Synthesis and Characterization of Novel Bismaleimides Derived from Arylene Phosphine Oxides and Ether-Ketones

by

Paul A. Wood, III

Dissertation submitted to the Faculty of the Virginia Polytechnic Institute and State University in partial fulfillment of the requirements for the degree of

DOCTOR OF PHILOSOPHY

in

Chemistry

APPROVED:

J. E. McGrath, Chairman

H. W. Gibson

J. G. Mason

J. S. Riffle

T. C. Ward

December, 1991

Blacksburg, Virginia

Synthesis and Characterization of Novel Bismaleimides Derived from Arylene Phosphine Oxides and Ether-Ketones

by

Paul A. Wood, III
Committee Chairman: Dr. J. E. McGrath
Department of Chemistry
(ABSTRACT)

Bismaleimides containing either bisphenoxy phosphine oxide or bisphenoxy carbonyl linkages have been synthesized in high yields from bis(4-fluorophenyl)phenyl phosphine oxide or para-[bis(4-fluorobenzoyl)]benzene via a two step process. The respective activated aryl halides were first reacted with aminophenates under nucleophilic conditions to form diamines which were subsequently reacted with maleic anhydride to yield first the bismaleamic acid and then catalytically cyclodehydrated to afford the bismaleimides.

The materials were characterized by a number of spectroscopic and chromatographic methods to ensure that the intended structures were quantitatively obtained. DSC analysis of the phosphine oxide bismaleimides showed that they have crystalline melting points around 100°C and cured to reasonably tough networks which exhibited glass temperatures around 380-400°C by DMTA and TMA. The phosphine oxide bismaleimides demonstrated an exothermic curing peaks >180°C, suggesting that a practical processing range exists.

Qualitatively the networks show excellent flame resistance compared to commercial controls. In contrast, the ether ketone bismaleimides showed higher melting behaviors and also had glass transition temperatures around 400°C.

This dissertation is dedicated to my father and friend,

Paul A. Wood, Jr.

Acknowledgement

Words are not eloquent enough to express the deep appreciation we have for Professor James E. McGrath

There is only the reality of energy's

thermodynamic and kinetic transformations

Paul Wood

December 1991

Table of Contents

List of Figures

Page

List of Schemes

List of Tables

I. Introduction

Historically, epoxies have been the major resin chosen for advanced composites and adhesives due to their outstanding adhesion, good impact resistance, solvent resistance and ease of processability. However, the structural performance of epoxies are limited to relatively low temperature applications of approximately 180°C in dry and 110°C in wet atmospheres. This significantly restricts epoxies from high performance, high temperature aerospace applications.

Higher temperature performance resins are needed for composite applications where epoxies cannot be used. But unfortunately, as high temperature properties are incorporated into resins, the ease of processability is often reduced. Bismaleimides are well known to be important thermosetting resin systems that have developed at a rapid rate during the last decade. Bismaleimides are preferred as matrix resins for composites over epoxies when high temperature resistance, good hot-wet environmental stability and improved fire, smoke and toxicity properties are required.

A wide variety of bismaleimides have been prepared with the aim of tailoring specific resin properties by simply changing the structure and molecular weight of the diamine used for the synthesis. In principle, it has been shown that

essentially any diamine or amine terminated prepolymer can be converted into the corresponding bismaleimide.

One of the advantages of aromatic bismaleimides is their high glass transition temperature, which is required for many aerospace applications. The methylenedianiline based systems, although considered widely to be the work horse of the BMI Industry, have been found to be both extremely brittle and undesirably contain quantities of the carcenogenic precursor methylenedianiline in the polymerization mixtures. This large degree of brittleness no doubt results from the high crosslink density due to the short bismaleimide segments. The brittle bismaleimide networks result in composites with microcracks and low damage tolerance. Bismaleimides have the inherent advantage of not emitting volatiles during network formation, which can cause detrimental structural defects, since crosslinking occurs via carbon-carbon double bonds.

Bismaleimides derived from aromatic diamines are crystalline compounds with relatively high melting points. Unfortunately, the high melting temperature of the uncured bismaleimide results in a narrow processing window. Once the bismaleimide resin melts, it immediately begins to cure, making processing difficult for the neat resins. After the material cures, the network cannot be processed. One means to overcome this drawback is to copolymerize the bismaleimide

with comonomers such as: diamines via Michael addition reaction, o,o'-diallylbisphenols, vinyl ester resins, allylphenoxyimides and a varity of others. Such chain extension improves the processability and reduces the melting point and the inherent brittleness of the bismaleimides. In practice, bismaleimides are prereacted with an aliphatic branched diamine to produce a lower melting or even a liquid precursor, which has a wider thermal processing window relative to its flow behavior and network formation. However, the aliphatic incorporation lowers the ultimate heat resistance of the BMI system.

It would be advantageous to produce a somewhat tougher BMI system which again would cure without any volatiles eliminated that would be based upon less environmental hazardous precursors, relative to the methylenedianiline based systems. It is also desirable to prepare systems that can liquefy at relatively low temperatures and possess an adequate processing window while still retaining a high temperature resistance network. These needs have led to this investigation of new BMI chemistry.

The principal purpose of this investigation was to synthesize novel bismaleimides that are processable, have high glass temperatures, that are thermo-oxidatively stable, and have improved toughness. Potential applications for materials with these physical properties are as advanced

composite matrix resins, structural adhesives, electronic components and for fire resistant materials and specialty coatings.

Several synthetic approaches were employed in this investigation to improve the toughness and processability without sacrificing thermo-oxidative stablility, relative to the methylenedianiline systems. One rationale was to increase the molecular weight between maleimide crosslinks and to insert flexible bridging units between the aromatic rings. Another strategy was to incorporate meta maleimides and to use bulky side groups. These schemes evolved into the use of bisphenoxy phosphine oxide and bisphenoxy carbonyl containing bismaleimides.

The literature review of this dissertation is divided into three main sections: 1) Bismaleimides, 2) Synthetic Compendium and 3) Requirements for Heat-Resistant Polymers. The intent was to cover what bismaleimides are, their uses, advantages and disadvantages, how bismaleimides are made and a background on types of molecular structures that are required for heat-resistant polymeric systems.

II. Literature Review

A. Bismaleimides

1. Introduction Maleimide 1 and a large number of N-substituted maleimides, such as N-phenylmaleimide 2 have been prepared and shown to homo- and copolymerize by radical and anionic mechanisms (1). Maleimides copolymerized with vinyl monomers lead to materials with greater structural stiffness and higher thermal stability compared to the parent vinyl polymers (2). In addition, maleimide copolymerization offers such property advantages as improved impact and tensile strength, adhesion, resistance to water, solvents and electrical stress (3). The relatively rigid 1,2-disubstituted olefin structure of maleimides is a result of their five-membered planar ring which hinders rotation of the imide residues around the backbone chain of the macromolecule:

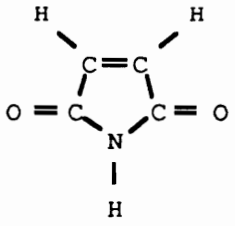

1

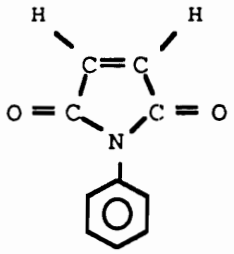

2

Planarity results in the possibility of cis and trans enchainment. Cubbon examined Courtauld models that showed there is considerable steric hindrance to the polymerization

in the cis configuration. He concluded that three types of polymers can be formed assuming that the trans opening of the double bonds takes place exclusively as shown in Figure 1 (4,5): (a) all of the rings are on the same side of the backbone chain, i.e., threo di isotactic, (b) the rings are on alternate sides of the backbone chain, i.e., threo di syndiotactic and (c) the rings may be randomly distributed on either side of the backbone chain. Recently Okamoto and coworkers reported the asymmetric polymerization of N-phenylmaleimide initiated with complexes of butyllithium and chiral ligands led to optically active polymers (5). They concluded optical activity resulted if enchainment was predominantly one of the two trans N-phenylmaleimide structures shown in Figure 1.

Kodak and IBM have employed copolymers containing maleimides as base-soluble binders for positive photoresists materials (6,7). Polystyrene substituted with pendant maleimide groups have been utilized in photocrosslinking reactions for photographic film applications (8,9). Dow has prepared maleimides with cyanate-functional pendant groups that have been copolymerized to prepare polycyanates, polymaleimides, polyepoxides and other vinyl compounds which cure to give thermosets with good mechanical properties and water resistance (10). Unsaturated polyesters have been modified with maleimides to obtain composites with improved

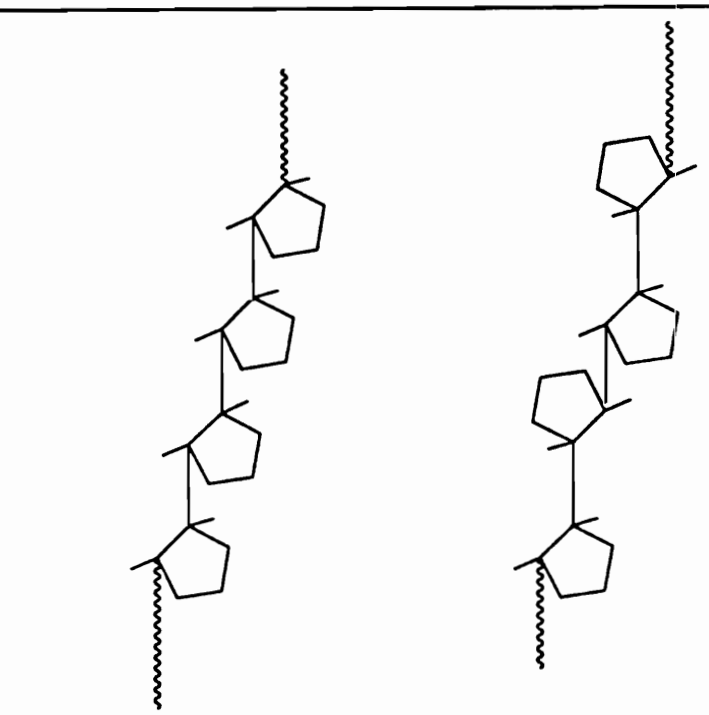

Threo Di Isotactic

Threo Di Syndiotactic

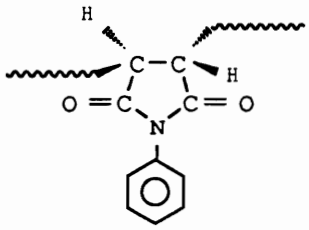

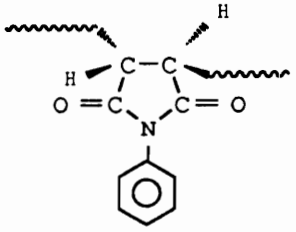

Two Possible
Trans Structures

Figure 1

Configuration of Poly-N-Substituted Maleimides (4,5)

heat resistance, while other polymeric systems, such as urethanes, cyanoacrylates, polysiloxanes and epoxies have also been modified with maleimides to obtain improved fiber, adhesives, coatings and laminates (1). Diene polymers have been crosslinked with maleimides yielding elastomers with improved heat resistance known as Hypalon® Rubbers (DuPont) (11). For example, chlorobutyl rubber has been cured with various maleimides (12).

Currently of more interest is the use of bismaleimides 3 derived from methylenedianiline and maleic anhydride, in relatively high temperature composite systems. Bismaleimides

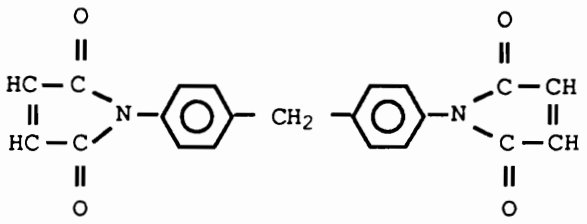

3

are a comparatively new class of thermosetting polymers that have developed at an astounding rate during the last decade (13). Traditionally, epoxies have been the major resin chosen for advanced composites and adhesives (14). However, the problem with epoxies is that their upper temperature range for structural performance is limited to approximately 180°C in dry and 110°C in a wet atmosphere (15). Higher temperature performance resins are needed for composites in applications where epoxies cannot be used, but unfortunately

as high temperature properties are increased, the ease of processability of the resins is reduced (16). Industry favors bismaleimides as matrix resins for composites over epoxies when high temperature resistance, good hot-wet environmental stability and improved fire, smoke and toxicity properties are required (17).

An extensive assortment of bismaleimides have been prepared with the goal of modifying specific resin properties by simply altering the structure and molecular weight of the diamine used in the bismaleimide synthesis. These variations can be used to adjust the solubility, melt temperature and viscosity of the uncured resin and improve the thermo-oxidative stability of the thermoset and optimize the fracture toughness (18). In principle, Stenzenberger has shown that any aromatic diamine or amino terminated prepolymer can be converted into the corresponding bismaleimide (15). Indeed, the patent literature describes many diamines that have been converted to the corresponding bismaleimide (19). In just the last two years over 500 new patents and applications have appeared on bismaleimides (20).

Bismaleimides derived from aromatic diamines are crystalline compounds generally with high melting temperatures. Table 1 and 2 shows the melting temperatures for various N,N'-substituted bismaleimides. Unfortunately, the high melting temperature of the uncured bismaleimide

Table 1

Melting Points of Bismaleimide Monomers

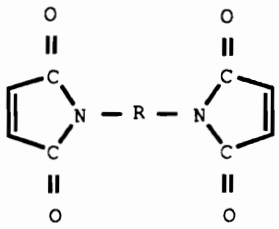

-R-	m.p. (°C)	Ref.
$-(CH_2)-$	171	21,22
$-(CH_2)_2-$	190-192	22,23
$-(CH_2)_6-$	137-140	23
$-(CH_2)_8-$	117-122	23
$-(CH_2)_{10}-$	111-115	23
$-(CH_2)_{12}-$	110-112	23
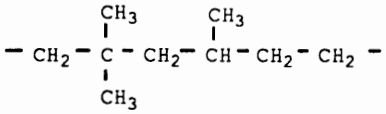	70-130	24
	243-244	25,26
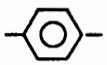	250	24,25,27
	202-203	21,22,24,25
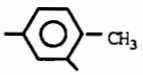	174-176	23
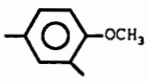	174-175	15

Table 1

Melting Points of Bismaleimide Monomers (con't)

-R-	m.p. (°C)	Ref.
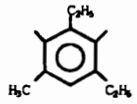	146-150	15
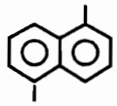	397	21
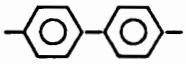	340-349	21,22
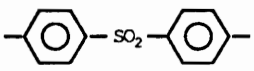	252-252	15,21,25
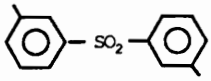	210-211	15
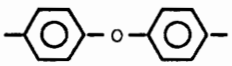	172-178	23,28,29
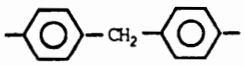	155-157	22,23,30,28
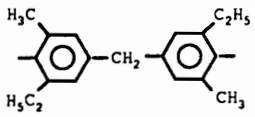	150-154	15
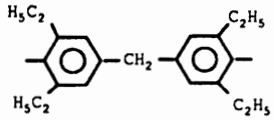	149-151	15
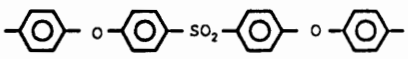	250	31
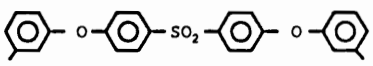	90-100	32

Table 1

Melting Points of Bismaleimide Monomers (con't)

-R-	m.p. (°C)	Ref.
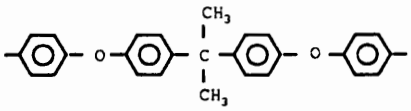	120	33
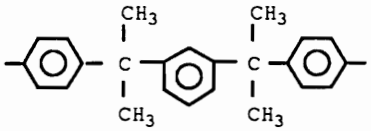	70	34
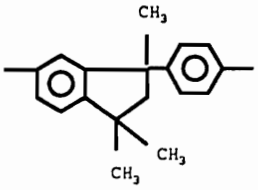	90-100	14
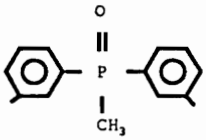	195	35
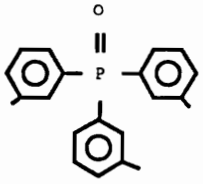	145	36
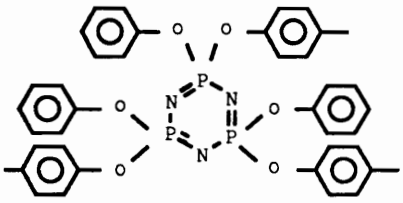	-	37,38,39

results in a narrow processing window. Once the bismaleimide resin melts, it immediately begins to cure making processing difficult for the neat resins. Presently 4,4'-bismaleimidodiphenylmethane 3 is the most widely used bismaleimide in commercial resin formulations due to the low price and availability of the starting materials (15).

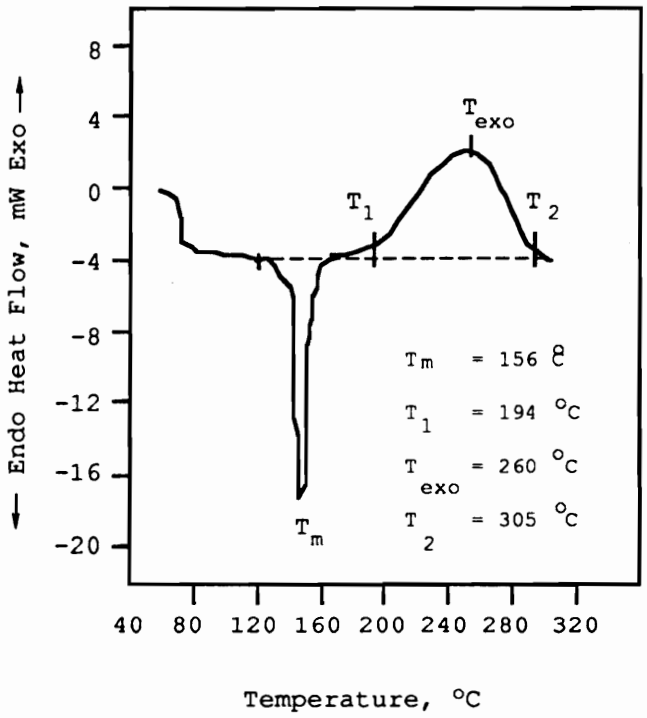

However, this material suffers from a narrow processing window as shown above by the differential scanning calorimetry thermogram (DSC), where T_m is the endothermal peak melting temperature of the bismaleimide resin, T_1 the on-set temperature of the curing reaction, T_{exo} the exothermic maximum peak of cure and T_2 the completion of the curing

reaction (40). The processing window is the temperature span between the resin melting (T_m) and T_1, while the area above the baseline drawn from T_1 to T_2 is the exothermic heat of polymerization (ΔH of cure).

The major advantage of aromatic bismaleimide networks is their high glass transition temperature, which is required for numerous aerospace applications (41). The primary disadvantage of crosslinked aromatic bismaleimides is their inherent brittleness resulting in composites with low damage tolerance and microcracks. This is due to the high crosslink density as a result of the short bismaleimide segments. One means to overcome this drawback is to copolymerize the bismaleimide with comonomers such as diamines via Michael addition (42), o,o-diallylbisphenols (43-46), vinyl ester resins (47), allylphenoxyimides (48) and a host of other methods. The Michael addition copolymer is obtained by a nonstoichiometric reaction between the bismaleimide and diamine as shown in Scheme 1 (42). The reaction is performed in the melt (or in solution) to give a predetermined low molecular weight crosslinkable prepolymer. A stoichiometric imbalance of diamine with excess bismaleimide results in an oligomer with maleimide terminated end-groups. The resulting prepolymer is fusible, soluble and processable. The oligomer can then be cured via maleimide carbon-carbon double bonds. Such chain extension improves the processability and reduces

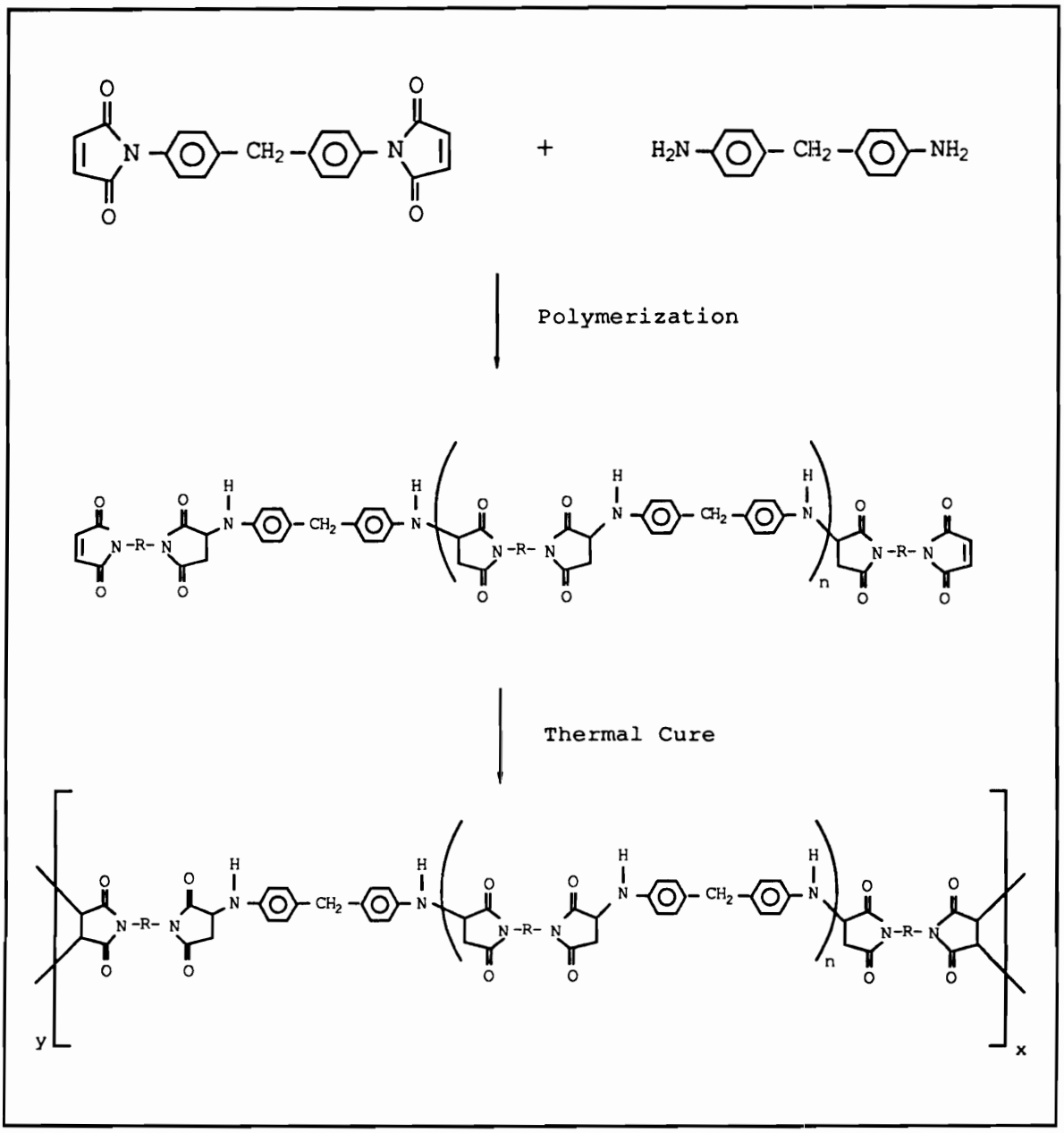

Scheme 1

Bismaleimide/Michael Addition Copolymerization (42)

the melting temperature and the inherent brittleness of the bismaleimides (40). In practice, the bismaleimide 3 is prereacted with an aliphatic branched diamine to produce an eutectic or even liquid precursor, which has a wider thermal processing window relative to its flow behavior and network formation. However, crosslinking aliphatic systems with aromatic bismaleimides reduces the thermal stability and hence the use of these material for high temperature applications. Figure 2 demonstrates the correlation between structures and melting behavior via differential scanning calorimetry for some well known eutectic and Michael type of bismaleimides (49).

Another method to improve bismaleimide fracture resistance is simply by increasing the molecular weight between crosslinks, this lowers the crosslink density yielding a less brittle material. Maleimide terminated amorphous poly(arylene ether ketone) oligomers 4 have been prepared with substantial increases in toughness relative to

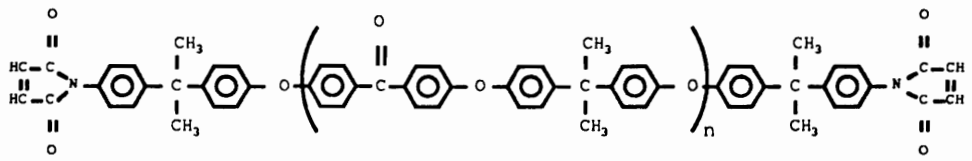

4

the simple bismaleimide 3 (50). Interestingly, it was demonstrated that the ability to control the final glass transition temperature of the network could be accomplished

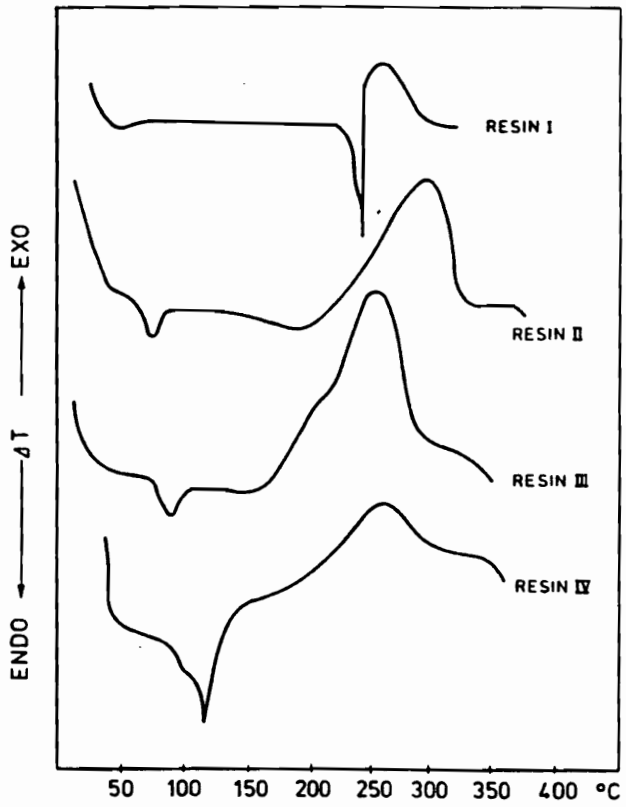

DSC scans showing melting and polymerization behavior of bismaleimide resins.

Structures and Melting Behavior of Bismaleimide Resins

RESIN NO	RESIN STRUCTURE	MELTING BEHAVIOUR
I	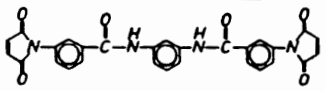	Fp. 238 - 245 °C
II	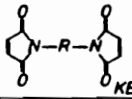 EUTECTIC TERNERY MIXTURE KERIMID 353	LIQUIFYABLE Fp. 70 - 125 °C VISCOSITY 140cP/120°
III	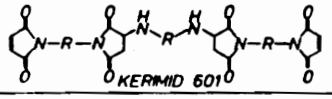 KERIMID 601	MELTABLE Fp 40 - 110 °C
IV	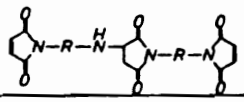	MELTABLE Fp 80 - 115 °C

Figure 2

Structures and Melting Behavior of Bismaleimide Resins (49)

by varying the molecular weight of the starting poly(arylene ether ketone) oligomer. As the oligomer molecular weight was lowered, the crosslink density increased leading to a corresponding increase in the T_g of the network as a result of decreased chain mobility. A variety of other maleimide-terminated thermoplastics have been prepared based on polysulfones (51,52), polyimides (53) and poly(amide-imides) (54). Aromatic polyketones with pendent maleimide groups have been prepared with good thermal and thermo-oxidative stability (55).

Epoxy-based resins are often toughened by the incorporation of a second dispersed phase. Typically, rubber or hard particles are added that serve to increase the number of energy absorption mechanisms available to the matrix. It is believed that the rubber particles act as stress concentrating locations allowing tougher materials to be prepared through crazing and shear band formation mechanisms (56). For example, carboxyl or amine terminated low molecular weight liquid poly(butadiene-*co*-acrylonitrile) copolymers have been used (57). Blending epoxies with tough, ductile engineering thermoplastics like polyethersulfones (58) or polyetherimides (59) is presumed to improve fracture toughness by an energy absorption mechanism known as "crack pinning" where the crack front is impeded by the hard impenetrable particles, creating new fracture surfaces (60).

These toughing approaches have also been applied to bismaleimides.

The modification of bismaleimides networks with carboxyl terminated poly(butadiene-*co*-acrylonitrile) rubbers has been reported with increase in toughness without significant reduction in the heat resistance of the material (61). However, ultimately the limited thermo-oxidative stability of the rubber component is not suitable for a high temperature thermoset applications (18). Improvement in fracture toughness of neat bismaleimide networks by greater than 100% has been described using polybenzimidazole as the hard particle additive (62).

A recent strategy in toughing and also resistance to microcracking in fiber reinforced composites has been accomplished by the copolymerization of bismaleimide 3 with diallylphenyl compounds, in particular o,o'-diallylbisphenol-A 5 (52,63-70):

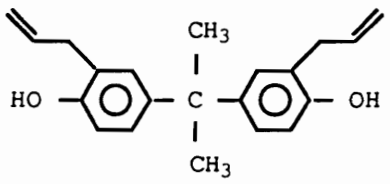

5

These formulations are now commercially available from Ciba-Geigy (Matrimid® 5292: o,o'-diallylbisphenol-A) (65) and Shell/Technochemie (Compimide TM 121: a proprietary

allylphenyl compound) (67,70). The resulting copolymer network is much tougher compared to the homo-bismaleimide thermoset. The exemplary advantage of 5 is that it acts as both a reactive diluent, i.e., liquid at room temperature, dissolving the bismaleimide and as a toughening agent (68). This solvent-free two-component bismaleimide system results in a low viscosity mixture that is easily hot melt processable for advanced composites and high performance structural adhesives. The molar ratio of the bismaleimide and diallyl compound can be varied for different structure/property relationships, however, large excess of the diallyl compound should be restricted in order to preserve high temperature stability (18). Optimum copolymer networks are prepared by an approximate 2:1 molar ratio of bismaleimide/diallylphenol (68). Variations from this ratio result in either brittle (lower than 2:1) or plasticized (higher than 2:1) thermosets. Significant improvements in fracture toughness of thermoplastic polysulfones, poly(ether phosphine oxide)s and polyimides with reactive end-groups have also been achieved by copolymerizing with bismaleimide 3 and o,o'-diallylbisphenol-A (52).

2. Background Aromatic bismaleimides are relatively low molecular weight monomers or oligomers terminated with maleimide end-groups. Conventional cyclic polyimides are distinguished from bismaleimides by the

presence of the phthalimide structure in their linear polymer backbone, while the three-dimensional polymeric bismaleimide lacks the incorporation of the aromatic ring in the cyclic imide structure. A comparison of bismaleimide and polyimide structure is illustrated in Figure 3.

The reactivity of the maleimide double bond is a consequence of the electron-withdrawing nature of the two adjacent carbonyl groups. The relative ease of maleimide polymerization is also due to release of ring strain during opening of the double bond (71). This results in a very electron-deficient double bond, as shown below by the resonance structures of N-phenylmaleimide 6 (15):

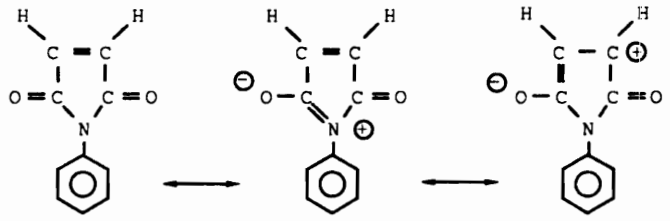

6

Aromatic bismaleimides offer higher glass transition temperatures and thermal stabilities compared to aliphatic structures as a result of additional bond energy gain through resonance stabilization. Crosslinking also enhances the thermal stability and glass transition temperature while increasing the hydrolytic and chemical resistance. Variation in the isomeric position of the maleimide end-group can have an profound influence on the melting behavior and enthalpy of

Bismaleimides

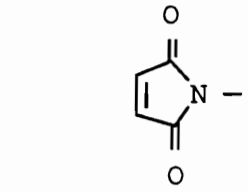

Maleimide

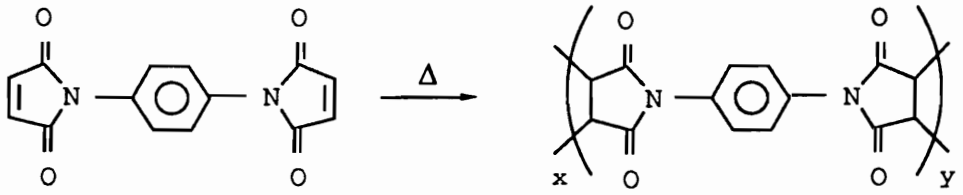

Polyimides

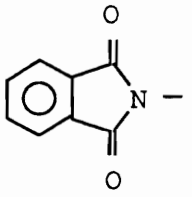

Phthalimide

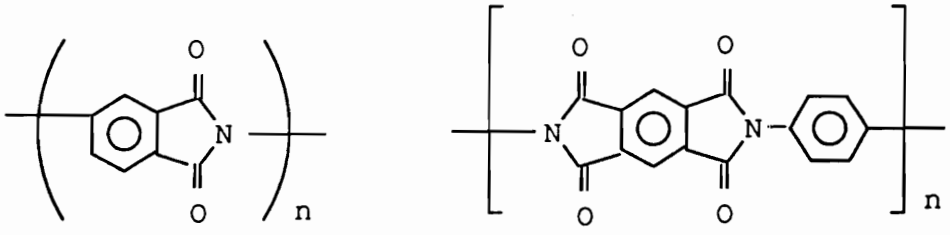

Figure 3

Comparison of Bismaleimide and Polyimide Structures

polymerization (ΔH of curing) as shown in Table 2 (72). Section II.C. outlines the requirements for heat-resistant polymers. In general, Stenzenberger has observed for bismaleimides containing the same structure between maleimide end-groups, differing only in the para and meta-position of the end-groups, the meta-isomer has the lower melting transition and the higher enthalpy of polymerization while the para-isomer has the lower enthalpy of polymerization. While no reason was given for these enthalpic differences, it is possibly due to the para-maleimide being less sterically hindered and therefore more readily accessible to neighboring maleimides for crosslinking compared to the meta-isomer.

Bismaleimides are typically synthesized from maleic anhydride and diamine compounds as shown in Scheme 2 (15,22,29,30). This classical method by Searle proceeds by a two-step condensation process. The reaction is carried out in solvents such as N-methylpyrrolidinone (NMP), dimethylformamide (DMF), acetone or chloroform at room temperature. In the first step, the corresponding bismaleamic acid is formed quantitatively as an intermediate (15). This step is analogous to the amic acid formed in polyimides. The second step is the cyclodehydration of bismaleamic acid to bismaleimide (imidization) via thermal or chemical dehydration. Typically, thermal dehydration can be performed in DMF at 40-60^{o}C (or in the melt), while acetic

Table 2

Comparison of Ether and Ether-Ketone Bismaleimides (72)

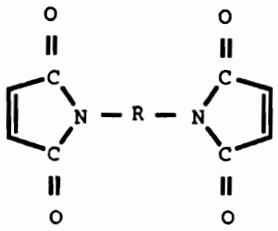

—R—	DSC Data[1] Mp (°C)	T_{MAX}[2] (°C)	$\Delta H_{pol.}$[3] (J/g)
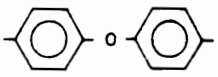	173–176	286	135
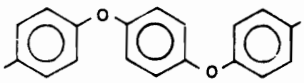	239	252	187
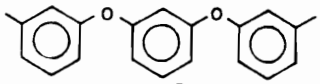	163	254	221
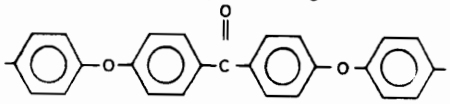	239	250	160–180
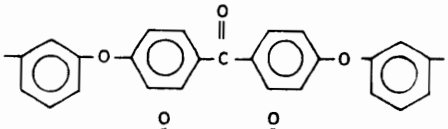	85–91	304	222
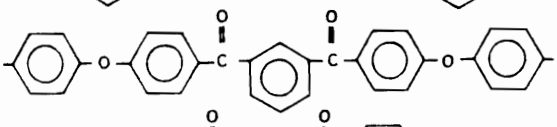	226	285	113
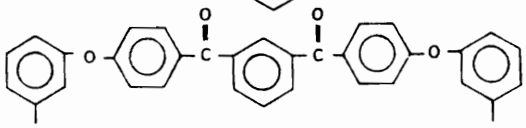	60–65	314	224

1 DSC = Differential Scanning Calorimetry, heating rate 10°C min
2 T_{MAX} = cure exotherm peak maximum
3 ΔH_{pol} = heat of polymerisation

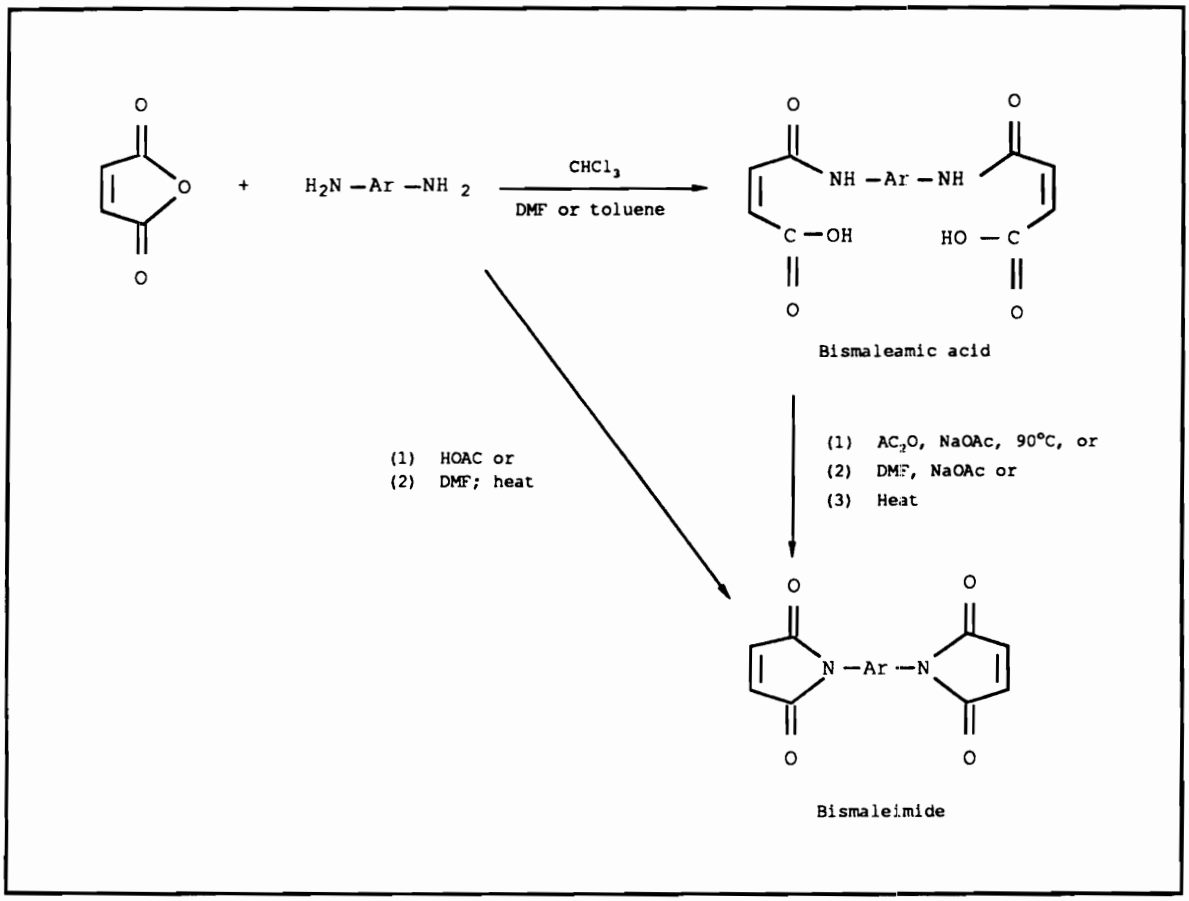

Scheme 2

Typical Synthesis of Bismaleimide (15)

anhydride and sodium acetate can be used as the chemical imidization agents. Similarly, N-substituted maleimides can be prepared from alkyl or aryl amines and maleic anhydride; maleimide 1 is synthesized from maleic anhydride and ammonia.

Derivative structures of maleimide are shown in Figure 4. Succinimide is the saturated version of the maleimide group obtained by either hydrogenation of the maleimide group or from condensation of an amine with succinic anhydride (or acid) and subsequent cyclodehydration. Maleimide groups have been reported containing methyl and halogen substitutions on the double bonds (3,35,36,73,74). These modifications were exploited to augment the electropositive nature of the maleimide carbon-carbon double bond and hence the reaction rate either by inductive or steric affect. Electron withdrawing substituents, such as chlorine, increase the electropositive character of the carbon-carbon double bond and therefore the reaction rate with nucleophilic agents; whereas the electrophilic nature of the double bond can be decreased using electron donating substituents like the methyl group (citraconimide). Maleimides can be homopolymerized or crosslinked as bismaleimides across the carbon-carbon bond as shown in Figure 4. Substitution of the carbonyl oxygen leads to mono- and bis-alkenylation of maleimides (75). While, acetanilides, N-maleimido-N'-acetylaminos and isoimides are intermediates in the

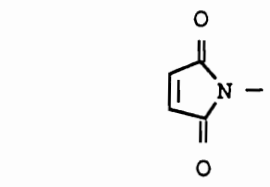

Maleimide

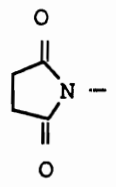

Succinimide

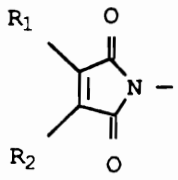

Substituted Maleimide
$R_1 = R_2 = CH_3$, F, Cl

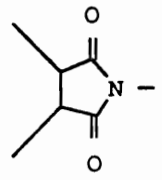

Homo or Crosslinked-
Maleimide

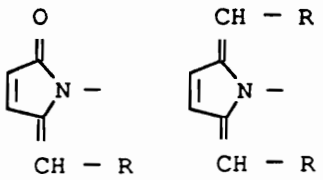

Mono or bis-
(alkenyl)amine

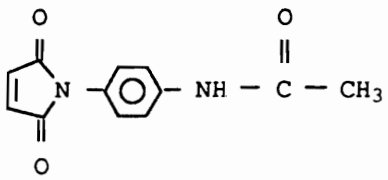

N-maleimido-
N'-acetylamino

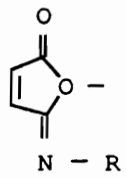

Isoimide
(Isomaleimide)

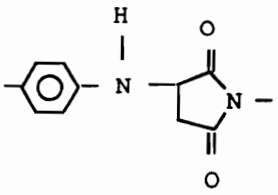

Aspartimide

Figure 4

Derivatives of Maleimide

synthesis of maleimides under certain reaction conditions. The Michael addition of an aromatic amine across the maleimide double bond described in Scheme 1 results in the aspartimide structure shown in Figure 4.

3. **Reactions of Bismaleimides** Maleimide and N-substituted maleimides readily undergo free radical and anionic initiated homopolymerizations (71). It was commonly believed until the early 1960's that 1,2-disubstituted ethylenes would not homopolymerize due to steric hindrance (76). However, the high heat of polymerization of maleimide indicates that steric repulsions between neighboring groups in the polymer backbone are not very large (77). Maleimides have been solution and melt polymerized using peroxides and azo compounds as free radical initiators (22,71,77-81).

Grundschober first reported the homopolymerization of maleimides and the crosslinking of bismaleimides by simply heating the monomers to between 150 and 400°C as depicted 7 (28,82). The mechanism of the thermally induced curing reaction probably involves a free radical crosslinking of bismaleimides through the electron deficient double bonds. However, in reviewing the literature, the main support for a free radical crosslinking mechanism was the observation that hydroquinone could inhibit the formation of the network structure (15,78,83) and that the rate of curing can be markedly increased by employing an organic free radical

initiator (51). The rates of thermal, self-initiated polymerizations are much slower than the corresponding polymerizations initiated by the thermal homolysis of a free radical initiator (84).

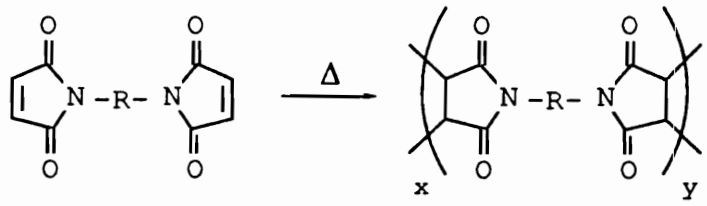

7

Most thermally initiated organic reactions have been found to involve the formation of free radicals that generally require high reaction temperatures (85,86). The occurrence of true thermal polymerizations can be difficult to establish since trace impurities in the monomers or reaction vessel often prove to be the actual initiators; in most cases of self-initiated polymerization, the identity of the initiating radicals and the mechanisms by which they are formed remain obscure (86). Electron spin resonance spectroscopy (ESR) studies of growing polymer chain radicals formed by thermal initiation are made difficult by the high reactivity of free radicals at the usually required high temperatures (85). Brown and Sandreczki recently reported studies of bismaleimide cure reactions by ESR (87). They concluded that radical mechanisms were involved in the thermal crosslinking of bismaleimides, probably as a result

of hydrogen atom abstraction reactions.

The electrophilic maleimide carbon-carbon double bond is especially labile to nucleophilic attack, undergoing a Michael addition type of reaction under mild conditions with amines, phenols, thiols and a variety of nucleophilic agents (21,42,88,89,90,91). For example, the nucleophilic reaction of 4,4'-bismaleimidodiphenylmethane and 4,4'-diaminodiphenylmethane is outlined in Scheme 1.

Anionic polymerization of maleimide and N-substituted maleimides has been described by various authors (4,5,71,77,80,92,93-99). A variety of nucleophilic reagent have been used to initiate the homo and crosslinking reaction of maleimides. Cubbon investigated the polymerization of N-substituted maleimides initiated with n-butyllithium (4). He observed that N-phenylmaleimide proceeds in a "living" polymerization in toluene at -78°C, with the characteristic deep red color accompany the propagating carbanion. The rate of the n-butyllithium initiated polymerizations was enhanced by changing the solvent to tetrahydrofuran which is a common feature of solvent separated ion pairs in lithium-carbanion diene chemistry. Marvel in the mid-1960's described the base-initiated polymerization of maleimides using alkali-metal tert-butoxides, butyllithiums and other bases (93). Hagiwara et al. recently continued the anionic polymerization of N-phenylmaleimide initiated with tert-butoxides 8 (92,94-

98). Their results indicated that polymerization of N-phenylmaleimide is initiated at the carbon-carbon double bonds and propagates through opening of the double bonds without any side reactions such as abstraction of hydrogen at the double bond, carbonyl addition or ring opening of the cyclic imide group.

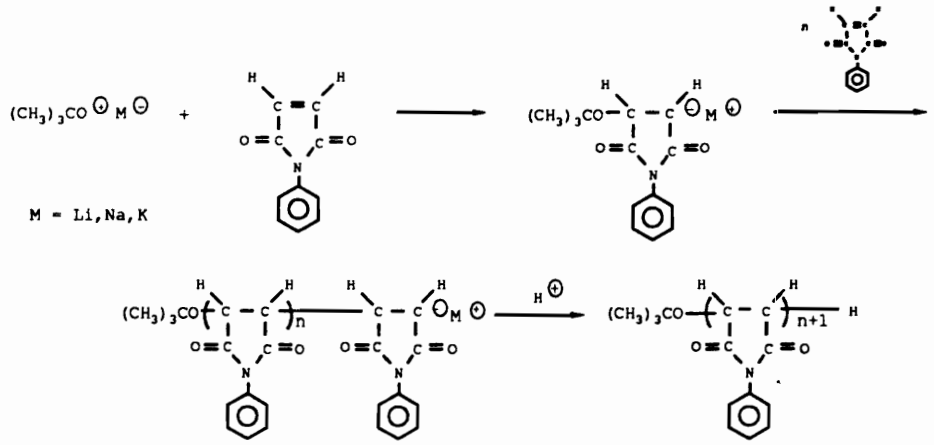

8

Hodge and colleagues have demonstrated that triphenylphosphine initiates polymerization of N-phenylmaleimide by an anionic mechanism. This reaction was carried out in dimethylformamide at 60°C with essentially quantitative yield (99). They eloquently showed by ^{31}P-NMR that initiation proceeds by a Michael addition of the phosphine to the olefinic bond of maleimide group, while propagation then consist of successive Michael addition of the anion to maleimide as shown in Scheme 3. In a similar manner imidazoles have been used to initiate the polymerization of maleimides (17,100,101).

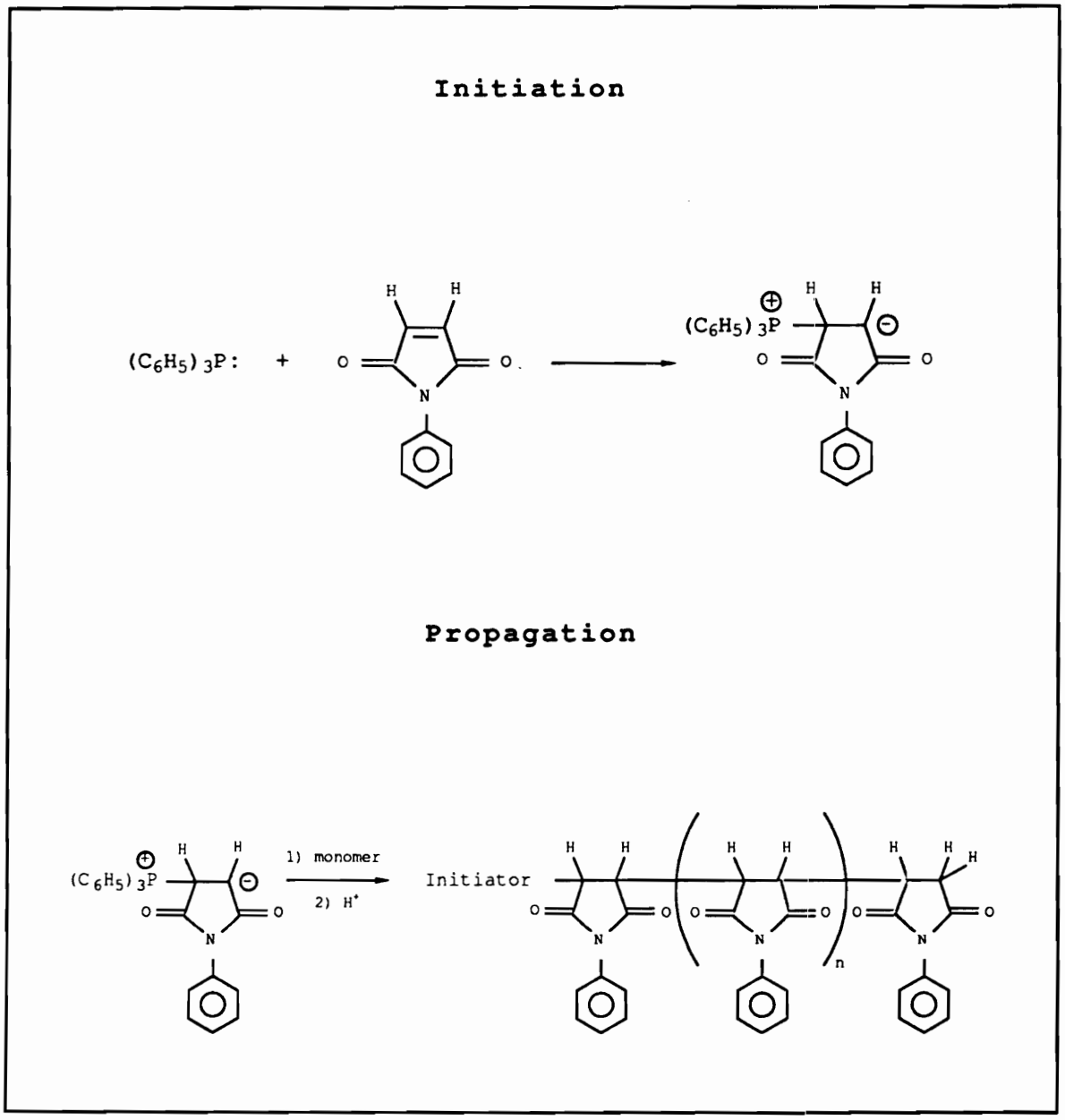

Scheme 3

Triphenylphosphine Polymerization of N-Phenylmaleimide (99)

Triphenylphosphine offers a novel initiation route to the crosslinking of bismaleimide resins for high temperature, high performance application (102). Conventionally, organic peroxides have been employed as free radical initiators for bismaleimide resins. However, organic peroxides are not very suitable for the high temperature melting bismaleimides (Table 1 & 2), since organic peroxides decompose into radicals at temperatures well below these melting temperatures. Essentially, the organic free radicals are depleted at temperatures require for crosslinking the maleimides carbon-carbon double bonds. Ideally, the initiator needs to be activate at temperatures corresponding to the bismaleimide melting transition. Triphenylphosphine has a melting point of 80°C and a boiling point >360°C, making it suitable for melt polymerization of bismaleimides.

An unique application of the maleimide carbon-carbon double bond is the A-B reactive monomers to polymerize linear non-phthalimide polyimides 9, where B delineates a functional group that will react with the double bond. Marvel prepared base-initiated polymerization of maleimide 1 with the repeating bond N-succinimide (93). While, Stenzenberger (15,72) and Harwood (103) et al. have investigated various N-substituted reactive B-groups such as aniline, allyl, allyl esters, amide allyl esters, benzocyclobutene (104), N-benzocyclobutene phthalimide (104)

and ethynyl phenyls (105). Many of these monomers have relatively low melting transitions and polymers with relatively high T_g, making them attractive for matrix resins and adhesives.

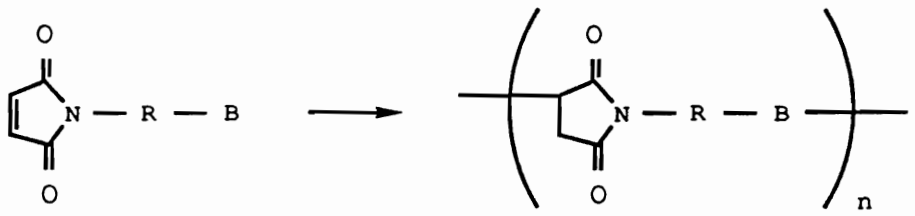

9

Group-transfer polymerization is a new technique that has recently been employed to polymerize maleimides (106-108). This mechanism proceeds in a living manner using tetracoordinate silanes, organotins or organogermaniums as group-transfer catalysts and Lewis acids or bifluorides, cyanides or azides as cocatalysis.

Bismaleimides are highly reactive bisdienophiles in Diels-Alder reactions with a variety of bisdienes like biscyclopentadienones 10 (109), α-pyrones (110), thiophene dioxides (111), bisfuvenes (112), divinylbenzene (113-115) and in pentadiene crosslinking in nadimide-terminated polyimides as shown in Figure 13. Diels-Alder systems can also be crosslinked by reacting the bismaleimide in excess to ensure maleimide end groups (72). However, bismaleimides based on Diels-Alder chemistry have not been greatly exploited commercially (116).

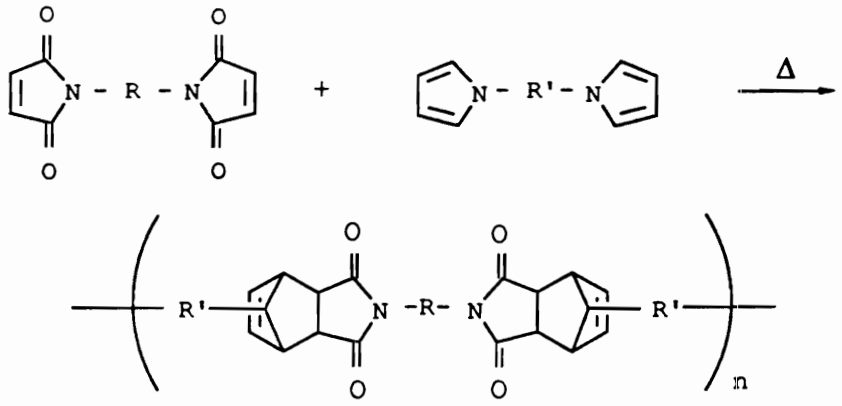

10

More important are the so called addition 'ene'-reactions of bismaleimide double bonds and allyl-type of olefinic bonds (15). These are the copolymerization between bismaleimides and diallylphenyl or diallylphenol compounds, for example o,o'-diallylbisphenol-A 5, was previously mentioned. The chemical characterization of the copolymer structures has been determined by ^{1}H-NMR (48), ^{13}C-NMR (117) and thermal properties by differential scanning calorimetry (118). The proposed synthetic route is illustrated in Scheme 4 (72). As shown the allylphenol and the maleimide react to form a linear chain extension by an 'ene'-reaction followed by a Diels-Alder reaction. The network forms in relatively large molecular crosslink segments, resulting in a copolymer network that is much tougher vs the bismaleimide alone. A recent variation of these reactive diluents is the allylnadic imide blended with bismaleimides (69,119,120).

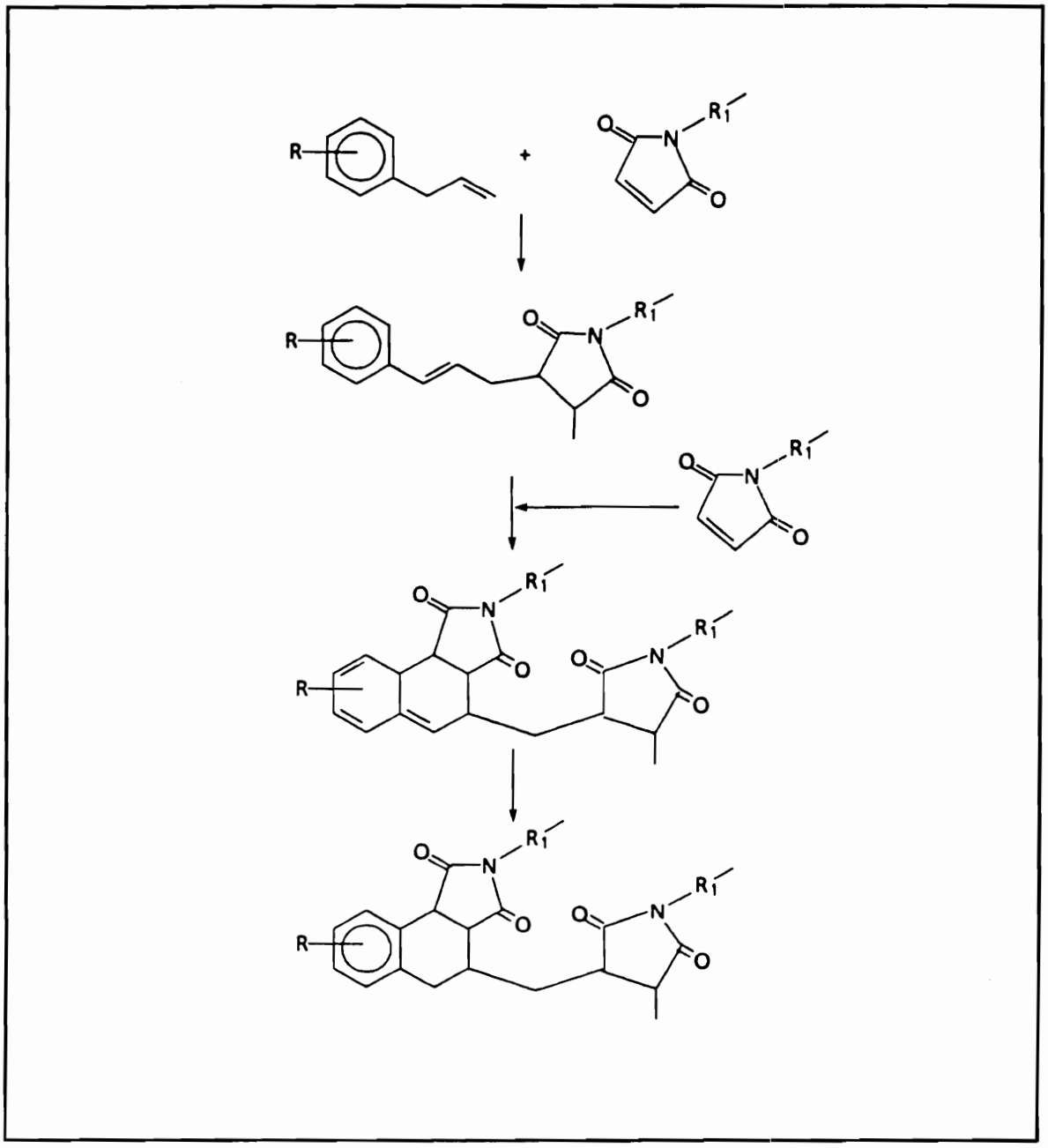

Scheme 4

Proposed Network Structure of Bismaleimide and o,o'-Diallylbisphenol-A (72)

Bisbenzocyclobutenes react with bismaleimides in a Diels-Alder reaction to form either linear polyimides as shown in Scheme 5 or crosslink systems depending on the molar ratio between the two reactants (13,121).

Biscyanates or cyanate-terminated oligomers have been reacted with bismaleimides to form a copolymer network known as triazine resins or BT-resins (B for bismaleimide; T for triazine) (15,72). This system is very versatile because a variety of formulation can be applied for different properties. Epoxies, acrylates and o-diallylphthalate are a few of the reactive diluents that have been used to modify the triazine-resins. Scheme 6 depicts the proposed bismaleimide-cyanate copolymerization (72,122). BT-resins are reported to be used by Mitsubishi for printed circuit boards and multilayer printed wiring boards (15).

4. Curing of Thermosets Polymers that are joined together in a three-dimensional structure are referred to as networks, thermosets or crosslinked polymers. While the network process is referred to as crosslinking, curing, thermosetting or network formation. Networks are formed when a monomer or oligomer has reactive functional groups that can form covalent bonds with another monomer or oligomer. The monomer must have a functionality (*f* indicates the number of reactive group per molecule) greater than 2 to form networks. For example, the carbon-carbon double bond in N-

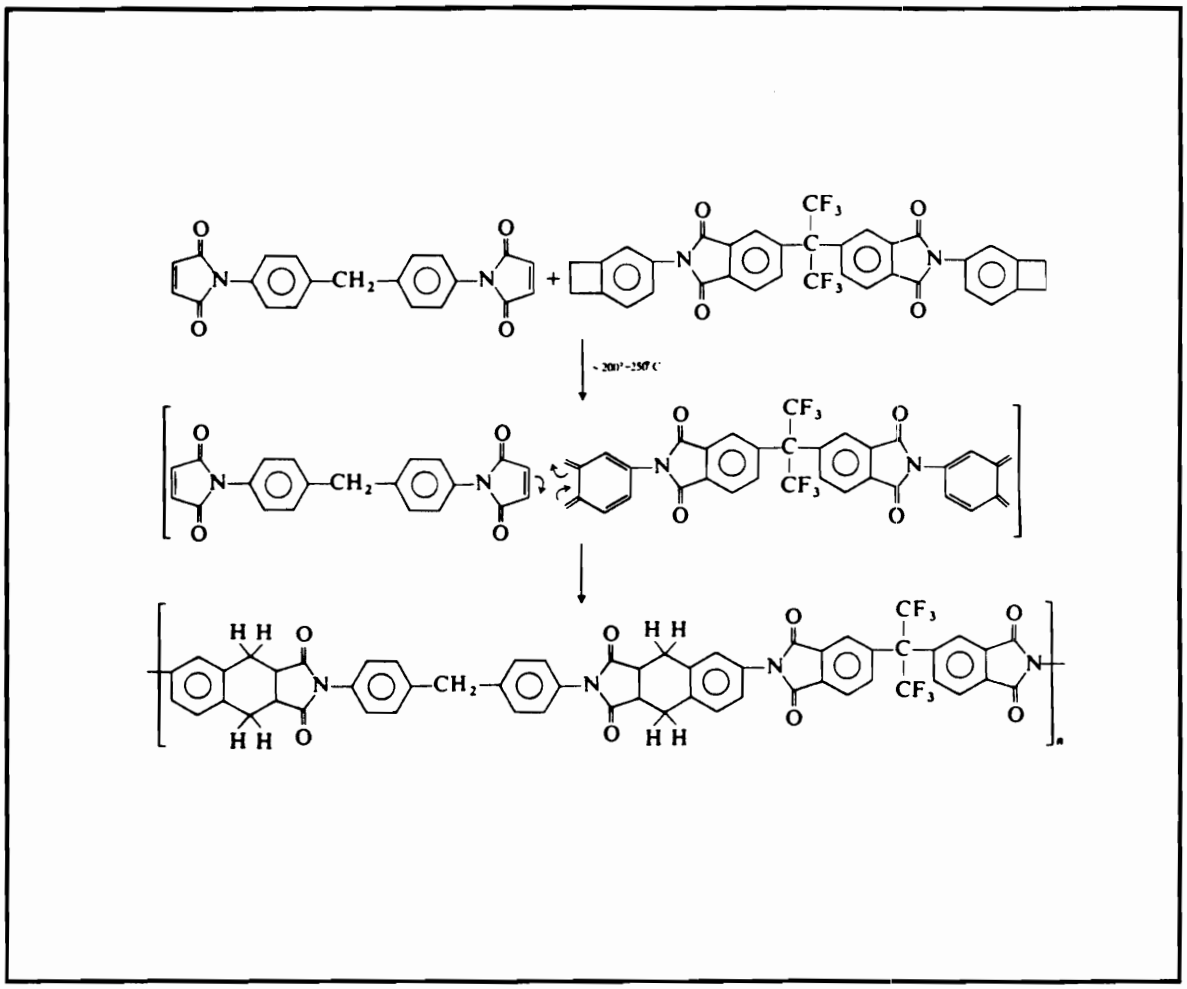

Scheme 5

Benzocyclobutene/Bismaleimide Copolymerization (13,121)

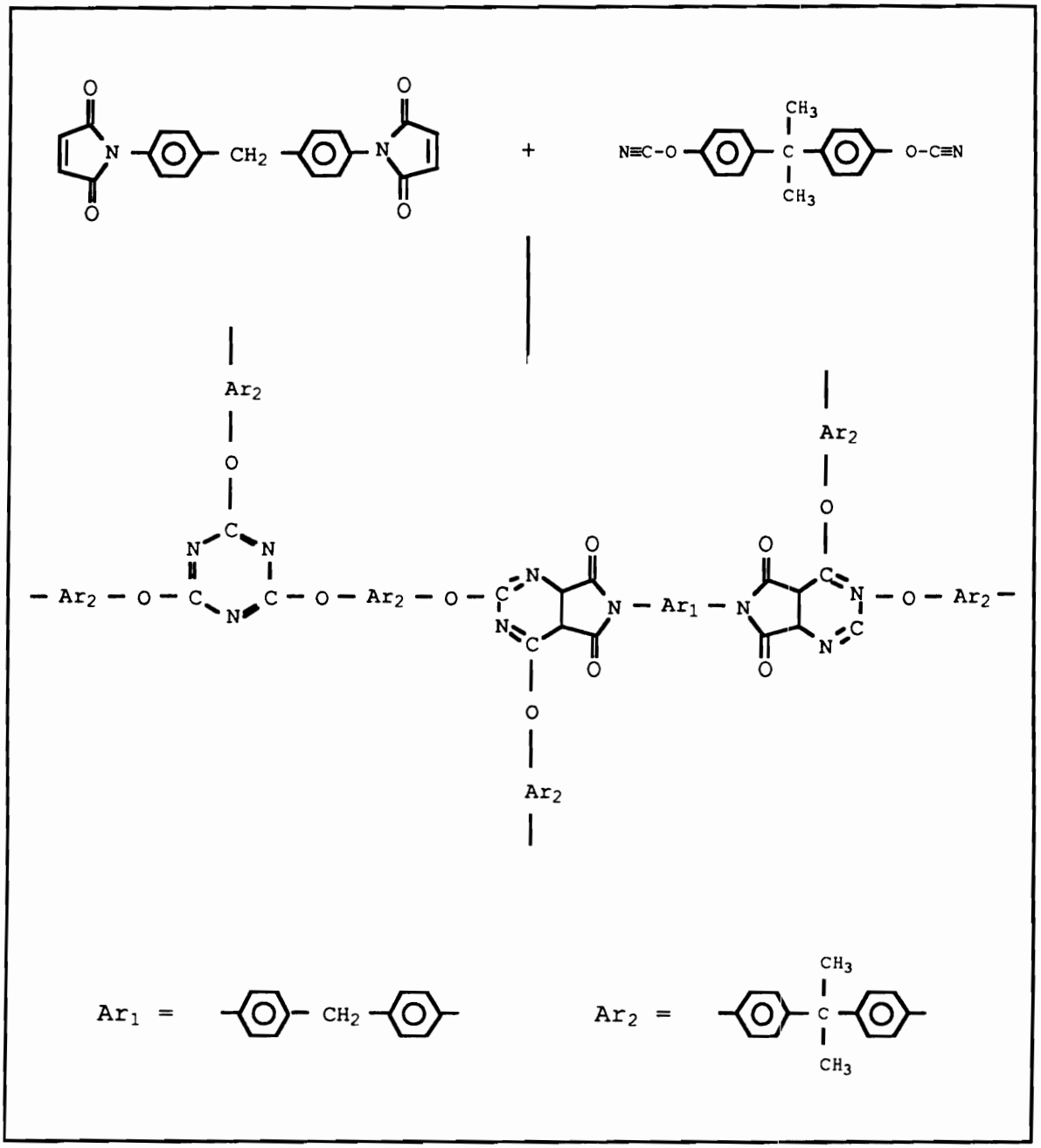

Scheme 6

Proposed Bismaleimide-Cyanate Copolymerization (72)

phenylmaleimide has a functionality of 2 leading to a linear homopolymer, while incorporation of more than one maleimide group per monomer or oligomer leads to $f > 2$ and hence to network formation as shown in Figure 5. Bismaleimides have a functionality of 4, while Mikroyannidis (123) recently has reported tetramaleimides with a functionality of 8. Other functional groups that lead to crosslinked polymers are listed in Table 14.

Curing begins with the linear polymerization of chains followed by branching and crosslinking. The molecular weight increases rapidly until the chains become linked into a three-dimensional network of infinite molecular weight. The degree of conversion that marks the transformation from a viscous liquid to the onset of a infinite network is known as the gel point and can be defined by the functionality, reactivity and stoichiometry of the reactants (124-131). Viscosity undergoes a tremendous increase as the gel point is approached with the number average molecular weight remaining small and the weight average molecular weight going to infinity while the material becomes elastic (129,132). The gel point is observed as a knee in the viscosity curve shown below for a generalized plot of viscosity change vs curing time at a given temperature. The system has a viscosity η_o at time zero (133). The exothermic heat of crosslinking given off initially produces a viscosity decrease η_1; as the

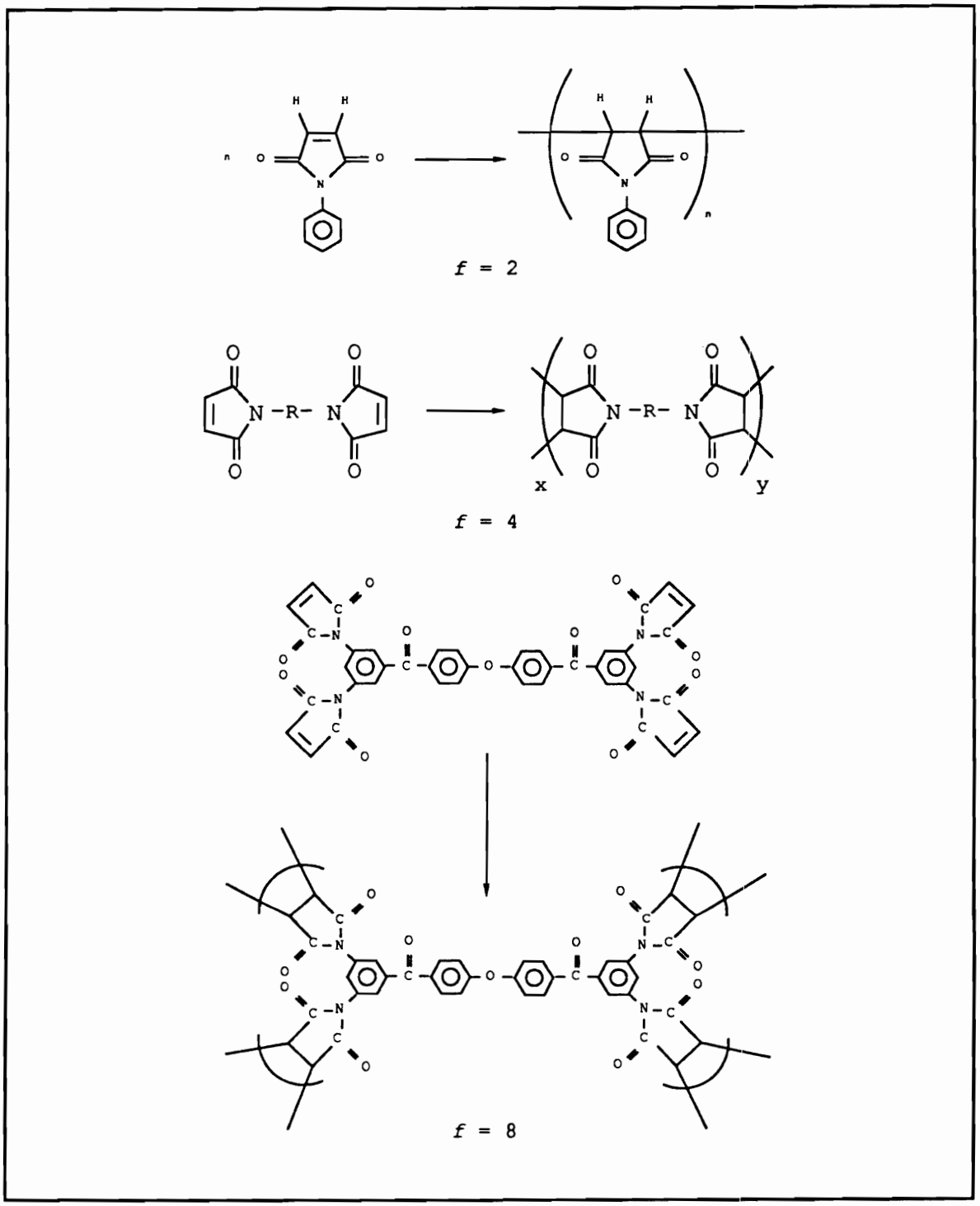

Figure 5

Functionality of Maleimides

cure progresses the molecular weight and branching rapidly increase with the viscosity going to infinity.

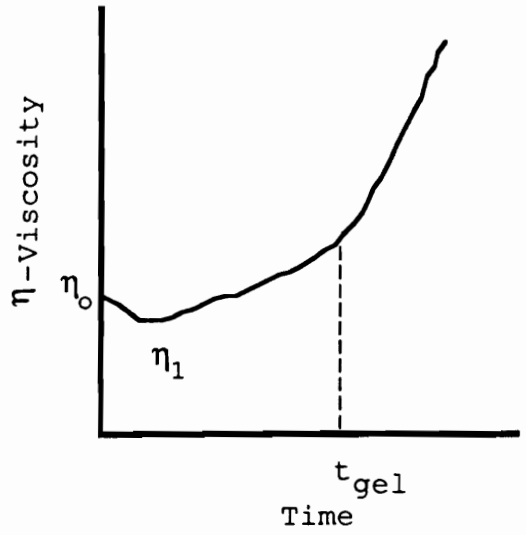

Preceding gelation the system is soluble and fusible, while after the gel point there exist both a soluble (sol fraction) and an insoluble (gel fraction) material. Gelation does not stop the crosslinking process. Further crosslinking leads to polymers with considerable increases in T_g and ultimate physical properties that are rigid, insoluble and infusible. Differential scanning calorimetry can be utilized to measure the extent of crosslinking and the rate of conversion, while torsional braid analysis (TBA) and dynamic mechanical analysis (DMA) and in some cases thermal mechanical analysis are used to determine gelation.

The T_g of a thermoset increases as a function of conversion due to advancement in molecular weight in the pregel stage and in the number of crosslinks in the postgel stage (125). However, at a given cure temperature, the T_g of the network may become coincidental with the cure temperature. This phenomenon is known as vitrication (i.e., glassy or solid state). Under this condition curing is essentially terminated since in the glassy state there is not sufficient chain mobility for reactive groups to collide together. Vitrication also does not necessarily indicate that the network is completely crosslinked (126). Subsequent crosslinking may be continued by heating the network above the current T_g, allowing sufficient chain mobility for reactive groups to come together.

Manufacturing products out of thermoset resins requires crosslinking in place. For example, in compression molding; resin transfer molding (RTM) (134) applications or "staging" techniques where the resin is reacted to some degree of conversion and then processed, since a fully cured thermoset is not capable of flowing and therefore cannot be processed into an object. Thermosets have been in practice classified as A-, B- and C-stage polymers depending on their extent of reaction compared to the extent of reaction at gelation (84). The A-stage refers to either the unreacted or slightly polymerized monomer, the B-stage to systems close to the gel

point and the C-stage to "fully" cured networks. The properties of networks are depended on their structure and therefore on methodology in preparing them (127). In processing and developing the ultimate properties of thermosets it is important to know the extent of conversion and the history of how the network was reached if useful materials are going to efficiently be prepared. Figure 6 (A) illustrates how a typical cure schedule can be generated from a plot of some mechanical property change vs curing time at a given temperature and pressure (133). Practical properties are often achieved at some partial degree of cure, since the time to achieve full cure may not gain any appreciable advantage in mechanical properties. An optimized combination of properties can also be determine in a similar manner as depicted in Figure 6 (B) (133).

Phase diagrams have been especially useful in understanding the curing process. Three basic types of phase diagrams have been developed for thermosets: a) Time-Temperature-Transformation Cure (TTT) Diagram (126,128,129) and Conversion-Temperature-Transformation (CHT) Diagram (135-137), b) Conversion-Temperature-Transformation (CTT) Diagram (135-137) and c) T_g-Temperature Property (T_g-TP) Diagram (137). In all four of these diagrams temperature is represented on the ordinate, while the abscissa is used for the extent of cure.

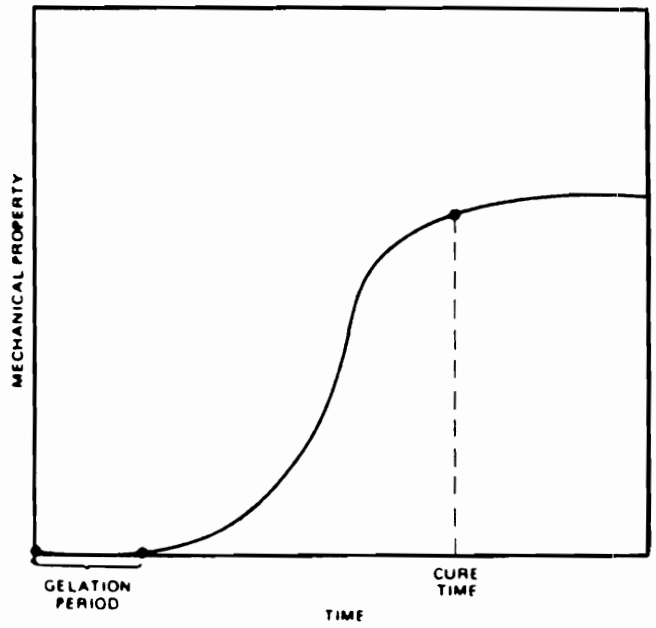

(A) Mechanical Property of a Thermoset vs Cure Time

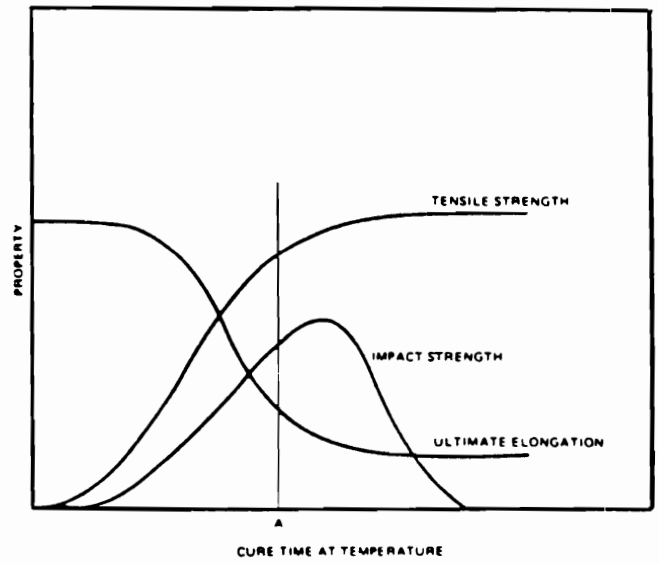

(B) Optimization of Cure Schedule for a Thermoset

Figure 6
Cure Schedule Optimizations (133)

Time-temperature-Transformation (TTT) diagrams originally developed for formulating metal alloys have been applied by Gillham et al. (126,128,129) for thermosetting systems. The TTT diagram outlines in a convenient fashion the temperature of cure vs the times to gelation, vitrification, full cure and thermal degradation. Figure 7 displays a TTT isothermal cure diagram for a generic thermosetting system (130). The diagram shows the specific states of matter possible during curing, i.e., liquid (with successive isoviscous contours differing by a factor of ten), sol/gel rubber, elastomer, gelled glass, ungelled glass and char. The three possible critical temperatures shown are: T_{go}, the glass transition temperature of the reactants, $_{gel}T_g$, the glass transition temperature at which gelation and vitrification occur concurrently and $T_{g\infty}$, the maximum glass transition temperature of the fully cured system. The full-cure line represents when $T_g = T_{g\infty}$ and splits the gelled glass region into two sections, a sol/gel glass and gel glass that is fully cured. The A-, B- and C-stage notation corresponds to the ungelled glass, sol/gel glass (i.e., the gelled glass region between the full-cure line and the gelation line) the and gel glass, respectively. The vitrification curve shown is S-shaped, which is also characteristic for linear step and chain-growth polymerizations (128,135).

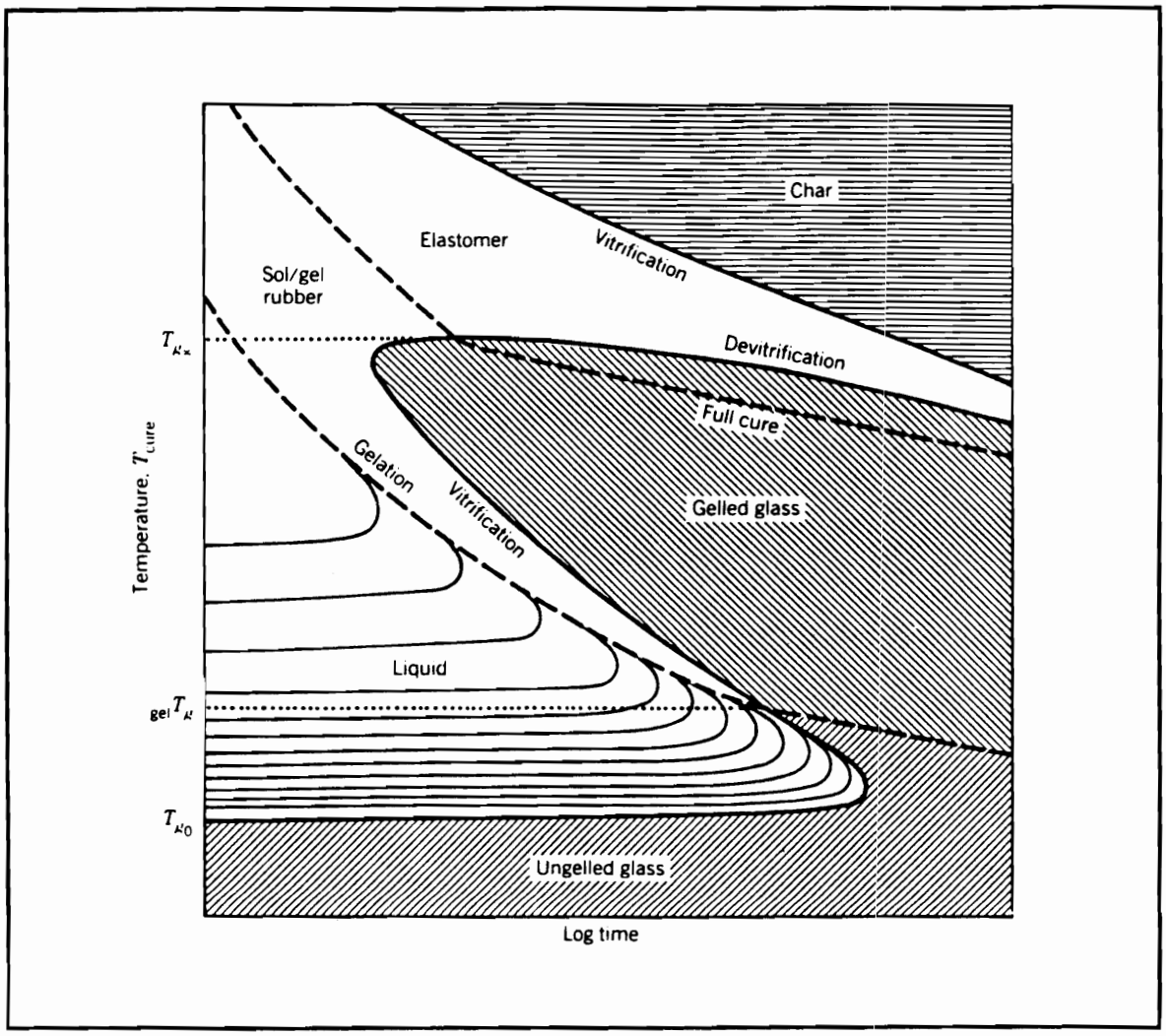

Figure 7

Time-Temperature-Transformation (TTT) Isothermal Cure Diagram for a Thermosetting System (130)

TTT diagrams offer a practical way of establishing cure schedules in manufacturing processes. Evaluation of the full cure is important in determining the ultimate structure-property relationships, since only then can different cure schedule be compared. If the curing history of the network is not well-defined, then its properties cannot be compared in a meaningful way with those cured by a different schedule (129). Curing above the maximum T_g of the material is the most straightforward procedure in obtaining $T_{g\infty}$. In high heat-resistant systems, where heating above the maximum glass transition temperature can lead to degradation, the full-cure line in Figure 7 offers an alternative pathway in achieving a completely cured system without thermal degradation. In a similar manner, the TTT diagram is helpful in showing if a specific cure schedule is leading to materials where the T_g of the gel is coincidental with the cure temperature, i.e., gelation has occurred below the vitrification line, which implies the system needs to be either cured longer or at a higher temperature to fall above the full-cure line inside the gelled glass region. Knowledge of the minimum time and the corresponding temperature for full-cure is industrially important for efficient processing (130).

An extension of the TTT diagram is the Continuous-Heating-Transformation diagram which describes dynamic cure paths at series of different rates as indicated in Figure 8

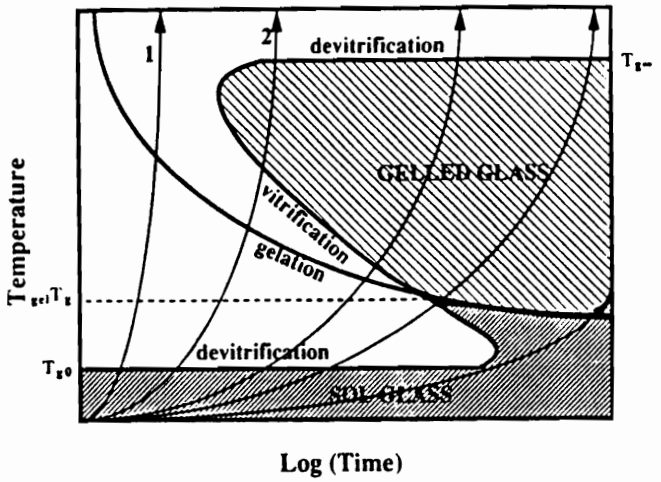

(A) Continuous-Heating-Transformation Diagram

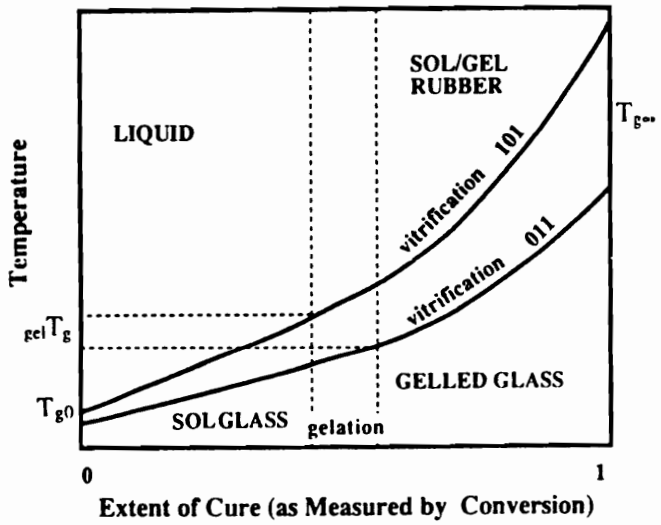

(B) Conversion-Temperature-Transformation Diagram

Figure 8

Cure Diagrams for Thermosetting Systems (137)

(A) where rate 1 > rate 2 (curves with arrows)(138). CHT diagrams are useful in molding technology to obtain full cures without going through vitrification (135). Both the TTT and CHT diagrams allow cure paths to be consider with respect to the kinetically controlled reaction region, (i.e., the liquid and sol/gel rubber regions) and the diffusion controlled reaction region (i.e., the sol glass and sol/gel glass region). In this manner, run away reactions can be avoid by choosing the proper slow rate of heating. This is done in such a way that the reaction rate is controlled by the T_g increasing coincidentally with the cure temperature until the full cure is reached or in a similar fashion by choosing an isothermal cure temperature that is not too high.

Conversion-Temperature-Transformation diagrams are helpful in examining the influence of functionality of the reactants with respect to gelation, vitrification and steric hindrance of the reactants and products (135-137). Figure 8 (B) (137) illustrates the different phases appearing in a CTT diagram, in a similar manner to the TTT diagram, except in this case the extent of cure is given by the partial degree of conversion instead of log-time. The two vitrification curves shown are for reactants with different functionalities where 101 > 011. These curves conveniently show the extent of cure at gelation.

A new cure diagram, the T_g-Temperature Property diagram (T_g-TP) introduce by Gillham el al. can be used to examine the physical properties of both the fully and partially cured thermoset (Figure 9) (137). This diagram is also somewhat analogous to the TTT diagram except that the extent of cure is given in terms of the glass transition temperature which results in linearization of the T_g-TP diagram. The physical properties of the system can be isolated into distinct regions by the different transition lines, i.e., gelation ($_{gel}T_g$), glass transition, end of the glass transition ($_eT_g$) and the β-transition ($T\beta$). Significantly, shown are the glass and β-transition temperatures increasing with increasing extent of cure. The T_g-TP diagram can be used to show the differences in physical properties (like modulus and density) before and after gelation in the different regions with the extent of cure.

5. **Spectroscopic Characterization of Aromatic Bismaleimides** Fourier transform infrared and nuclear magnetic resonance spectroscopy offer a convenient method in deducing the structure of bismaleimides and intermediate compounds. These spectroscopic techniques are also useful in characterizing the crosslinking of the maleimide carbon-carbon double bond (139-141). Fry and Lind recently investigated the curing of bismaleimides by solid-state ^{13}C-NMR which was able to detect quantitative differences in

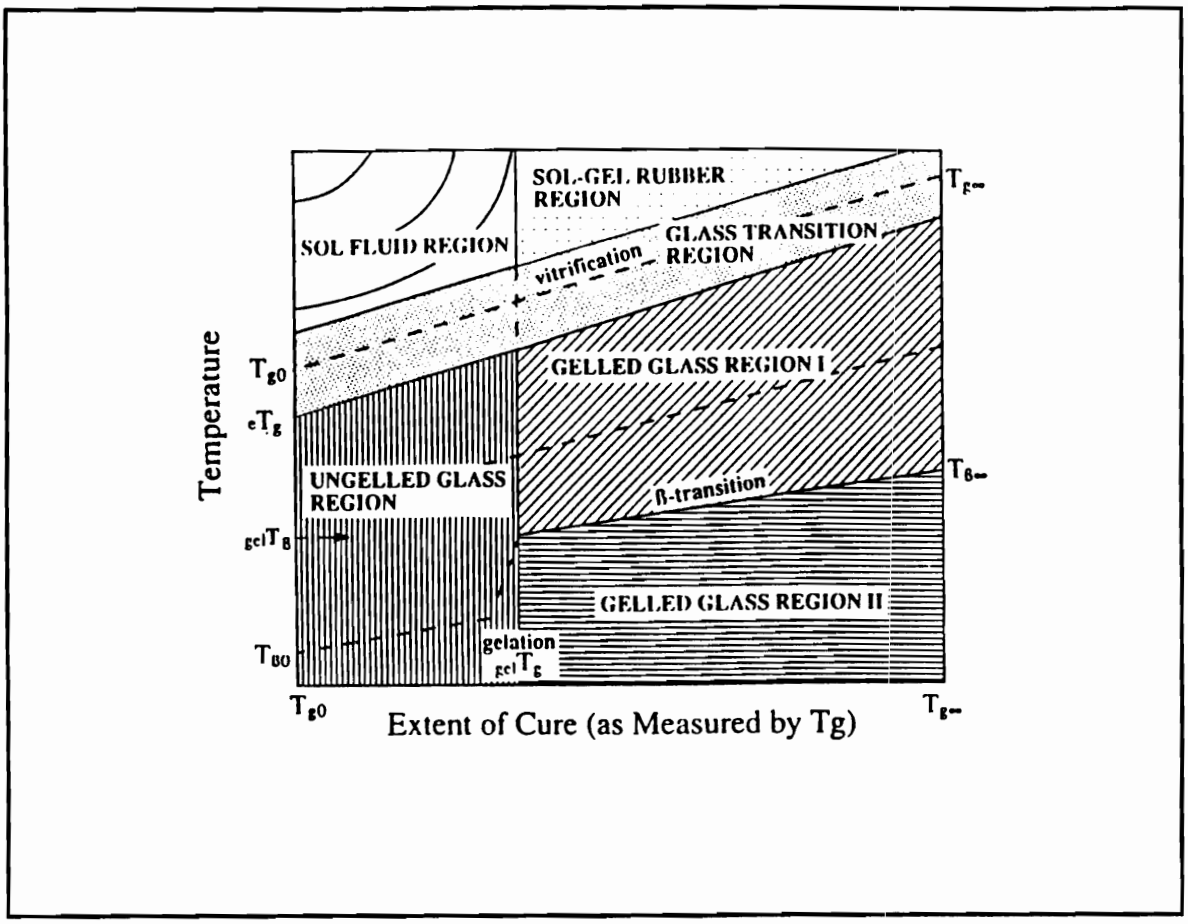

Figure 9

T_g-Temperature-Property Diagram

for Thermosetting Systems (137)

chemical structure brought about by different cure schedules (141). Solid-state ^{13}C-NMR is especially suited for the analysis of bismaleimide composites. Electron spin resonance (ESR) spectroscopy has been utilize to characterize the free radical structure of N-substituted maleimide formed by γ-irradiation and subsequent polymerization via the ethylenic double bonds (142,143). While, Brown and Sandreczki have reported the thermally induced radical initiation of bismaleimides probably by hydrogen atom abstraction reactions as determined by ESR (87).

Table 3 list reported assignments for IR absorption bands and Table 4 the ^{1}H-NMR; ^{13}C-NMR chemical shifts for bismaleimides and intermediate compounds. While, Figure 10 shows the IR spectra of N-phenylmaleamic acid and the corresponding imide, N-phenylmaleimide (145).

6. Applications of Bismaleimides High performance-heat resistant polymers are used for a variety of applications including matrices for advanced composites, adhesives, coatings, films and electronic applications. Crosslinking has been an useful technique in achieving these advanced materials. It is a major requirement to prepare materials that do not contain voids, since this can have a catastrophic effect on the mechanical properties. Consequently, a lot of emphasis has been devoted to reactive end-capped monomers and oligomers that do not emit volatiles

Table 3

IR Absorption Frequencies for Bismaleimides and Intermediates

Group	Wavelength (cm^{-1})	Ref.
$Ar-NH_2$ aromatic amines	3500-3400 s (doublet, stretch)	144
-(C=O)- maleamic acid	1715 (stretch)	145,148
ν(C=O) maleimide	1770 w (in phase)	139;146
ν(C=O) maleimide	1705 vs (out of phase)	139;146
ν(C=O) succinimide	1773 m (in phase)	139;146
ν(C=O) succinimide	1700 vs (out of phase)	139;146
ν(C=O) maleic anhydride	1850;1175 (doublet)	147
C=O maleimide	643 m (in plane bending)	146
C=O succinimide	636 m (in plane bending)	146
C=O maleimide	550 w (out of plane deformation)	146
C=O maleimide	556 w (out of plane deformation)	146
ν(=C-H) maleimide	3109-3099 m	139
ν(C-N-C) maleimide	1149 vs	139
ν(C-N-C) succinimide	1188 vs	139

Table 4

^{1}H-, ^{13}C-NMR Spectral Data for Bismaleimides and Intermediates

Group	^{1}H (ppm)	^{13}C (ppm)	Ref.
$Ar-NH_2$ aromatic amines	5.0-3.0	-	144
-(C=O)-OH maleamic acid	13.9	206	148
C=O maleimide	-	169	141
C=O crosslinked maleimide	-	175	141
C=O succinimide	-	183.6	147
C=O maleic anhydride	-	164.3	147
=C-H maleimide	7.0	 134	148 147
-C-H succinimide	2.73	30.3	147
=C-H maleic anhydride	7.1	136.6	147
H-C=C-H cis-maleamic acid	6.30,6.55	-	148

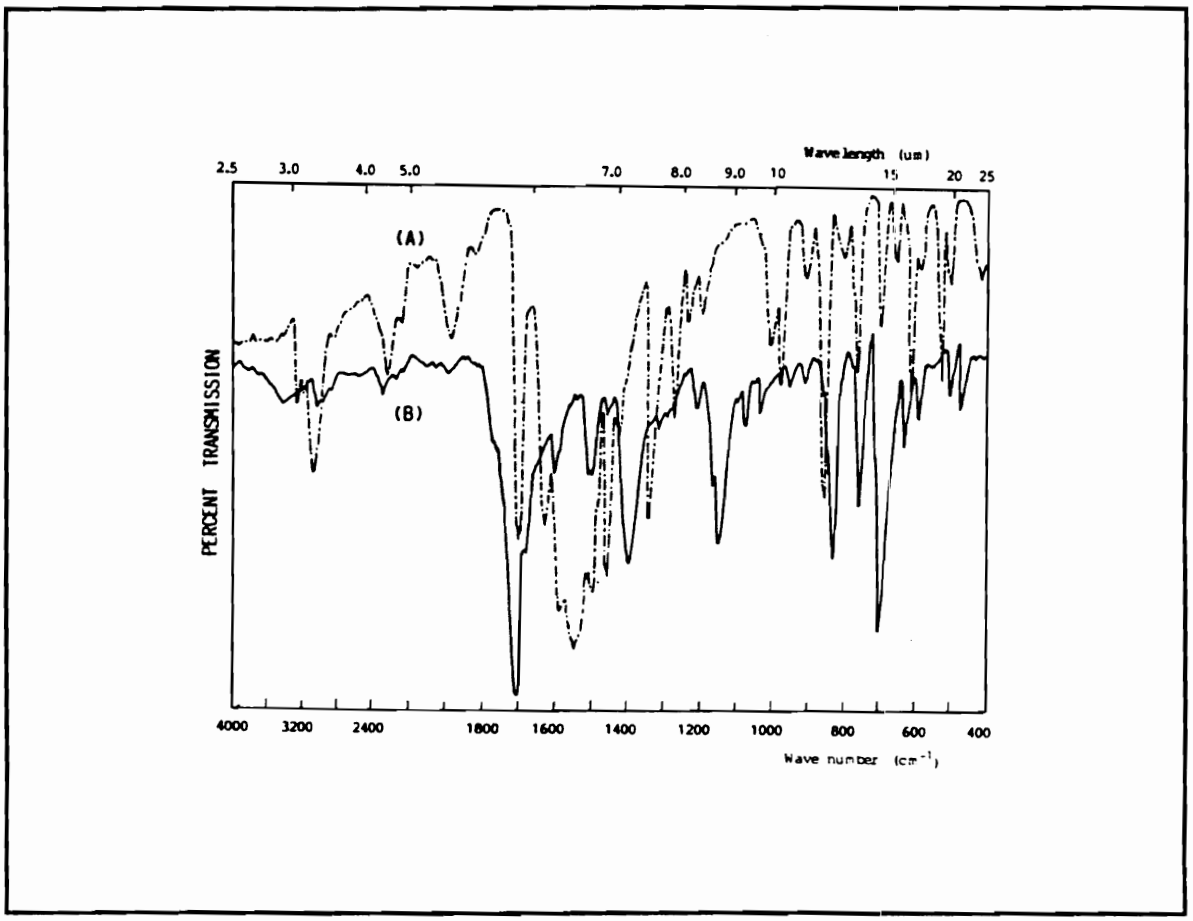

Figure 10

Infared Spectra of (A) N-Phenylmaleamic Acid and

(B) N-Phenylmaleimide (145)

via maleimides and acetylenes.

These thermoset resins have found their largest market so far in military aircraft, both in primary and secondary structural components in addition to engine parts (149). For example, the Advanced Tactical Fighter (ATF) (Northrop/McDonnell Douglas YF-23) expected to begin production in 1996 and be operational by 1999 is estimated to be composed of 45-50% composite (150). Each ATF will contain approximately 8,000-10,000 pounds of composites, which equates to about 3,000 pounds of matrix resin (151). By comparison, the 1970's vintage F-15 aircraft fighter contains only 2.2% composites, while the F-18 has just 9.9% composites. A great deal of the high heat-resistance demands of advanced military aircraft is due to aircraft engines becoming more and more integrated deeper into the airframe (150). Northrop/McDonnell Douglas plan to use bismaleimides resins in many area on the YF-23, for instance, the current prototypes have composite sections in the aft fuselage around the engine bays; skin panels on the aft fuselage have been demonstrated to be 20% lighter vs aluminium structures. This section of bismaleimide/graphite skin panel is one single piece that eliminates 8,000 individual fasteners, thus representing lower production cost.

Grumman has successfully employed bismaleimides in a wide variety of advanced aerospace structures since the early

1970's, for instance, as a composite matrix for the nacelle anti-ice plenum on the DC-8 jet engines; radomes, fuselage structures for Fighter/Attack aircraft and is currently evaluating their use in the airframe of the army's Bell/Grumman helicopters (152). Almost every large aerospace company is currently evaluating bismaleimides and/or planning to use them in future productions. For example: General Dynamics uses bismaleimides in the F-16XL fighter cranked-arrow wing skins, ribs, flaps and for firewalls in helicopters (114,115,153); Rockwell/Brunswick in the B-1 bomber radomes (152); British Aerospace for radomes for the Concorde and Tornado (134). A recent feature article in SAMPE Journal on the stealth F-117A fighter and B-2 bomber reports that polyimides and bismaleimides are among the best dielectric transparency polymers, however, the article does not provide the specific classified materials used in these aircraft (154).

However, eventually the largest user of these materials will be the commercial aircraft industry because of the weight/fuel efficiency and increased payload over their aluminum counterparts (155). Twenty-five thousand gallons of fuel per plane per year is saved with just 10% saving in weight (149). However, current incorporation of composites on U.S. commercial aircraft is just 3% (156). For example, the structural weight of the Boeing 767 and 757 is about 3%

composite, however, this translates into approximately 30% of these aircraft's surface area (157). While the European Aerobus commercial aircraft is currently composed of 16% composites (156). Boeing's newest commercial aircraft the 777, expected to be in service in 1995 will be composed of 10-12% composite (157). Boeing is also planning to build a 1000 High Speed Commercial Transport aircraft that will have a structural weight of approximately 40-50% composite compared to the all aluminum European SST (156). At an estimated value of $200/kg for prepregs, this represents over five million dollars for just one plane. This aircraft will have a maximum air speed of 2.4 Mach generating an upper wing surface temperature of 188°C. These requirement represent demanding challenges for composite matrix resins and adhesives.

In 1970 America held 91% of the world's aerospace market while in 1987 it was down to 65%. Currently, advanced composites are becoming an integral part of emerging technologies for the American aerospace industry to retain its competitive edge (156). Bismaleimides are one of the major composite resins that will play a leading role in military and commercial aircraft because of their relatively ease of processability, high mechanical properties, environmental stability, long storage shelf life, acceptable cost and versatile methods of fabrication.

B. Synthetic Compendium

1. Overview Heat-resistant bismaleimides are prepared from aromatic diamines and maleic anhydride as outlined in Scheme 2. This two step process can be performed *in situ* without the need to isolate the bismaleamic acid intermediate, with imidization either by thermal or chemical cyclodehydration. The properties and performance of the bismaleimide network are primarily dependent on the diamine structure used in this synthesis. The effect of modifying the maleimide backbone, i.e., incorporation of specific chemical groups or structural variations, are discussed in sections II.A. and II.C. The methods used to prepare aromatic diamines and subsequent cyclodehydration of the corresponding bismaleamic acid are discussed in this section. Aromatic diamines and amine-terminated arylene ether ketone oligomers are conveniently prepared by aromatic nucleophilic substitution reactions which was the principal method used to synthesize these materials via activated aryl halides, for this dissertation.

2. Preparation of Aromatic Diamines Aromatic diamines are used in the preparation of many polymers like polyurethanes, polyureas, polyamides, azo polymers, polyimines, polyamidines, polyimides, polyasparimides and bismaleimides. A large variety of methods exist for the synthesis of aromatic amines (158). Industrially, the

diamines are typically prepared by the reduction of aromatic nitro compounds, which are easily made by nitration techniques (159-162). Some of the conventional methods that have been used to prepare aromatic diamines monomers are by Friedel-Crafts reaction, condensation reactions and aromatic nucleophilic substitution reactions. These procedures are briefly outlined below.

Friedel-Crafts acylation does not occur on rings substituted with strong electron-withdrawing groups like the nitro. However, a novel approach has been to use nitro substituted benzoyl chloride to prepare bis(nitrobenzoyl)arylene ethers which are then reduced to the diamine, as shown below (163).

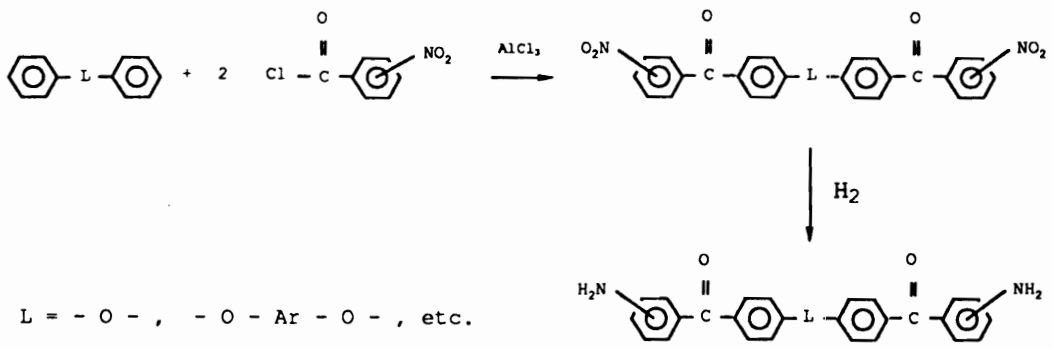

The dinitro monomers can be prepared in high yields by reacting a 2-, 3-, or 4-nitrobenzoyl halide with a diphenyl ether compound in the presence of aluminum chloride or other Lewis acids. Reduction of nitro compounds by hydrogenation is generally the preferred method of amine formation since

the dinitro compounds are quantitatively converted to the diamine.

Methylenedianiline (MDA) can be prepared by the condensation of aniline and formaldehyde under acidic conditions using excess aniline (164). The reaction is somewhat complex, going through several intermediates before the carbocation alkylates aniline to yield MDA as simplified below (165).

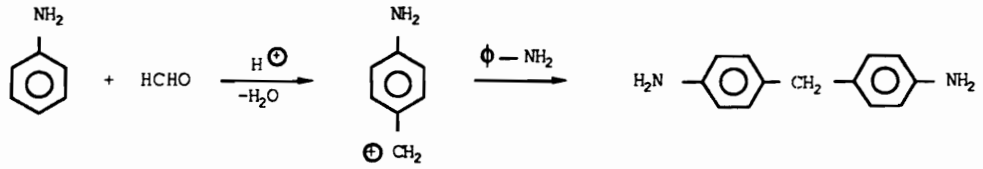

A versatile method that has been applied to prepare a large variety of aryl diamine monomers derived from bishalides, bisphenols and bisnitro compounds is by the aromatic nucleophilic substitution reaction as outlined:

a) Bisphenolates and 4-halonitrobenzene can be reacted to prepare bis(nitrophenyl)arylene ethers with good yields, which are subsequently reduced to the diamine (166,167):

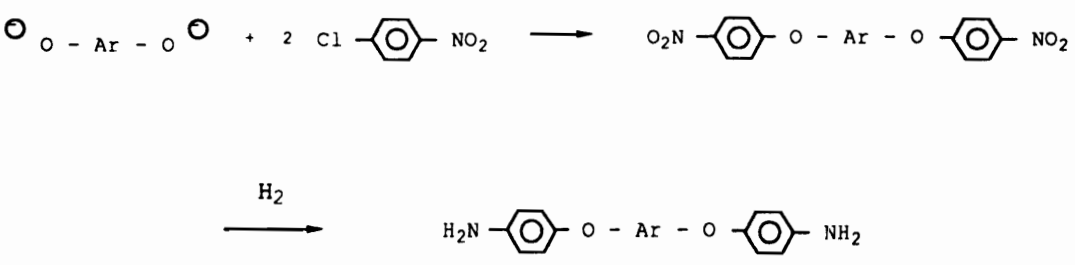

The reaction is done under oxygen free, anhydrous conditions using cuprous halide catalysts in non-acidic solvents. The reaction does not occur if halide substituted anilines are used in place of 4-halonitrobenzene, possibly due to catalyst deactivation by the amino group.

b) Bisphenolates and m-dinitrobenzene can be used to prepare diamines by the reduction of the corresponding bisnitro compounds via the nitro-displacement reaction (161,168):

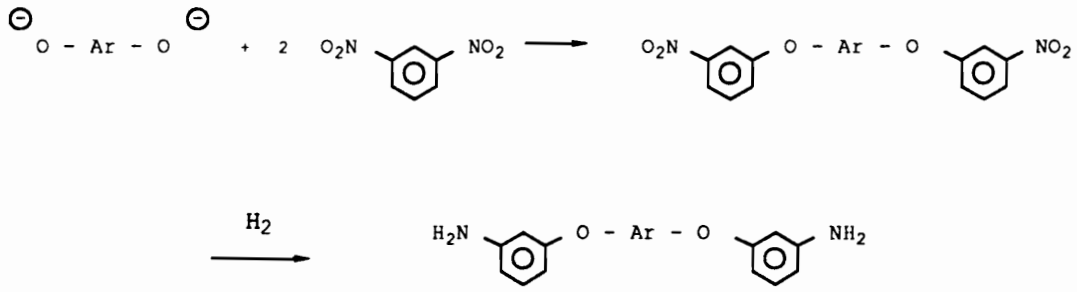

This method offer a convenient means to prepare aromatic ether bonds in high yields using bisphenolates under anhydrous conditions.

c) Aminophenols and activated bishalo compounds under nucleophilic conditions yield aryl ether ketone or sulfone diamines (31,51,169-176). This reaction proceeds rapidly and free of side reactions in anhydrous aprotic polar solvents at elevated temperatures (170). The diamine can also be prepared using p-nitrophenolate in place of aminophenolates, however this reaction is relatively slow (169,171).

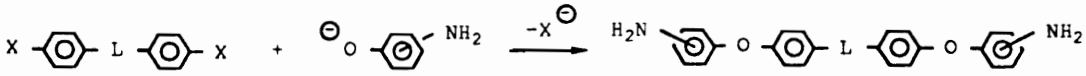

X = F, Cl L = - CO - , - SO_2 - , etc.

d) Aryl ether diamines have been prepared via Ullmann ether synthesis with aminophenols and aryl bishalides. Aromatic halides without activating substituents do not yield aryl ethers cleanly, however etherification is improved using the copper-catalyzed condensation of the aryl halide and phenolate (169).

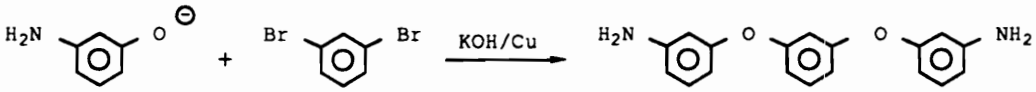

3. <u>Aromatic Nucleophilic Substitution Reactions</u> In nucleophilic substitution reactions a substrate is attacked by a nucleophile to form a new bond, while a leaving group departs with an electron pair. The nucleophile is a base possessing an unshared pair of electrons that forms the bond with a positive site on the substrate. Alkyl halides readily undergo nucleophilic reactions, whereas aromatic halides are comparatively unreactive toward nucleophilic reagents. In alkyl halides the carbon bonded to the halogen is sp^3-hybridized, while in the aryl halides this bond is shorter, stronger and more stable via sp^2-hybridization.

Aromatic nucleophilic substitution reactions are referred to as a S_NAr mechanism and may be thought of as an addition-elimination reaction (177). The mechanism consist of two steps, with the first step usually the rate-determining as show below:

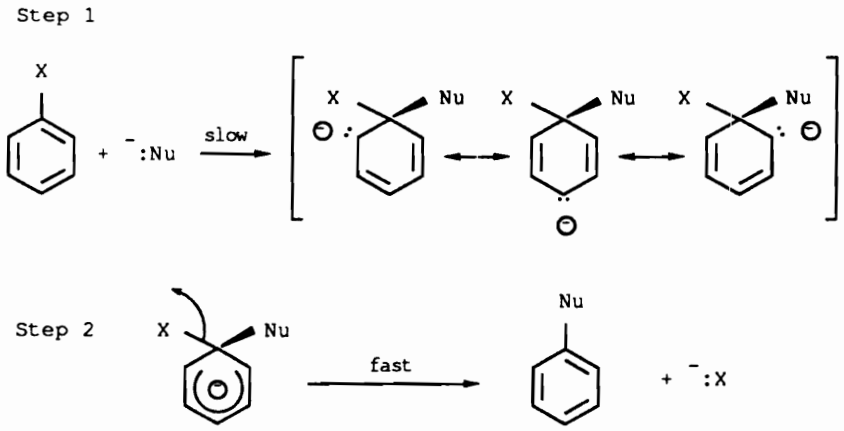

The attacking nucleophile ($^-$:Nu) forms a new bond with the carbon bonded to the eventual halide leaving group (X), giving an intermediate. In the second step, the leaving group is then displaced only after the nucleophile has established a permanent bond.

In simple aryl halides, S_NAr reactions require rather vigorous reaction conditions or else very strong nucleophiles to force the reaction to proceed, notwithstanding, these reaction are of major industrial importance (178). For example, chlorobenzene is converted into phenol by aqueous sodium hydroxide only under very harsh conditions at temperatures over 350°C. However, the reactivity of aryl

halides are greatly increased toward nucleophilic attack when certain groups are located para or ortho to the halide leaving group. For example, the nitro group has a powerful inductive as well as resonance effect favoring the S_NAr reaction (179). Resonance structures for the intermediate formed by reaction of p-nitrochlorobenzene and sodium hydroxide is shown below:

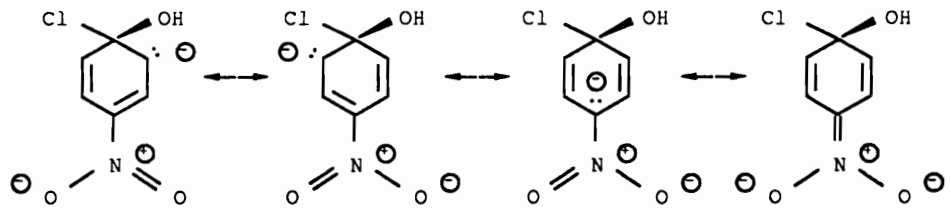

Intermediates of this nature are stable complexes, referred to as Meisenheimer salts. The negative charge is stabilized by the conjugated pentadienyl anion and by resonance delocalization by groups that can accommodate the charge. Electron-withdrawing groups like the nitro stabilize the system, in particular if they are para or ortho to the leaving group, since this is where the negative charge is the greatest. While, electron-donating substituents deactivate the system especially if they are found para or ortho to the departing group. An electron-withdrawing group meta to the leaving group has little effect on reactivity of an aryl halide, since it is not possible for the negative charge in the ring to delocalized into the meta substituent.

Many electron-withdrawing groups other than the nitro have been used to activate halogen elimination in S_NAr reactions like $-N(CH_3)_3^+$, -CN, -COOH, $-SO_3H$, -CHO, etc. (169,178). Most of the electron-withdrawing group used are for relatively low molecular weight molecules, while only a few have found utility in polymer chemistry. In particular the carbonyl (-CO-) and sulfone ($-SO_2-$) groups are chiefly used to prepare monomers and polymers (170,171,180). Here again, these group are effective in stabilizing the Meisenheimer intermediate by accepting the negative charge from the ring as indicated below (181-184):

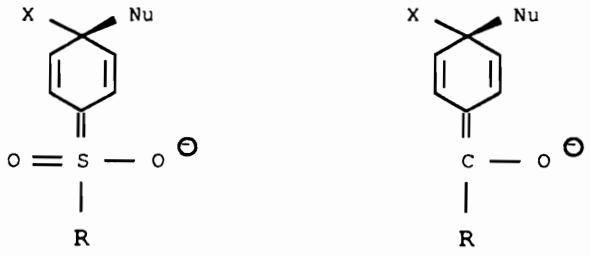

In general, fluoride is the best leaving group of the halogens, with the order of elimination usually: F > Cl > Br > I, with some exceptions (169,185-187). The halogen reactivities decrease in the order: para > ortho > meta-substitution relative to the activating group, with ortho-halogen substitution being less reactive due to steric hindrance (183). Fluorine, being the most electronegative of the halogens, causes the largest decrease in electron density

on carbon of the aryl carbon-fluorine bond ($C^{\delta+}-F^{\delta-}$). This results in a faster attack by a nucleophile on the electropositive carbon compared to the other halogens. Nucleophilic attack is least hindered when fluorine is the leaving group, since it has the smallest atomic volume of the halogens. Electron-withdrawing groups also activate leaving groups other than just halogens in S_NAr reactions. Many of the established leaving groups in aliphatic nucleophilic substitutions are also common departing groups in S_NAr reactions (177,178). An approximate order of displacement of commonly used leaving groups in comparison to halides is: F > NO_2 > OTs > SOPh > Cl,Br,I > N_3 > NR_3^+ > OAr,OR,SR,SO_2R,NH_2; with a strong dependent on the nucleophile used (169).

Leaving groups can be displaced by a variety of nucleophiles in S_NAr reactions. The relative reactivity of nucleophiles depends on the nature of the substrate, leaving group and reaction conditions. Nucleophilicity is in general a function of base strength, leading to a very approximate order of nucleophilicity in S_NAr reactions: NH_2^- > Ph_3C^- > $PhNH^-$ > ArS^- > RO^- > R_2NH > ArO^- > OH^- > $ArNH_2$ > NH_3 > I^- > Br^- > Cl^- > H_2O > ROH (169,177). The S_NAr reaction has resulted in an important commercial method for the preparation of polysulfones and polyetherketones via the formation of ether linkages, in addition to monomers like aromatic diamines containing carbonyl, sulfone and ether connecting group.

Typically, the nucleophilic phenolates are prepared from bisphenols or phenol derivative like aminophenols using a stoichiometric amount of aqueous sodium hydroxide in aprotic solvents, followed by the removal of water by azeotropic distillation using chlorobenzene. Water removal is critical to prevent hydrolysis of the activated halide. Excess of sodium hydroxide should be avoided to prevent hydrolysis of the activated halide (170) or cleavage of the ether linkage (183). An alternate method that is unaffected by excess base, uses anhydrous potassium carbonate as the base to form the phenolate which is soluble in an aprotic solvent/toluene azeotrope (189). Potassium carbonate is a weak base that reacts with phenols only at elevated temperatures (>140°C) without the hydrolysis of the halide. Sodium or potassium are the only useful counterions for phenolates in polar aprotic solvents since the lithium, calcium and magnesium phenolates are insoluble (170,190). The reactivity of the phenolate is also influenced by ring substitution, with the more basic phenolate being more reactive. In this case electron-donating groups increase the basicity of the phenolate, while withdrawing groups delocalize the negative charge on the phenolate oxygen, reducing nucleophilicity (191).

S_NAr reactions in general require aprotic solvents such as dimethylsulfoxide, dimethylacetamide, dimethylformamide,

N-methylpyrrolidinone, etc., for smooth, high yield reactions to occur (170,178,189,192,193). Figure 11 shows the structure of some of the more commonly used aprotic solvents for S_NAr reactions. These are polar solvents of moderately high dielectric constants that do not contain acidic hydrogens. Polar aprotic solvents are important in S_NAr reactions because they are excellent in solvating cations but very poor at solvating anions as shown for dimethyl-sulfoxide:

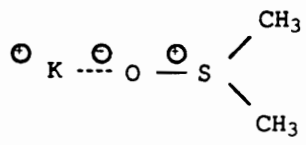

Strong Attraction

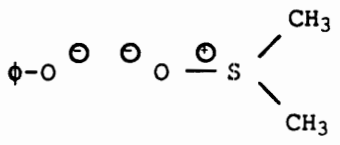

Strong Repulsion

The dipole moment for the aprotic solvent is larger compared to protic solvents with the negative end of the dipolar well exposed to solvate the cation. Since the positive end of the dipole is well-shielded, aprotic solvents poorly solvate the anion, with the net effect of concentrating the nucleophilic anion (179). This results in the nucleophile not having to fight its way out of a crowd of solvent molecules compared to protic solvents, allowing the aromatic nucleophilic substitution to proceed faster (179).

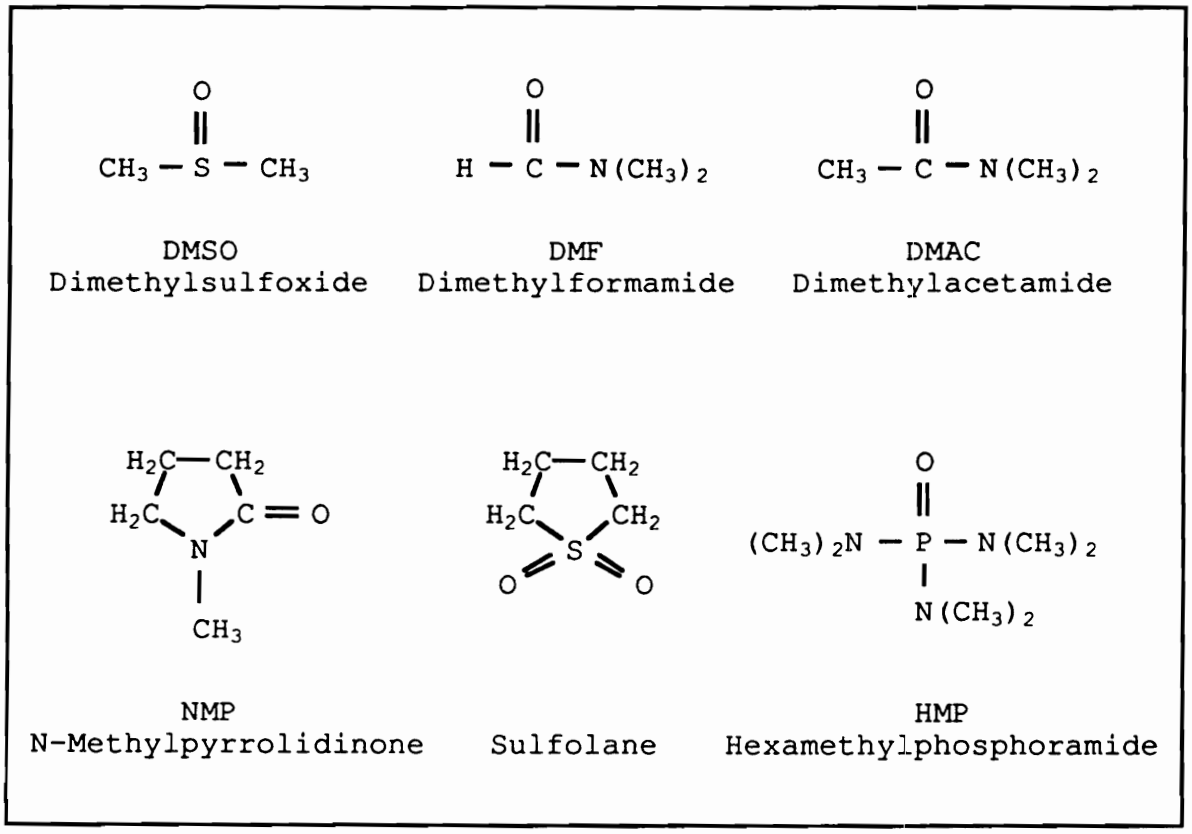

Figure 11

Polar Aprotic Solvents

Anions are best solvated by solvents having polar hydrogen bonds, which is lacking in aprotic solvents.

4. Imidization of Amic Acids The synthesis of maleimides were first reported for the reaction of aliphatic primary amines with maleic anhydride without providing much detail to the characterization of the materials (194-197). While the synthesis of the more important N-aryl maleimides was described by Searle using acetic anhydride and sodium acetate for imidization (30). This classical method is now a standard procedure for the synthesis of bismaleimides, which proceeds by a two-step condensation as outlined in Scheme 2. In the first step, an intermediate maleamic acid is prepared at ambient temperature, while imidization can be achieved either by thermal or chemical cyclodehydration. As outlined in Scheme 7, amic acid is form by a nucleophilic acyl substitution reaction of an aryl amine (or a primary aliphatic amine) with maleic anhydride. One of the carbonyl carbon is attacked by the amine (or diamine in the case of bismaleimides) nucleophile with the formation of a tetrahedral intermediate followed by ring opening. The amic acid is then produced by nitrogen deprotonation to the carboxylate anion.

Scheme 7 also illustrates the pathway to maleimides by thermal cyclodehydration of amic acid via condensation of water. In general, this is not a satisfactory method because

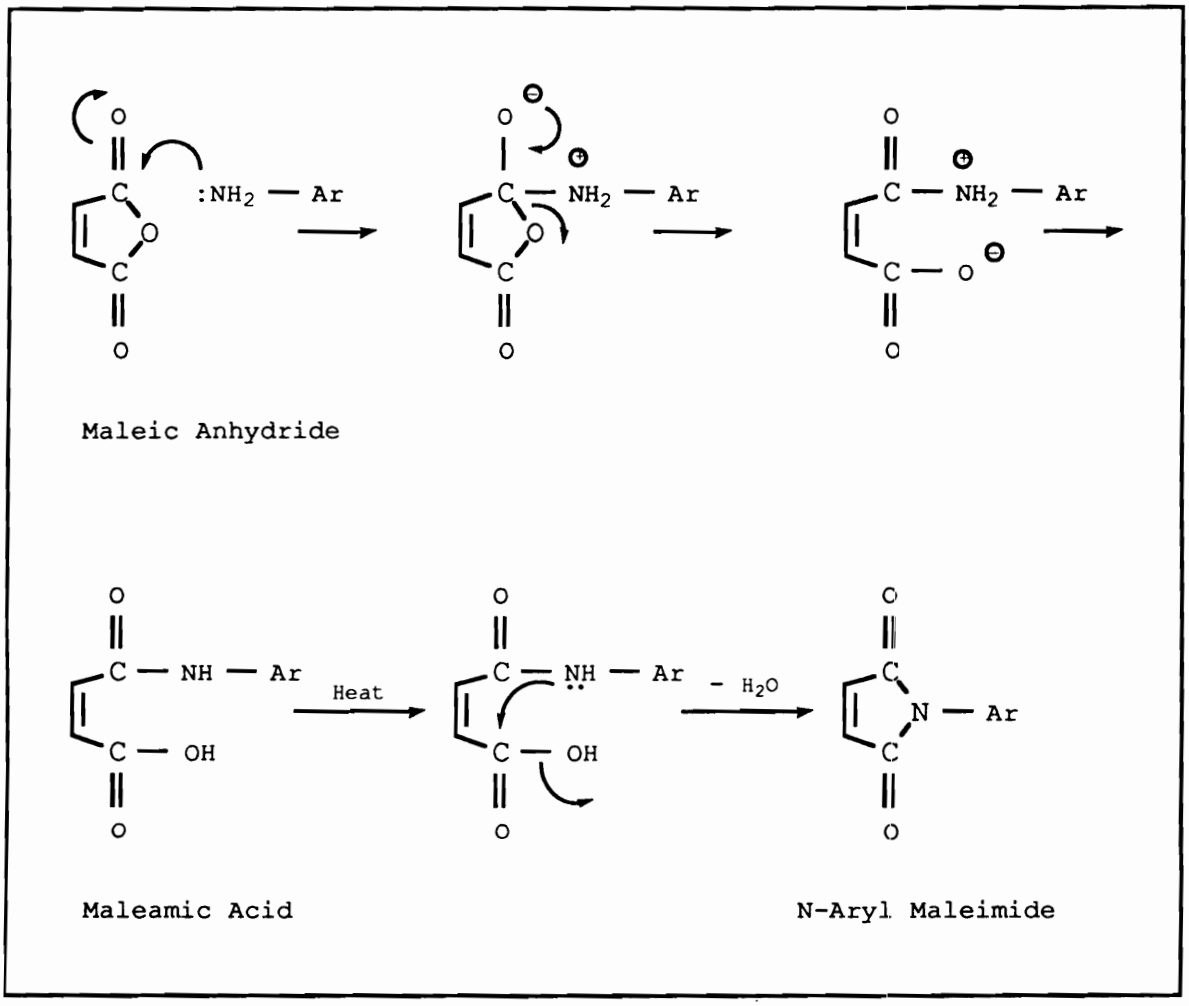

Scheme 7

Thermal Imidization of Maleamic Acid

of low yields of maleimides and polymerization of the carbon-carbon double bonds at the high temperatures required for imidization (30,198,199). Chemical assisted imidization of amic acids, as shown in Scheme 8, by sodium acetate and acetic anhydride offers a milder reaction with good yields. Sodium acetate is used to abstract the carboxylic proton for subsequent formation of maleamide anhydride via acetic anhydride. Indeed, the maleamide anhydride will not form without the presence of the acetate (200). Dehydration forms the thermodynamically stable five-membered imide ring. The dehydration also depends on the basicity of the leaving group, with $^{-}$OAc being a weaker base compared to $^{-}$OH, such that chemical imidization provides a lower energy pathway for ring closure vs thermal imidization. Acetic anhydride also acts as an efficient water scavenger for preventing amic acid hydrolysis.

In the older literature, many other amic acid cyclodehydration techniques exist for example, the use of reagents such as: phosphorus pentaoxide (201), acetyl chloride (201), thionyl chloride (202), boiling in acetic acid (203,204), azeotropic removal of water using p-cymene (205) and heating in the presence of triethylamine (206). More recently, as evident by the number of citations on bismaleimide preparations, many variations of older imidization techniques as well as novel ones are being

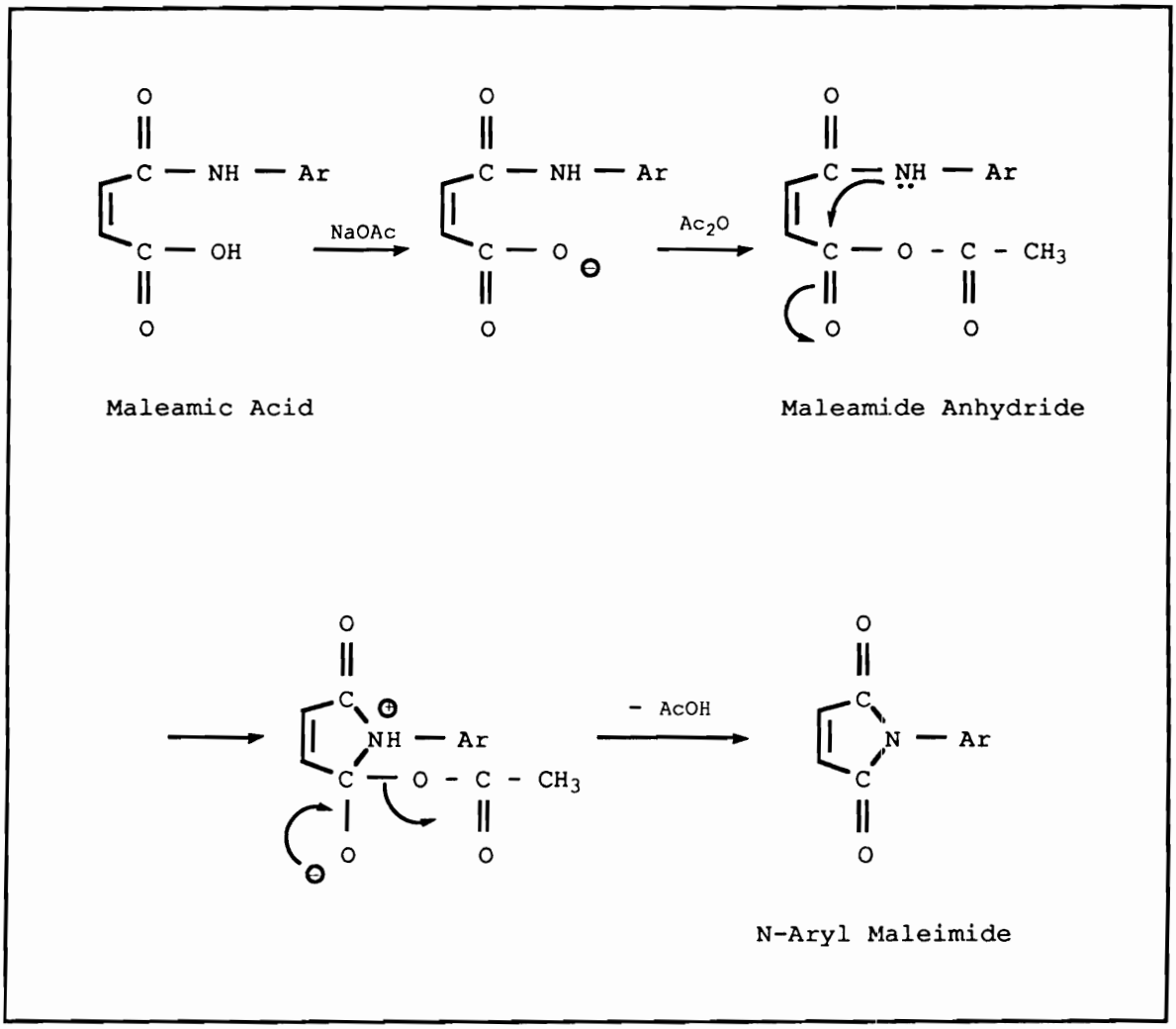

Scheme 8

Chemical Imidization of Maleamic Acid

utilized. For example, Butler et al. report yields of 99% bismaleimide using triethylamine to first convert maleamic acids to the amine and then cyclodehydrating using acetic anhydride and $Ni(OAc)_2 \cdot H_2O$ (207). Another variation of the sodium acetate/acetic anhydride technique is to add salts like KCl, KBr, KNO_3, $MgCl_2$, $Fe_2(SO_4)_3$, etc. to imidize amic acids with >80% yields (208). Alkali metal carbonates have also been added to the standard sodium acetate/acetic anhydride method to also produce yields >80% (209). A Japanese patent describes >90% bismaleimide yields in the presence of phosphoric acid using an o-xylene azeotrope distillation (210).

Isoimides under certain reaction conditions have been reported for the cyclodehydration of amic acids either as side reactions in imidizations or as desired products as shown below for the generalized N-arylmaleimides. For example, ethyl chloroformate-triethylamine (211), perchloric acid (212), thionyl chloride (213) and trifluoroacetic anhydrides (211,214,215) catalyzed imidizations have been described to yield isoimides. These methods are said to give rise to both maleimide and isoimide, the relative amounts being dependent on reaction conditions. The acetic anhydride-sodium acetate method has also been found yield isoimides at low temperatures (216) or when the reaction is run without sodium acetate (215), generally with very low

yields. Much of the literature dealing with isoimides is rather dated and not thoroughly characterized, with different papers reporting different products via the same reagents; therefore they should be consider with caution (1). In any event, relative high yields of maleimides are obtained from the corresponding maleamic acids with the $Ac_2O/NaOAc$ procedure, because any isoimides formed very readily rearrange to the maleimide, especially in the temperature range normally used with this technique (1).

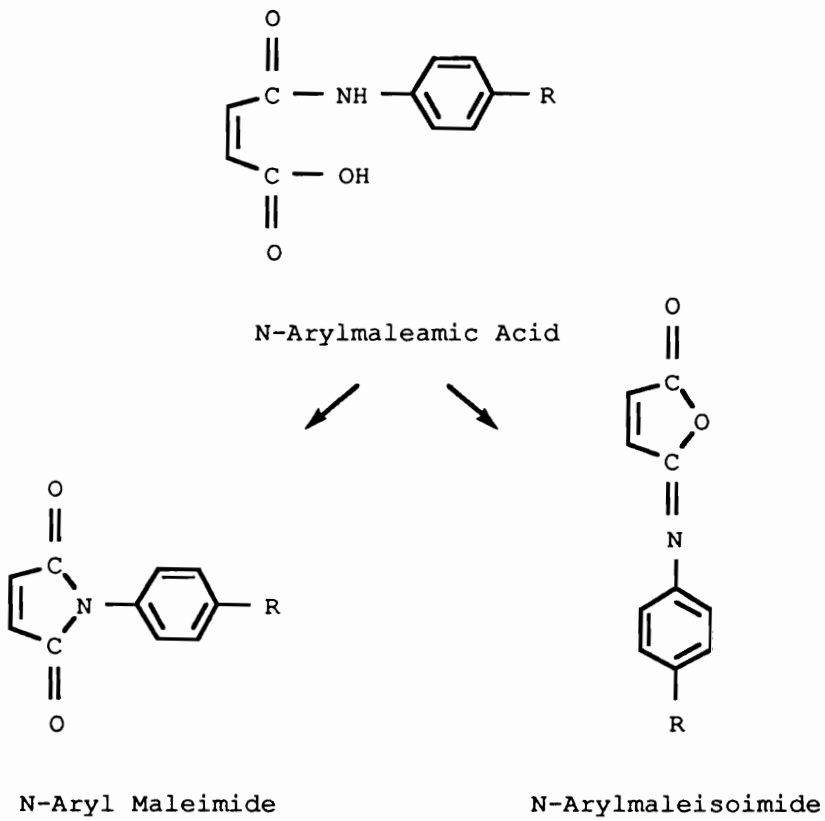

C. Requirements for Heat-Resistant Organic Polymers

1. Background The search for high temperature polymers has been an inquisitive endeavor for the past thirty years. The main momentum for the development of heat-resistant polymers has come from the aerospace industry (217). One of the first and most common class of heat-resistant polymers is the polyimide which was originally reported by Bogert and Renshaw in 1908 (218). Early activities in high temperature polymers was accelerated by the discovery that heterocyclic and aromatic amide polymers exhibited the ability to withstand extreme temperatures (219). For instance, E. I. du Pont de Nemours & Company commercialized the aromatic polyamide fiber Nomex® and polyimide film Kapton® (220,221). In the 1950's research was launched to meet the demand for functional and structural heat-resistant polymers for advanced aircraft, weapon systems and for the electronic industry (222). Early studies on high heat-resistant polymers focused primarily on the synthesis of new types of thermo-oxidatively stable polymers and paid little attention to cost, processability, performance or to actual application temperature. However, it is now recognized that a successful system must exhibit a favorable combination of price, processability and performance (223).

Progress in heat-resistant polymers has been dominated by the counterbalancing constraints of thermal stability versus processability. The difficulty is that most polymers bearing good thermo-oxidative stability are associated with increases in strength, modulus, rigidity and softening point. Unfortunately, this in general lowers the solubility, tractibility, moldability and overall processability (224). Frequently, a tradeoff is required at the sacrifice of thermal stability in order to produce a material that is useable. As a consequence, effort has been centered on improved synthetic schemes of existing heat-resistant polymers or on structural modifications for enhanced processing without the coexistent loss of thermal stability. Subsequently, relatively few of the many reported high temperature polymers have actually achieved commercial success.

However, many important commercial benefits resulted from this research having little or nothing to do with their high thermal properties (225). These advantages include: low density (a high strength-to-weight ratio), ease of processing (compared to ceramics and metals), availability of wide structural variations, range of properties and the ability to have properties tailored to a specific use by changes in chemical structures (226). For example, in aerospace applications, the reduced weight brought about by high

strength/weight ratios and high stiffness/weight leads to the potential for lower component cost (227). For each kg of weight saved on a Boeing 747 by replacing metal components with polymers is worth approximately $450, while this amount displaced on the space shuttle is valued at $30,000 over the lifetime of the vehicle (228).

Polymers possessing serviceability at high temperatures, in addition to high strength, rigidity, chemical and solvent resistance find a variety of uses not related to thermal stability. As shown in Table 5, these material properties can be applied to several extreme service environments (224). Some of the applications include: high-modulus fibers used in auto tire cords and "bullet proof vest" (aromatic polyamides, Kevlar)(116); thermal-protective clothing used as fabric for astronaut's clothing (polybenzimidazole)(229); osmotic membranes used for both gaseous and liquid separations (polyimides)(230); adhesives used for supersonic aircraft (polyphenylquinoxalines)(223,231); and a multitude of commercial exploits as listed in Table 6 (232,233).

Organic compounds typically melt below 250°C and as a rule degrade below 300°C. For polymers to be considered heat-resistant, stability must be defined in terms of time and temperature with regards to the thermal stress (226). Increases in the exposure temperature or time shortens the expected lifetime of the material. As a guideline, heat-

Table 5

Applications, Properties and Detrimental Factors (224)

Aerospace	Geothermal	Undersea
Properties Needed		
Strength to Weight Ratio Adhesion Modulus Abalation Thermal Stability	Hydrolytic and Thermoreductive Resistance Elasticity	Adhesion Impermeability Marine Growth Resistance Corrosion Prevention
Detrimental Forces		
Temperature Oxidation Stress Water	Temperature Hydrolysis Reduction H_2S Abrasion	Hydrolysis Time

Table 6

Applications For Heat-Resistant Polymers (232,233)

* Structural Resins (Adhesives, Composites, Foams and Moldings) for Advanced Aircraft, Space Vehicles and Missiles
* Jet Engine Components (Fan Blades, Ducting, Cowling; Bushings)
* Electronic/Microelectronic Components (Circuit Boards, Moldings, Insulation)
* Binding Systems in Brake Shoes, Abrasive Wheels and Cutting Discs
* Automotive Components (Connecting Rods, Wrist Pins, Pistons)
* Gaskets, Sealants and Tubing
* Castings, Nozzles, Etc. for Geothermal Energy Conversion Systems
* Coating on Cookware (Non-Stick Interior and Decorative Exterior)
* Ablators (Thermal Protection Systems)
* Nuclear Reaction Components (Coolants, Insulations, Structural Parts)
* Conveyor Belts (Treating and Drying of Materials)
* Filters (Hot Exhaust Stacks)
* Pipes (Chemical Processing and Energy-Generating Plants)
* Fire Resistant Materials (Protective Clothes and Parachutes)
* Reinforcements (High Modulus/High Strength Fiber and Ribbons)

resistant polymers are defined as materials that retain mechanical properties for thousands of hours at 230°C, hundreds of hours at 300°C, minutes at 540°C or seconds up to 760°C (233). For illustration, Figure 12 shows the approximate use temperatures for several aerospace adhesive applications as function of service life (16). Thermal resistance customarily means the lowest temperature at which the polymer begins to undergo chemical and property changes.

The requirements for the use of a polymer at high temperatures can be stated as (217):

1. Retention of mechanical properties/high softening point; high glass transition temperature;
2. High resistance to thermal breakdown;
3. High resistance to chemical attack, i.e., oxidation and hydrolysis.

2. <u>General Principles</u> The most important criterion for thermal resistance is the retention of physical properties in a specific environment at an elevated temperature for a stated amount of time (225). Table 7 categorizes some of the major chemical and physical factors that influence heat-resistance. Evaluation of polymer

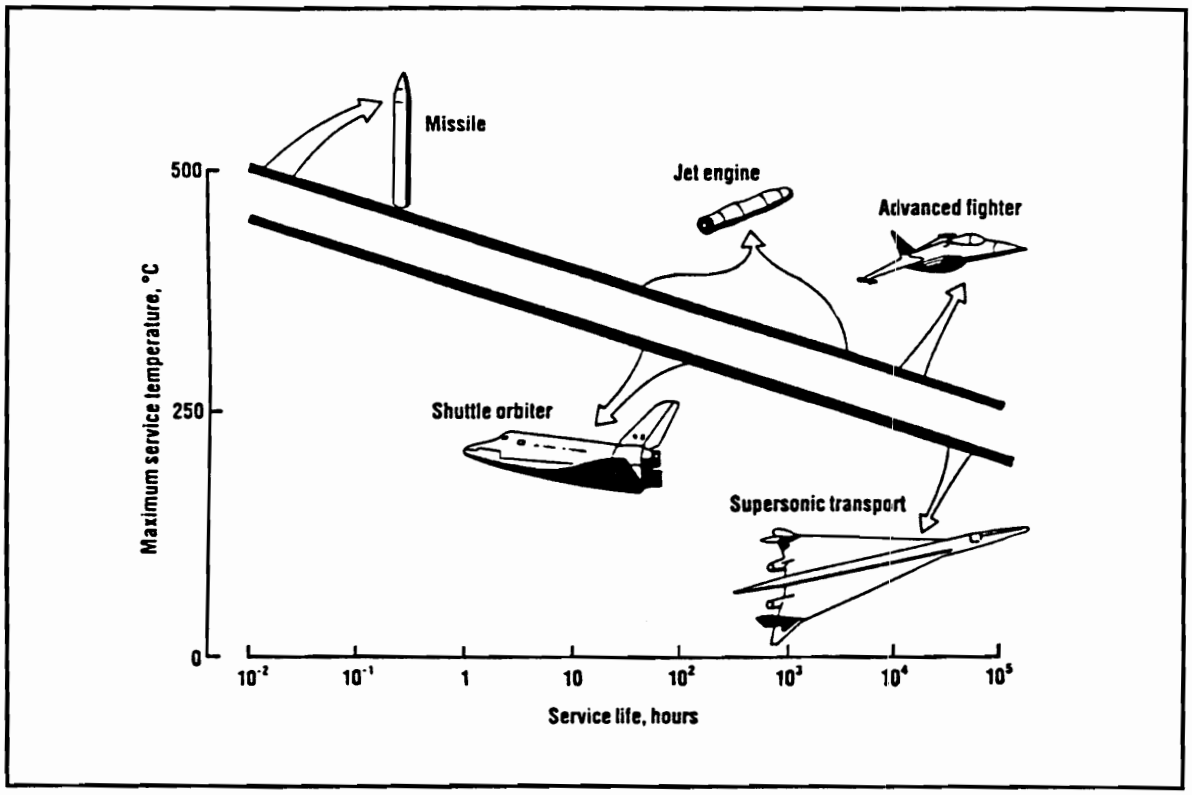

Figure 12

Approximate Use Temperature as a Function of Service Life for Several Aerospace Adhesive Applications (16)

Table 7

Factors Which Contribute To Heat Resistance (232)

Chemical Factors

* Primary Bond Strength
* Secondary Bonding Forces (Hydrogen Bonding, Van Der Waals Forces)
* Resonance Stabilization
* Mechanism Of Bond Cleavage (Recombination, Unzipping)
* Molecular Symmetry (Regularity Of Structure)
* Rigid Intrachain Structure
* Crosslinking And Branching

Physical Factors

* Molecular Weight
* Molecular Weight Distribution
* Close Packing (Order Or Crystallinity)
* Molecular (Dipolar) Interactions
* Purity

degradation mechanisms has led to the following generalizations for attaining high thermal stabilities (217):

1. Only the high-energy bonds should be used.
2. Low energy degradation pathways should be avoid.
3. Resonance stabilization should be optimized.
4. Normal bond angles should be utilized.
5. Polybonding should be engaged as much as possible.

Of these the primary bond strength is the single most important criterion to thermal stability. Degradation begins when the temperature increases to the point where vibrational energy causes bond rupture, in particular on the weakest bonds present in the polymer (234). In general, catastrophic changes in mechanical properties can be observed when only one percent of the main chain bonds have been broken.

Bond dissociation energies primarily signify the vulnerability of bonds to thermal cleavage, indicating the relative thermal stability of polymers. High heat-resistant polymers must have bonds with high bond dissociation energies. However, predicting relative thermal stabilities of polymers is not as direct as comparing bond strengths of different bonds (235). Conclusions from studies on the thermal stability of model compounds have to be treated with caution, the results cannot always be considered as a

reliable guide to the stability of the same structural units when incorporated in a polymeric environment (236). The mechanism of bond cleavage must also be considered, since structural features and vulnerability of a bond to other species that allow degradation by low-energy processes must be excluded. Table 8 lists bond dissociation energies commonly found in polymeric systems (179,237,238). The bond dissociation energy of a carbon-carbon single bond is approximately 348 kJ/mole while a carbon-carbon double bond is approximately 682 kJ/mole. An additional 167-290 kJ/mole is gain through resonance stabilization in aromatic carbon-carbon bonds. In ring structures, breaking of one bond does not necessarily lead to a decrease in molecular weight since there is a lower probability that two bonds will rupture within the same ring. As an outcome, aromatic and heterocyclic rings are used extensively in heat-resistant systems.

Additional thermal stability and strength can be gained through secondary bonding interactions. Secondary forces determine the attraction between neighboring chains (cohesion) and in turn affect the magnitude of the glass transition temperature, the melting temperature and solubility. Cumulative effect of these interactions along the polymer backbone results in a large electrostatic field of attraction holding the individual chains together. When

Table 8

Bond Dissociation Enthalpies (kJ/mole) (236-238)

C-H	413	C-C	348	C=C	682	C≡C	962
N-H	391	N-N	161	N=N	418	N≡N	941
O-H	463	O-O	139	O=O	498	C≡N	891
Si-H	319	S-S	226	N=O	607		
B-H	294	C-O	361	C=O	732		
P-H	318	C-N	307	C=N	617		
S-H	347	Si-C	328	C=S	536		
		Si-O	445				
		Si-N	437				
		C-F	428				
		C-S	273				
		C-Cl	340				
		C-B	374				
		B-O	777				
		B-N	386				
		P-C	580				
		P-O	528				

the temperature is raised, a point will be reached where the secondary forces are overcome freeing the chains to slide past one another, i.e., to flow. Dipole-dipole interactions and hydrogen bonding can also contribute 25-41 kJ/mole of energy toward stability. The strength of secondary bonding forces increases with increasing polarity and decreases sharply with increasing distance between groups.

Crosslinking is another procedure to enhance the thermal stability of a polymer. This method also serves to increase the softening point or glass transition temperature; hydrolytic and chemical resistance (239). Generally, as the crosslink density increases, so does the heat resistance. Ultimately, an infusible, intractable and insoluble polymer is produced. However, this is accompanied by decreases in impact strength, elongation at break and reversible extensibility. Crosslinking improves the heat-resistance in a polymer essentially because the three-dimensional structure impedes the rotation of backbone bonds and since there are more bonds to break.

The most successful approaches to high-temperature polymers have been based upon aromatic and heterocyclic rings as a result of their rigidity, crystallinity and the ability to participate in extended resonance conjugation. For main chains containing phenylene rings the para-linked rings have the highest heat-resistance. This structure also has a very

high softening point and is generally considered as the standard to which all other systems are compared to. In fact, poly-p-phenylene has been reported to melt above 530°C (240) and may be stable up to 800-900°C (234). However, this system is extremely stiff and results in an intractable material with low solubility that is very difficult to process. These types of materials are commonly referred to as "brick dust".

Another method to improve on the processability is by incorporating meta- and ortho- isomers, but this subsequently lowers the thermal stability and the glass transition temperature. The order of thermal stability gained by polymers for various phenylene, aromatic and heterocyclic rings with regard to ring orientation is: para- > meta- > ortho-.

Considerable improvement in processability and solubility has resulted by incorporation of flexible linking (bridging) groups between the aromatic or heterocyclic rings which promote rotational freedom. However, the insertion of linking groups ultimately decreases the inherent thermal and thermo-oxidative stability of these materials. Bridging groups should be employed that offer high resistant to thermal, oxidative and hydrolytic attack while not offering low energy mechanisms for degradation. Thermally stable polymers that are intractable can be modified by the

incorporation of methylene groups or aliphatic chains between aromatic and/or heterocyclic groups producing a polymer that is easier to process. However, the aliphatic character greatly reduces the thermal stability. Table 9 list many of the linking groups that have been used (217,241); of those that sacrifice the least to thermal stability are (217):

$$-CO- \quad , \quad -COO- \quad , \quad -CONH- \quad , \quad -S- \quad , \quad -SO_2- \quad ,$$
$$-O- \quad , \quad -[-CF_2-]_n- \quad , \quad -[-C(CF_3)-]-$$

The following relative order of stability can be derived for some of the more common aromatic systems (241):

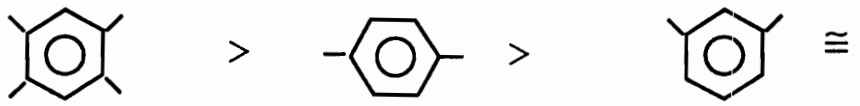

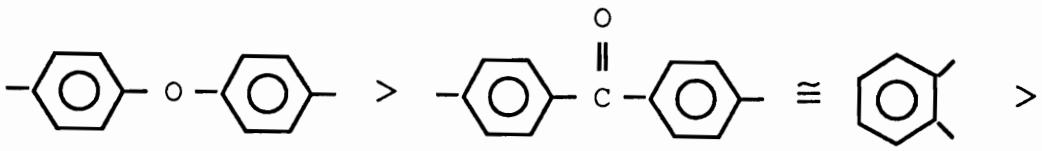

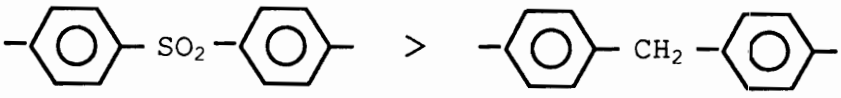

Table 9

Linking Groups Used Between Aromatic Rings (217,240)

$-CH_2-$	-CO-	-NH-	-S-
$-CH_2CH_2-$	-CO-O-	-N=N-	-S-S-
$-C(CH_3)_2-$	-CO-O-CO-	-CO-NH-	-SO-
-CH=CH-	-O-CO-O-	-CO-NH-NH-CO-	$-SO_2-$
-C≡C-		-NH-CO-CO-NH-	$-SO_2-O-$
-C(CN)=CH-		-NH-CS-NH-	$-SO_2-NH-$
$-[CF_2]_n-$			
$-C(CF_3)_2-$			
-O-			
$-C(CF_3)(C_6H_5)-$			
$-C(C_6H_5)=C(C_6H_5)-$			

Use of linking groups that are electron-withdrawing, i.e., -CO- and -SO_2-, are generally more stable than those that are electron-donating units, i.e., -O- (233,242). Aliphatic linking units and aliphatic pendent should be avoided for good thermal and thermo-oxidative stability. Lee has recently summarized the T_g-structure relationship of polyimides and other semi-rigid polymers such as polyquinolines and polyquinoxalines. He concluded that there is a universal relative bridging effect, as well as an isomerization effect for a ring/linking repeating unit (242). That is, a flexible linking group imparts almost the same type of properties no matter what semi-rigid polymer it is incorporated into. Lee concludes that a relative bridging effect can be considered as a rigidity index of a repeating unit and the flexible linking group can be correlated to a rotational barrier energy. Furthermore, the T_g's of semi-rigid polymers should be meticulously a function of the cohesive energy density, the relative flexibility of their bridging group and the concentration of the bridging groups within their repeating units (243).

3. <u>Thermally Stable Polymers</u> There are overall two important strategies to the synthesis of thermally stable polymers: high bonding energy and restrictive bond rotation.

High bonding energy is achieved by utilizing aromatic ring structures to maximize the advantage of resonance

stabilization. For example, Marvel ("Father of high-temperature polymers,") (244) worked on one of the first completely aromatic polymers, poly(p-phenylene), 11 (245).

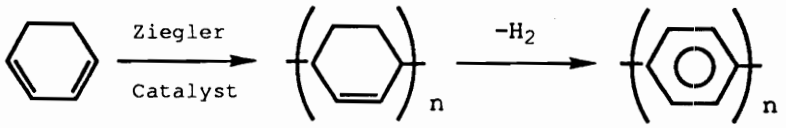

11

Aromatic systems with C-O, C-N and C-S in the chain as in the heterocyclics are very thermally stable. Marvel's innovative studies also led to the development of the heterocyclic polybenzimidazole, 12 (229).

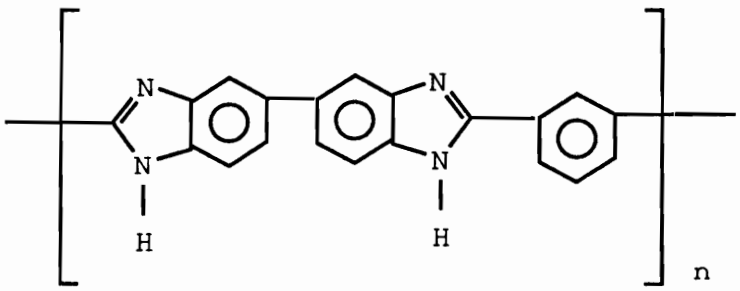

12

Restricting the motions of bond in polymers can lead to either rigid or crosslinked structures. The linear bonding between aromatic and heterocyclic structures fabricates rigid systems producing high glass transition temperatures and/or crystalline melting points. Crystallinity has limited use in heat-resistant systems due to the more strenuous processing

conditions and lower solubilities. Rings can be immobilized into planar structures that restrict either the conformation or hinder the rotation of the ring around the main chain of the polymer. Planar rings can be achieved by the incorporation of C=O groups as in polyimides, 13 or by C=N units, for example, in polybenzimidazoles 12, polybenzoxazoles and polybenzothiazoles. Or by using both of

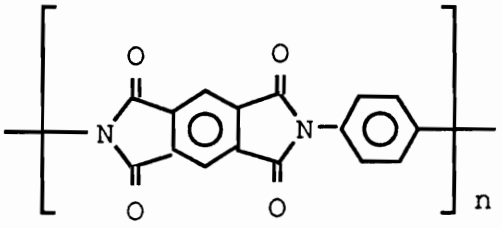

13

these groups in the same structure for instance in the copolyimide isoindoloquinazolinediones, 14 (246,247).

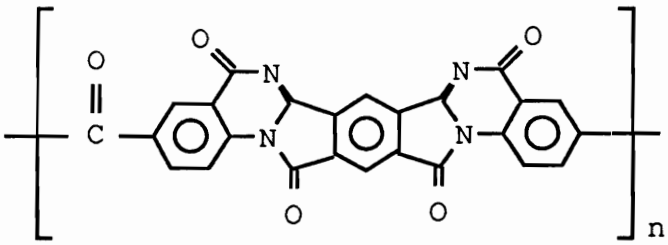

14

Ladder and spiro polymers are examples of double-stranded (ordered linear networks) polymers that also possess

increased heat-resistance because of their stiffness due to restrictive bond rotation. Molecular structures of this type can undergo a single bond cleavage in the chain without a decrease in molecular weight, not resulting in deterioration of properties, unless two or more bonds break in the same ring (248).

Aromatic or heterocyclics can be restricted into three-dimensional infusible networks by the incorporation of either pendent or terminal reactive groups that undergo addition crosslinking reactions. Currently, the most frequently used functional end-groups are maleimides, nadimides, acetylenics, and styrls for the preparation of thermally crosslinkable systems that do not give rise to volatile byproducts. As an example, NASA developed polyimides terminated with nadimide end-groups as shown in Figure 13 (16,72,222,249).

In general, high heat-resistant polymers can be classified into five categories:

1) Step-growth Polymers, i.e., those prepared by polymerizing aromatic rings together either directly or by linking groups via condensation reactions (see Table 10);
2) Heterocyclic Polymers, i.e., macromolecules synthesized by combining aromatic rings with heterocyclic systems (see Table 11);

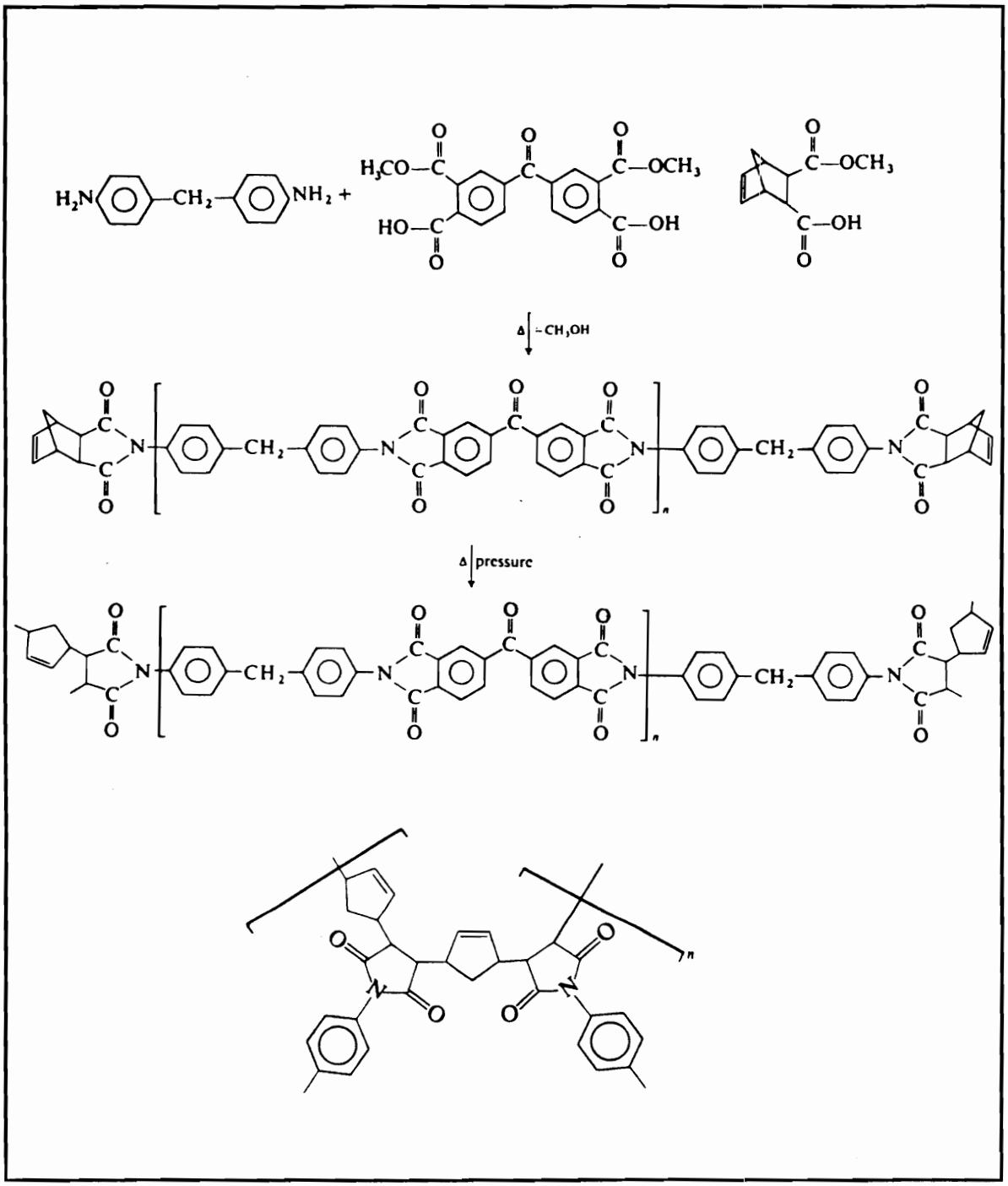

Figure 13

Thermosetting Polyimide (16,72)

Table 10

Step-Growth Polymers

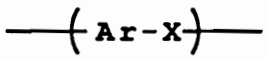

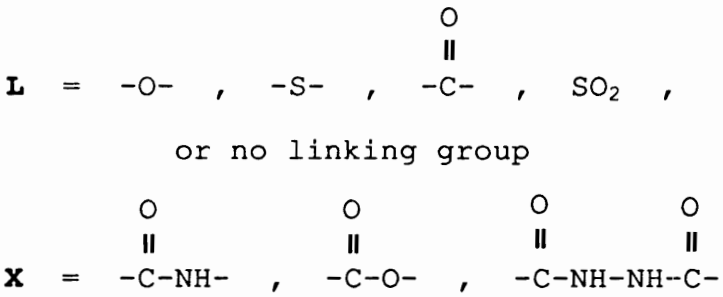

Polymers: (Ref.)
poly(amide)s (250)
poly(ester)s (251)
poly(benzyl)s (252)
poly(hydrazide)s (253)
poly(phenylene)s (254)
poly(phenylene ether sulfone)s (175,183)
poly(phenylene ether ketones)s (255)
poly(phenylene oxides, sulfide)s (256)

Table 11

Heterocyclic Polymers

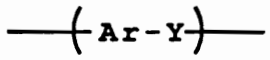

Q = -O- , -S- , -NR- ; R: H , C_6H_5

X = -O- , -S- , $-SO_2-$,  , $-C(CF_3)_2-$,

or no linking group

Ar = 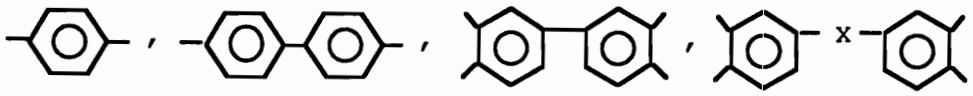

Y = 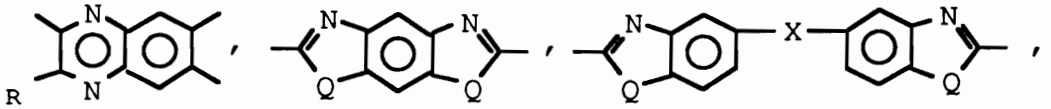

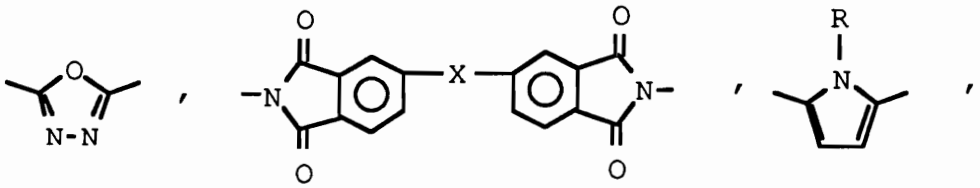

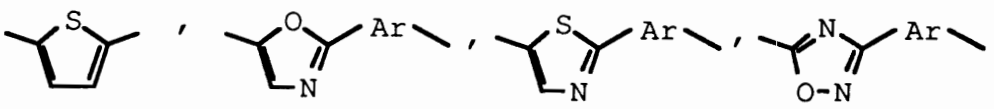

Polymers: (Ref.)

poly(imides)s (257)	poly(benzimidazoles)s (262)
poly(oxazole)s (258)	poly(1,3,4-oxadiazole)s (263)
poly(thiazole)s (259)	poly(1,2,4-oxadiazole)s (264)
poly(quinoxaline)s (260)	poly(phenylenepyrrole)s (265)
poly(benzoxazole)s (261)	poly(phenylenethiophene)s (226)

3) Step-growth/Heterocyclic Copolymers, i.e., simple condensation linkages combined with aromatic and heterocyclic rings (see Table 12);
4) Ladder and Spiro Polymers, i.e., heterocyclic polymers that are based on double strands (see Table 13);
5) Thermosetting Polymers, i.e., crosslinked polymers prepared from 1-4 (see Figure 13 and Table 14).

4. Determination of Heat-Resistance There are essentially two ways in which polymer property degradation occurs in temperature-dependent processes (217). The "softening or glass transition temperature" of a polymer is a reversible change dependent upon temperature only. While irreversible degradation is when the polymer is permanently changed, this is both time- and temperature-dependent. Ideally, it is the irreversible process that we are talking about when considering thermal stability. Such that, heat stability and flammability are concerned with actual chemical changes (i.e., material destruction), while softening and glass transition temperature are indicative of morphological transformations.

A variety of thermal analytical techniques are available to assess heat-resistance. Thermal analysis is defined as methods in which a specific physical property of a material

Table 12

Step-Growth/Heterocyclic Copolymers

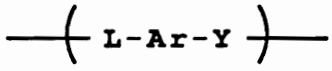

Q = -O- , -S- , -NR- ; R: H , C_6H_5 ,

X = -O- , -S- , $-SO_2-$,  , 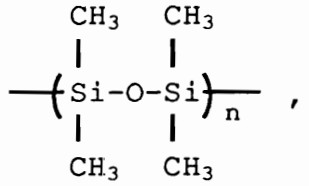 ,

or no linking group

L = 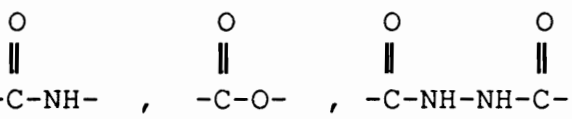

Ar = 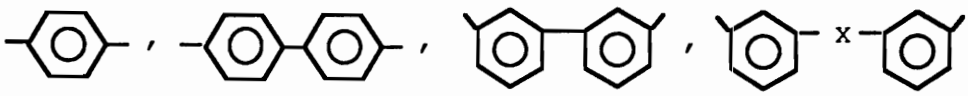

Y = 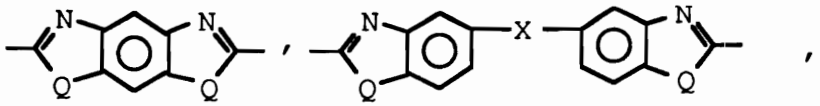 ,

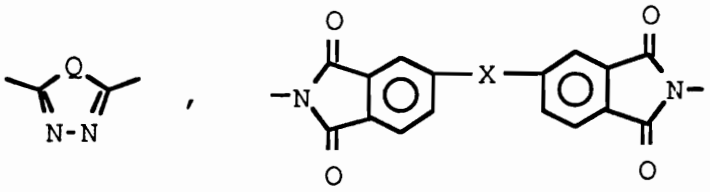

Polymers: (Ref.)
poly(ester-imides)s (266) poly(siloxane-imide)s (268,269)
poly(amide-imides)s (267) poly(amide-hydrazide)s (270)

Table 13

Ladder and Spiro Polymers

Ladder

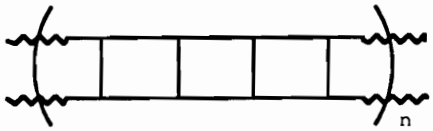

Poly(pyrazinopyrazine) (88)

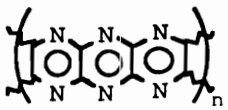

Poly(perinaphthalene) (89)

Poly(imidazopyrrolone) (90)

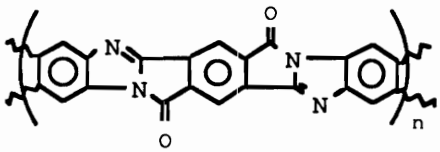

Spiro

Poly(spiroamide) (91)

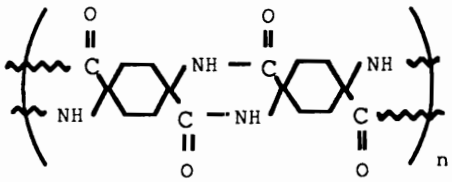

Poly(spiroketal) (92)

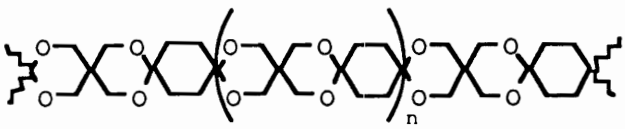

Table 14

Thermosetting End-Groups

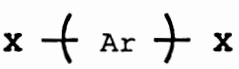

Function (Ref.)	**X**, Reactive End-Group
Styrl (276)	$-CH=CH_2$
Ethynyl (277)	$-C\equiv CH$
Nitrile (278)	$-C\equiv N$
Cyanate (222)	$-OC\equiv N$
Cyanamide (279)	$-NHC\equiv N$
N-Cyanourea (280)	$-NH-CO-NH-C\equiv N$
Phenylethynyl (281)	$-C\equiv C-$ 
Phenylbutadiynyl (281)	$-C\equiv C-C\equiv C-$ 
Phenylbutenynyl (281)	$-C\equiv C-CH=CH-$ 

Table 14

Thermosetting End-Groups (con't)

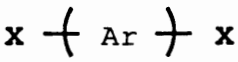

Function (Ref.)	X, Reactive End-Group
Phthalonitrile (282)	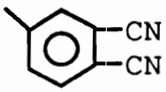
Benzocyclobutene (283)	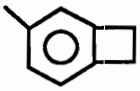
Biphenylene (284)	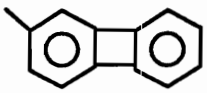
Maleimide (30)	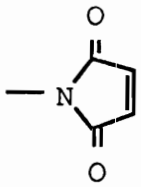
Nadimide (72)	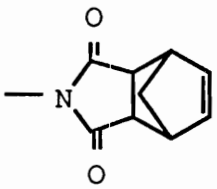

and/or of its reaction products is measured as a function of temperature while the material is exposed to a controlled temperature program (284). The routinely used techniques are (286-288):

a) Thermogravimetric analysis (TGA), which measures changes in sample weight resulting either from chemical or physical transformations as a function of temperature or time;
b) Differential thermal analysis (DTA) ascertains the chemical and physical changes that are accompanied by a loss or gain of heat in a polymer as temperature is decreased, increased or held isothermally and differential scanning calorimetry (DSC) which gives quantitative information about these heat changes;
c) Thermomechanical analysis (TMA) and thermo-dilatometry are methods for assessing the dimensional changes in polymers as a function of temperature and time;
d) Dynamic mechanical thermal analysis (DMTA) provides information on the dynamic modulus and/or damping of a material measured under oscillatory load as a function of temperature as the material is subjected to a controlled temperature program;

e) Dielectric thermal analysis (DETA) evaluates the dielectric properties of a material as a function of temperature and frequency, providing the dielectric constant (ε'), dielectric loss (ε'') and the dissipation factor (tan δ).

f) Evolved gas detection (EGD) and evolved gas analysis (EGA), mass spectrometry, gas chromatography, etc., are coupled with any of the above methods for on-line analysis of volatile products;

g) Other "hyphenated" techniques, that combine a number of existing methods together, for example, interfacing DSC or TGA with FTIR and/or NMR spectroscopy.

Dynamic TGA is the most widely used technique for evaluating heat-stability of polymeric materials (241,289,290). Dynamic TGA is popular for a number of reasons, foremost because this method readily provides the onset temperature at which major irreversible polymer degradation occurs at. Also, because the measurements are rapid, reproducible and simple to perform while there are a wide variety of available instruments to choose from, which allow different sample atmospheres to be used. Solids or liquids can be measured with essentially no sample preparation required and very small samples are needed.

Figure 14 represents a typical TGA thermogram of benzimidazoles measured both in air and nitrogen atmospheres (235,291). Dynamic TGA measures weight changes while scanning though a predefined temperature range at a fairly rapid rate that can be regarded as indicative of short-term stability assessment. While, isothermal TGA aging testing may give a more accurate prediction of lifetime service of a polymer.

While dynamic and isothermal TGA do not measure softening or melting, DSC or DTA can be utilized to determine the glass transition temperature or crystalline melting as shown in Figure 15 for an idealized DSC or DTA thermogram (116). For highly crosslinked systems like bismaleimides, the network may be so rigidly confined that a glass transition temperature may not be observed by DSC. However, the softening temperature may often be conveniently determined by TMA using the penetration mode. In this technique, the sample rests on a quartz stage surrounded by a furnace while a quartz probe with a small tip and a predefined load on it is applied to the polymer surface. The TMA measures the linear displacement of the penetration probe as the furnace is run through the predetermined heating program. The movement of the probe is translated into an electrical signal by a linear variable differential transformer as a function of temperature (or time). When the

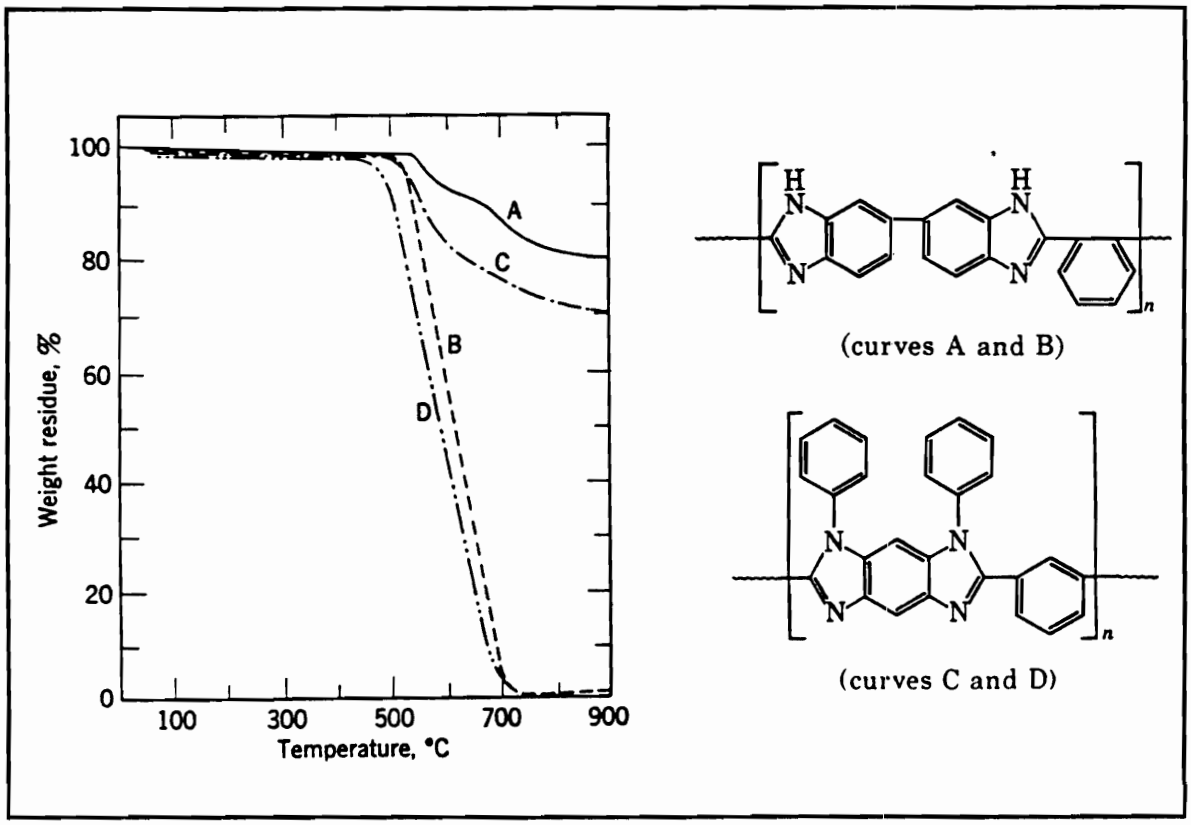

Figure 14

Thermogravimetric Analysis Curves of Benzimidazoles at 2.5°C/min with curves A & C under N_2; curves B and D in air (235,291)

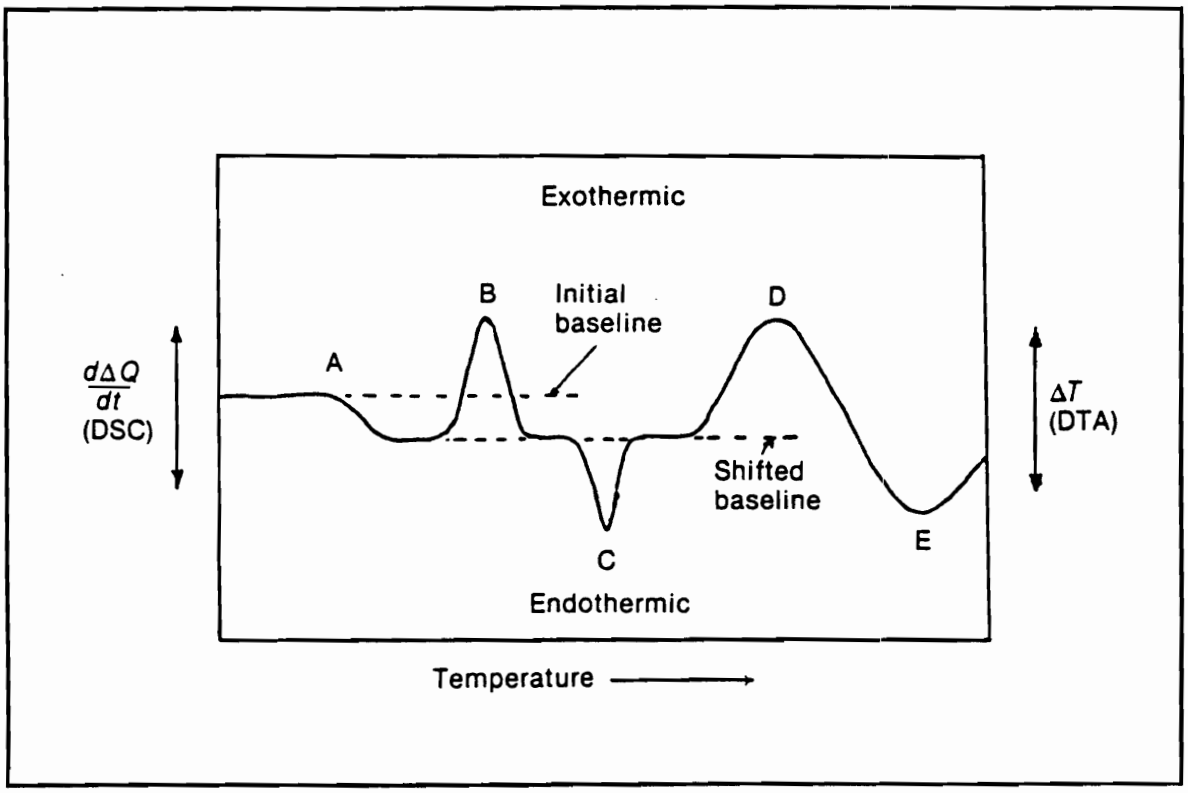

Figure 15

A Generalized Differential Scanning Calorimetry or Differential Thermal Analysis Curve: (A) Glass Transition Temperature; (B) Crystalline Melting Point; (C) Crystallization; (D) Crosslinking and (E) Vaporazation (116)

sample reaches its softening point it can no longer support the load on the probe and it penetrates into the polymer. The softening temperature is not identical to the glass transition temperature but is associated with the large-scale decrease in modulus at the glass temperature (124). However, it has been shown to correlate well with the glass transition temperature and most people quote the softening temperature as the glass transition temperature.

5. **Flammability and Flame Resistance** Polymeric materials, whether synthetic or natural account for most of the combustible material found in fatal fires (292). Many polymers like polyolefins are inherently flammable. Combustion of a polymer begins with it being heated and volatilized in a highly complex process. This can be initiated by thermal radiation, via convection (proximity to heat source) or conduction (direct contact to heat source). When a polymer reaches the temperature at which the weakest bonds start to rupture, this is referred to as polymer degradation and at first only results in minor changes in structure and properties, like discoloration. While at higher temperatures a more extensive proportion of the bonds breakdown and decomposition occurs (293). Essentially, there are two consecutive chemical transformation that occur when a material burns, decomposition and combustion, which are interrelated with ignition and thermal feedback (294).

Combustion occurs in a series of steps. When a polymer is exposed to an remote heat source, its temperature increases to the point where decomposition begins and combustible gases are given off. After the gases ignite the temperature increases until the volatilization is fast enough for combustion to be self-sustaining. Some polymers will burn as long as the heat source is in close proximity, but stop burning when the source is removed. This is known as a self-extinguishing polymer, for example polycarbonates. Some hydrocarbon polymers like α-methyl-styrene or methyl methacrylate burn with the volatiles being high in monomer because the polymer chain unzips by a free radical process (295). The monomer in turn decomposes into smaller molecules that diffuse toward the flame. The gases then react with oxygen at the flame front to produce the flame.

This process can be shown by the following idealized burning polymer that decomposed by low energy unzipping processes (296):

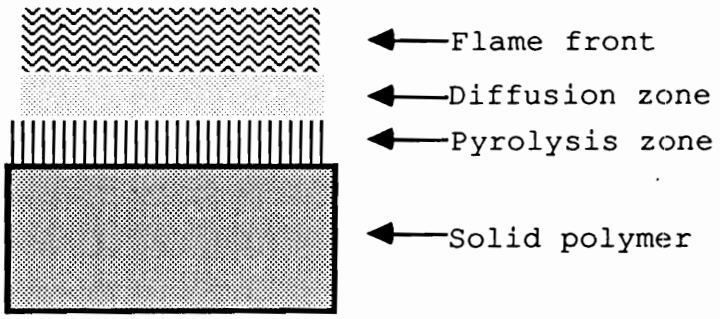

This simplified view is analogous to the burning of a candle, i.e., the wax of a candle does not burn directly but must be first transformed into a volatile fuel by the heat of the flame. With either the burning candle or polymer we can obtain a detailed chemical description of the combustion by such analytical techniques as TGA-MS.

Three main factors for sustained combustion are fuel (polymer), oxygen and heat. The basis of fire suppression is to interfere with one or more of these interrelated stages:

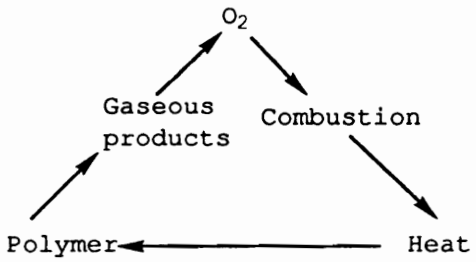

There are three broad approaches to promoting flame resistance of polymeric systems, most have been achieved by the use of additives to affect the various stages of the combustion cycle (297): 1) retarding the flame formation and propagation process in the vapor phase (diffusion zone); 2) promoting the formation of "char" in the pyrolysis zone and 3) dilution of the polymer with materials (fillers) that promote nonflammability or that endothermically cool the pyrolysis zone. Approximately 90% of the commercial flame retardants being used in the United States belong to one of

these six chemical classifications: alumina trihydrate; organochlorine compounds; organobromine compounds; organophosphorus ester compounds; antimony oxides and boron compounds (292).

Retardation of combustion in the vapor phase has been approached by adding flame retardants or by modifying the polymer by copolymerizing with a monomer that imparts flame resistance. Combustion in the vapor phase occurs by a series of complex free radical reactions, therefore, radical scavengers have been added to polymers to reduce the concentration of radical in the vapor phase. This type of retardant acts by being released along with the combustible polymer. Halogenated compound have been extensively used as flame retardants since they efficiently trap radicals, however, a serious disadvantage of halogenated additives is the smoke and toxicity of the hydrogen halide that is given off during the burning.

Flammability can also be reduced by inhibiting the gaseous products from diffusing toward the flame by char formation and carbonization. Char acts as barrier that insulates the polymer from the thermal energy that would otherwise continue the cycle of fuel generation and degradation. It has been shown that the amount of char formed is a measure of the polymers flame resistance and which is indicative of the polymer's structure (294).

Further heating produces a carbonaceous surface residue that can be described as a conglomerate of loosely linked small graphitic regions (298). Polymers that have high thermal stability due to aromatic and/or heterocyclic structures have greater tendencies to condense into aromatic chars, producing less flammable gaseous products for the flame, for example, poly(phenylene oxides), polycarbonates and polysulfones. Crosslinked, ladder and spiro structures also lead to flame resistance since bond rupture in these structures does not generate combustible fuel gases, furthermore, char and carbonization formation are promoted.

The third method involves the use of inorganic fillers or materials that decompose to give off nonflammable gases or products that decompose endothermically to cool off the substrate. Aluminium oxide trihydrate is a filler that can act both as a heat sink to prevent the polymer from reaching temperatures at which breakdown leads to gaseous products and as an endothermic cooler since its approximately 35% water content is released upon decomposition. The water vapor acts to absorb energy from the flame and reduces the fuel temperatures. Also, sodium bicarbonate is used since it decomposes to form carbon dioxide which reduces the combustible gases.

Phosphorus containing compounds have been used for both vapor and pyrolysis-phase flame retardants or by both phases

simultaneously. Synergistic interaction with phosphorus based retardants have been reported for other elements, for example, nitrogen and halogens (292,293,299). The performance of a particular phosphorus compound greatly depends on the polymer that is being considered (300). Triphenylphosphine oxide and triphenylphosphate have been proposed to inhibit flames by a vapor-phase mechanism involving the trapping of free radicals (291,301):

$$(C_6H_5)PO \longrightarrow PO\bullet,\ P\bullet;\ P_2$$

$$H\bullet + PO\bullet + M \longrightarrow HPO + M$$

$$HO\bullet + PO\bullet \longrightarrow HPO + \bullet O\bullet$$

$$HPO + H\bullet \longrightarrow H_2 + PO\bullet$$

$$P_2 + \bullet O\bullet \longrightarrow P\bullet + PO\bullet$$

$$P\bullet + \bullet OH \longrightarrow PO\bullet + H\bullet$$

Phosphorous-containing bismaleimides have been reported by Varma (see Table 1) that have outstanding flame resistance (302). These crosslinked materials have been shown to be flame resistance by both vapor and pyrolysis-phase mechanisms. A significant portion of phosphorus was observed in the char and also in the gaseous and pyrolysis products. Gas-phase inhibition of combustion was attributed to the free radical trapping of hydrogen radicals.

The current trend in flame retardants is gradually shifting toward the replacement of vapor-phase active

additives with pyrolysis-phase char forming systems (292,297). However, large amounts of fire-retardant additives can have detrimental effects on polymer properties. Many flame-retardant additives also reduce the thermal stability of the polymer system because the additives themselves are thermally labile. Therefore, it would seem logical in preventing polymer combustion to design polymers incorporating structures that are thermally stable, that do not have low energy decomposition pathways and have proven flame resistance. For example, triphenylphosphine oxide has been show to be very effective in flame retardation, however, this additive is not commonly used commercially (303). Incorporation of the triphenylphosphine oxide unit into the main chain, and hence the inherent fire-resistance of the polymer would seem to be the optimum design. This dissertation reports on some new bismaleimides based on aromatic ether phosphine oxide units that show excellent flame resistance. (304).

III. Experimental

A. Reagents and Purifications

1. Reaction Glassware and Techniques Monomer and polymer synthesis were conducted in pyrex glassware. All glassware was cleaned with dilute hydrofluoric acid; rinsed with dilute sodium hydroxide then distilled water and dried prior to use.

Pyrex round bottom flasks used in synthesis were fitted with nitrogen inlets, overhead mechanical stirrers with pyrex shafts and teflon paddles, thermometers, water condensers and Dean Stark traps as needed. Ground joints were wrapped with teflon tape. Silicone oil was used to seal the stirring shaft. Nitrogen was dried by passing through a series of three Drierite® columns before entering the reaction flask. A silicone oil bubbler was used to regulate the nitrogen flow. Flasks were heated using silicone oil baths on hot plates. Care was taken to properly rinse the aluminium weighing pans and glassware of residual weighed reagents into the reaction flask.

Solvents were distilled in an all pyrex glass distillation apparatus using a water aspirator equipped with a Drierite® column. A heating mantle was used to heat the system.

Sublimations were conducted in a Kontes #100 sublimation apparatus, heating with a silicone oil bath while using a dry

ice/isopropanol cold finger and a mechanical vacuum pump that contained an in line dry ice/isopropanol cold trap. Crystals to be sublimed were covered with a sheet of filter paper prior to sublimation to prevent contamination from sputtering of the unpure crystals. A silicone oil bath was used to heat the sublimation apparatus.

2. Solvents

a. N,N-Dimethylacetamide (Fisher, reagent grade) was stirred over crushed calcium hydride for one week and then distilled under reduced pressure from calcium hydride. Dimethylacetamide was stored in a round bottom flask sealed with a rubber septum and degassed with dry nitrogen.

b. Acetone (Fisher, reagent grade) was either stirred over molecular sieves (Fisher) for one week and distilled under reduced pressure from molecular sieves or used as received (Fisher, HPLC grade). Acetone was stored in a round bottom flask sealed with a rubber septum and degassed with dry nitrogen.

c. Chlorobenzene (Aldrich, reagent grade) was stirred over phosphorus pentoxide for one week and then distilled from phosphorus pentoxide under reduced pressure. Chlorobenzene was stored in a round bottom flask sealed with a rubber septum and degassed with dry nitrogen.

d. Toluene (Fisher, reagent grade) was either stirred over calcium hydride for one week and distilled under

reduced pressure from calcium hydride or used as received (Fisher, HPLC grade). Toluene was stored in a round bottom flask sealed with a rubber septum and degassed with dry nitrogen.

e. Tetrahydrofuran (Fisher reagent grade) was either stirred over sodium/benzophenone overnight and distilled under reduced pressure from sodium/benzophenone or used as received (Fisher, HPLC grade). Tetrahydrofuran was stored in a round bottom flask sealed with a rubber septum and degassed with dry nitrogen.

3. Monomers

a. Bisphenol A (Dow Parabis®) [2,2-Bis(4-hydroxyphenyl)propane or Bis A] was kindly supplied by Dow Chemical USA. Bisphenol A was dried at 60°C under vacuum for 24 hours in a vacuum oven and stored in a desiccator.

b. Bis(4-fluorophenyl)phenyl phosphine oxide bis(4-fluorophenyl)phenyl phosphine oxide was either prepared by Carrington Smith (305) or supplied by Akzo America, Inc. and used as supplied. Bis(4-fluorophenyl)phenyl phosphine oxide was stored in a desiccator until needed. Bis(4-fluorophenyl)phenyl phosphine oxide was made by a Grignard procedure using 4-fluorophenylmagnesium bromide and phenylphosphonic dichloride.

c. Para-[bis(4-fluorobenzoyl)]benzene (monomer grade) was kindly supplied by BASF. Para-[bis(4-

fluorobenzoyl)]benzene was vacuum oven dried at 100°C for 24 hours and stored in a desiccator.

d. Bis(4-fluorophenyl)methyl phosphine oxide was either supplied by Carrington Smith (305) or prepared by the same method. Bis(4-fluorophenyl)methyl phosphine oxide was stored in a desiccator until needed. Bis(4-fluorophenyl)methyl phosphine oxide was made by a Grignard reaction using 4-fluorophenylmagnesium bromide and methylphosphonic dichloride.

e. 4,4'-Methylenebis(cyclohexylamine)-20 (PACM-20, mixture of isomers: 20% cis / 80% trans) was supplied by Air Product & Chemicals, Inc. and used as received.

f. 4,4'-Methylenebis(cyclohexylamine)-48 (PACM-48, mixture of isomers: 48% cis / 52% trans) was supplied by Air Product & Chemicals, Inc. and used as received.

g. 2,2',5,5'-Tetramethylmethylenedi(cyclohexylamine) (RC-589, ratio of isomers not determined) was supplied by Air Product & Chemicals, Inc. and used as received.

h. 1,3-Bis(aminomethyl)cyclohexane (RC-389, ratio of isomers not determined) was supplied by Air Product & Chemicals, Inc. and used as received.

i. 3,3'-Dimethyl-4,4'-diaminodicyclohexyl-

methane (RC-589-DMBCHA, ratio of isomers not determined) was supplied by Air Product & Chemicals, Inc. and used as received.

j. 4,4'-Methylene(aminobenzyl)cyclohexylamine (RC-589-4-BENZYL-CHA, ratio of isomers not determined) was supplied by Air Product & Chemicals, Inc. and used as received.

4. Chemicals

a. Meta-aminophenol (Aldrich) was sublimed generally twice to obtain pure white crystals at 100°C. Meta-aminophenol was stored in a 24/40 round bottom flask equipped with a rubber septum and degassed with dry nitrogen.

b. Para-aminophenol (Aldrich) generally required four sublimations to obtain pure white crystals using an oil bath at 100°C. It was best to sublime p-aminophenol just before use and minimize its exposure to air. Para-aminophenol could be stored under nitrogen in a 24/40 round bottom fitted with a rubber septum, however p-aminophenol would show signs of oxidation within a few weeks.

c. 2,2'-(4-Hydroxyphenyl-4-aminophenyl)-propane (MBA: mono amine of Bis A) was prepared (176,306) and supplied by Greg Lyle (50,239,307). 2,2'-(4-Hydroxyphenyl-4-aminophenyl)propane was sublimed once before use and stored in a 24/40 round bottom flask equipped with a rubber septum and degassed with dry nitrogen.

d. Methylphosphonic dichloride (Aldrich) was used as received.

e. Acetic anhydride (Aldrich) was stirred over thin shavings of magnesium for one week and distilled from magnesium. Acetic anhydride was stored in a 24/40 round bottom flask equipped with a rubber septum and degassed with dry nitrogen.

f. Maleic anhydride (Aldrich) was sublimed once at 60°C and stored in a 24/40 round bottom flask equipped with a rubber septum and degassed with dry nitrogen.

g. Sodium acetate (Aldrich) was used as received.

h. Potassium carbonate (Fisher) was crushed and vacuum oven dried for 24 hours at 100°C and stored in a desiccator.

B. Monomer Synthesis

1. Aromatic Ether Phosphine Oxide Monomers

a. Bis(meta-aminophenoxy)triphenyl phosphine oxide

Bis(meta-aminophenoxy)triphenyl phosphine oxide was either supplied by Dr. Attila Gungor (308) or synthesized by the following modifications as described below.

A 1 liter four-neck round bottom flask was fitted with a Dean Stark trap, water condenser, nitrogen inlet, overhead mechanical stirrer and a thermometer. The activated halide bis(4-fluorophenyl)phenyl phosphine oxide (0.0955 mole) was added to the flask followed by m-aminophenol (0.2102 mole)

and potassium carbonate (0.1261 mole). Dimethylacetamide (226 ml) and toluene (56 ml) were added next. The Dean Stark trap was filled with toluene. The system was refluxed at 145°C for 4 hours with the observance of water collecting into the Dean Stark trap. Toluene was removed from the Dean Stark trap until the reaction temperature increased to 155°C. The reaction was then allow to proceed for another 2 hours; the solution was tan in color. The solution was filtered to remove the inorganic salts and the filtrate was neutralized with acetic acid. At this point the filtrate could be either precipitated in 25-50 ml portions in a blender containing 500 ml distilled water or the filtrate distilled using a Buchi rotovapor apparatus to dryness and then redissolved in the minimum amount of ethanol and precipitated in water. The bis(m-aminophenoxy)triphenyl phosphine oxide precipitate was then stirred in three liters of distilled water and filtered using a Buchner funnel. The precipitate was washed with 3-6 liters of distilled water while in the Buchner funnel. The white bis(m-aminophenoxy)triphenyl phosphine oxide precipitate was then vacuum dried for 48 hours at 60°C. Bis(m-aminophenoxy)triphenyl phosphine oxide: yield 96%; DSC @ 10°C/min: T_m 84°C; FTIR (KBr) aromatic (N-H) stretch at 3336 and 3453 cm^{-1}; ^1H-NMR ($CDCl_3$) aromatic amine protons at 3.8 ppm.

b. Bis(para-aminophenoxy)triphenyl phosphine oxide was synthesized in much the same manner as described above for bis(m-aminophenoxy)triphenyl phosphine oxide with the following exceptions. A 250 ml round bottom flask was charged with bis(4-fluorophenyl)phenyl phosphine oxide (0.0318 mole), potassium carbonate (0.0420 mole) and freshly sublimed p-aminophenol (0.0699 mole). Dimethylacetamide (75 ml) and toluene (19 ml) were added and nitrogen gas was turned on. Care was taken to minimized the exposure of p-aminophenol to air. The system was refluxed at 145°C for 4 hours and then the reaction temperature was increased to 155°C for 2 hours. The solution was red in color. The solution was filtered to remove the inorganic salts and the filtrate was neutralized with acetic acid.

The filtrate was distilled to dryness using a Buchi rotovapor apparatus and redissolved in the minimum amount of ethanol. This was then precipitated in distilled water using a blender. The precipitated bis(p-aminophenoxy)triphenyl phosphine oxide was stirred in 3 liters of distilled water, filtered and washed with 3-6 liters of water. The bis(p-aminophenoxy)triphenyl phosphine oxide precipitate was vacuum oven dried for 48 hours at 60°C. Bis(p-aminophenoxy)triphenyl phosphine oxide: yield 93%; DSC @ 10°C/min: T_m 98°C; FTIR (KBr) aromatic (N-H) stretch at 3343

and 3439 cm^{-1}; ^1H-NMR ($CDCl_3$) aromatic amine protons at 3.65 ppm.

c. **Bis(meta,para-aminophenoxy)triphenyl phosphine oxide** was prepared by a procedure similar to bis(m-aminophenoxy)triphenyl phosphine oxide and bis(p-aminophenoxy)triphenyl phosphine oxide. A 100 ml round bottom, three-neck flask was equipped with an overhead stirrer, nitrogen inlet with a thermometer adaptor, Dean Stark trap and a water condenser. The reactor was charged with bis(4-fluorophenyl)phenyl phosphine oxide (0.0160 mole), potassium carbonate (0.0211 mole), m-aminophenol (0.0176 mole) and freshly sublimed p-aminophenol (0.0176 mole). Dimethylacetamide (38 ml) and toluene (10 ml) were added. The system was refluxed at 145°C for 4 hours and then increased to 155°C for 2 hours. The solution was a deep turquoise blue. The solution was filtered and neutralized with acetic acid. The precipitated bis(m,p-aminophenoxy)triphenyl phosphine oxide was worked up in the same manner as described above for bis(p-aminophenoxy)triphenyl phosphine oxide. Bis(m,p-aminophenoxy)triphenyl phosphine oxide: yield 91%; DSC @ 10°C/min: T_m 83°C; FTIR (KBr) aromatic (N-H) stretch at 3336 and 3446 cm^{-1}; ^1H-NMR ($CDCl_3$) aromatic amine protons at 3.84 and 3.73 ppm.

d. **Bis(aminophenylisopropylidenephenoxy)-triphenyl phosphine oxide** was prepared similarily to bis(m-aminophenoxy)triphenyl phosphine oxide and bis(p-aminophenoxy)triphenyl phosphine oxide. A 100 ml round bottom reactor was charged with bis(4-fluorophenyl)phenyl phosphine oxide (0.0160 mole), potassium carbonate (0.0211 mole) and 2,2'-(4-hydroxyphenyl-4-aminophenyl)propane (MBA) (0.0352 mole). Dimethylacetamide (55 ml) and toluene (14 ml) were then added. The system was refluxed at 145°C for 4 hours and then increased to 155°C for 2 hours. The solution had a light yellow color. The solution was filtered and neutralized with acetic acid. The precipitated bis(aminophenylisopropylidenephenoxy)triphenyl phosphine oxide was worked up in the same manner as described above for bis(p-aminophenoxy)triphenyl phosphine oxide. Bis(aminophenylisopropylidenephenoxy)triphenyl phosphine oxide: yield 96%; DSC @ 10°C/min: T_m 90°C; FTIR (KBr) aromatic (N-H) stretch at 3377 and 3446 cm^{-1}; ^1H-NMR ($CDCl_3$) aromatic amine protons at 3.57 ppm.

e. **Bis(meta-aminophenoxy)diphenylmethyl phosphine oxide** was prepared similarily to bis(m-aminophenoxy)triphenyl phosphine oxide and bis(p-aminophenoxy)triphenyl phosphine oxide. A 100 ml round bottom reactor was charged with bis(4-fluorophenyl)methyl phosphine oxide (0.0051 mole), potassium carbonate (0.0067

mole) and m-aminophenol (0.0112 mole). Dimethylacetamide (12 ml) and toluene (3 ml) were then added. The system was refluxed at 145°C for 4 hours and then increased to 155°C for 2 hours. The solution was yellow in color. The solution was filtered and neutralized with acetic acid. The precipitated bis(m-aminophenoxy)diphenylmethyl phosphine oxide was worked up in the same manner as described above for bis(p-aminophenoxy)triphenyl phosphine oxide. Bis(m-aminophenoxy)diphenylmethyl phosphine oxide: yield 92%; DSC @ 10°C/min: T_m 70°C; FTIR (KBr) aromatic (N-H) stretch at 3336 and 3446 cm^{-1}; ^1H-NMR ($CDCl_3$) aromatic amine protons at 3.75 ppm.

f. Bis(meta-maleimidophenoxy)triphenyl phosphine oxide was prepared by first forming the intermediate bismaleamic acid by adding bis(m-aminophenoxy)triphenyl phosphine oxide (0.1543 mole), maleic anhydride (0.3703 mole) and acetone (537 ml) to a 2 liter four-neck round bottom flask fitted with a nitrogen inlet, overhead mechanical stirrer, thermometer and a water condenser. The yellow bismaleamic acid precipitated out of solution after 5 minutes at room temperature. The precipitated solution was stirred for an additional hour. The bismaleimide was then prepared *in situ* using acetic anhydride (108 ml) and sodium acetate (9.3 g) while refluxing. The mixture became homogeneous at reflux and was

allowed to proceed for an additional 3 hours. The homogeneous brown solution was then filtered and the filtrate reduced in volume by distilling using a Buchi rotovapor apparatus. The solution was precipitated in water using a blender and washed several times with distilled water. The light tan bismaleimide was vacuum oven dried for 48 hours at 60°C. Bis(m-maleimidophenoxy)triphenyl phosphine oxide: yield 95%; DSC @ 10°C/min: T_m 92°C ,T_1 180°C (onset of cure), T_{exo} 220°C (maximum peak of cure); FTIR (KBr) maleimide (C=O) stretch at 1716 cm^{-1}, maleimide (=C-H) stretch at 3070 cm^{-1}; ^1H-NMR ($CDCl_3$) maleimide protons at 6.79 ppm; ^{13}C-NMR ($CDCl_3$) carbonyl carbons at 168.94 ppm.

g. **Bis(para-maleimidophenoxy)triphenyl phosphine oxide** was prepared in the same manner outlined above for bis(m-maleimidophenoxy)triphenyl phosphine oxide. The intermediate bismaleamic acid was made by adding bis(p-aminophenoxy)triphenyl phosphine oxide (0.0203 mole), maleic anhydride (0.0487 mole) and acetone (75 ml) to a 250 ml four-neck round bottom flask. The bismaleimide was prepared *in situ* using acetic anhydride (14 ml) and sodium acetate (1.22 g). Bis(p-maleimidophenoxy)triphenyl phosphine oxide: yield 98%; DSC @ 10°C/min: T_g 107°C ,T_1 180°C (onset of cure), T_{exo} 223°C (maximum peak of cure); FTIR (KBr) maleimide (C=O) stretch at 1716 cm^{-1}, maleimide (=C-H) stretch at 3070 cm^{-1};

^{1}H-NMR ($CDCl_3$) maleimide protons at 6.84 ppm; ^{13}C-NMR ($CDCl_3$) carbonyl carbons at 169.39 ppm.

h. Bis(meta,para-maleimidophenoxy)triphenyl phosphine oxide was prepared in the same manner outlined above for bis(m-maleimidophenoxy)triphenyl phosphine oxide with the following exceptions. The intermediate bismaleamic acid was made by adding bis(m,p-aminophenoxy)triphenyl phosphine oxide (0.0081 mole), maleic anhydride (0.0195 mole) and acetone (38 ml) to a 100 ml three-neck round bottom flask. The bismaleimide was prepared *in situ* using acetic anhydride (6 ml) and sodium acetate (0.5 g). Bis(m,p-maleimidophenoxy)triphenyl phosphine oxide: yield 99%; DSC @ 10°C/min: T_m 93°C , T_1 180°C (onset of cure), T_{exo} 279°C (maximum peak of cure); FTIR (KBr) maleimide (C=O) stretch at 1716 cm^{-1}, maleimide (=C-H) stretch at 3070 cm^{-1}; ^{1}H-NMR ($CDCl_3$) maleimide protons at 6.815, 6.828 and 6.829 ppm; ^{13}C-NMR ($CDCl_3$) carbonyl carbons at 169.36 and 169.03 ppm.

i. Bis(maleimidophenylisopropylidene-phenoxy) phosphine oxide was prepared in the same manner outlined above for bis(m-maleimidophenoxy)triphenyl phosphine oxide with the following exceptions. The intermediate bismaleamic acid was synthesized by adding bis(aminophenylisopropylidenephenoxy)triphenyl phosphine oxide (0.0082 mole), maleic anhydride (0.0197 mole) and acetone (41 ml) to a 250 ml four-neck round bottom flask.

The bismaleimide was prepared *in situ* using acetic anhydride (6 ml) and sodium acetate (0.5 g). Bis(maleimidophenyl-isopropylidenephenoxy)triphenyl phosphine oxide: yield 95%; DSC @ 10°C/min: T_g 113°C , T_1 180°C (onset of cure), T_{exo} 216°C (maximum peak of cure); FTIR (KBr) maleimide (C=O) stretch at 1716 cm^{-1}, maleimide (=C-H) stretch at 3070 cm^{-1}; ^1H-NMR ($CDCl_3$) maleimide protons at 6.82 ppm; ^{13}C-NMR ($CDCl_3$) carbonyl carbons at 169.6 ppm.

j. Bis(m-maleimidophenoxy)diphenylmethyl phosphine oxide was prepared in the same manner outlined above for bis(m-maleimidephenoxy)triphenyl phosphine oxide. The intermediate bismaleamic acid was made by adding bis(m-aminophenoxy)diphenylmethyl phosphine oxide (0.0023 mole), maleic anhydride (0.0055 mole) and acetone (8 ml) to a 100 ml three-neck round bottom flask. The bismaleimide was prepared *in situ* using acetic anhydride (2 ml) and sodium acetate (0.2 g). Bis(m-maleimidophenoxy)diphenylmethyl phosphine oxide: yield 93%; DSC @ 10°C/min: T_g 77°C , T_1 180°C (onset of cure), T_{exo} 261°C (maximum peak of cure); FTIR (KBr) maleimide (C=O) stretch at 1716 cm^{-1}, maleimide (=C-H) stretch at 3070 cm^{-1}; ^1H-NMR ($CDCl_3$) maleimide protons at 6.81 ppm; ^{13}C-NMR ($CDCl_3$) carbonyl carbons at 169.0 ppm.

2. **Aromatic Ether Ketone Monomers**

a. Para-[bis(meta-aminophenoxybenzoyl)]-benzene was synthesized in a three liter four-neck round

bottom flask fitted with a Dean Stark trap, water condenser, nitrogen inlet, overhead mechanical stirrer and a thermometer. The activated halide p-[bis(4-fluorobenzoyl)]-benzene (0.6000 mole) was added to the flask followed by m-aminophenol (1.3200 mole) and potassium carbonate (0.7900 mole). The Dean Stark trap was filled with toluene. Dimethylacetamide (1444 ml) and toluene (361 ml) were added next and the reaction was refluxed at 145°C for 4 hours. Toluene was removed from the Dean Stark trap until the reaction temperature increased to 155°C. The reaction was allowed to proceed for another 2 hours, after which the reaction solution was filtered to remove the inorganic salts. The filtrate was neutralized with acetic acid and reduced in volume by distillation using a Buchi rotovapor apparatus. The neutralized solution (25-50 ml portions) was precipitated in a blender containing 500 ml (1:3) methanol/water. The precipitate was filtered and boiled twice in 4 liters of methanolic water for 1 hour and filtered. The p-bis(m-aminophenoxybenzoyl)benzene precipitate was vacuum oven dried at 60°C for 48 hours. Para-[bis(m-aminophenoxy-benzoyl)]benzene: yield 99%; T_m 163-164°C (melting point apparatus), FTIR (KBr) aromatic (N-H) stretch at 3364 and 3418 cm^{-1}, benzoyl carbonyl stretch at 1648 cm^{-1}; ^1H-NMR [$(CD_3)_2SO$] aromatic amine protons at 5.3 ppm.

b. **Para-[bis(para-aminophenoxybenzoyl)]-benzene** was synthesized by the same procedure as described above for p-[bis(m-aminophenoxybenzoyl)]benzene with the following changes. Para-[bis(p-aminophenoxybenzoyl)]benzene was prepared in a 500 ml four-neck round bottom flask using p-[bis(4-fluorobenzoyl)]benzene (0.6000 mole) and p-aminophenol (0.1320 mole) and potassium carbonate (0.0790 mole). Dimethylacetamide (145 ml) and toluene (36 ml) were used. Para-[bis(p-aminophenoxybenzoyl)]benzene: yield 99%; T_m 179-180°C (melting point apparatus), FTIR (KBr) aromatic (N-H) stretch at 3364 and 3418 cm^{-1}, benzoyl carbonyl stretch at 1648 cm^{-1}; ^1H-NMR [$(CD_3)_2SO$] aromatic amine protons at 5.1 ppm.

c. **Para-[bis(aminophenylisopropylidene-phenoxybenzoyl)]benzene** was synthesized by the same procedure as described above for p-[bis(m-aminophenoxybenzoyl)]benzene with the following changes. Para-[bis(aminophenylisopropylidenephenoxybenzoyl)]benzene was prepared in a 100 ml three-neck round bottom flask using p-[bis(4-fluorobenzoyl)]benzene (0.0099 mole) and 2,2'-(4-hydroxyphenyl-4-aminophenyl)propane (0.0220 mole) and potassium carbonate (0.0132 mole). Dimethylacetamide (35 ml) and toluene (9 ml) were used. Para-[bis(aminophenyl-isopropylidenephenoxybenzoyl)]benzene: yield 96%; FTIR (KBr) aromatic (N-H) stretch at 3350 and 3439 cm^{-1}, benzoyl carbonyl

stretch at 1648 cm^{-1}; ^{1}H-NMR [$(CD_3)_2SO$] aromatic amine protons at 4.8 ppm.

d. Para-[bis(meta-maleimidophenoxybenzoyl)]benzene was prepared in a 5 liter four-neck round bottom flask equipped with a water condenser, nitrogen inlet, overhead mechanical stirrer and a thermometer. Para-[bis(m-aminophenoxybenzoyl)]benzene (0.4994 mole), maleic anhydride (1.1986 mole) and acetone (2341 ml) were added to the reactor and stirred; immediately a yellow bismaleamic acid precipitate formed. The reaction was stirred for an additional hour. The bismaleimide was then prepared *in situ* by the addition of acetic anhydride (351 ml) and sodium acetate (21.9 g) while refluxing. The mixture became homogeneous at reflux and precipitated after approximately three hours. The light tan bismaleimide precipitate was washed in 4 liters of (1:3 v/v) hot methanol/water, filtered and washed several times in hot methanolic water. The p-[bis(m-maleimidophenoxybenzoyl)]benzene was vacuum oven dried for 48 hours at 60°C. Para-[bis(m-maleimidophenoxybenzoyl)]benzene: yield 92%; DSC @ 10°C/min: T_m 203°C; FTIR (KBr) maleimide (C=O) stretch at 1716 cm^{-1}, benzoyl carbonyl stretch at 1648 cm^{-1}, maleimide (=C-H) stretch at 3070 cm^{-1}; ^{1}H-NMR ($CDCl_3$) maleimide protons at 6.8 ppm; ^{13}C-NMR ($CDCl_3$) carbonyl carbons at 169.58 ppm, benzoyl carbons at 195 ppm.

e. Para-[bis(para-maleimidophenoxybenzoyl)]benzene was synthesized by the same procedure as described above for p-[bis(m-maleimidophenoxybenzoyl)]benzene with the following changes. Para-[bis(p-maleimidophenoxybenzoyl)]benzene was prepared in a 1 liter four-neck round bottom flask. Para-[bis(p-aminophenoxybenzoyl)]benzene (0.0500 mole), maleic anhydride (0.1200 mole) and acetone (234 ml) were used to form the intermediate bismaleamic acid. The bismaleimide was then prepared by the addition of acetic anhydride (35.1 ml) and sodium acetate (2.2 g). Para-[bis(p-maleimidophenoxybenzoyl)]benzene: yield 94%; FTIR (KBr) maleimide (C=O) stretch at 1716 cm^{-1}, benzoyl carbonyl stretch at 1648 cm^{-1}, maleimide (=C-H) stretch at 3070 cm^{-1}; ^{1}H-NMR ($CDCl_3$) maleimide protons at 6.8 ppm; ^{13}C-NMR [$(CD_3)_2SO$] carbonyl carbons at 169.86 ppm, benzoyl carbons at 193 ppm.

f. Para-[bis(maleimidophenylisopropylidenephenoxybenzoyl)]benzene was synthesized by the same procedure as described above for p-[bis(m-maleimidophenoxybenzoyl)]benzene with the following changes. Para-[bis(maleimidophenylisopropylidenephenoxybenzoyl)]benzene was prepared in a 100 ml three-neck round bottom flask. Para-bis[(aminophenylisopropylidenephenoxybenzoyl)]benzene (0.0068 mole), maleic anhydride (0.0163 mole) and acetone (34 ml) were used to form the intermediate bismaleamic acid. The

bismaleimide was then prepared by the addition of acetic anhydride (5.0 ml) and sodium acetate (0.41 g). Para-[bis(maleimidophenylisopropylidenephenoxybenzoyl)]benzene: yield 90%; DSC @ 10°C/min: T_m 112°C; FTIR (KBr) maleimide (C=O) stretch at 1716 cm^{-1}, benzoyl carbonyl stretch at 1655 cm^{-1}, maleimide (=C-H) stretch at 3070 cm^{-1}; ^1H-NMR ($CDCl_3$) maleimide protons at 6.8 ppm; ^{13}C-NMR [$(CD_3)_2SO$] carbonyl carbons at 169.53 ppm, benzoyl carbons at 194.59 ppm.

3. Cycloaliphatic Bismaleimides

a. 4,4'-Methylenebis(cyclohexylmaleimide)-

20 was prepared in a 250 ml four-neck round bottom flask equipped with a water condenser, nitrogen inlet, overhead mechanical stirrer and a thermometer. The liquid 4,4'-methylenebis(cyclohexylamine) (5.0000 g), maleic anhydride (5.6012 g) and acetone (68 ml) were added to the reactor and stirred. The reaction was homogeneous for the first five minutes, then precipitated out of solution as the intermediate bismaleamic acid. The reaction was stirred for an additional hour. The bismaleimide was prepared *in situ* by the addition of acetic anhydride (17 ml) and sodium acetate (1.4 g) while refluxing. Once the acetic anhydride and sodium acetate were added to the bismaleamic acid and brought up to reflux in acetone, the mixture became homogeneous. The reaction was refluxed for three hours. The reaction mixture was filtered and the resulting homogeneous brown solution was

precipitated in water using a blender and rewashed several times with water. The light brown bismaleimide precipitate was vacuum oven dried for 48 hours at 60°C. 4,4'-Methylenebis(cyclohexylmaleimide)-20: yield 94%; FTIR (KBr) maleimide (C=O) stretch at 1703 cm^{-1}, maleimide (=C-H) stretch at 3090 cm^{-1}; ^{1}H-NMR [$(CD_3)_2SO$] maleimide protons at 6.9 ppm; ^{13}C-NMR [$(CD_3)_2SO$] carbonyl carbons at 169 ppm.

b. 4,4'-Methylenebis(cyclohexylmaleimide)-48 was prepared in the same manner as described above for 4,4'-methylenebis(cyclohexylmaleimide)-20. The liquid 4,4'-methylenebis(cyclohexylamine)-48 (5.0000 g), maleic anhydride (5.6012 g) and acetone (68 ml) were used to form the intermediate bismaleamic acid. While the bismaleimide was prepared by the addition of acetic anhydride (17 ml) and sodium acetate (1.4 g). 4,4'-Methylenebis(cyclohexylmaleimide)-48: yield 94%; FTIR (KBr) maleimide (C=O) stretch at 1703 cm^{-1}, maleimide (=C-H) stretch at 3090 cm^{-1}; ^{1}H-NMR [$(CD_3)_2SO$] maleimide protons at 6.9 ppm; ^{13}C-NMR [$(CD_3)_2SO$] carbonyl carbons at 171 ppm.

c. (2,2',5,5'-Tetramethylmethylenebis-(cyclohexylmaleimide) was prepared in the same manner as described above for 4,4'-methylenebis(cyclohexylmaleimide)-20. The liquid 2,2',5,5'-tetramethylmethylenedi(cyclohexylamine) (5.0000 g), maleic anhydride (4.4520 g) and acetone (60 ml) were used to form the intermediate

bismaleamic acid. While the bismaleimide was prepared by the addition of acetic anhydride (27 ml) and sodium acetate (2.3 g). 2,2',5,5'-Tetramethylmethylenedi(cyclohexylmaleimide): yield 90%; FTIR (KBr) maleimide (C=O) stretch at 1710 cm^{-1}, maleimide (=C-H) stretch at 3090 cm^{-1}; ^{1}H-NMR [$(CD_3)_2SO$] maleimide protons at 6.9 ppm; ^{13}C-NMR [$(CD_3)_2SO$] carbonyl carbons at 171 ppm.

e. 1,3-Bis(maleimidomethyl)cyclohexane was prepared in the same manner as described above for 4,4'-methylenebis(cyclohexylmaleimide)-20. The liquid 1,3-bis(aminomethyl)cyclohexane (5.0000 g), maleic anhydride (8.2861 g) and acetone (85 ml) were used to form the intermediate bismaleamic acid. While the bismaleimide was prepared by the addition of acetic anhydride (25 ml) and sodium acetate (2.1 g). 1,3-Bis(maleimidomethyl)cyclohexane: yield 32%; FTIR (KBr) maleimide (C=O) stretch at 1730 cm^{-1}, maleimide (=C-H) stretch at 3090 cm^{-1}; ^{1}H-NMR [$(CD_3)_2SO$] maleimide protons at 6.9 ppm; ^{13}C-NMR [$(CD_3)_2SO$] carbonyl carbons at 171 ppm.

f. (3,3'-Dimethyl-4,4'-dimaleimidodicyclo-hexylmethane was prepared in the same manner as described above for 4,4'-methylenebis(cyclohexylmaleimide)-20. The liquid 3,3'-dimethyl-4,4'-diaminodicyclohexylmethane (5.0000 g), maleic anhydride (4.9422 g) and acetone (64 ml) were used to form the intermediate bismaleamic acid. While the

bismaleimide was prepared by the addition of acetic anhydride (30 ml) and sodium acetate (2.5 g). 3,3'-Dimethyl-4,4'-dimaleimidodicyclohexylmethane: yield 97%; FTIR (KBr) maleimide (C=O) stretch at 1710 cm^{-1}, maleimide (=C-H) stretch at 3090 cm^{-1}; ^{1}H-NMR [$(CD_3)_2SO$] maleimide protons at 6.9 ppm; ^{13}C-NMR [$(CD_3)_2SO$] carbonyl carbons at 165 ppm.

h. 4,4'-Methylene(maleimidobenzyl)cyclohexylmaleimide was prepared in the same manner as described above for 4,4'-methylenebis(cyclohexylmaleimide)-20. The liquid 4,4'-methylene(aminobenzyl)cyclohexylamine (5.0000 g), maleic anhydride (5.7660 g) and acetone (69 ml) were used to form the intermediate bismaleamic acid. While the bismaleimide was prepared by the addition of acetic anhydride (17 ml) and sodium acetate (1.5 g). 4,4'-methylene-(maleimidobenzyl)cyclohexylmaleimide: yield 93%; FTIR (KBr) maleimide (C=O) stretch at 1716 cm^{-1}, maleimide (=C-H) stretch at 3090 cm^{-1}; ^{1}H-NMR [$(CD_3)_2SO$] maleimide protons at 7.1 ppm; ^{13}C-NMR [$(CD_3)_2SO$] carbonyl carbons at 169 ppm.

C. Maleimide-terminated Poly(arylene ether ketones)

1. Synthesis of Amine-terminated Poly(arylene ether ketones) A series of three amine-terminated poly(arylene ether ketones) with a bisbenzoylbenzene/bis A repeat unit (see Scheme 14 and Figure 66 for repeat unit) of n = 5, 10 and 20 for calculated molecular weights of 2,900,

5,500 and 10,500 g/mole were prepared for subsequent imidization to the maleimide moieties. Molecular weight control was calculated according to the Carother equation via addition of a monofunctional reagent (176). The procedure was the same for all three amine-terminated systems; only the 5,500 g/mole will be outlined.

A 1 liter four-neck round bottom flask was fitted with a Dean Stark trap, water condenser, nitrogen inlet, overhead mechanical stirrer and a thermometer. The activated halide p-[bis(4-fluorobenzoyl)]benzene (51.5694 g) was added to the flask followed by the addition of bis A (33.0494 g); m-aminophenol. Next, potassium carbonate (29.3 g) and dimethylacetamide (475 ml) and toluene (119 ml) were added to the reactor. The Dean Stark was filled with toluene. The system was refluxed at 145°C for 4 hours with the observance of water collecting into the Dean Stark trap. Toluene was removed from the trap until the reaction temperature increased to 155°C. The reaction was the allow to proceed for another 8 hours. The solution was filtered to remove the inorganic salts and the filtrate was neutralized with acetic acid. The filtrate was reduced in volume by distilling using a Buchi rotovapor apparatus and precipitated in a 25/75 (v/v) ratio of methanol to distilled water in a blender. The polymer was vacuum oven dried at 60°C for 24 hours. The yield was 96%.

2. Synthesis of Maleimide-terminated Poly(arylene ether ketones) The series of three amine-terminated poly(arylene ether ketones) described above were imidized by the following procedure as described for the 5,500 g/mole amine-terminated polymer.

Amine-terminated poly(arylene ether ketone) (25 g) was added to a 500 ml round bottom flask fitted with a water condenser, an inverse Dean Stark trap, overhead mechanical stirrer, nitrogen inlet and a thermometer. Next, maleic anhydride (1.2 g) and 118 ml of chlorobenzene was added to the reactor, stirred for 1 hour and refluxed for 24 hours. The solution was reduced in volume using a Buchi rotovapor apparatus and precipitated in a 25/75 (v/v) ratio of methanol to distilled water in a blender. The polymer was vacuum oven dried at 60°C for 24 hours.

D. Characterization

1. Proton Nuclear Magnetic Resonance ^{1}H-NMR solution measurements were performed on a high resolution Varian Unity 400 MHz NMR Spectrometer. Samples were dissolved and filtered using deuterated solvents like chloroform or methyl sulfoxide. Peaks were referenced relative to tetramethylsilane.

2. Carbon Nuclear Magnetic Resonance ^{13}C-NMR solution measurements were performed on a high resolution

Varian Unity 400 MHz NMR Spectrometer. Carbon NMR spectra's were routinely run on the same sample used for proton NMR.

3. Fluorine Nuclear Magnetic Resonance ^{19}F-NMR solution measurements were performed on a high resolution Varian Unity 400 MHz NMR Spectrometer. Hexafluorobenzene was used as the internal standard to reference peak locations, i.e., relative to -163 ppm and deuterated chloroform was used as the lock; these were sealed in a glass capillary tube. A sample for measurement was taken directly from reaction flask and pipeted into a NMR tube containing the internal standard capillary tube.

4. Solid-State Nuclear Magnetic Resonance ^{13}C-NMR solid state measurements were taken on a Bruker MSL-200 MHz NMR Spectrometer. Samples were crushed and packed into a spinning rotor for measurements. Measurements were kindly performed by Tom Glass of the Department of Chemistry: Analytical Services at Virginia Tech.

5. High Pressure Liquid Chromatography Monomer purity was determined using a Varian Liquid Chromatograph System 5500. An isocratic mobile reversed phase was employed that generally had the following solvent composition: 60 to 80% THF / 10 to 20% MeOH / 10 to 20% H_2O at room temperature and a flow rate of 1 ml/min. A DuPont Zorbax ODS C_{18} column was used with an RI detector.

6. **Intrinsic Viscosities** analysis were carried out at 25°C in a Ubbelohde viscometer generally using chloroform as the solvent.

7. **Fourier Transform Infrared Spectroscopy** (FTIR) measurements were taken on a Nicolet 10-DX Spectrometer. Monomer spectra were obtained from pressed KBr discs, while polymer spectra were taken from casted films on NaCl plates. Twenty-seven accumulated scans were routinely taken from 4000-600 cm^{-1} with a resolution of 4 cm^{-1} for each FTIR spectra.

8. **Differential Scanning Calimetry** (DSC) A Perkin-Elmer DSC-7 calorimeter was used to obtain thermograms of the crystalline endothermic melting temperature (T_m) and the exothermic heat of cure: (T_{exo}) maximum peak of cure, (T_1) on-set temperature for curing, and (T_2) temperature for completion of cure. The area under the exothermic DSC curve was used as the measure of the heat of curing (ΔH, curing). Thermograms were obtained at either 5 or 10°C/min. in a nitrogen atmosphere. Crimped aluminum Perkin-Elmer pans were used for routine analysis, while Perkin-Elmer high pressure screw-type pans were used for volatile samples. Temperature and enthalpy calibrations were performed using indium and zinc standards. Many thanks to Tom Danaher of the Perkin-Elmer Corp. and Dr. Robert O. Waldbauer (now at DuPont) for showing me the ropes of thermal analysis.

9. Thermogravimetric Analysis (TGA) were determined on a Perkin-Elmer Thermogravimetric Analyzer TGA-7. The TGA-7 was calibrated for temperature using nickel and perkalloy standards. Thermograms were performed at 10°C/min. in air or nitrogen atmospheres. Samples for TGA measurements were generally cut from sample bars that were prepared for DMTA analysis as described below.

10. Thermal Mechanical Analysis (TMA) were performed on a Perkin-Elmer Thermogravimetric Analyzer TMA-7. The TMA-7 was calibrated for temperature using indium and zinc standards. Thermograms were run at 10°C/min. in the penetration mode with a force of 2500 mN. Samples for TMA measurements were generally cut from sample bars that were prepared for DMTA analysis as described below.

11. Dynamic Mechanical Thermal Analysis (DMTA) DMTA's were obtained on a Polymer Laboratory Dynamic Mechanical Thermal Analyzer. Typically, bismaleimide sample bars (2.27 x 12.62 x 8.00 mm or 2.63 x 6.34 x 14.00 mm) were first formed in rubber molds by melting the samples in a vacuum oven and then cured at 220°C for 8 hours under vacuum. The bars were then removed from the molds and post-cured at 300°C for 4 hours using a convection oven in an air atmosphere. The dynamic mechanical behavior (log storage modulus ε' and log tan δ) was plotted as a function of temperature at a heating rate of 1°C/min. at 1 Hz. The

samples were mounted using a single cantilever clamp. The DMTA measurements were kindly run by Steve Wilkinson.

12. Titrations Molecular weights of amine and amic acid functional monomers and polymers were obtained by acid-base potentiometric titrations using a Mitsubishi Chemical Industries Microprocessor-Control Automatic Titrator Model GT-05. HBr was used as the titrant for aromatic amines and amic acids were titrated using tetramethyl ammonium hydroxide. The titrants were standardized with potassium hydrogen phthalate. Endpoints were detected by the first derivative of the potential versus volume titration curve. Amine samples were dissolved in chloroform, while amic acid samples were dissolved in dimethylacetamide. Three to five samples were generally titrated for each monomer with the average molecular weight taken.

13. Rheological Measurements Complex viscosity (η^*) were obtained from a Rheometrics Mechanical Spectrometer Model RMS-800 at 10 Hz with 1% strain.

IV. Results and Discussion

A. Aromatic Ether Phosphine Oxide Monomers and Thermosets

Aromatic ether phosphine oxide bismaleimides were prepared by a two-step process via synthesis of an aromatic amine and subsequent conversion to the maleimide. These two steps are shown in Scheme 9, for the synthesis of the aromatic diamine and in Scheme 10, for the bismaleimide preparation.

In the first step the diamine was prepared by a modification (189) of the classical aromatic nucleophilic substitution reaction. The activated aryl halide bis(4-fluorophenyl)phenyl phosphine oxide was reacted with the potassium salt of an aminophenol compound forming the ether bond by the displacement of the halide by the aminophenate. In this modification the aminophenate was formed *in situ* using the weak base potassium carbonate instead of sodium hydroxide in the polar aprotic solvent dimethylacetamide. As previously described in Section II.B.3. potassium carbonate reacts with phenols only at elevated temperatures without hydrolysis of the halide. Toluene was used as an efficient azeotroping agent to remove water via a Dean Stark trap. The temperatures employed were typical of those for activated halides in S_NAr reactions (50,189). Fluorine NMR was utilized to determine reaction time, by the disappearance of

Step 1

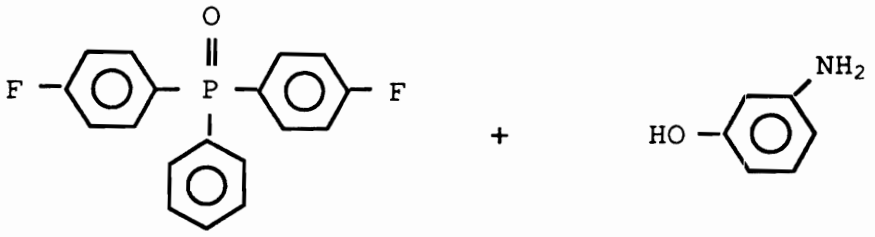

Bis(4-fluorophenyl)-
phenyl phosphine oxide

\+

m-Aminophenol

80:20% v/v DMAC To Toluene @ 20% Solids

K_2CO_3

Temperature: 145°C for 4 hours
155°C for 2 hours

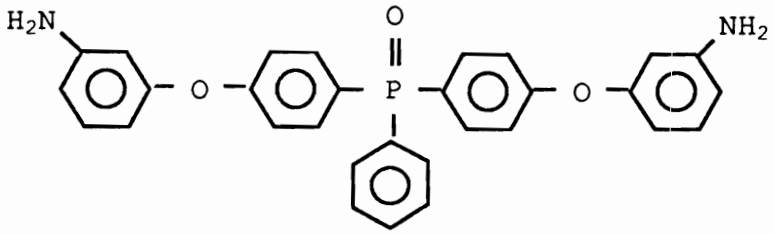

Bis(m-aminophenoxy)triphenyl phosphine oxide

Scheme 9

Synthesis of Bis(m-aminophenoxy)-
triphenyl phosphine oxide

Step 2

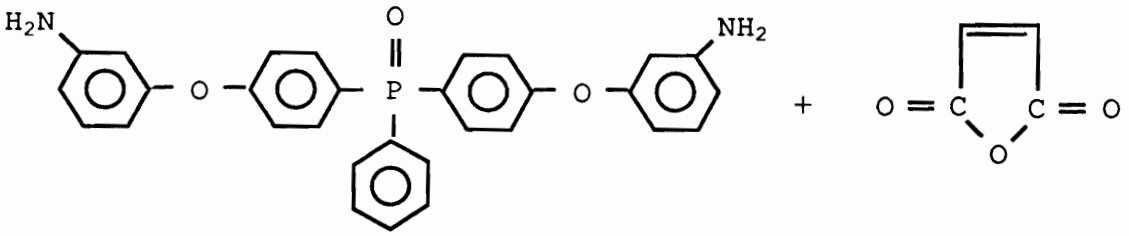

Bis(m-aminophenoxy)-
triphenyl phosphine oxide

Maleic anhydride

Acetone
Room Temperture
1 Hour

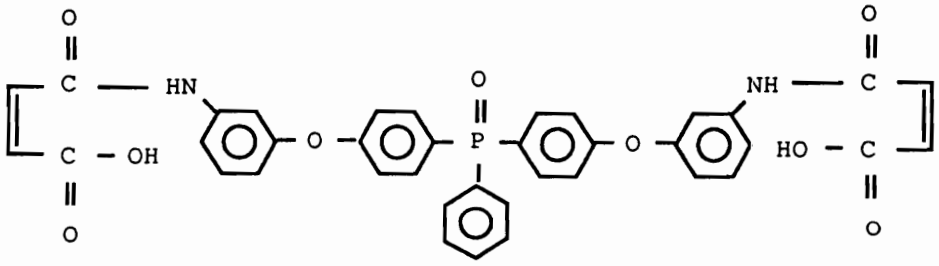

Bis(m-maleamic acid phenoxy)triphenyl phosphine oxide

Scheme 10

Synthesis of Bis(m-maleimidophenoxy)-
triphenyl phosphine oxide

Step 2 (con't)

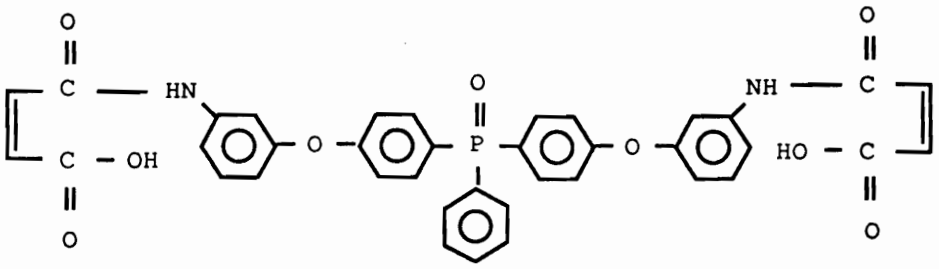

Bis(m-maleamic acid phenoxy)triphenyl phosphine oxide

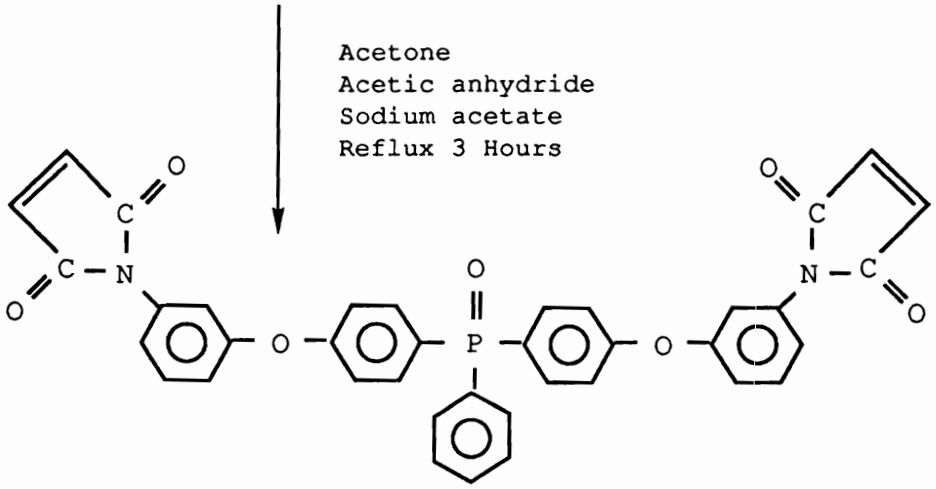

Bis(m-malemidophenoxy)triphenyl phosphine oxide

Scheme 10 (con't)

Synthesis of Bis(m-maleimidophenoxy)-

triphenyl phosphine oxide

of the activated halide's fluorine signal at -104.8 ppm taken at various times during the S_NAr reaction. The reaction appears to be complete in 3-4 hours at 145°C; an additional 2 hours at 155°C was used to ensure completion. A similar fluorine NMR determination of reaction time vs fluorine signal is shown in Figure 56 for p-bis(m-maleimidophenoxybenzoyl)benzene described in Section IV.B.

In the second step, the intermediate bismaleamic acid was formed *in situ* in acetone at room temperature using maleic anhydride. The bismaleimide was then formed by the cyclodehydration of bismaleamic acid using acetic anhydride and sodium acetate as described in Section II.B.4. and outlined in Schemes 8 (Section II.B.4.) and 10. This method of imidization was very convenient, since there was no need to isolate the bismaleamic acid and form the bismaleimide in a different solvent and reactor (148). Once the bismaleamic acid precipitated, acetic anhydride and sodium acetate were brought up to reflux temperature in acetone, the system became homogeneous to form the bismaleimide. A 10 to 20% mole excess of maleic anhydride was used to ensure difunctional maleimide incorporation. Maleic anhydride was easily washed from the final bismaleimide product.

Several structural variations of the ether triphenyl phosphine oxides were prepared by utilizing different aminophenols. Para-aminophenol, meta-aminophenol, a 50/50

mixture of the meta and para-aminophenols and 2,2'-(4-hydroxyphenyl-4-aminophenyl)propane shown below were employed to prepare the diamines. The diamines and succeeding bismaleimides formed from these aminophenols are listed in Tables 15 and 16. All of these monomers were prepared using essentially the same procedures as outlined in Schemes 9 and 10, with high yields (>90%) and high purity (>99%).

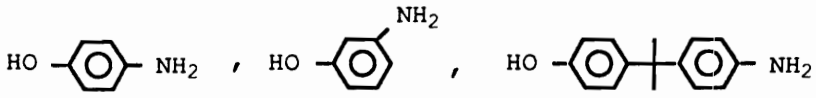

The monomers were characterized by a number of spectroscopic and chromatographic methods to ensure that the intended structures were quantitatively obtained. High pressure liquid chromatography was used to show that monomers were synthesized in high purity by the presence of sharp monomodal chromatographic peaks, for example as shown in Figure 16 for bis(m-aminophenoxy)triphenyl phosphine oxide. Acid-base potentiometric titrations of the diamines and bismaleamic acid confirmed the difunctionality of the monomers and molecular weights as represented in Figure 17 for bis(m-aminophenoxy)triphenyl phosphine oxide. Routinely, titrated molecular weights were within ±2 g/mole for all monomers. No endpoints were detected when bismaleimides were titrated for either amines or amic acids, further indicating conversion and purity of monomers.

Table 15

Structures and Melting Points of

Aromatic Ether Triphenyl Phosphine Oxide Diamines

Bis(aminophenoxy)-triphenyl phosphine oxides	T_m (°C), DSC
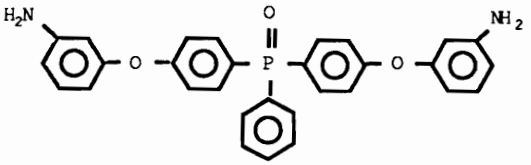	84
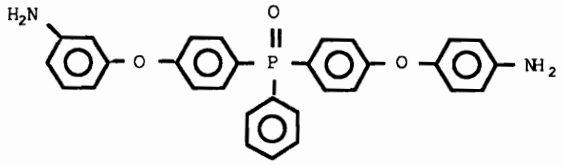	83
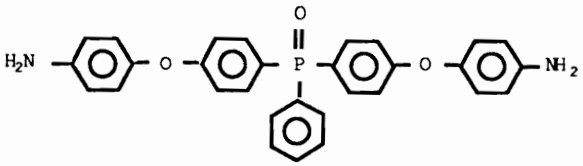	98
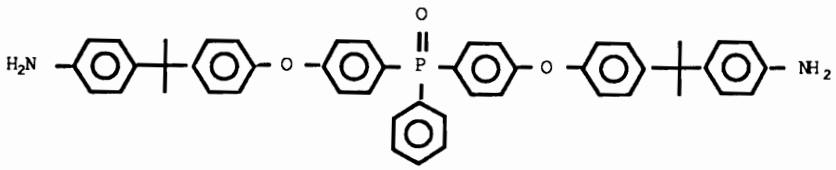	90

Table 16

Structures and DSC Thermal Data of

Aromatic Ether Triphenyl Phosphine Oxide Bismaleimides

Bis(maleimidophenoxy)-triphenyl phosphine oxides	T_m(or T_g)	T_1	T_1-T_m(or T_g)
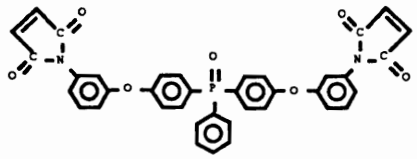	92	180	88
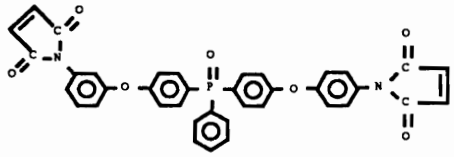	93	180	87
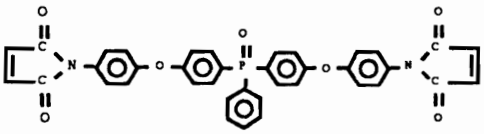	107(T_g)	180	73
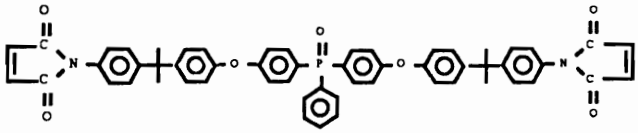	113(T_g)	180	67

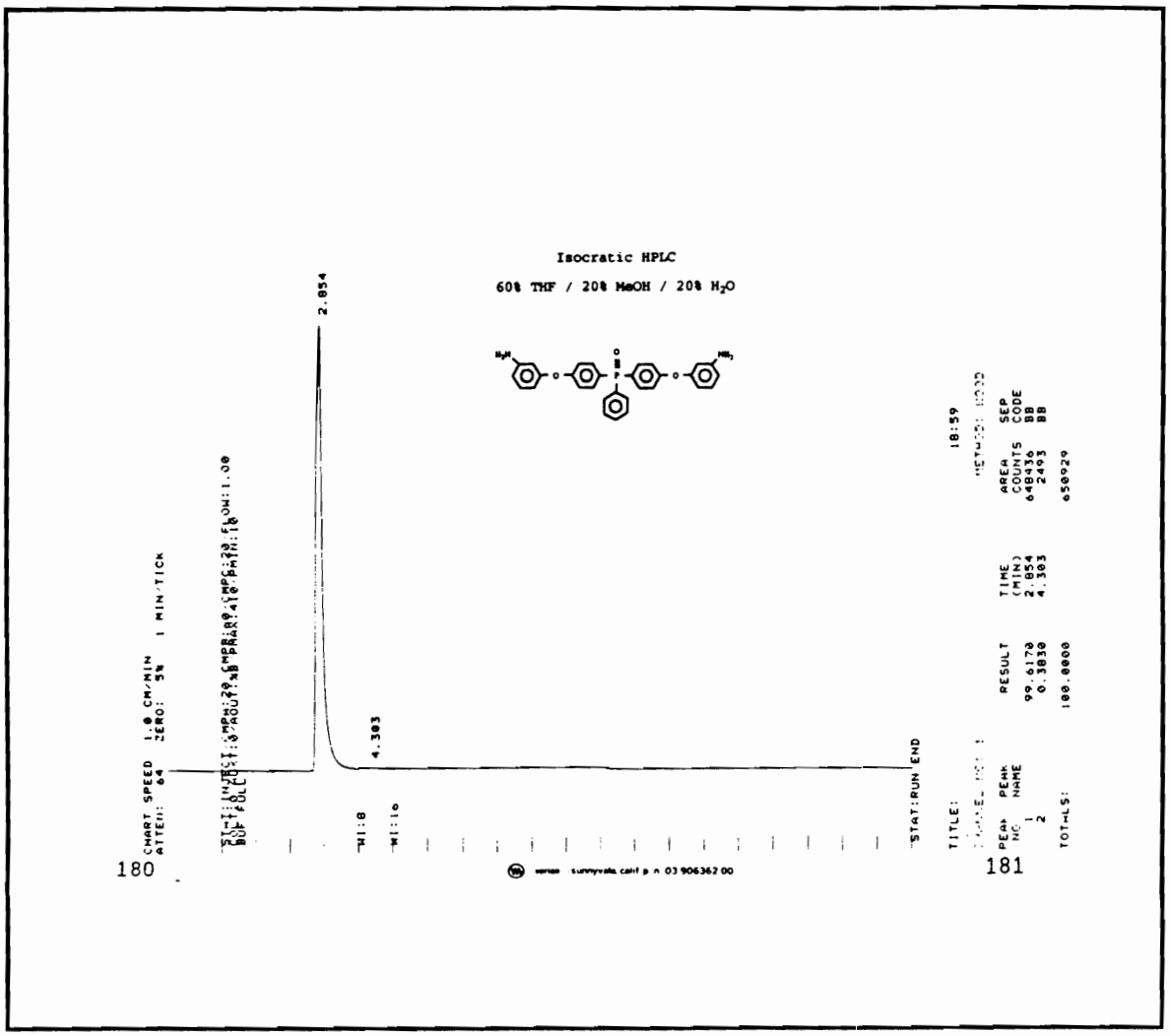

Figure 16

HPLC of Bis(m-aminophenoxy)-

triphenyl phosphine oxide

Amine Titrating Reagent: HBr
Sample Solvent: Chloroform

Amic Acid Titrating Reagent: TMAH
Sample Solvent: N,N-Dimethylacetamide

Sample	Calculated MW	Titrated MW
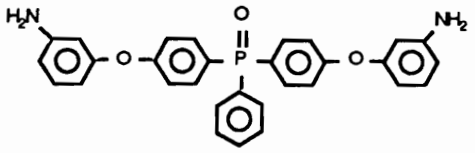	492	491
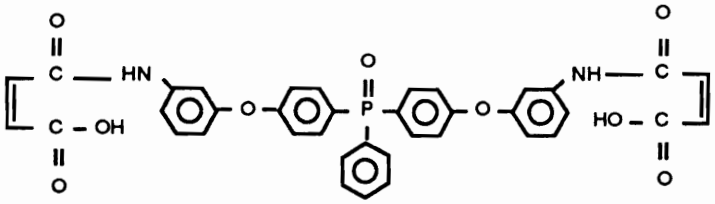	688	689
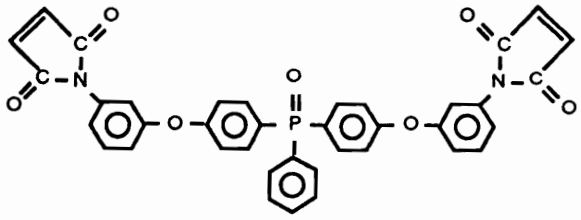	652	No Endpoint Detected

Figure 17

Potentiometric Titrations of

Ether Triphenyl Phosphine Oxide Monomers

Fourier transform infrared and nuclear magnetic resonance spectroscopy were convenient methods in determining the intermediate and bismaleimide structures as well as the progress of these reactions. These spectroscopic techniques were also useful in characterizing the crosslinking reaction.

For example, each stage in the preparation of bismaleimide made from meta-aminophenol is illustrated in Figures 18-21 utilizing FTIR. In Figure 18, for bis(4-fluorophenyl)phenyl phosphine oxide the peaks of interest are the aromatic (C-H) stretching at 3062 cm^{-1}, the (P=O) stretching at 1197 cm^{-1} and the aromatic (C-F) stretching at 1164 cm^{-1} . After reacting the activated halide in the first step, Figure 19 shows the appearance of an aromatic (N-H) stretching at 3336 and 3453 cm^{-1} resulting from the incorporation of the amine from meta-aminophenol and the disappearance of the aromatic (C-F) stretching. While in Figure 20 the appearance of the carbonyl stretching (C=O) from amic acid can be seen at 1716 cm^{-1}. And in Figure 21 the carbonyl and maleimide [(=C-H), @ 3070 cm^{-1}] bands are observed for the final bismaleimide product. Many of the other pertinent bands are identified in Table 3 in Section II.A.5.

For comparison, Figure 22 and Figure 23 show the amine and maleimide FTIR bands, respectively, for the para-,

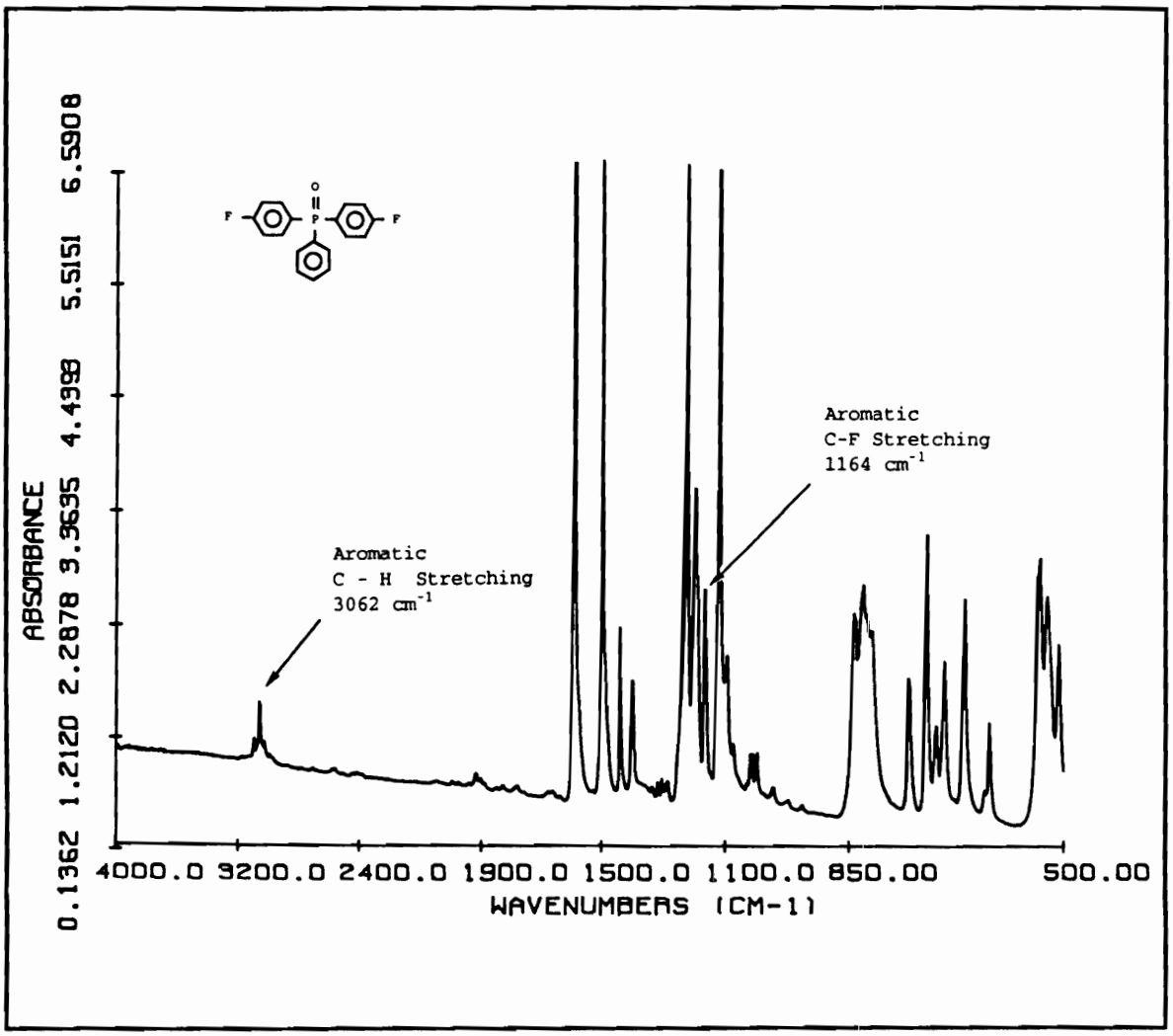

Figure 18

FTIR Spectra of Bis(4-fluorophenyl)-

phenyl phosphine oxide

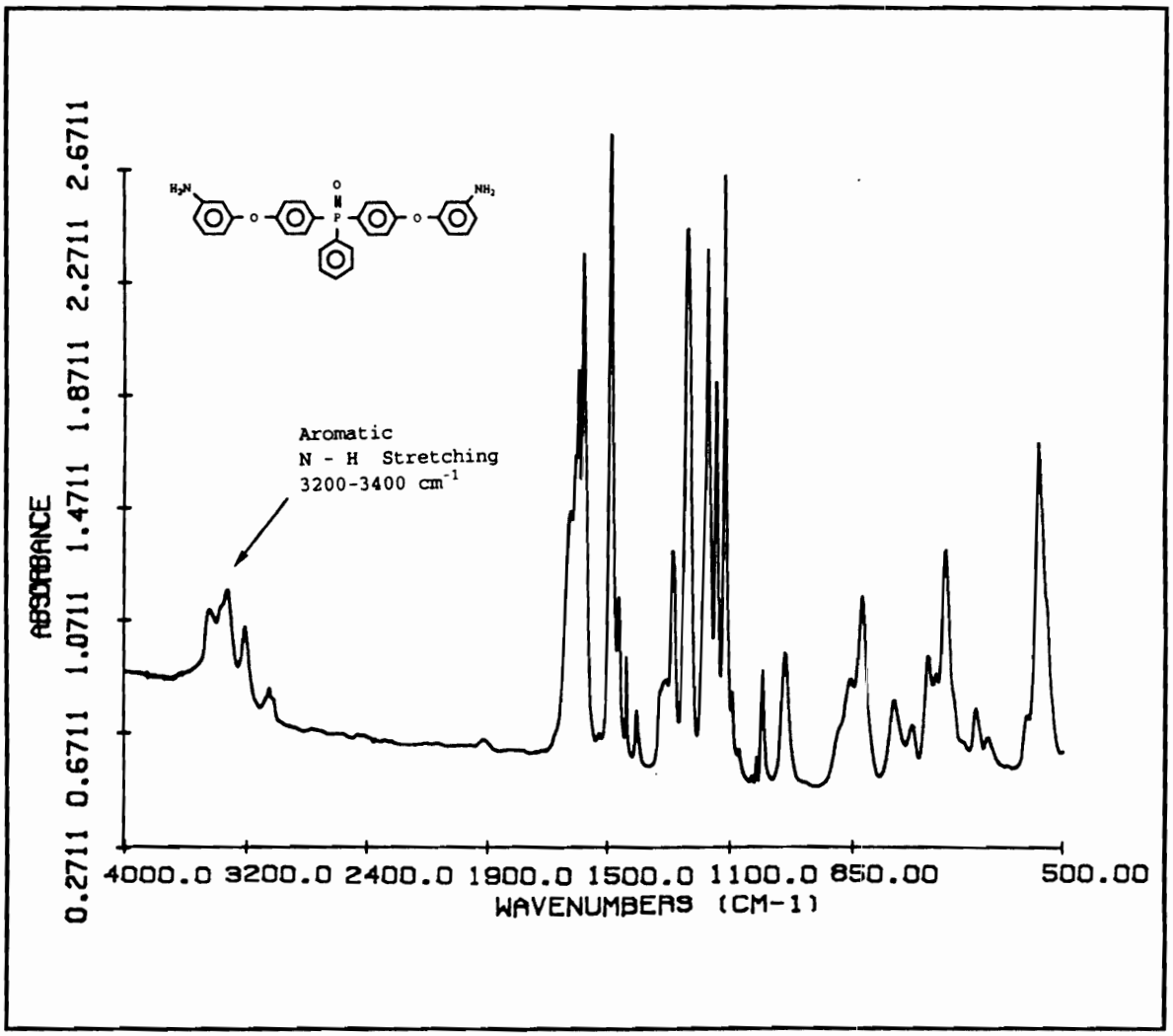

Figure 19

FTIR Spectra of Bis(m-aminophenoxy)-

triphenyl phosphine oxide

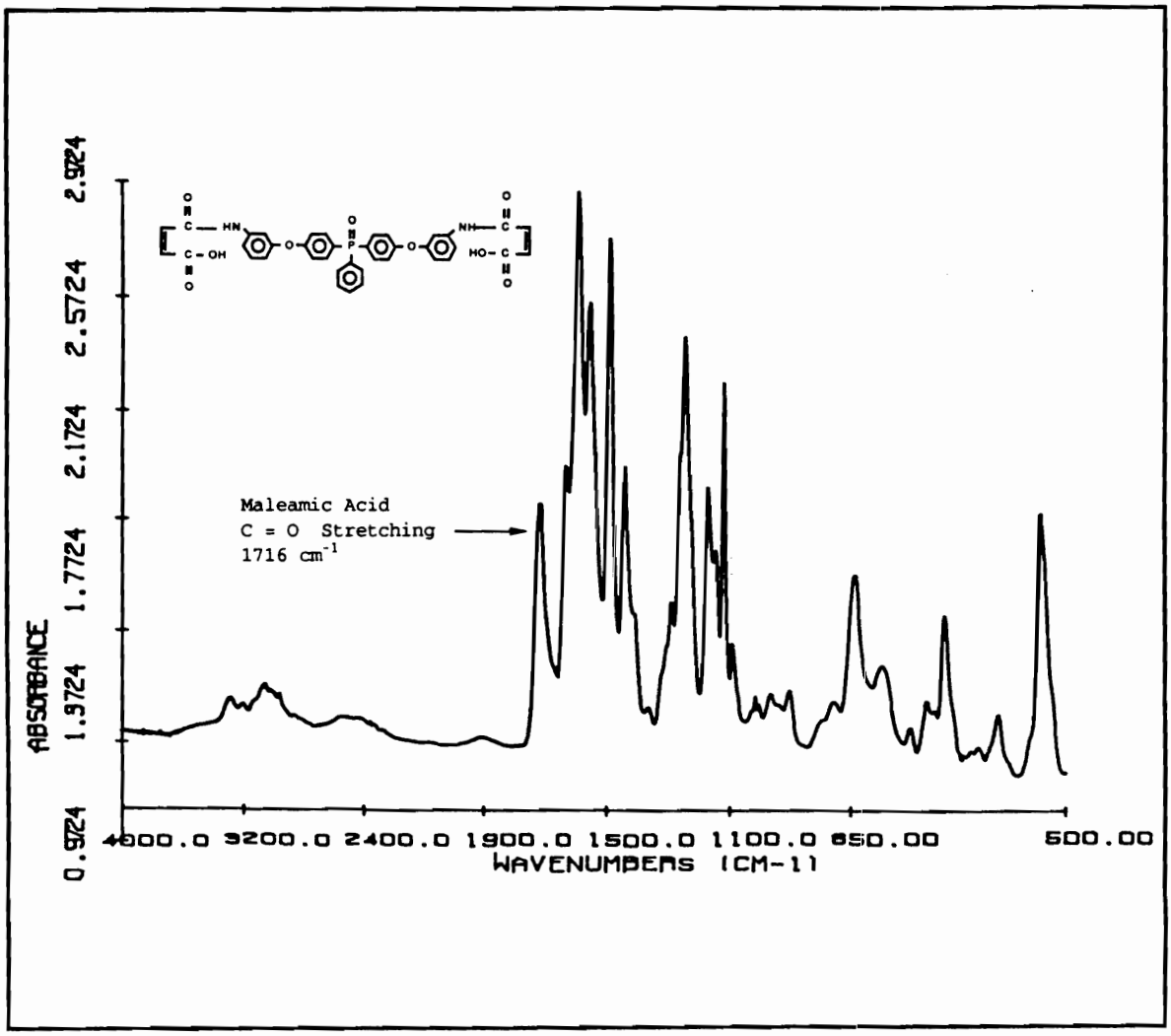

Figure 20

FTIR Spectra of Bis(m-maleamic acid phenoxy)-triphenyl phosphine oxide

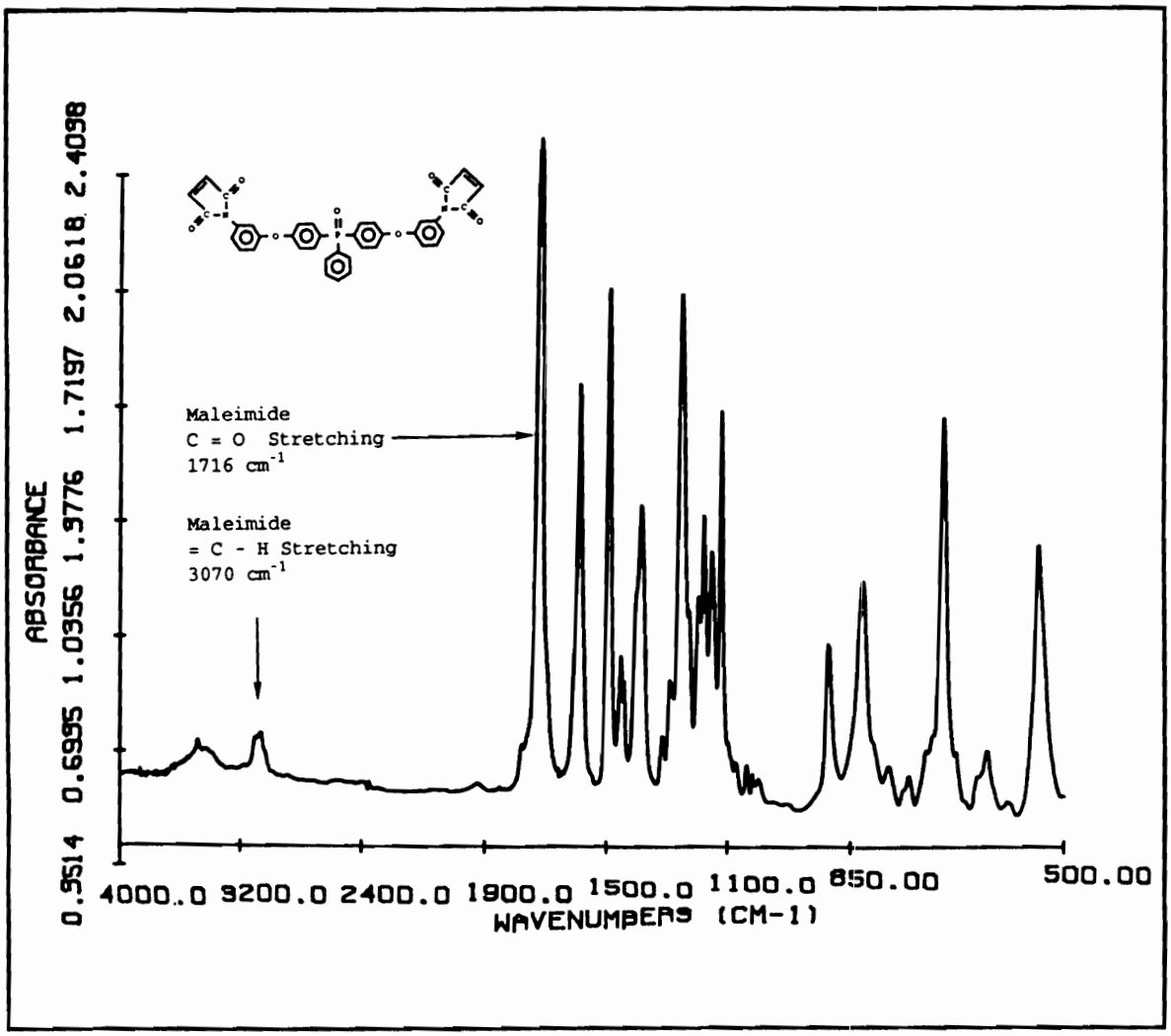

Figure 21

FTIR Spectra of Bis(m-maleimidophenoxy)-triphenyl phosphine oxide

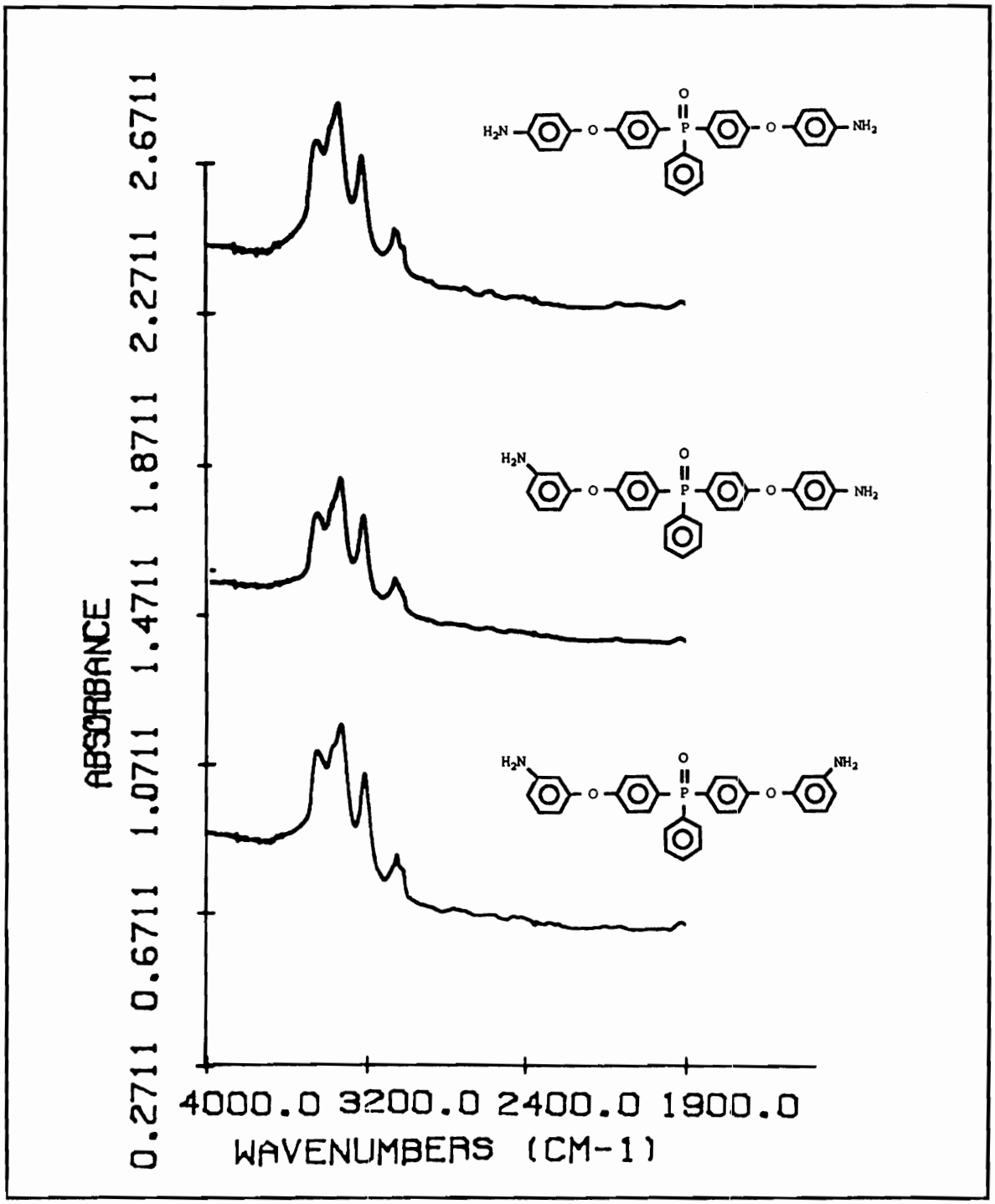

Figure 22

FTIR Comparison of Diamine Phosphine Oxide Isomers

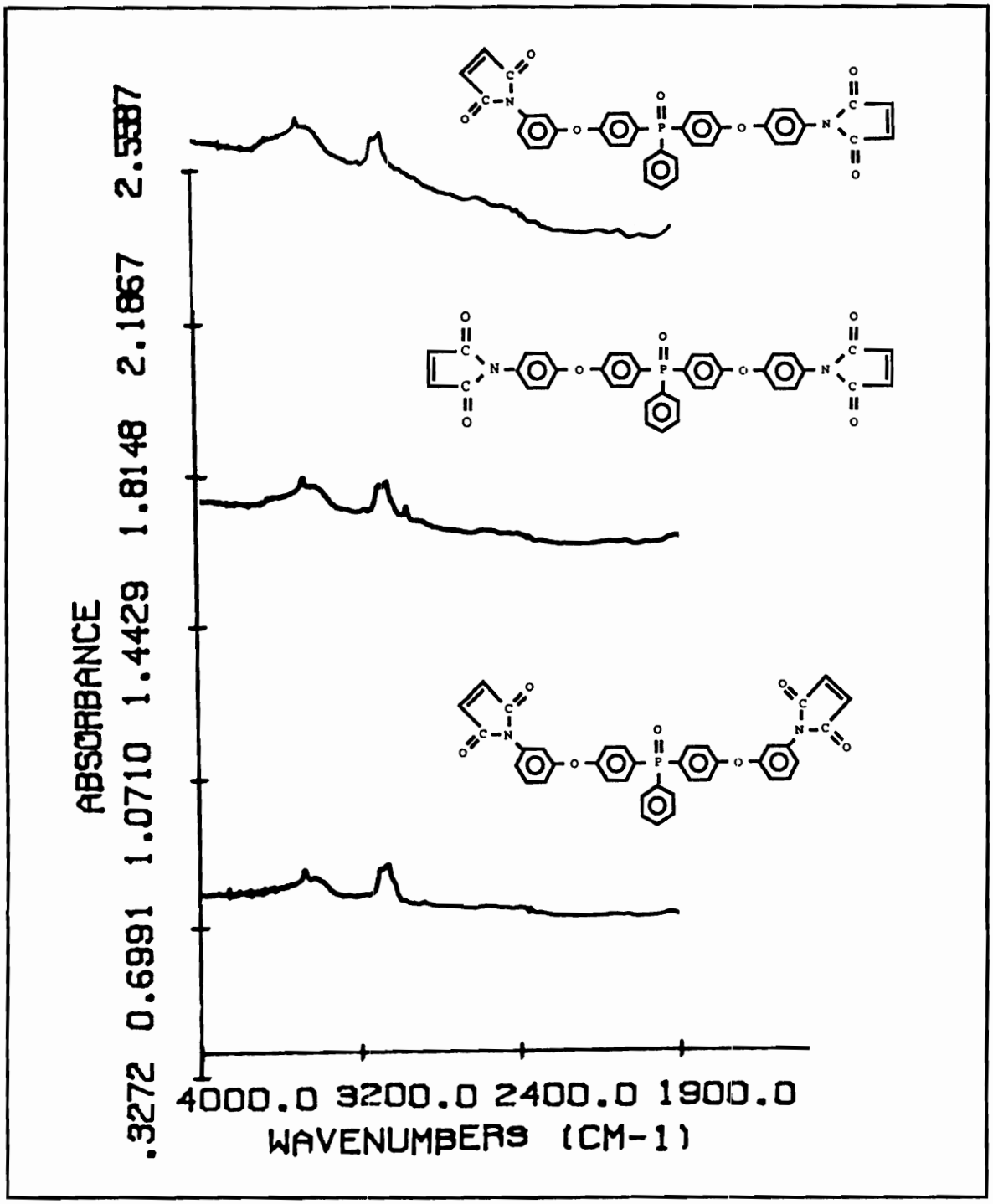

Figure 23

FTIR Comparison of Bismaleimide Phosphine Oxide Isomers

meta,para- and the meta-isomers of the ether triphenyl phosphine oxides. In Figure 22 the bands at 3453 and 3336 cm^{-1} are due to the aromatic amine (N-H) stretching, those at 3220 cm^{-1} to aromatic (C-H) stretching from the aminophenol ring and 3063 cm^{-1} to the aromatic (C-H) stretching on the triphenyl phosphine rings. While in Figure 23 the band at 3070 cm^{-1} is due to the carbon-hydrogen stretching of the maleimide ring for all three isomers.

In a similar manner the diamine and bismaleimide made from 2,2'-(4-hydroxyphenyl-4-aminophenyl)propane shows the characteristic nitrogen-hydrogen stretching and carbon-hydrogen stretching for the amines and maleimides, respectively, as shown in Figure 24. The carbonyl stretching at 1716 cm^{-1} can also be observed for the bismaleimide, as a result of the imidization. Also prominent are the asymmetric (C-H) stretching band at 2967 cm^{-1} resulting from the isopropylidene methyls.

Proton and carbon-NMR also confirmed the desired triphenyl phosphine oxide intermediate and bismaleimide structures. For instance, the proton NMR spectra are shown in Figures 25-27 for the meta derived ether triphenyl phosphine oxide. In Figure 25 for the diamine, the amine protons can be seen at 3.8 ppm, while in Figure 27 for the bismaleimide the amine protons have vanished and the

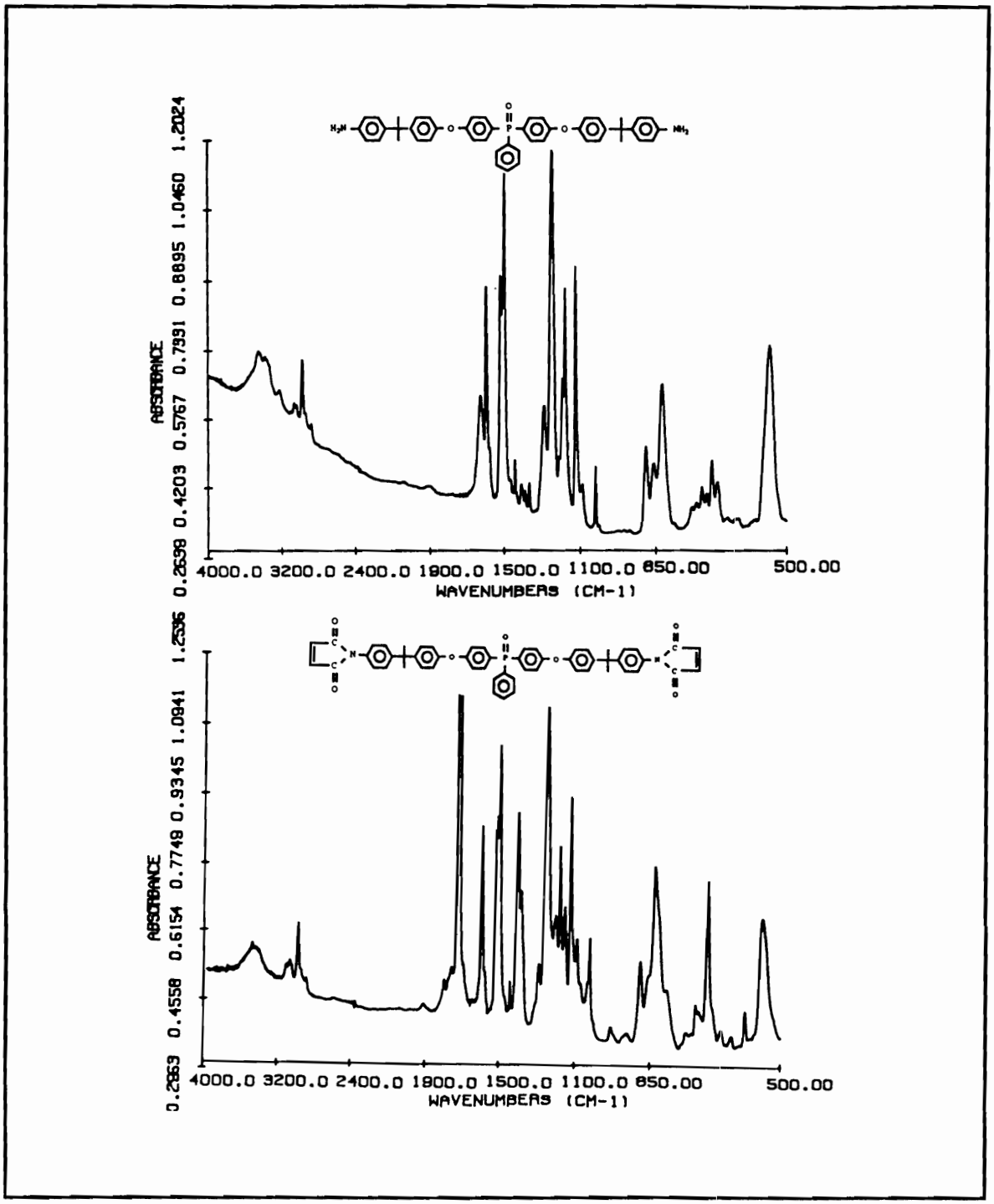

Figure 24

FTIR of 2,2'-(4-Hydroxyphenyl-4-aminophenyl)propane Derived Phosphine Oxide Diamine and Bismaleimide

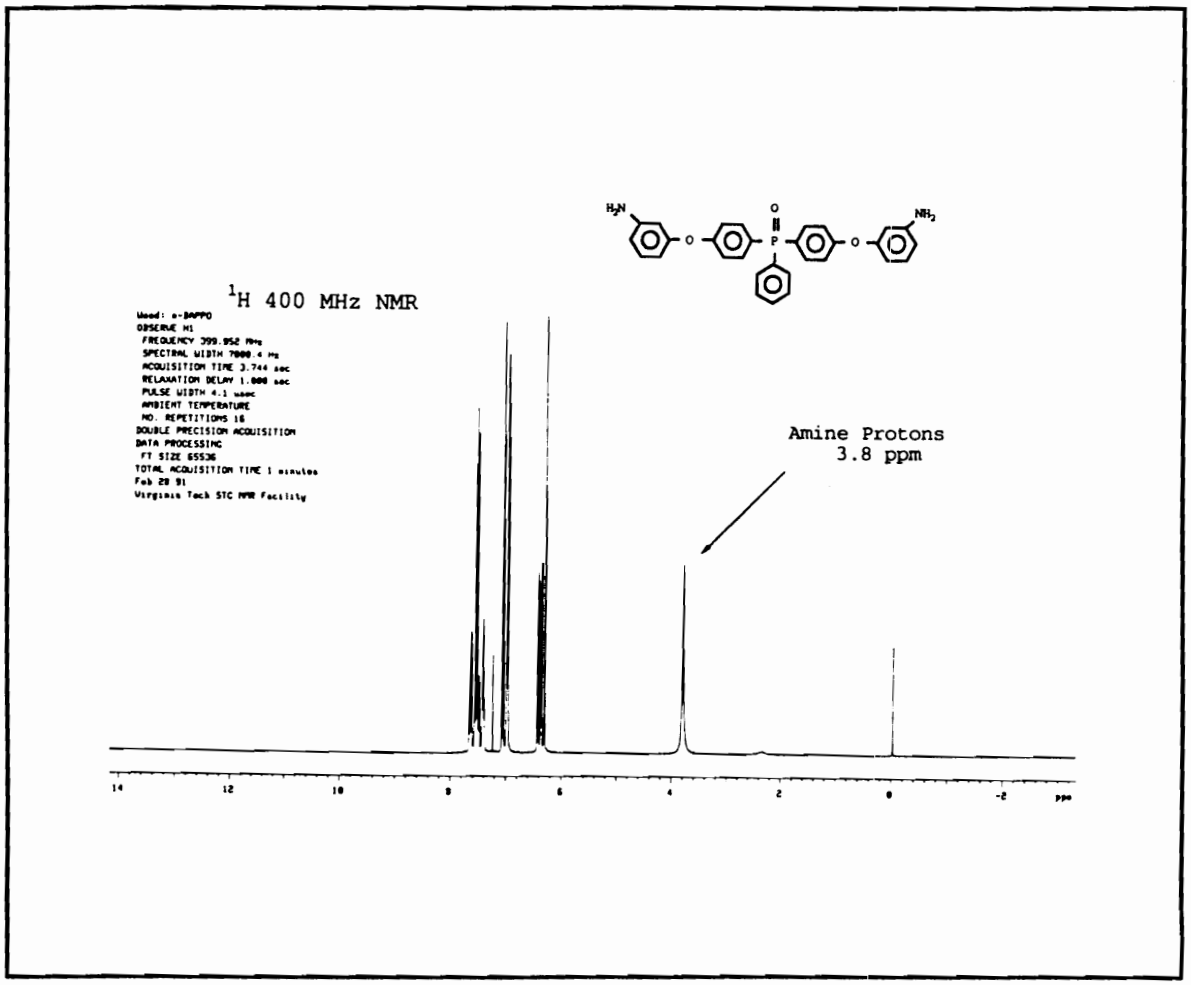

Figure 25

^{1}H-NMR of Bis(m-aminophenoxy)-

triphenyl phosphine oxide

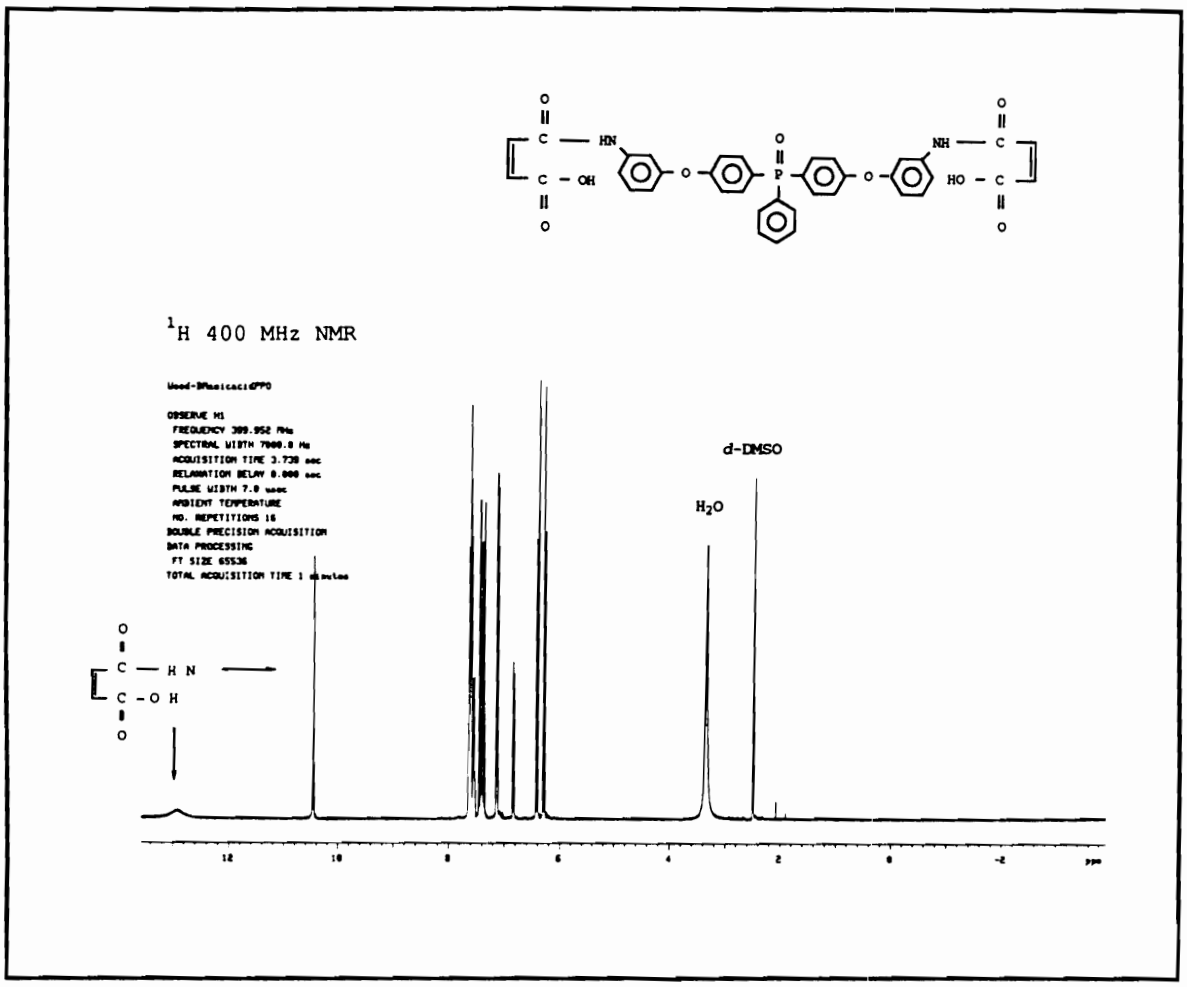

Figure 26

^{1}H-NMR of Bis(m-maleamic acid phenoxy)-triphenyl phosphine oxide

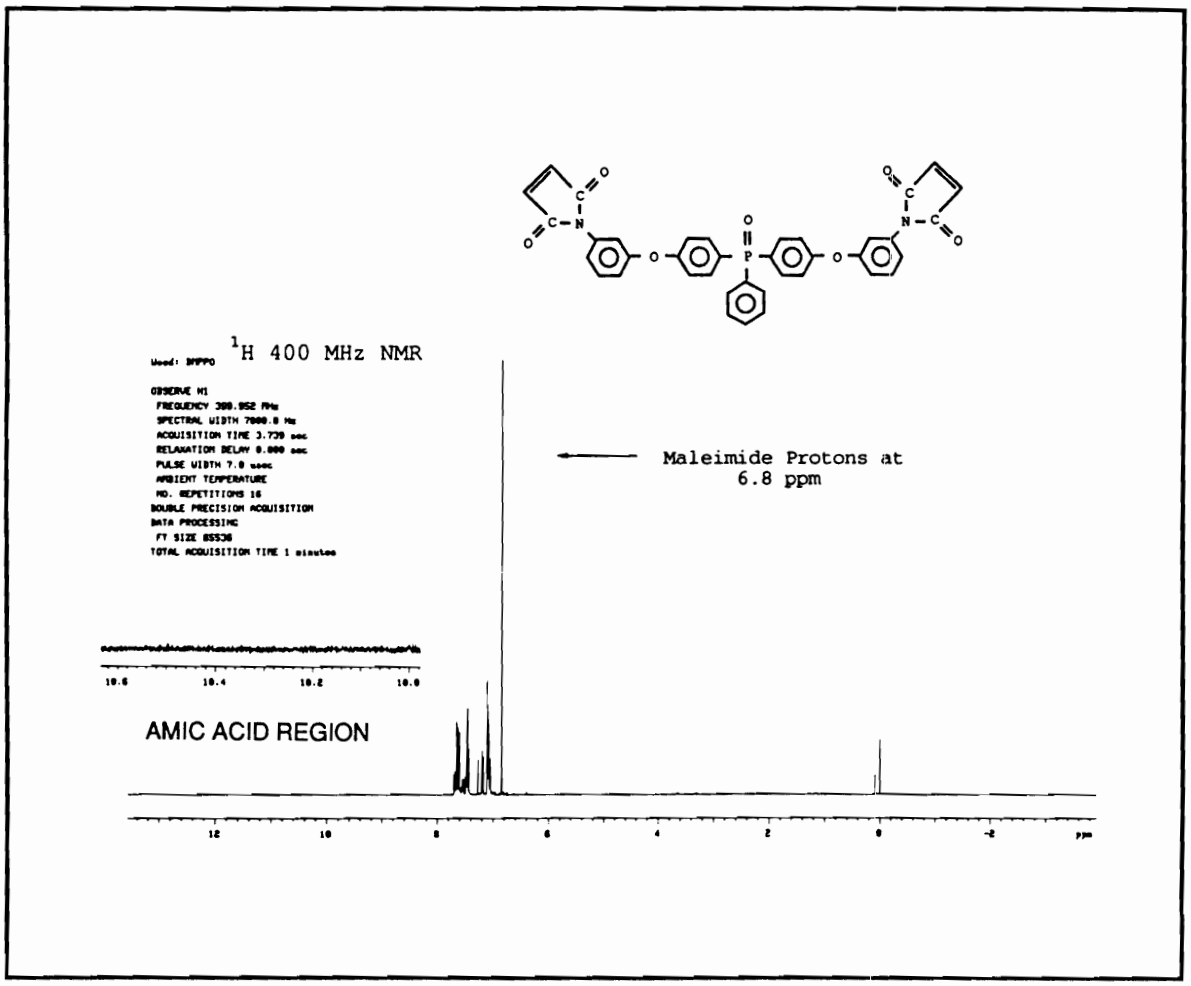

Figure 27

^{1}H-NMR of Bis(m-maleimidophenoxy)-

triphenyl phosphine oxide

maleimide protons appeared at 6.8 ppm. The intermediate bismaleamic acid shown in Figure 26 has the characteristic broad carboxylic protons signal centered at 13.9 ppm and the amide protons at 10.2 ppm. An expanded/enlarged scale of the amic acid region in Figure 27 for the bismaleimide shows that the conversion of bismaleamic acid to bismaleimide is complete with no residual amic acid detected. ^{13}C-NMR for the bismaleimide displays the expected carbonyl carbon at 169 ppm as illustrated in Figure 28.

A comparison of the 400 MHz proton and carbon-NMR for the para-, meta,para- and meta- ether triphenyl phosphine oxide diamines and bismaleimides reveals that the individual isomers can be distinguished as shown in Figures 29-33. The proton spectra to a degree are complicated due to the proton-phosphorus splitting. All spectra have been integrated and peaks assigned and will only be briefly presented here.

In Figure 29, the aromatic region was expanded for the proton spectra of the three diamine isomers. The para-derivative peaks at 6.63 and 6.82 ppm are the ortho protons relative to the oxygen and nitrogen, respectively, from the former p-aminophenol component. While the protons due to the triphenyl phosphine group can be divided into three sections. The group of peaks downfield of 7.6 ppm are the protons ortho to the phosphine oxide group, while the protons ortho to the ether bond are located upfield around 6.9 ppm. The protons

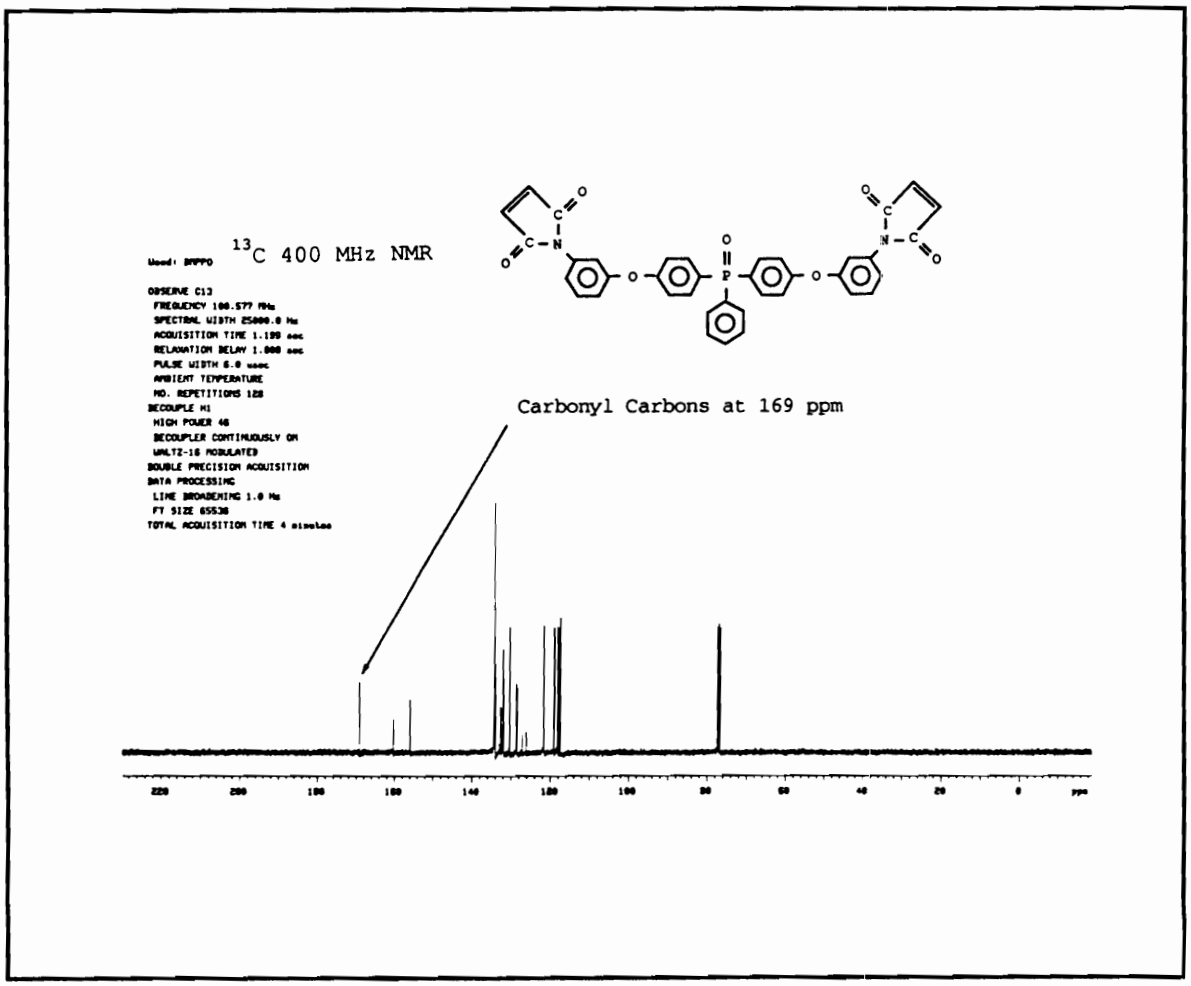

Figure 28

^{13}C-NMR of Bis(m-maleimidophenoxy)-triphenyl phosphine oxide

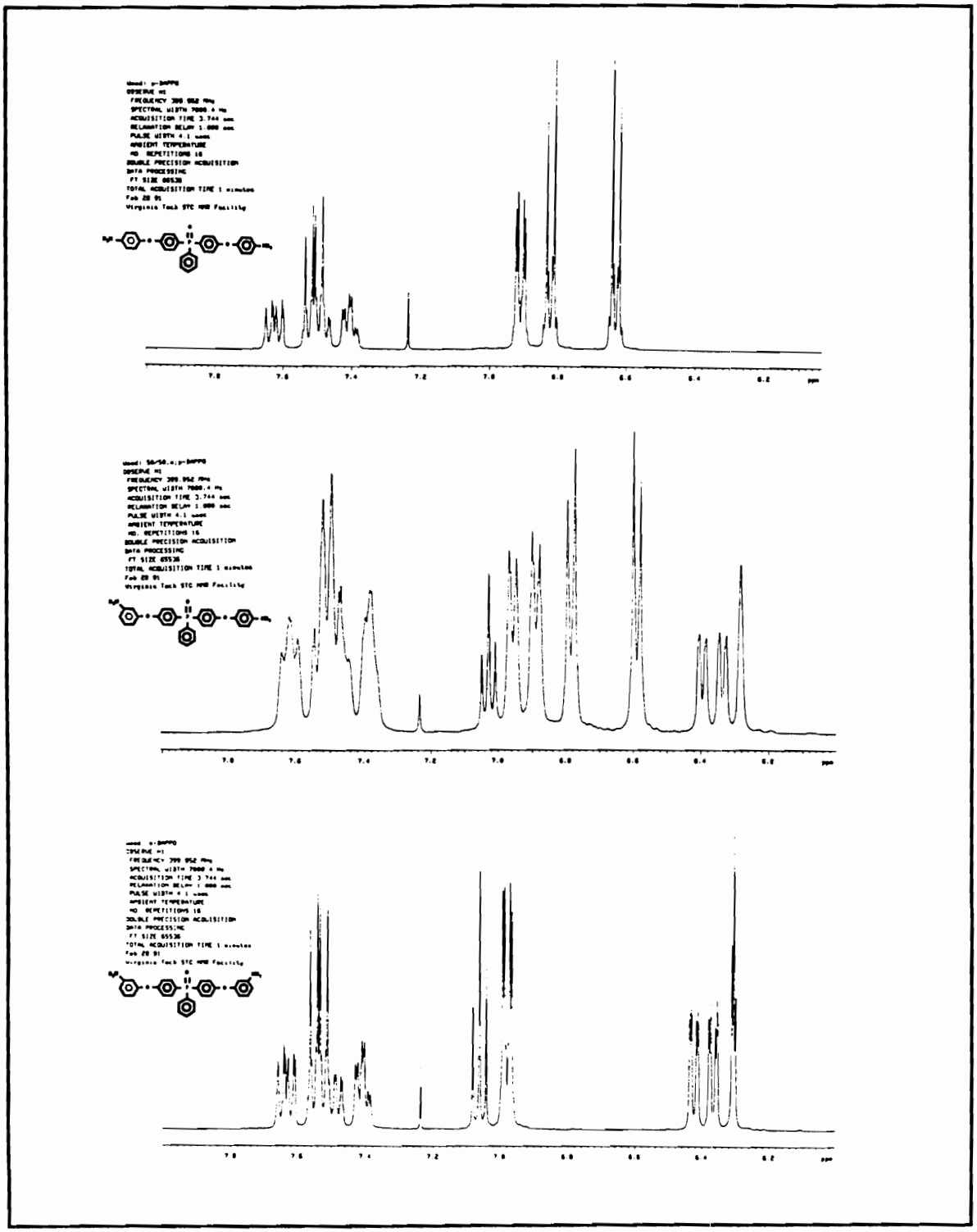

Figure 29

^{1}H-NMR Comparison of Diamine Phosphine Oxide Isomers

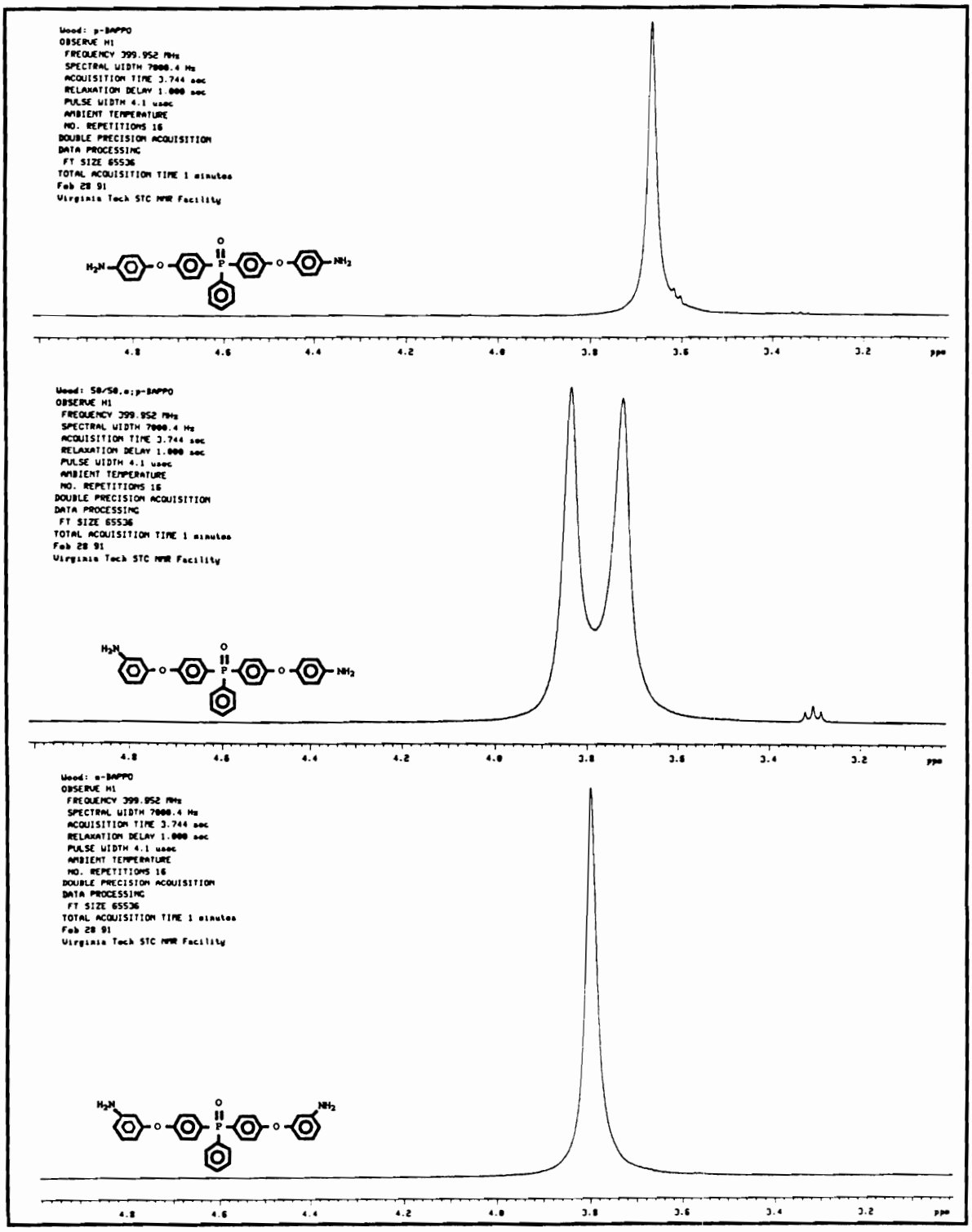

Figure 30

^{1}H-NMR Comparison of Phosphine Oxide Amine Protons

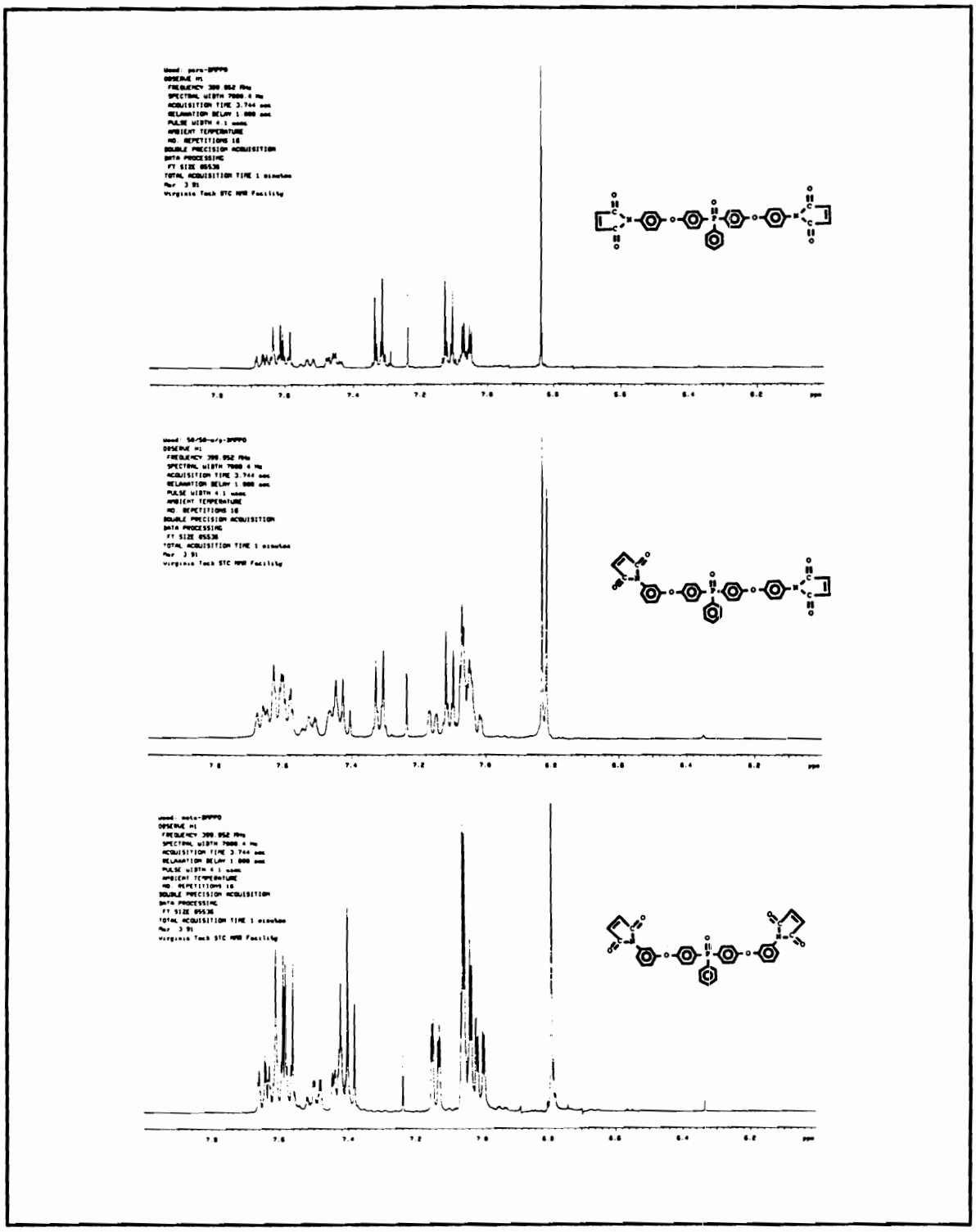

Figure 31

^{1}H-NMR Comparison of Bismaleimide Phosphine Oxide Isomers

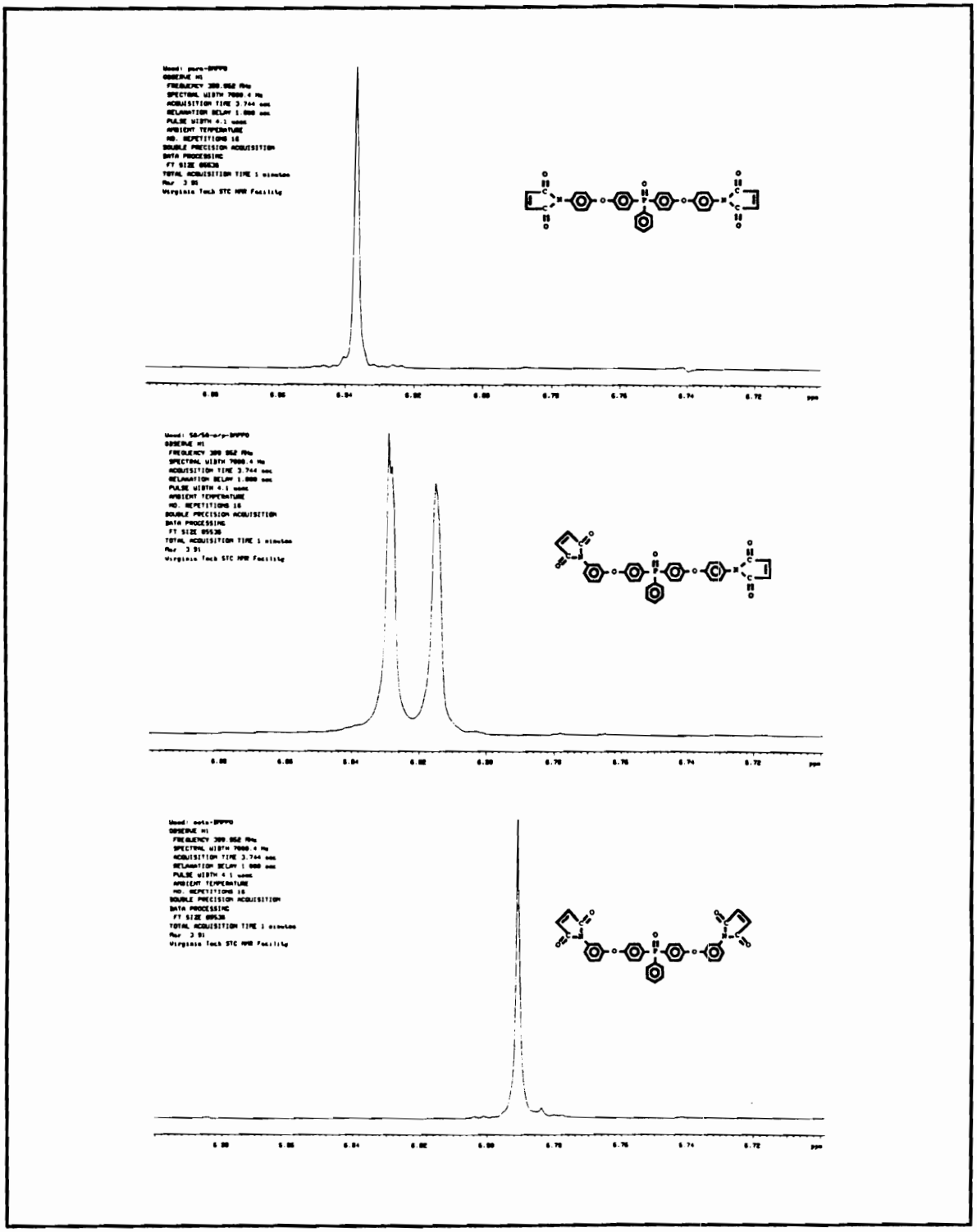

Figure 32

^{1}H-NMR Comparison of Phosphine Oxide Maleimide Protons

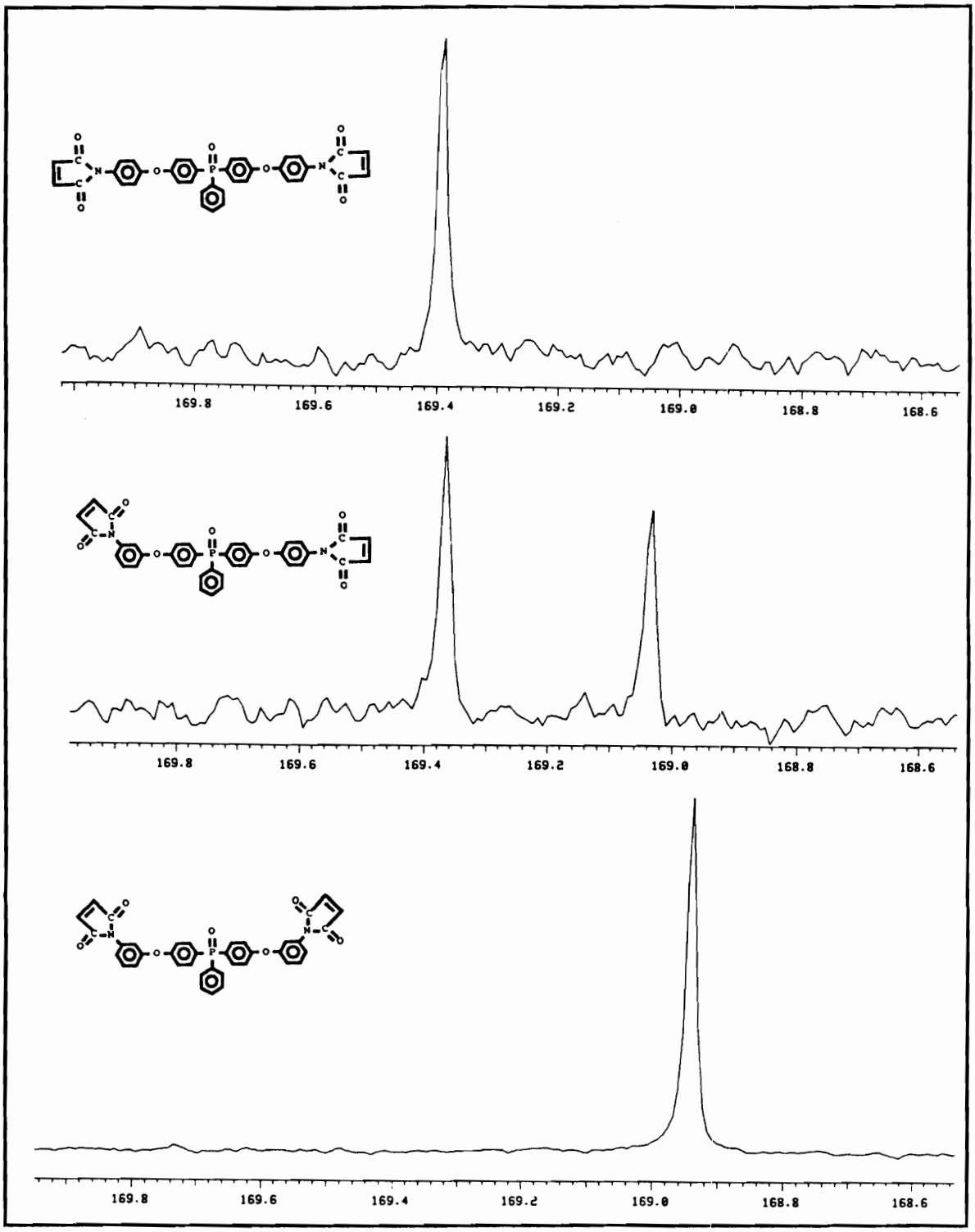

Figure 33

^{13}C-NMR Comparison of Maleimide Carbonyl Carbons

meta and para to the phosphine oxide on the pendent phenyl are centered around at 7.4 and 7.5 ppm, respectively. The peak at 7.24 ppm in all three spectra is the chloroform-*d* signal.

In the meta-derivative shown in Figure 29, the triphenyl phosphine oxide protons ortho to the ether bond are now centered around 7.26 ppm; the remaining protons are in approximately the same locations as in the para-derivative. However, the protons from meta-aminophenol are split into four groups. The peaks centered around 6.98 ppm is the proton in between the ether bond and the amine group, while the peak at 6.31 ppm is due to the proton meta to both the ether bond and amine group. And lastly, the two groups centered around 6.37 and 6.43 ppm are the protons next to the ether and amine groups, respectively. The meta,para-derivative diamine exhibits the intermediate spectra comprised of both the meta and the para-structures. Note, the meta,para-derivative diamine was prepared using a 50/50 mixture of the meta- and para-aminophenols as previously described. The diamine and subsequent bismaleimide prepared by this mixture should statistically yield one-third of each of the possible structures: para-, meta- and meta,para-isomers. However, this was not verified by HPLC, since the main interest in this structure was its melting behavior, which will be discussed shortly.

Figure 30 compares the expanded regions of the amine protons on the ether phosphine oxide diamines, with the meta amine protons being more deshielded vs the para amine protons, while the meta,para-derivative shows contribution from both isomeric positions. Proton-NMR can also distinguish between the meta and para-maleimide positions as shown in Figure 31 and 32. The aromatic region of the bismaleimides is expanded in Figure 31, showing the maleimide protons in the vicinity of 6.79 to 6.84 ppm for the three isomers. This region is further expanded in Figure 32, illustrating the ability to distinguish between the isomers. This resolving power is also shown in Figure 33 for the ^{13}C-NMR spectra of the maleimide carbonyl carbon in the vicinity of 168.9 to 169.5 ppm.

Proton and carbon-NMR were also used to confirm the 2,2'-(4-hydroxyphenyl-4-aminophenyl)propane derived diamine and bismaleimide structures. The proton spectra for the diamine displayed the characteristic aromatic peaks and the amine protons are located at 3.57 ppm. Both the diamine and bismaleimide isopropylidene proton signals are located at 1.6 ppm and the maleimide protons are shown at 6.8 ppm in Figure 34. The bismaleimide ^{13}C-NMR spectrum exhibited the carbonyl carbon signal at 169.5 ppm.

In addition to the diamines and bismaleimides prepared with the central triphenyl phosphine moiety, a diamine and

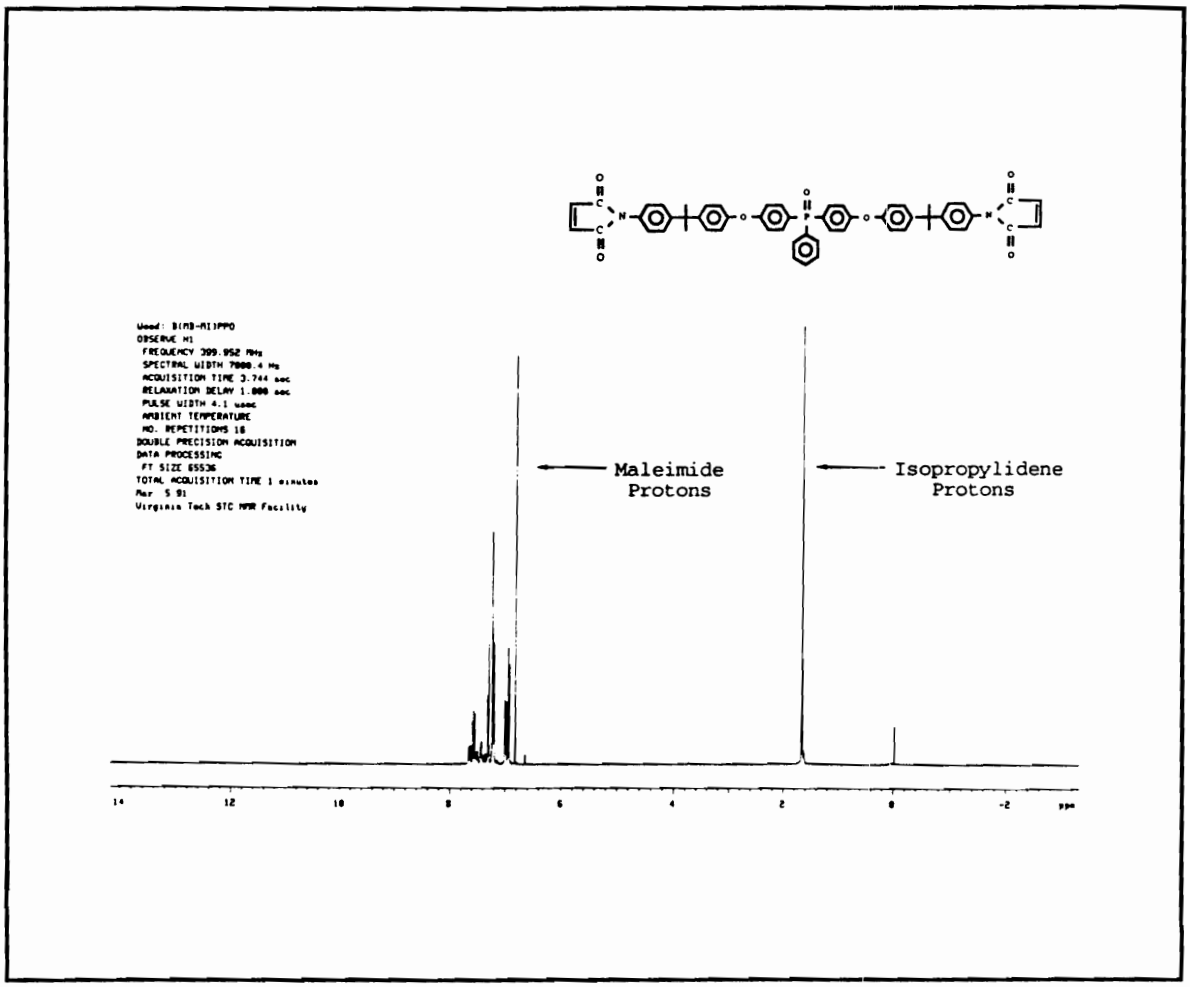

Figure 34

^{1}H-NMR of Bis(maleimidophenylisopropylidenephenoxy)-triphenyl phosphine oxide

corresponding bismaleimide were prepared by replacing the triphenyl phosphine oxide's pendent phenyl with a methyl group. In this case the diamine and bismaleimide were made in the same manner as described for the triphenyl phosphine oxides as outlined in Schemes 9 and 10, with the exception of substituting bis(4-fluorophenyl)methyl phosphine oxide shown below for the triphenyl halide moiety. Only the meta-derivative was prepared using meta-aminophenol.

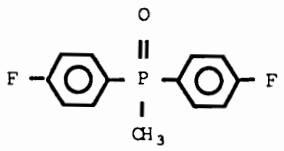

The methyl substituted ether phosphine oxide diamine and bismaleimide were characterized by the analogous methods described for the triphenyl systems. FTIR for the diamine exhibited the distinctive aromatic (N-H) stretching bands at 3336 and 3446 cm^{-1} as well as the (P-CH_3) stretching at 1402, 1304 and 882 cm^{-1}, while the bismaleimide showed the maleimide (=C-H) stretching at 3070 cm^{-1}. Proton-NMR for the diamine and bismaleimide; carbon-NMR for the bismaleimide are displayed in Figure 35. The pendent methyl protons appear at 1.9 ppm, while the peak for the aromatic amine protons are at 3.7 ppm. Again the characteristic maleimide carbonyl carbon signal was at 169 ppm and the pendent methyl carbon at 17 ppm.

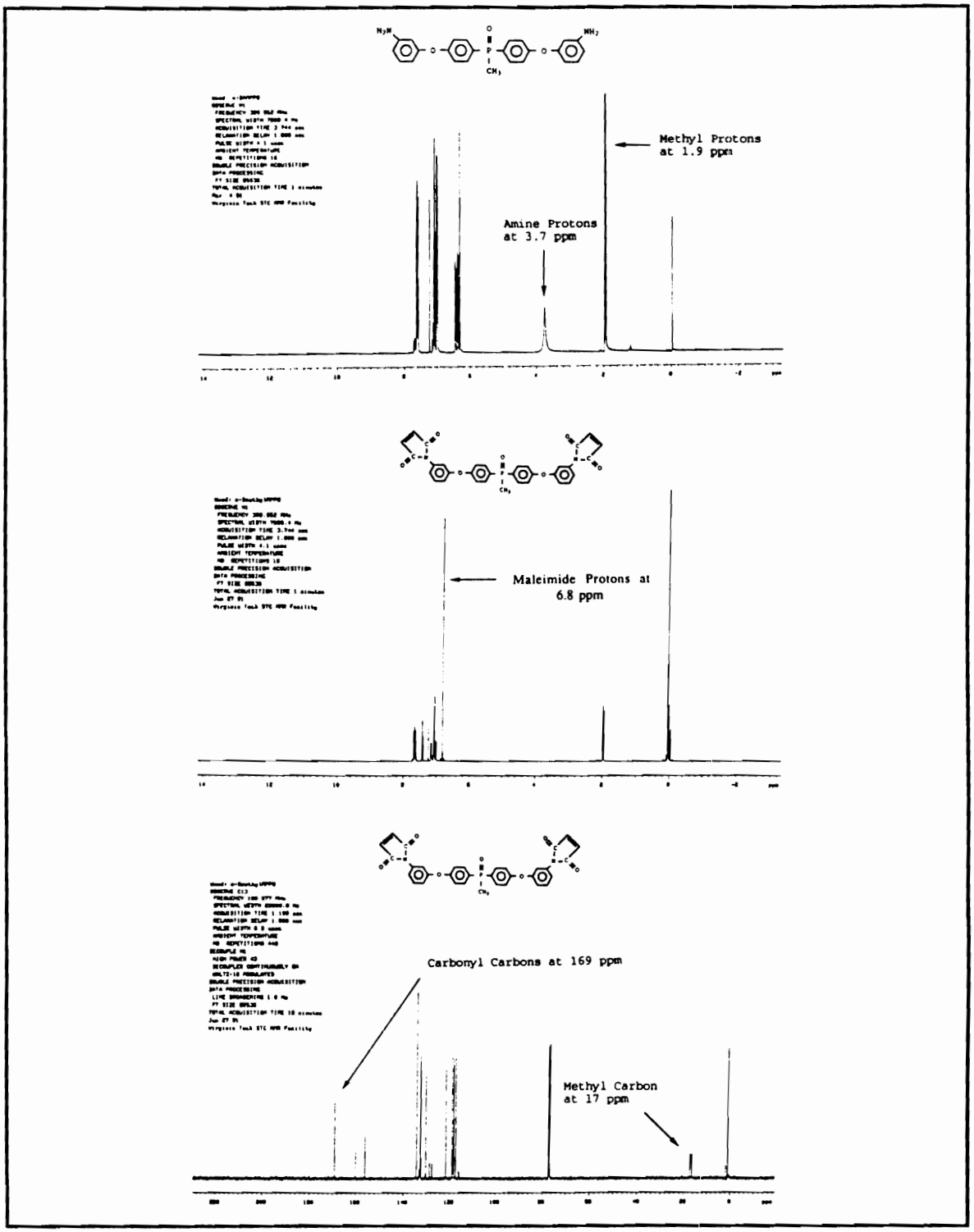

Figure 35

^{1}H and ^{13}C-NMR of Methyl Substituted Ether Phosphine Oxides

After confirming the phosphine oxide bismaleimides structures and purity, a detailed study of their thermal behavior was performed since ultimately this is one of the major properties of interest for these materials. As outlined in the literature review, thermosetting resins become infusible and insoluble as a consequence of chemical crosslinking reactions. The resins cannot be processed into shapes after being formed into a three-dimensional network. Therefore, it is of upmost importance to be able to easily process/mold the resins prior to curing. In general, bismaleimides derived from aromatic diamines have relatively high melting points as covered in the literature review. The high melting temperature of the uncured bismaleimide results in a narrow processing window, since once the resin melts, it immediately begins to cure as shown on page 13 for the methylenedianiline based bismaleimide. It is highly desirable to prepare systems that can liquefy at relatively low temperatures and possess an adequate processing window, while still retaining a high temperature resistant network.

The melting and curing behavior of the phosphine oxide monomers were characterized by DSC. Figure 36 shows an expanded scale dynamic DSC scan for the diamine bis(m-aminophenoxy)triphenyl phosphine oxide with a melting point of 84°C. While Tables 15 and 17 list the melting points as determined by DSC for the triphenyl and methyl based

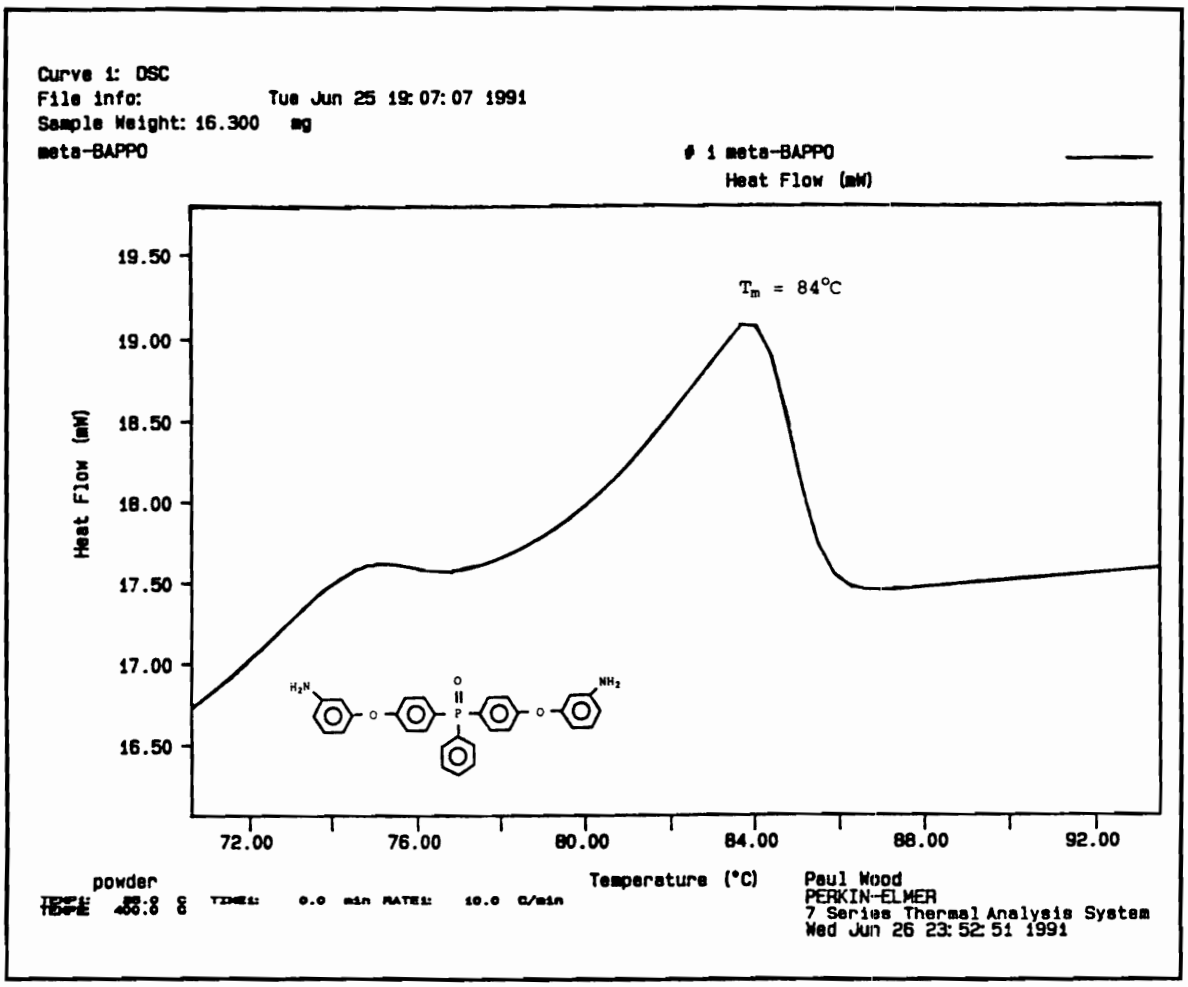

Figure 36

Dynamic DSC Scan of Bis(m-aminophenoxy)-triphenyl phosphine oxide

Table 17

DSC Thermal Data of

Aromatic Ether Methyl Diphenyl Phosphine Oxide Monomers

Bis Ether Diphenyl Methyl Phosphine Oxides	T_m	T_1	T_1-T_m
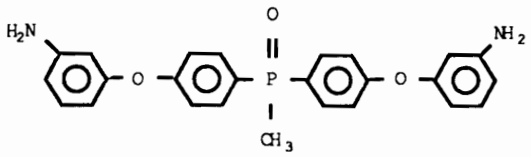	70	-	-
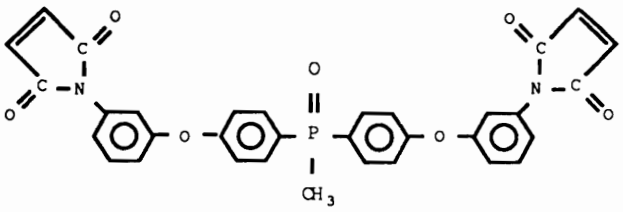	77	180	103

phosphine oxide diamines, respectively. All of these aromatic phosphine oxide diamines have relatively low melting points compared to many of the diamines reported in the literature, that were used to prepare the bismaleimides listed in Table 1. The phosphine oxide diamines have relatively sharp DSC melting points, further demonstrating their high purity.

The melting points or glass transition temperatures measured by DSC of the phosphine oxide bismaleimides are listed in Table 16; melting points for the triphenyl based systems and in Table 17 for the methyl substituted bismaleimide. All of the phosphine oxide bismaleimides exhibit remarkably low melting transitions, notably when compared with the bismaleimides outlined in Table 1. In Figure 37, the dynamic DSC scan shows that the uncured bis(m-maleimidophenoxy)triphenyl phosphine oxide melts around 92°C (T_m) and an exotherm indicating curing does not take place until more than 180°C (T_1), with a maximum peak exotherm noted at about 220°C (T_{exo}). The difference in temperature between the onset of crosslinking (T_1) and the melting temperature is known as the processing window. A relatively large window allows for an easier processing, while a narrow window makes it very difficult, if not impossible. All of the phosphine oxides listed in Tables 16 and 17 have more than adequate processing windows, especially compared to the largest

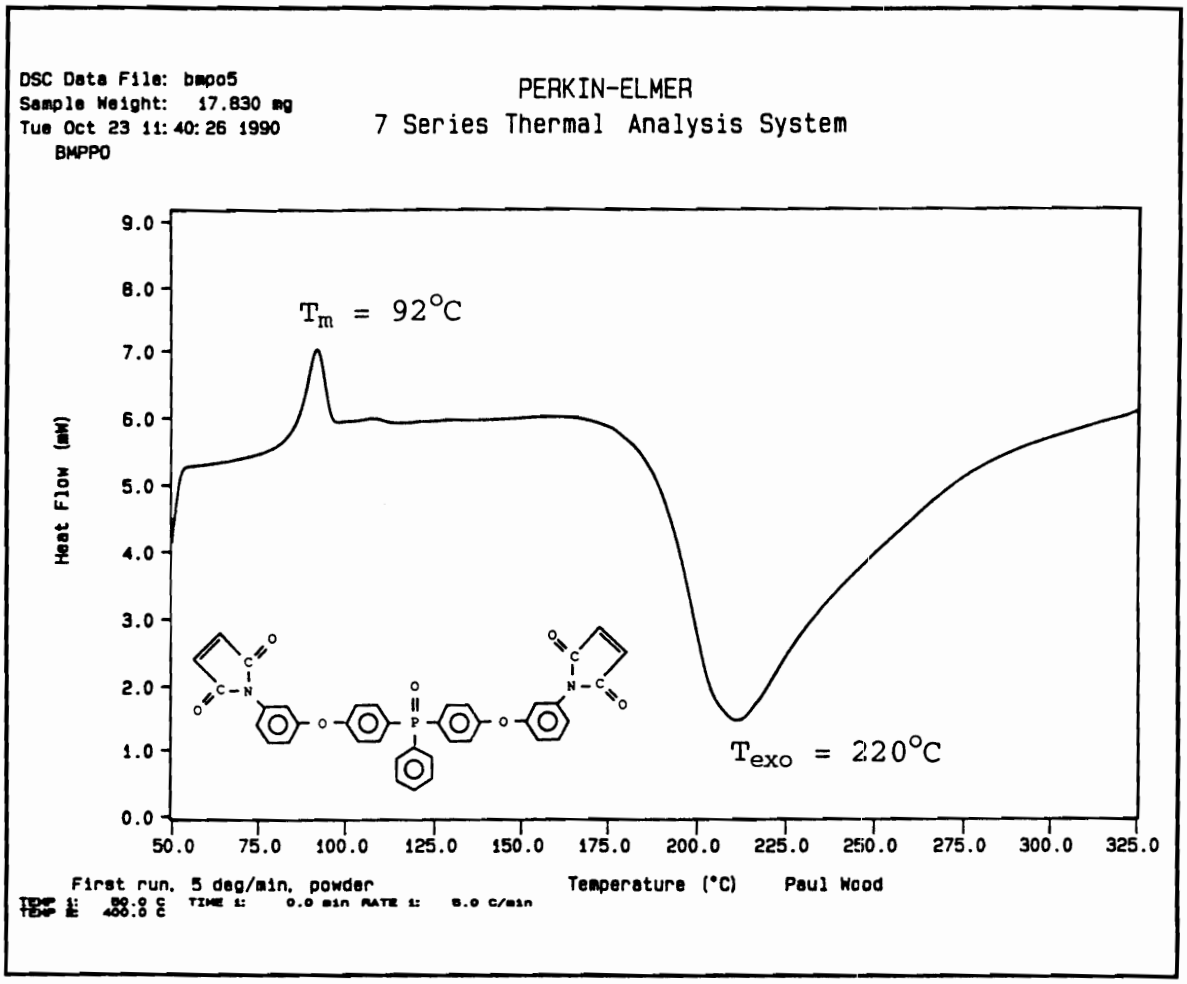

Figure 37

Dynamic DSC Scan of Bis(m-maleimidophenoxy)-triphenyl phosphine oxide

commercial bismaleimide 4,4'-bismaleimidodiphenylmethane, 3, and many of the aromatic bismaleimides reported in the literature. Table 16 and 17 list the approximate processing windows (T_1-T_m or T_g) for the triphenyl based bismaleimides and methyl substituted bismaleimide, respectively.

This particularly low melting behavior is further examined by the complex viscosity (η^*) taken for bis(m-maleimidophenoxy)triphenyl phosphine oxide as a function of temperature. As shown in Figure 38 the bismaleimide resin exhibits very low viscosities, especially when approaching higher temperatures, which is still well below the onset of curing. The complex viscosity measurements were stopped below the 180°C onset of cure temperature to prevent the rheometrics instrument's parallel plates from being stuck together by the network. Had the measurements been taken through the cure, the line shown would have leveled out and then risen astronomically high as the material cured.

The next important criterion to consider is the glass transition temperature of the phosphine oxide networks. The glass transition temperature is of upmost importance because it defines what applications a material may ultimately have. The goals of this investigation were to develop high performance, high temperature resistant bismaleimide networks for advanced composite matrix applications, structural adhesives, electronic applications, fire resistant materials

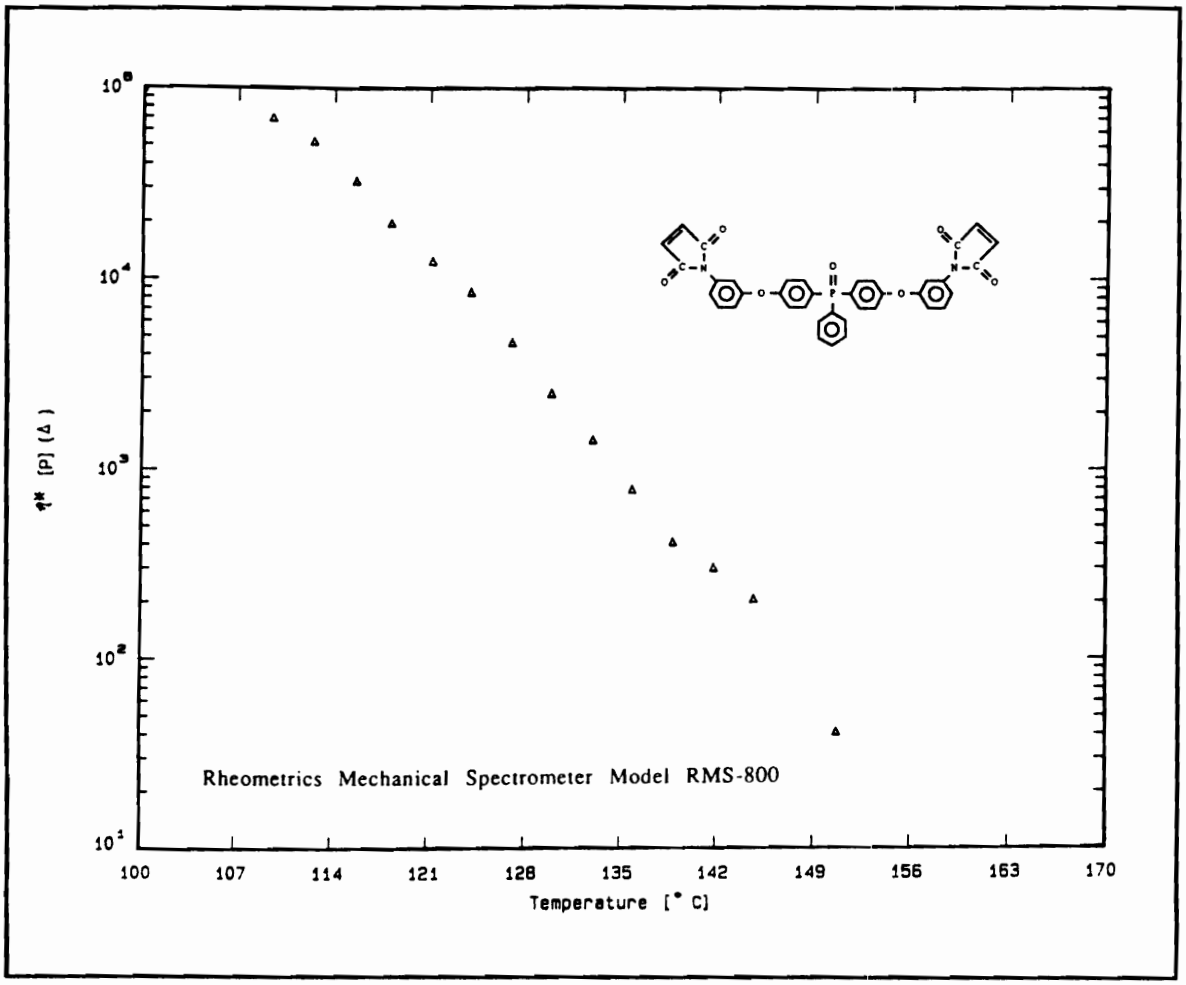

Figure 38

Complex Viscosity (η*) of Bis(m-maleimidophenoxy)-triphenyl phosphine oxide at 10 Hz with 1% Strain

and specialty coatings. Many of these applications require high glass transition temperature materials.

The glass transition temperatures of the phosphine oxide bismaleimide networks were determined by TMA. Correctly speaking TMA was used to obtain the onset softening temperature that is associated with the large-scale decrease in modulus at the glass transition (124). However, most people simply call the softening temperature of rigid thermosets the T_g. The cure schedules for TMA measurements were determined by selecting a series of temperatures along the exotherm of the DSC curve for the bismaleimide and post-curing sample bars for allotted times at those selected temperatures. For the "ultimate" glass transition temperature of the phosphine oxide bismaleimide networks, it was determined that at 300°C for four hours the T_g did not increase after longer cures.

Figure 39 shows the resulting high glass transition temperature of around 400°C for the bis(m-maleimidophenoxy)triphenyl phosphine oxide network cured at 300°C for 4 hours. The T_g's of the phosphine oxide bismaleimide networks are listed in Table 18. All of the phosphine oxide networks had high glass transition temperatures of around 400°C, with the exception of the 2,2'-(4-hydroxyphenyl-4-aminophenyl)propane derived and methyl substituted bismaleimides. This was expected since the more

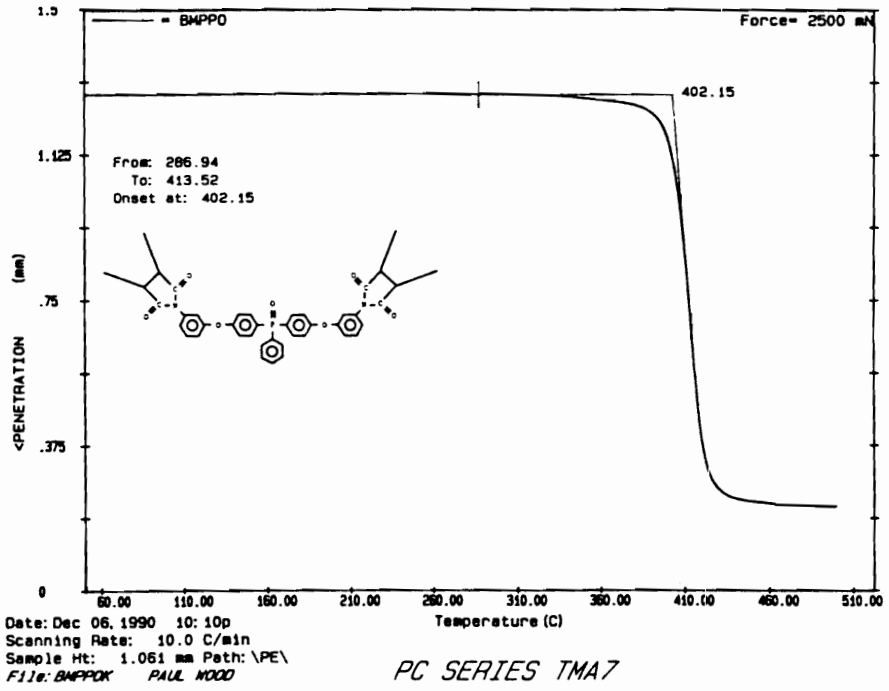

Figure 39

Dynamic TMA Scan of Bis(m-maleimidophenoxy)-triphenyl phosphine oxide

Table 18

TMA Glass Transition Temperatures of Phosphine Oxide Bismaleimide Networks Post-Cured at 300°C for 4 Hours

Bis(Maleimidophenoxy) Phosphine Oxide Networks	T_g
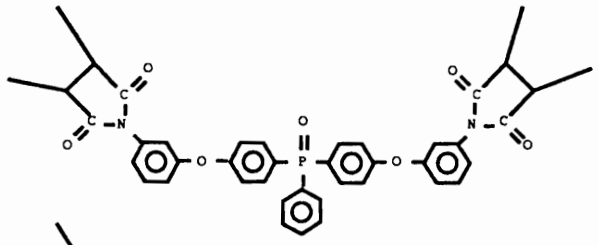	402
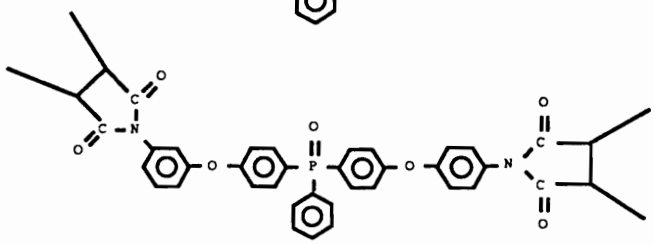	404
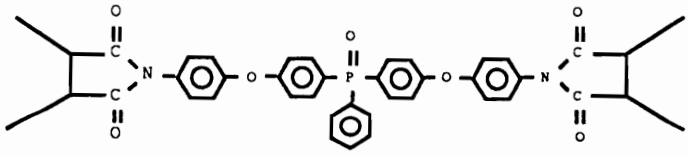	407
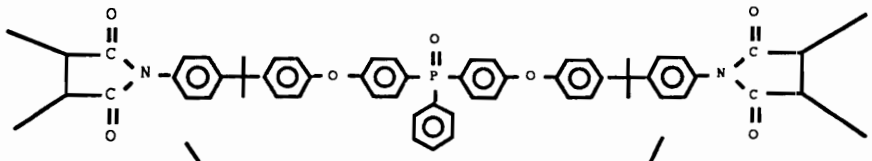	222
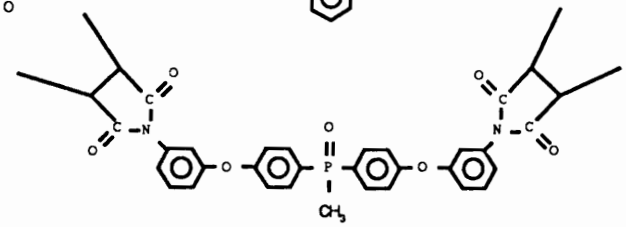	365

aromatic character incorporated into the bismaleimide, the higher the resulting T_g, and conversely tailoring in an aliphatic make-up attributes to lowering the T_g, especially in the case of adding isopropylidene linkages. The stiffness behavior as defined by glass transition temperature would suggest these phosphine bismaleimides could be used as structural adhesives and matrix resins, etc.

The T_g was also measured at approximately 380°C by DMTA as shown in Figure 40 for the bis(m-maleimidophenoxy)triphenyl phosphine oxide. Another interesting feature of this dynamic mechanical behavior plot is the presence of a β-relaxation peak at -100°C. The β-relaxation peak suggests that these materials may have improved fracture toughness relative to the methylene dianiline based bismaleimide, which shows no β-relaxation.

^{13}C Solid-state NMR was also another technique used to follow the progress of the phosphine oxide bismaleimide curing reaction. The bis(m-maleimidophenoxy)triphenyl phosphine oxide resin and the "fully" cured network carbon NMR signals are shown in Figure 41. As displayed for the uncured material, the maleimide carbonyl carbon has a signal at 169 ppm, just as in the solution carbon NMR shown in Figure 28. After post-curing the bismaleimide at 300°C for 4 hours, the maleimide carbonyl carbon signal shifts downfield to 175 ppm and the aliphatic nature of the saturated carbon-

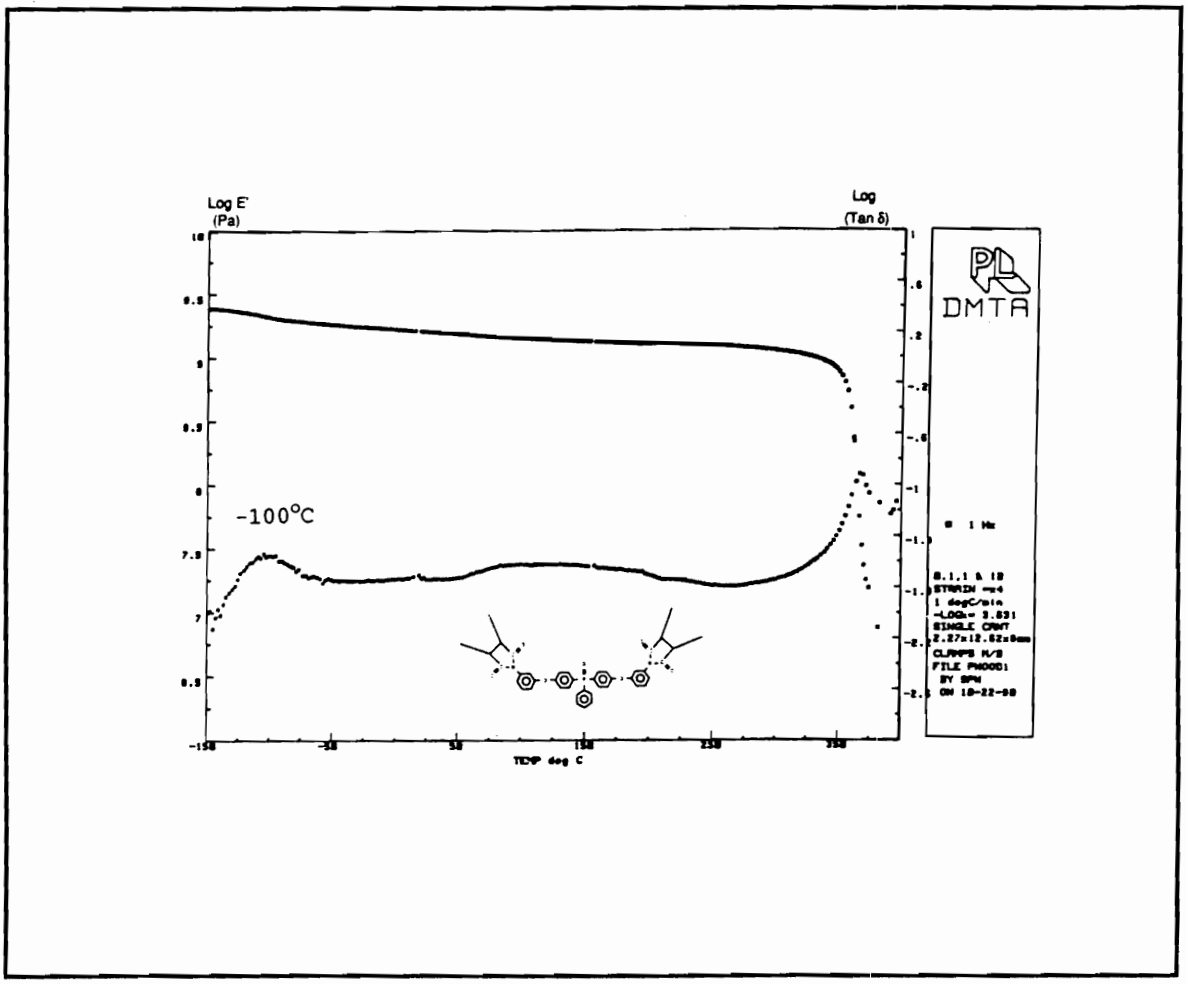

Figure 40

Dynamic Mechanical Behavior of Bis(m-maleimidophenoxy)-triphenyl phosphine oxide at 1 Hz

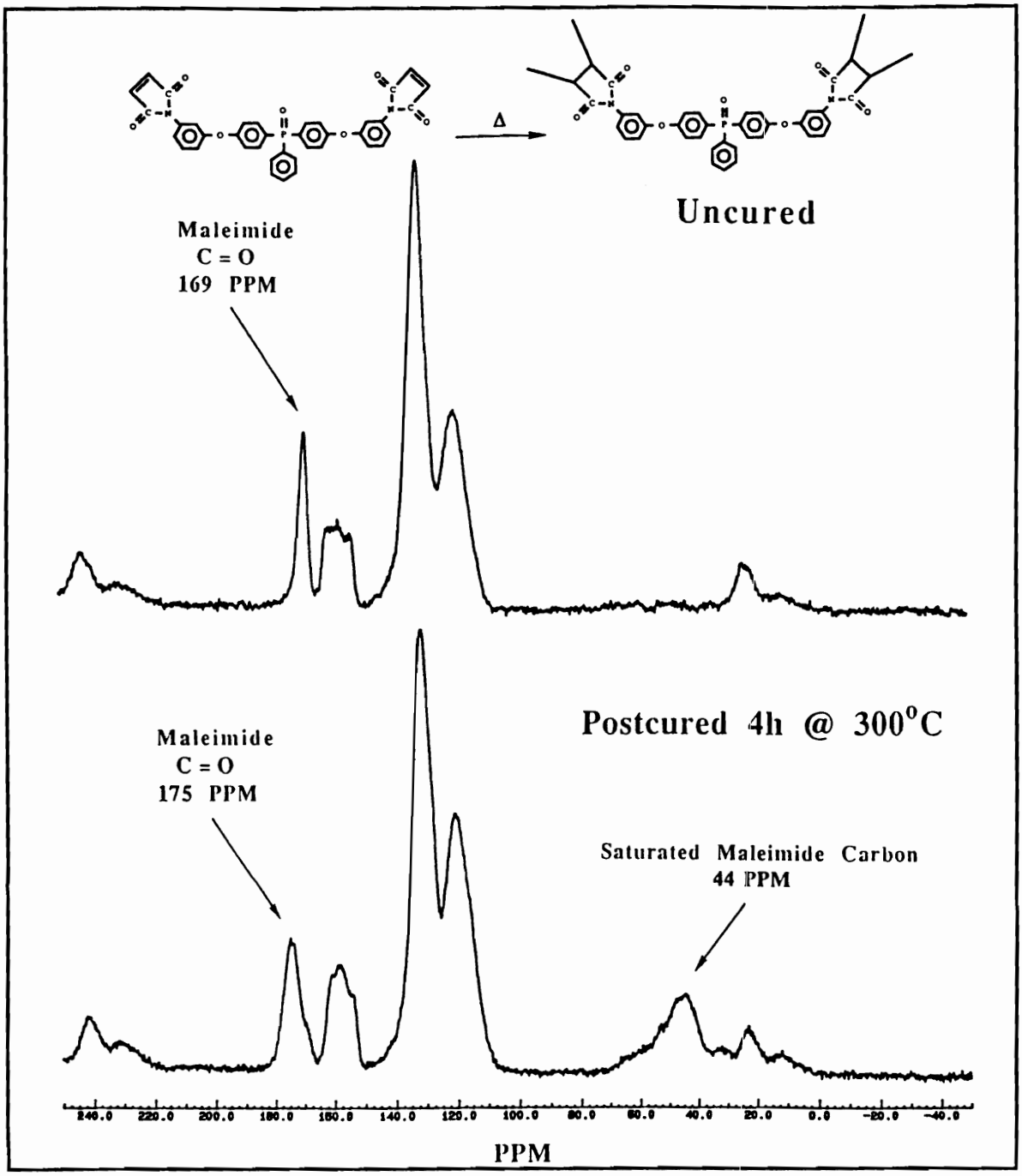

Figure 41

^{13}C-Solid State NMR of Uncured and Cured

Bis(m-maleimidophenoxy)triphenyl phosphine oxide

carbon maleimide bond is exhibited at 44 ppm. The peaks at 22 and 242 ppm are spinning side band of the aromatic carbon signals from 110 to 165 ppm. This method is particular useful since there are not many analytical methods to determine the chemical structure of solid samples, i.e., composites.

Dynamic and isothermal TGA scans of the cured phosphine oxide bismaleimides reveal that they have excellent thermal stability. For example, Figure 42 displays the thermo-oxidative behavior for bis(m-maleimidophenoxy)triphenyl phosphine oxide in both air and in nitrogen as measured by TGA. The TGA scan shows that it was stable in air to 400°C and demonstrates a significant char yield that is important in flame-resistance. Even at 700°C nearly 50% of the bismaleimide is still present in an air atmosphere, while 50% is present at over 900°C in nitrogen. Isothermal TGA, for example as shown in Figure 43 for the same material at 300°C for 12 hours in air showed no weight loss, which well meets the qualifications for many high temperature aerospace applications.

Preliminary tests by Harvey Grubbs show that the phosphine oxide networks are highly resistant to flame ignition and flame propagation; have low combustibility with a very low amount of smoke generated, all highly desirable properties (310).

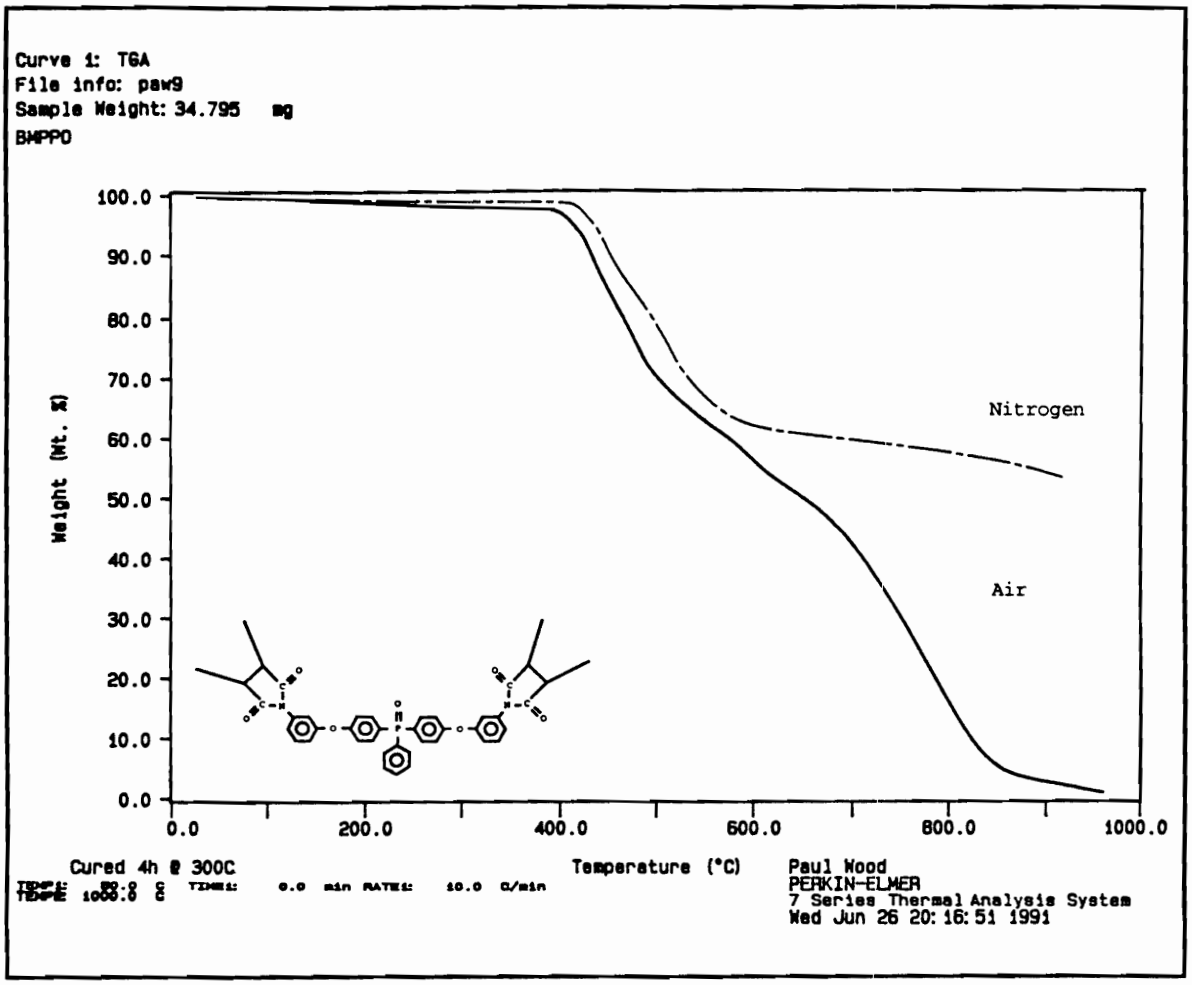

Figure 42

Dynamic TGA Scan of Bis(m-maleimidophenoxy)-triphenyl phosphine oxide in Air and Nitrogen

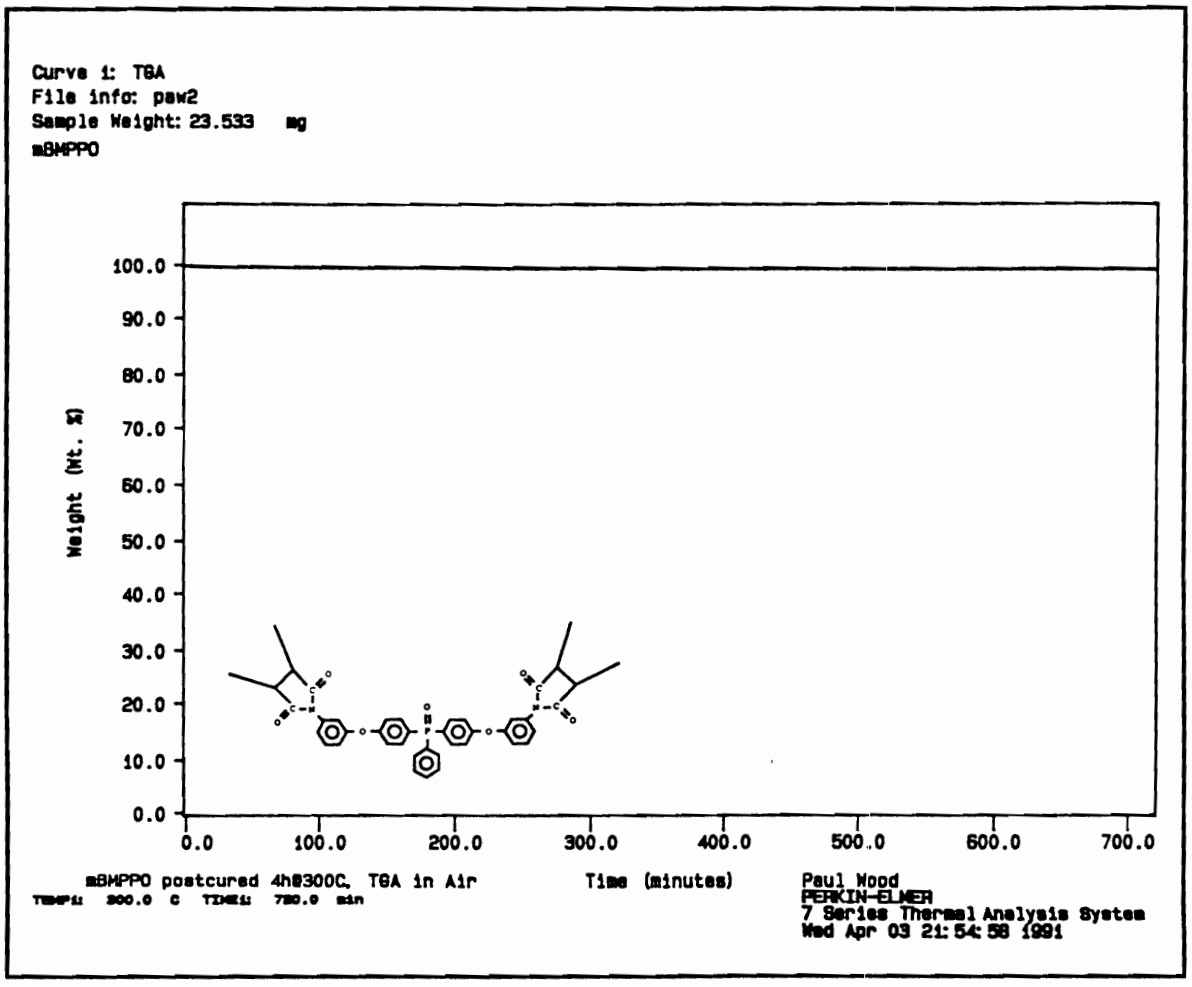

Figure 43

Isothermal TGA Scan of Bis(m-maleimidophenoxy)-triphenyl phosphine oxide in Air at 300°C for 12 Hours

Figures 44-55 show the DSC, TMA and TGA scans for the para-, meta,para-, 2,2'-(4-hydroxyphenyl-4-aminophenyl)-propane derived and methyl substituted phosphine oxide bismaleimides while their thermal data is tabulated in Tables 15-18. All of these materials exhibit excellent thermo-oxidative stable and adequate processing windows, which cure to a reasonably tough networks with high glass transition temperatures. Notice in Figure 46 and 49 that the para- and meta,para-bismaleimide networks have slightly higher char yields compared to the meta-bismaleimide, no doubt due to the higher stability para-maleimide incorporation. Substituting the methyl group in place of the phenyl ring in the meta-isomer had little effect on the thermo-oxidative stability of the bismaleimide network as shown in Figure 55. The methyl-substituted bismaleimide has a slightly higher char yield vs the meta-triphenyl moiety, probably due to the higher phosphorus content. However, the effect of incorporating the aliphatic isopropylidene groups along the main chain of the 2,2'-(4-hydroxyphenyl-4-aminophenyl)propane based bismaleimide is particularly apparent by TGA as shown in Figure 52. It appears that the isopropylidene based bismaleimide degrades by a different mechanism compared to the non-2,2'-(4-hydroxyphenyl-4-aminophenyl)propane moieties. Nevertheless, the 2,2'-(4-hydroxyphenyl-4-aminophenyl)propane based bismaleimide still has approximately the same thermal

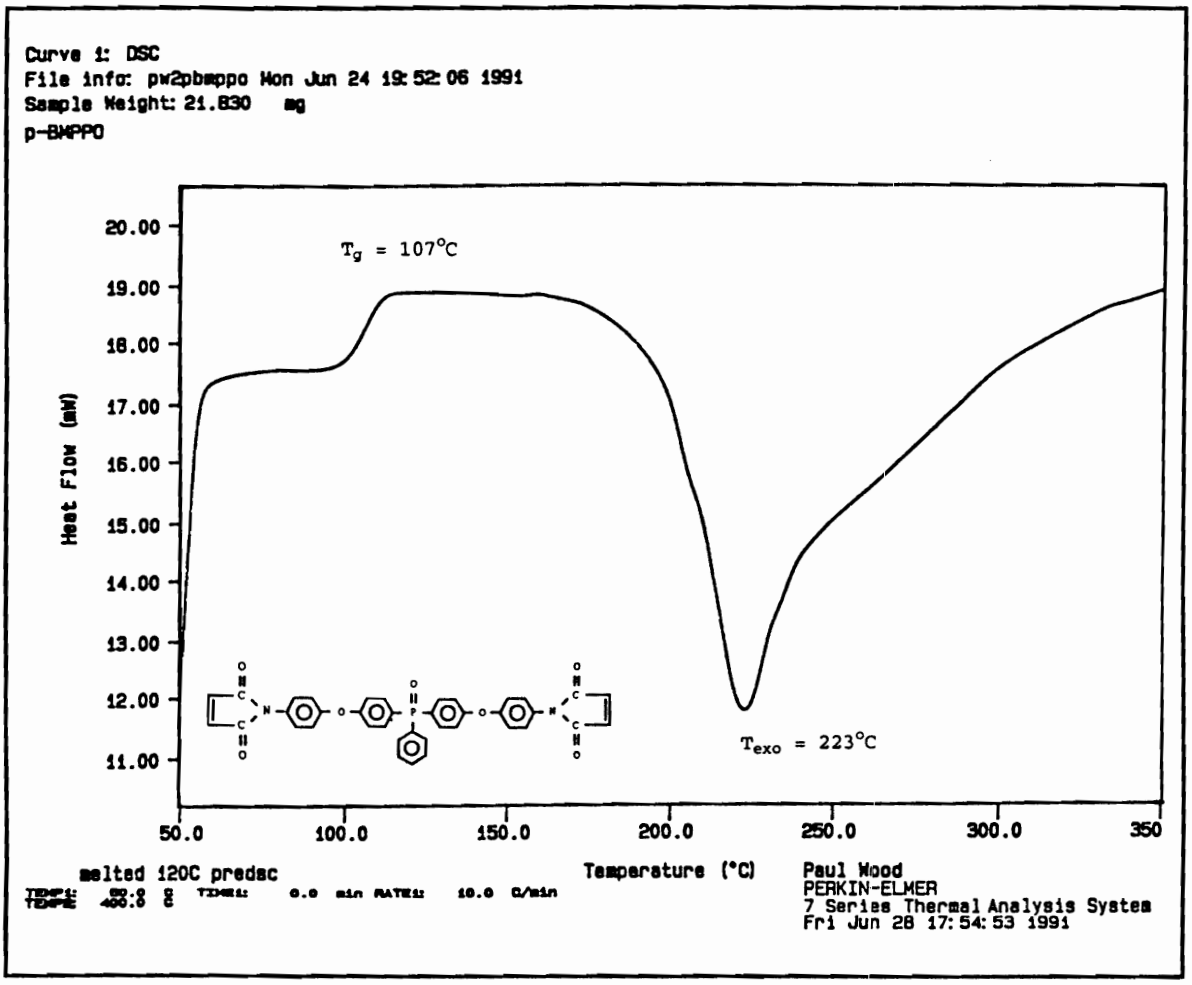

Figure 44

Dynamic DSC Scan of Bis(p-maleimidophenoxy)-triphenyl phosphine oxide

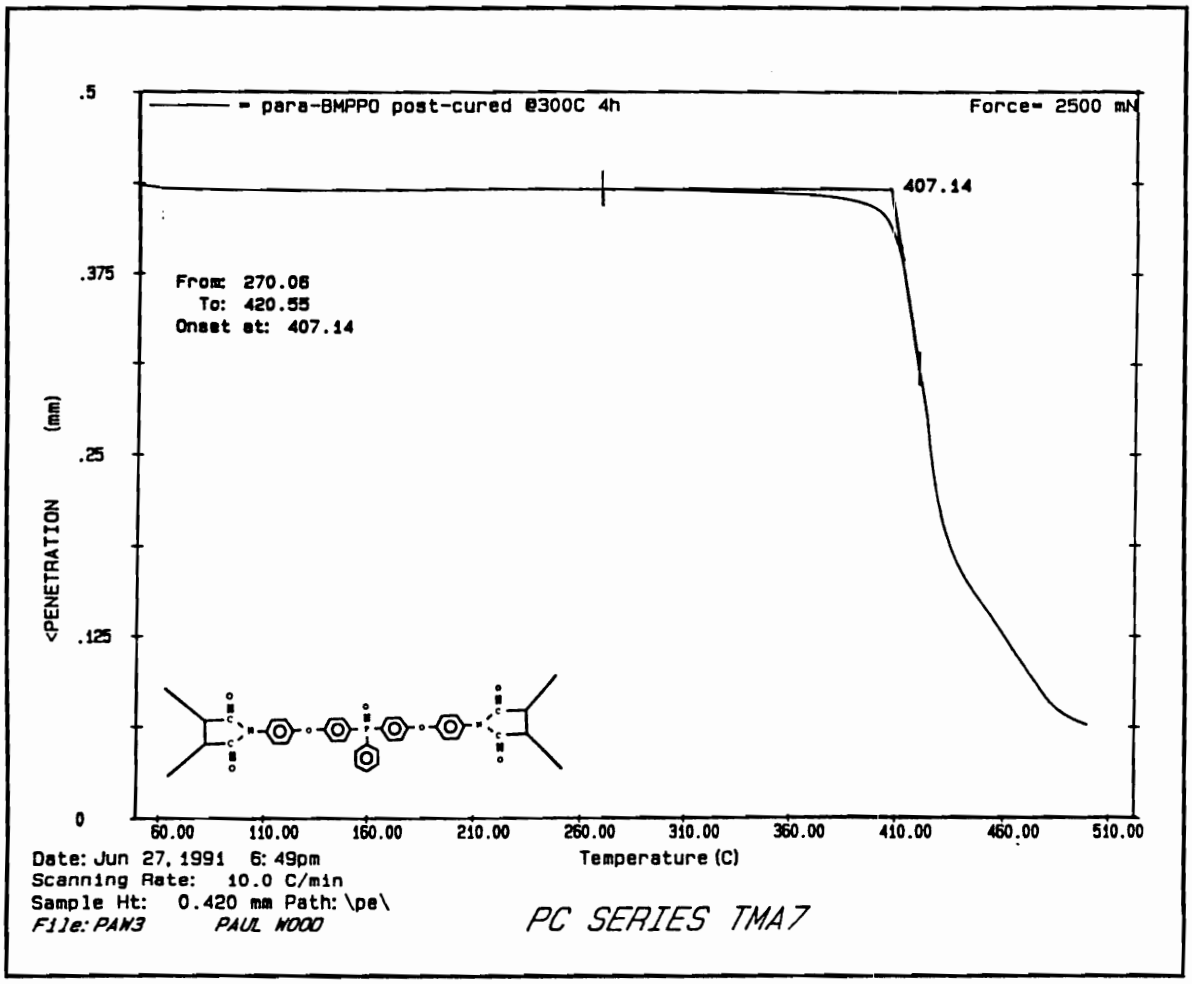

Figure 45

Dynamic TMA Scan of Bis(p-maleimidophenoxy)-triphenyl phosphine oxide

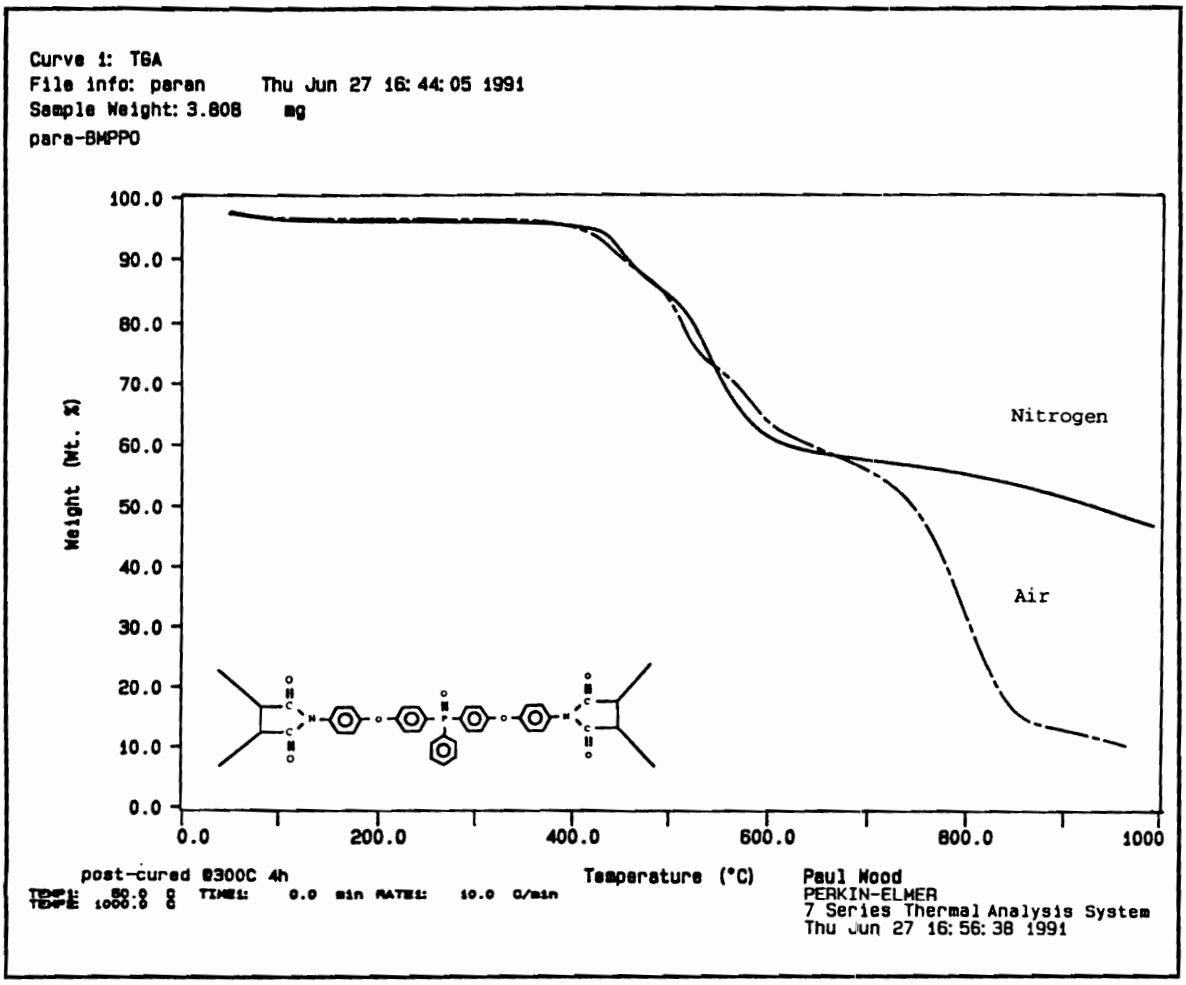

Figure 46

Dynamic TGA Scan of Bis(p-maleimidophenoxy)-triphenyl phosphine oxide in Air and Nitrogen

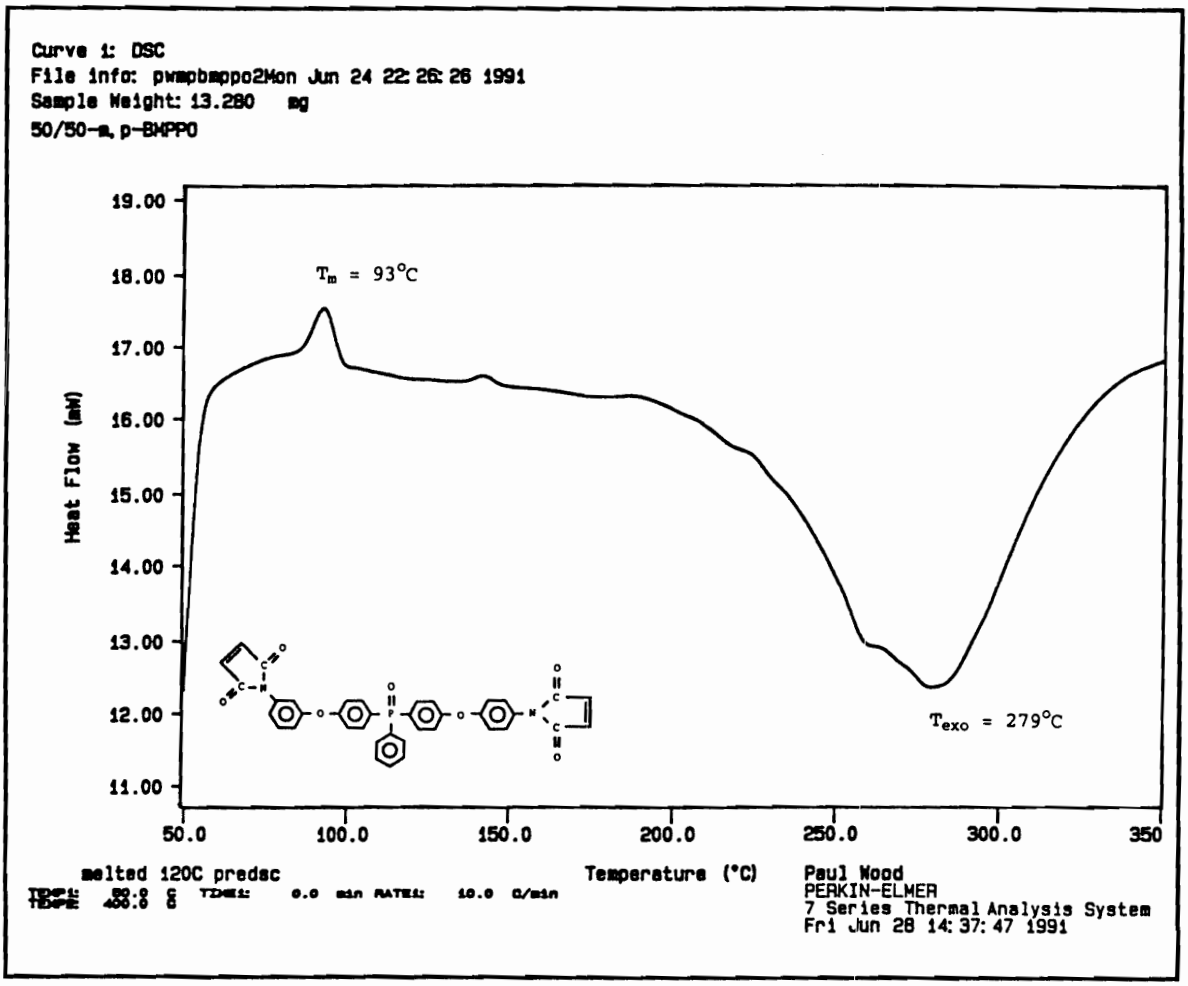

Figure 47

Dynamic DSC Scan of Bis(m,p-maleimidophenoxy)-triphenyl phosphine oxide

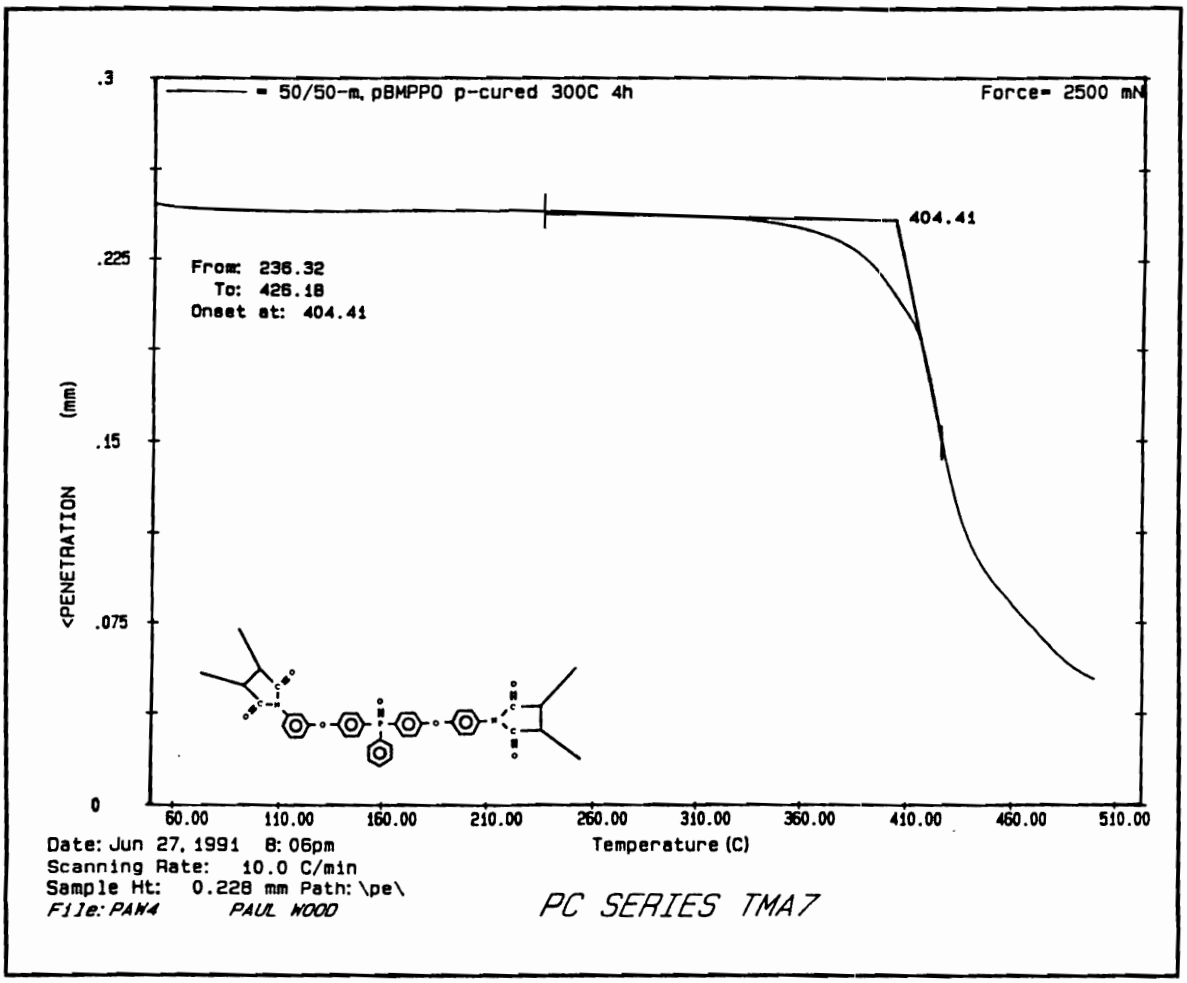

Figure 48

Dynamic TMA Scan of Bis(m,p-maleimidophenoxy)-triphenyl phosphine oxide

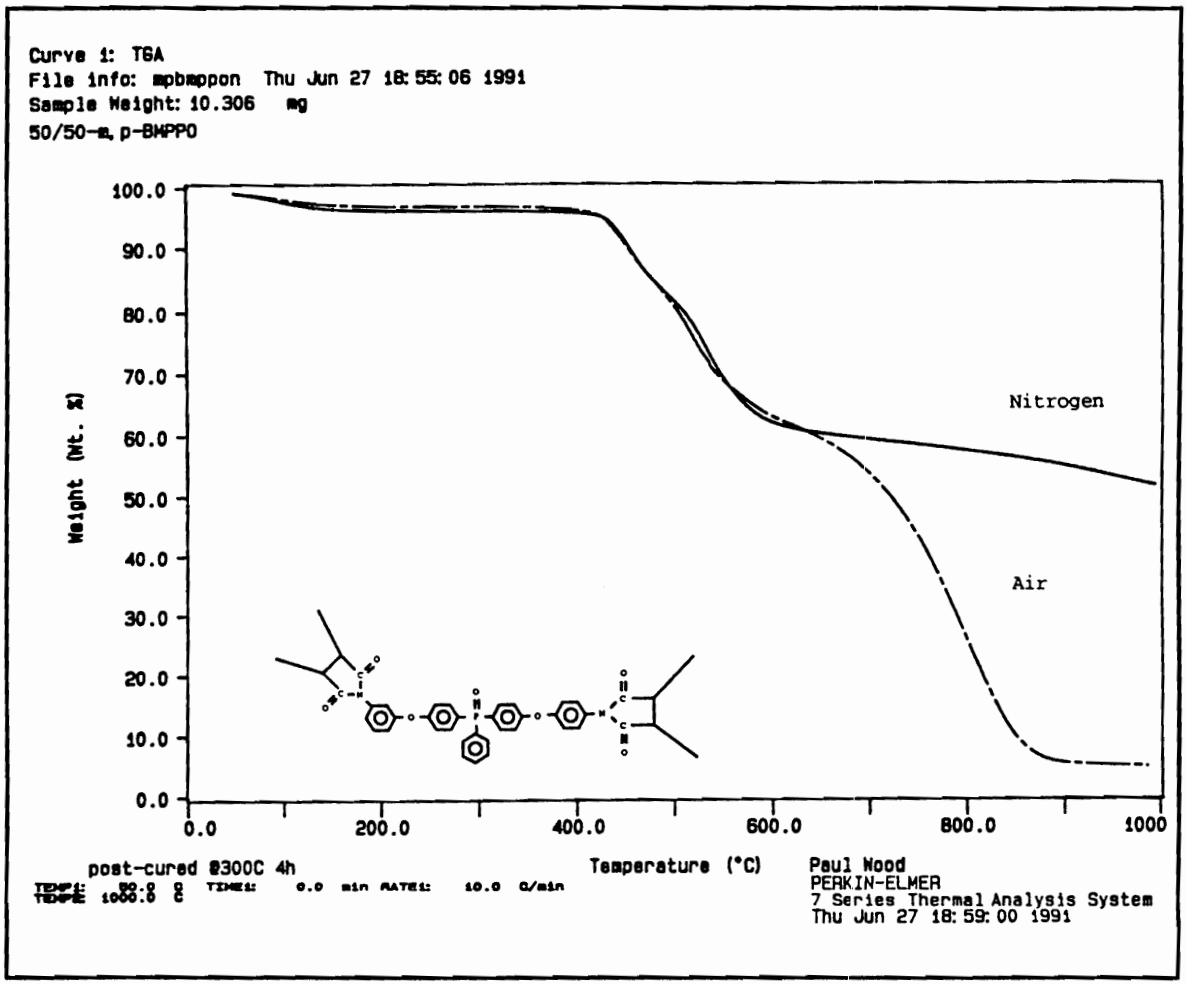

Figure 49

Dynamic TGA Scan of Bis(m,p-maleimidophenoxy)-triphenyl phosphine oxide in Air and Nitrogen

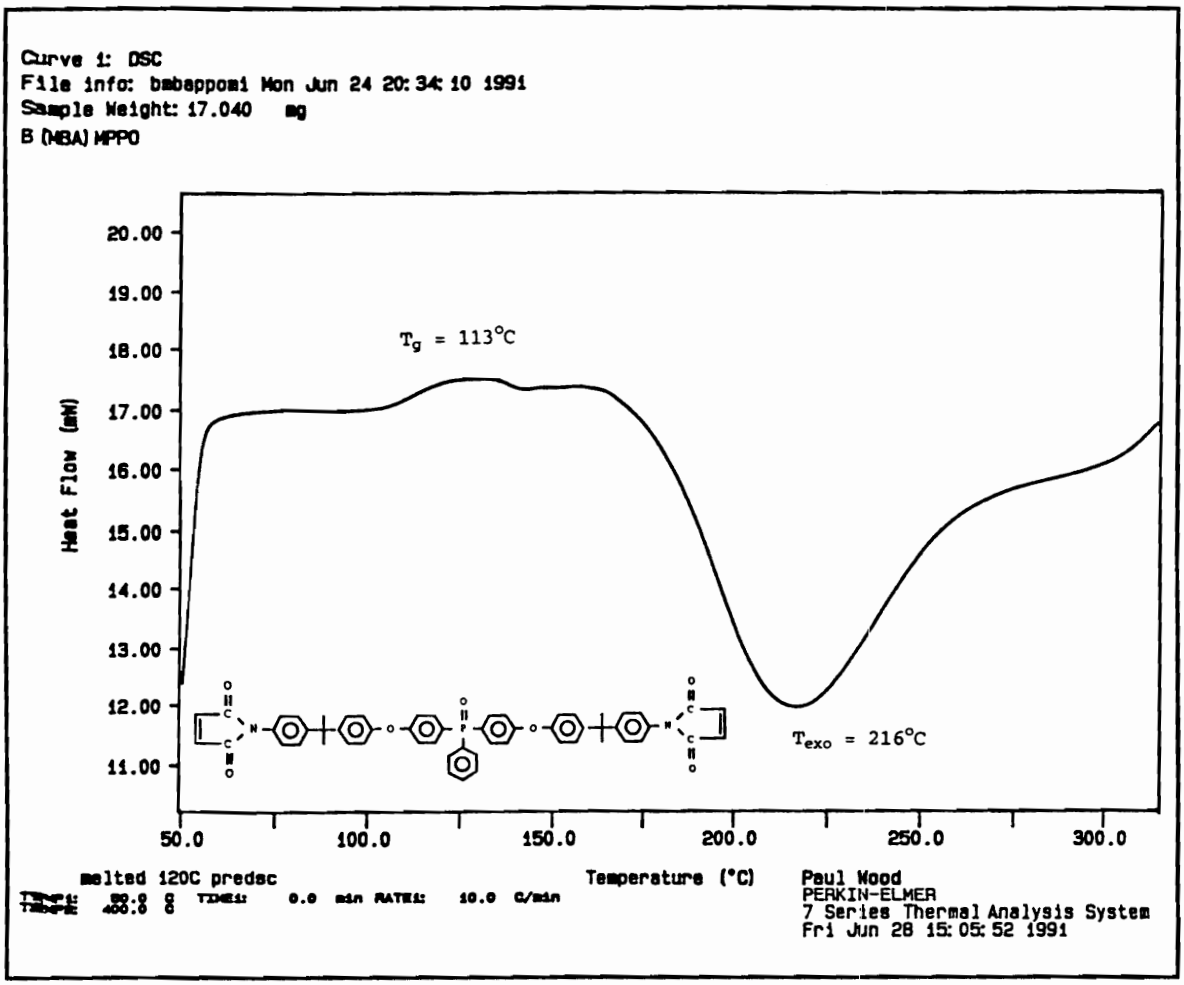

Figure 50

Dynamic DSC Scan of Bis(maleimidophenylisopropylidene-phenoxy) phosphine oxide

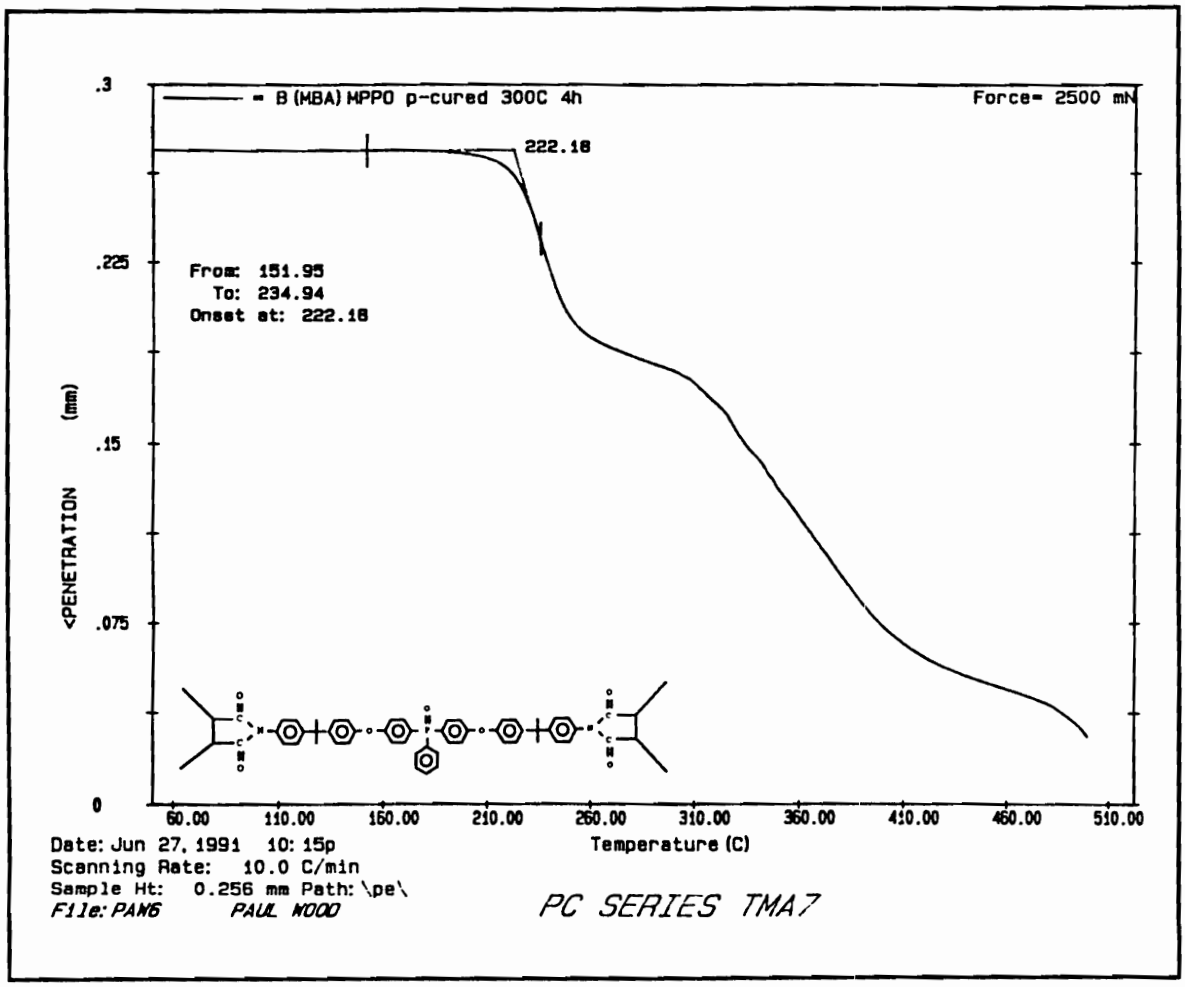

Figure 51

Dynamic TMA Scan of Bis(maleimidophenylisopropylidene-phenoxy) phosphine oxide

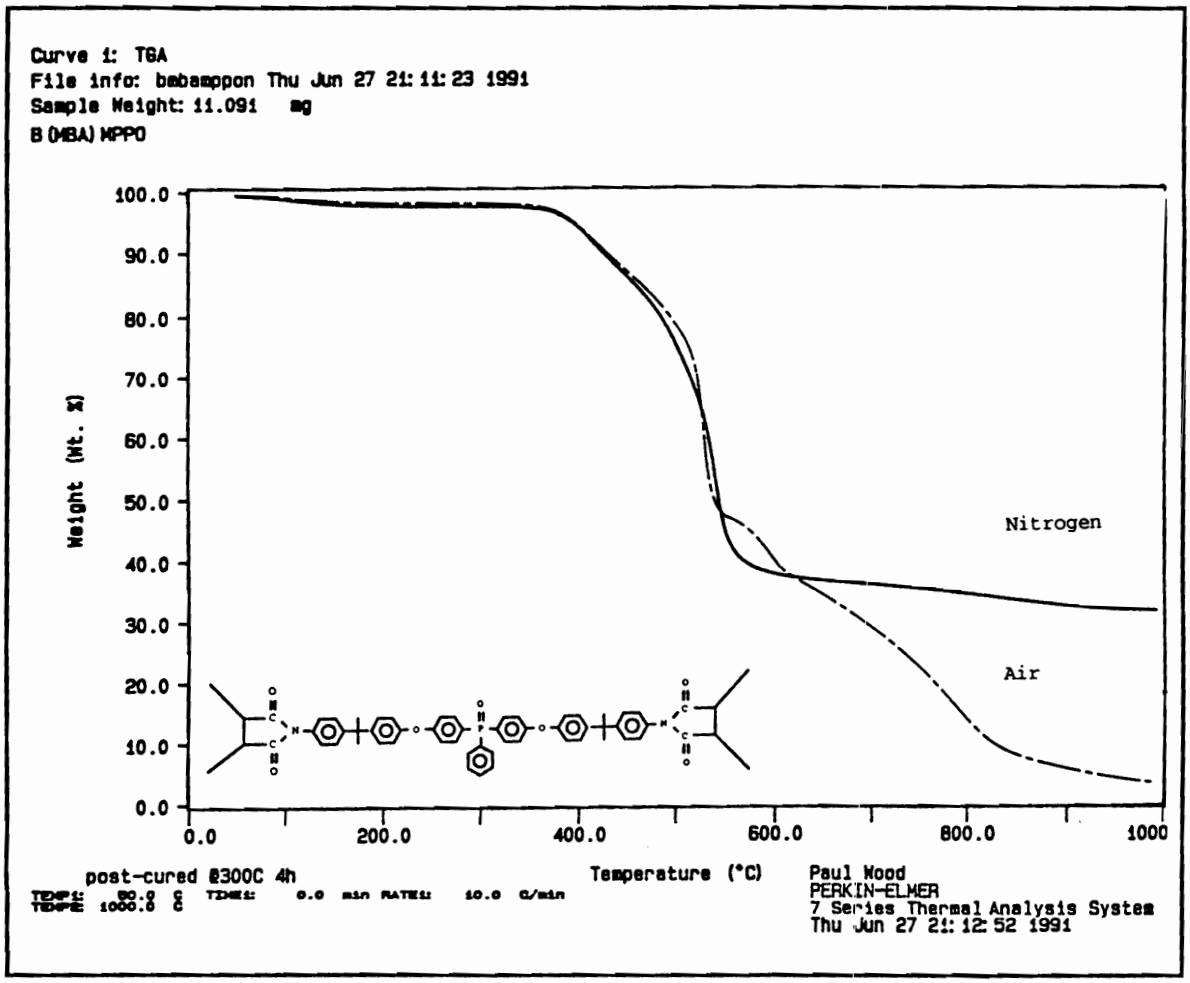

Figure 52

Dynamic TGA Scan of Bis(maleimidophenylisopropylidene-phenoxy) phosphine oxide in Air and Nitrogen

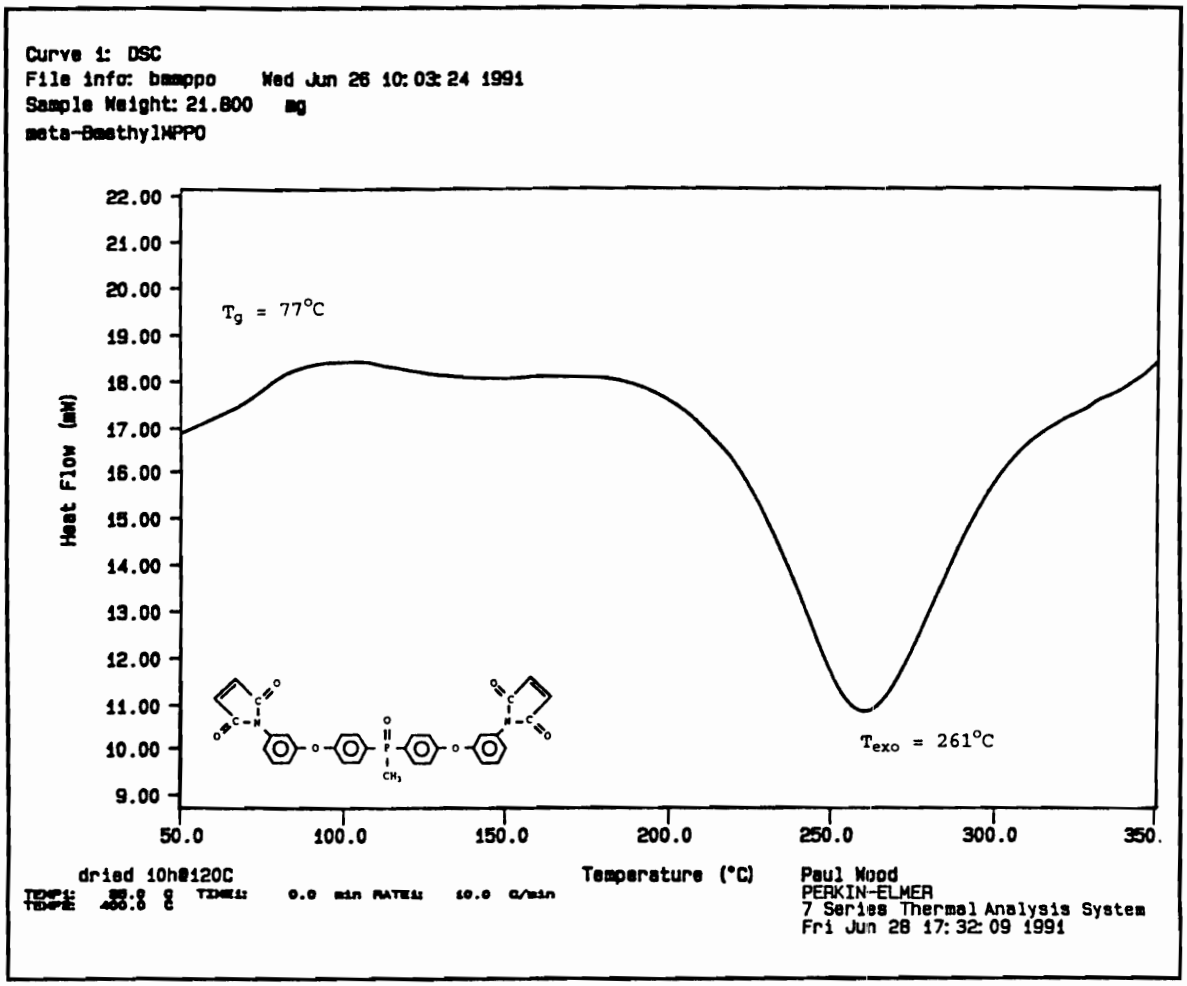

Figure 53

Dynamic DSC Scan of Bis(m-maleimidophenoxy)-diphenylmethyl phosphine oxide

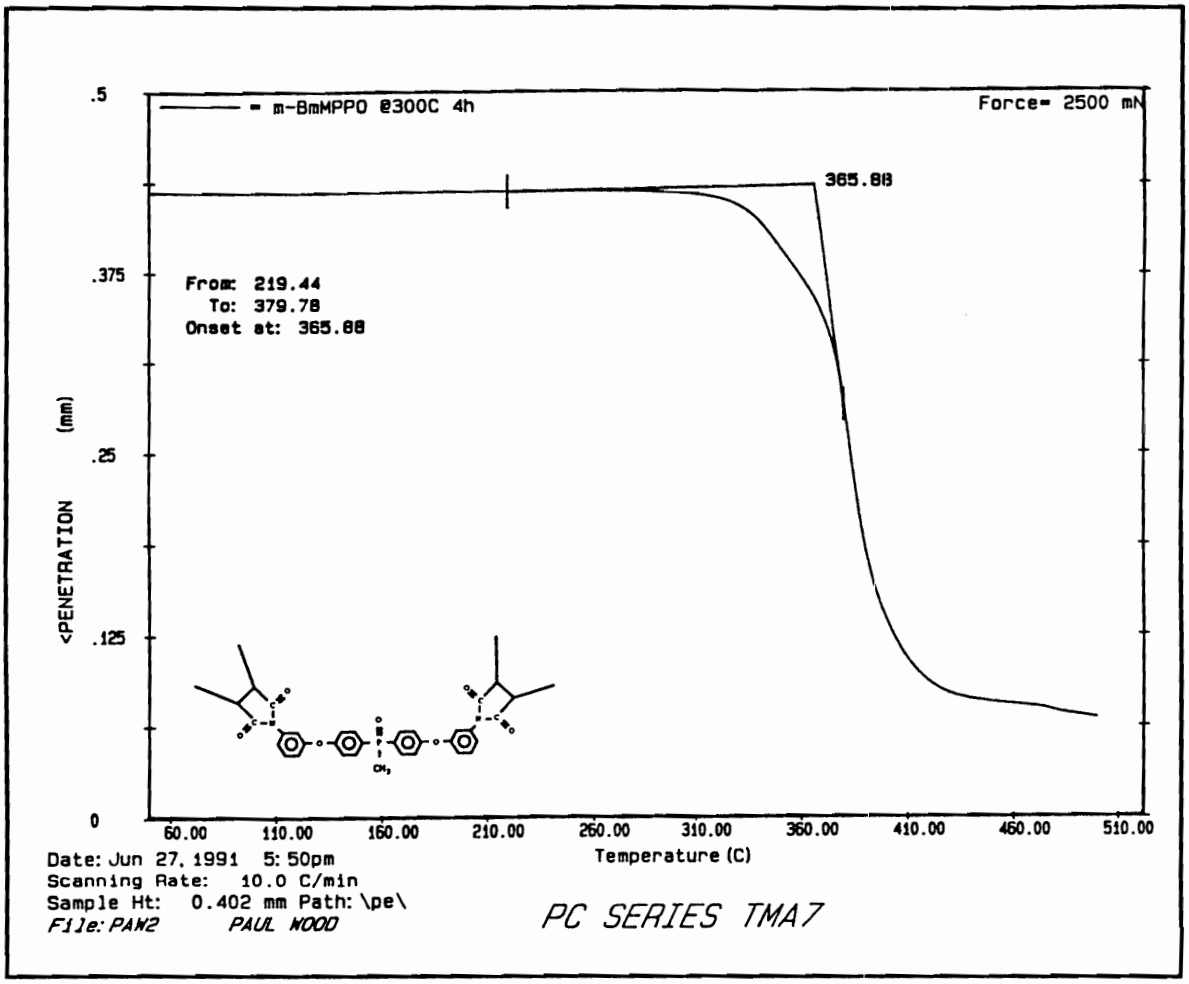

Figure 54

Dynamic TMA Scan of Bis(m-maleimidophenoxy)-diphenylmethyl phosphine oxide

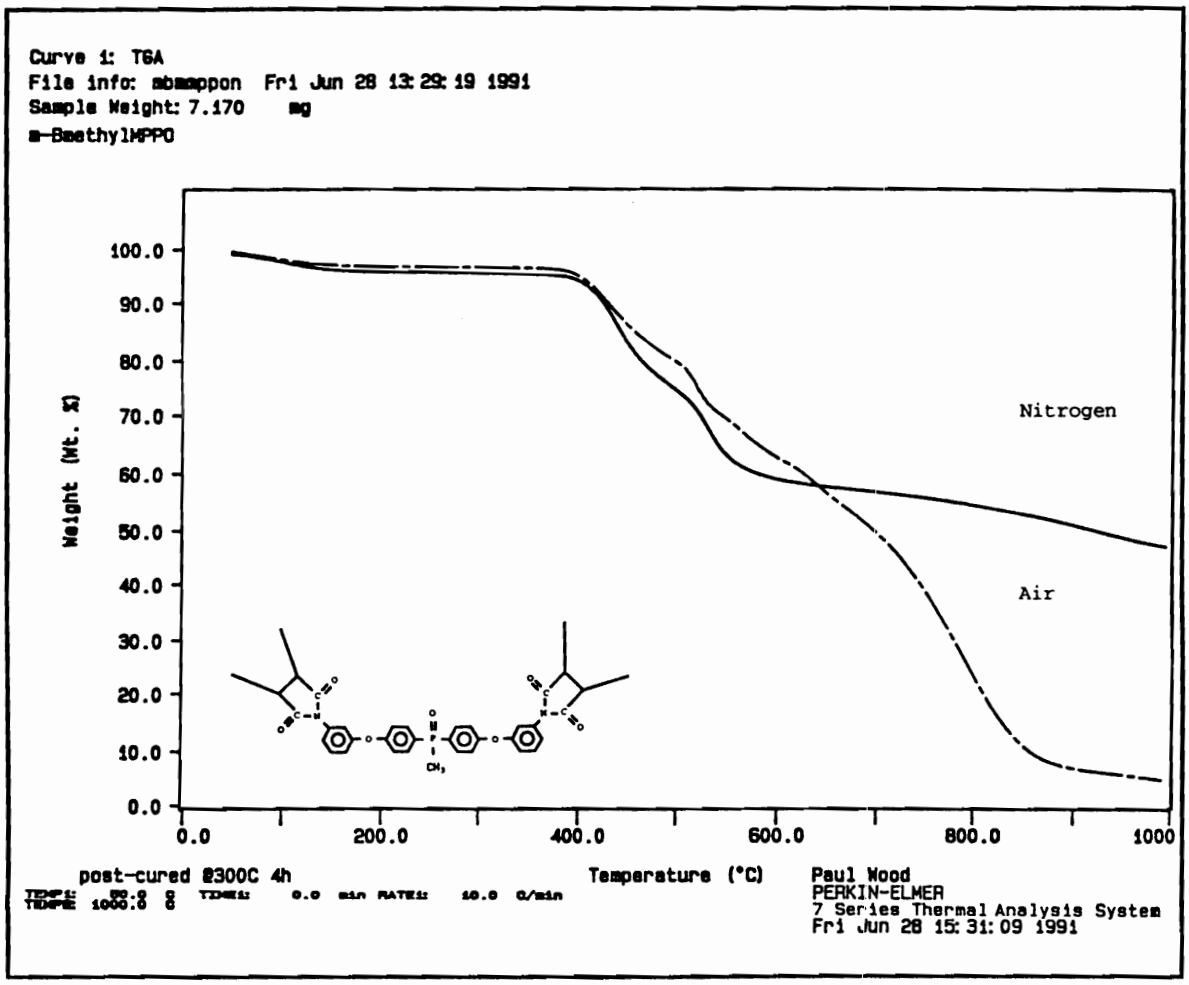

Figure 55

Dynamic TGA Scan of Bis(m-maleimidophenoxy)-diphenylmethyl phosphine oxide in Air and Nitrogen

stability as the other bismaleimides with weight loss not occuring until after 400°C in air and it also has a significant char yield.

Further mechanical properties outside the scope of this investigation need to be developed on these phosphine oxide bismaleimides, but first observations are that they are apparently much tougher materials than the methylene dianiline based bismaleimides. This will have to be confirmed by fracture toughness measurements.

B. Aromatic Ether Ketone Monomers and Thermosets

Aromatic ether ketone bismaleimides were prepared by a two-step process via synthesis of an aromatic diamine and subsequent imidization to the bismaleimide. These two steps are shown in Scheme 11, for the synthesis of the ether ketone diamine and in Scheme 12, for the bismaleimide. The reaction schemes and procedures were carried in essentially the same manner as previously described for the ether phosphine oxide bismaleimides. Three structural variations of the ether ketone monomers were prepared using meta-aminophenol, para-aminophenol and 2,2'-(4-hydroxyphenyl-4-aminophenyl)-propane. These monomers were prepared in high yields (>90%) and high purity (>99%).

In the course of determining the proper reaction conditions, the temperatures used in preparing the diamine were typical of those for activated halides in S_NAr reactions

STEP 1

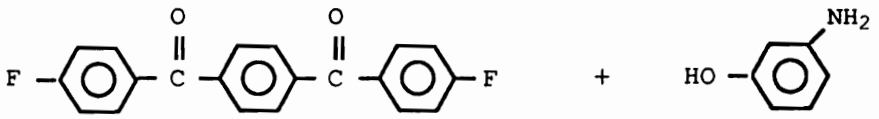

p-[Bis(4-fluorobenzoyl)]benzene + m-Aminophenol

80:20% v/v DMAC To Toluene @ 20% Solids

K_2CO_3

Temperature: 145°C for 4 hours

155°C for 2 hours

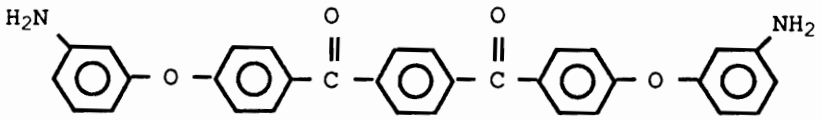

p-[Bis(m-aminophenoxybenzoyl)]benzene

Aminophenols = 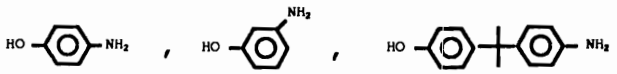

Scheme 11

Synthesis of Ether Ketone Diamine

STEP 2

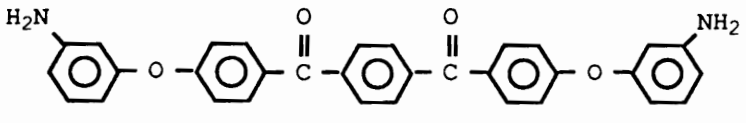

p-[Bis(m-aminophenoxybenzoyl)]benzene

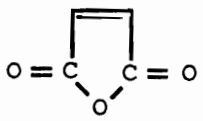

Maleic anhydride

Acetone
Room Temperture
1 Hour

p-[Bis(maleamic acid phenoxy benzoyl)]benzene

Acetone
Acetic anhydride
Sodium acetate
Reflux 3 Hours

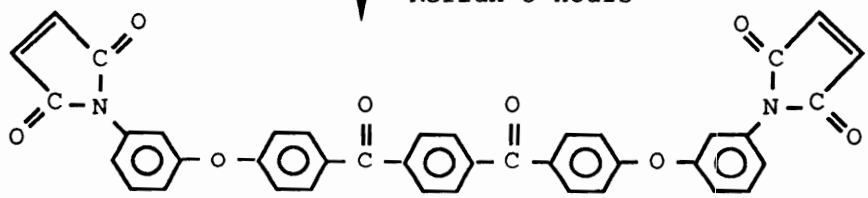

p-[Bis(m-maleimidophenoxybenzoyl)]benzene

Scheme 12

Synthesis of Ether Ketone Bismaleimide

of this type (50,189). In the first few attempts to develop the best procedure, a 2 to 1 mole ratio of m-aminophenol to p-[bis(4-fluorobenzoyl)]benzene was tried. However, subsequent molecular weight determinations by amine titrations showed that amine incorporation was not difunctional.

A very convenient method to follow the reaction was developed by measuring the disappearance of the fluoride from p-[bis(4-fluorobenzoyl)]benzene by fluorine NMR. Figure 56 shows the fluoride signal at around -106 ppm for the activated halide vs reaction time. Samples were pipeted from the reactor directly into NMR tubes without the need of working up the samples, since everything else in the reaction was transparent to the frequency measured. A hexafluorobenzene/chloroform-d internal standard sealed in a capillary tube was used to reference the peak.

For a 2 to 1 mole ratio the reaction appeared to be over in six hours, but the titrated molecular weight was off. In adjusting the ratio of aminophenol to p-[bis(4-fluorobenzoyl)]benzene at 145°C it was determined that a 5-10% mole excess of aminophenol was best. The reaction was complete in three hours, determined by the disappearance of fluoride signal when using an 10% excess of aminophenol. The S_NAr reaction was run at 145°C for an additional hour and then at 155°C for two hours to ensure completion. The

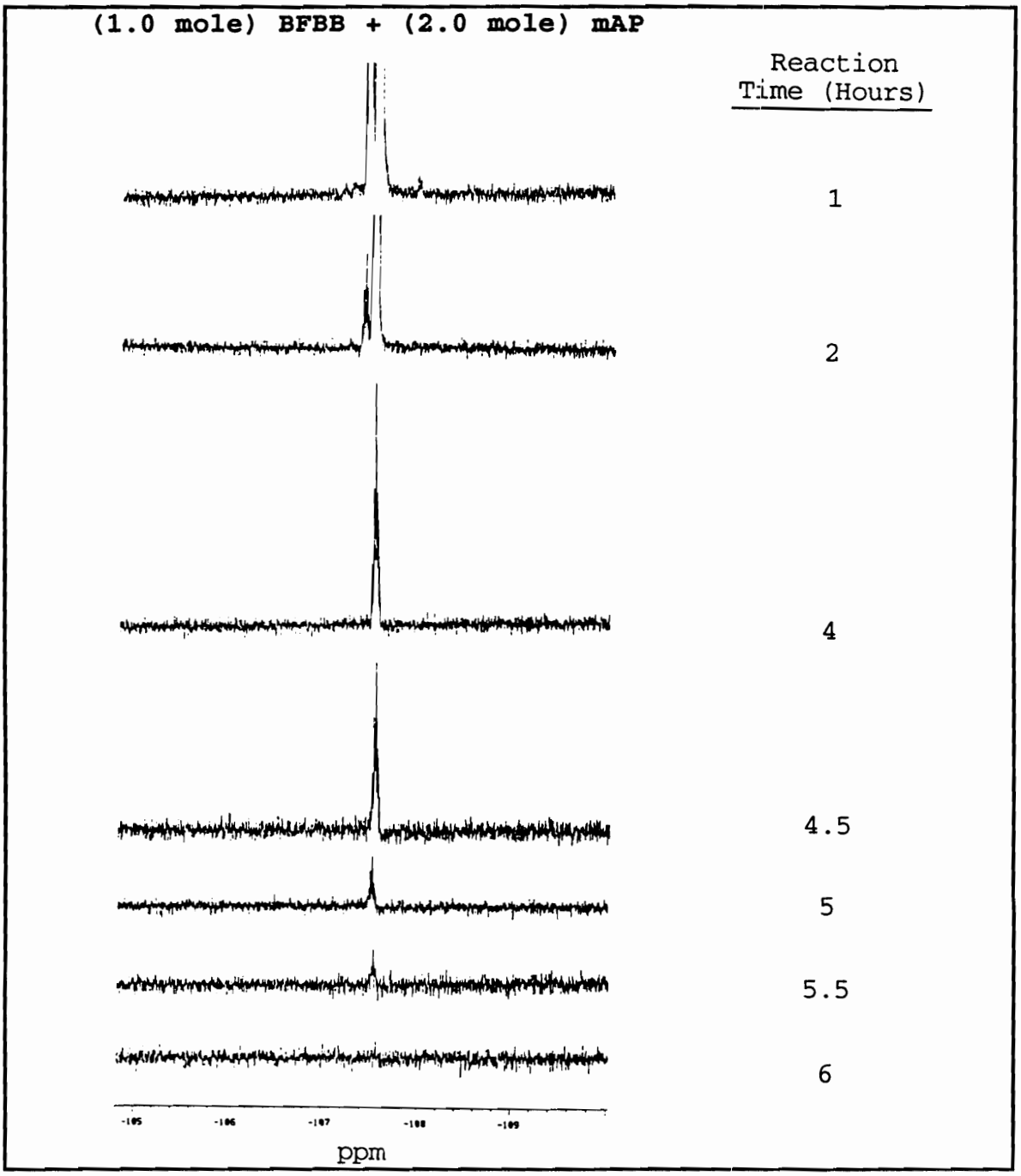

Figure 56

^{19}F-NMR of Ether Ketone Diamine Synthesis

aminophenols being soluble in water or methanol were easily removed from the diamine product.

The ether ketone monomers were characterized in the same manner as previously described for the ether phosphine oxide monomers. For example, Figure 57 shows a sharp monomodal HPLC trace for the ether ketone bismaleimide: p-[bis(m-maleimidophenoxybenzoyl)]benzene with a purity >99%. Molecular weight titrations for amines and amic acids were within ±2 g/mole for all monomers. Figure 58 illustrates the titrator's printout of the molecular weight determination for p-[bis(m-aminophenoxybenzoyl)]benzene.

FTIR and NMR were again used to confirm the chemical structure of all monomers. A FTIR example of p-[bis(m-aminophenoxybenzoyl)]benzene p-[bis(m-maleimidophenoxybenzoyl)]-benzene and is shown in Figure 59. The aromatic (N-H) stretching for the diamine and (=C-H) stretching for the bismaleimide can seen at 3400-3200 cm^{-1} and 3070 cm^{-1}, respectively. While the benzoyl and maleimide carbonyl (C=O) stetching are located at 1654 and 1716 cm^{-1}, respectively. Proton NMR for p-[bis(p-aminophenoxybenzoyl)]benzene shows a clean spectrum with the amine protons located at 5.1 ppm in Figure 60, while in Figure 61 the maleimide protons for p-[bis(m-maleimidophenoxybenzoyl)]benzene are seen at the expected 6.8 ppm. Carbon NMR for p-[bis(m-maleimidophenoxybenzoyl)]benzene in Figure 62 verifies the

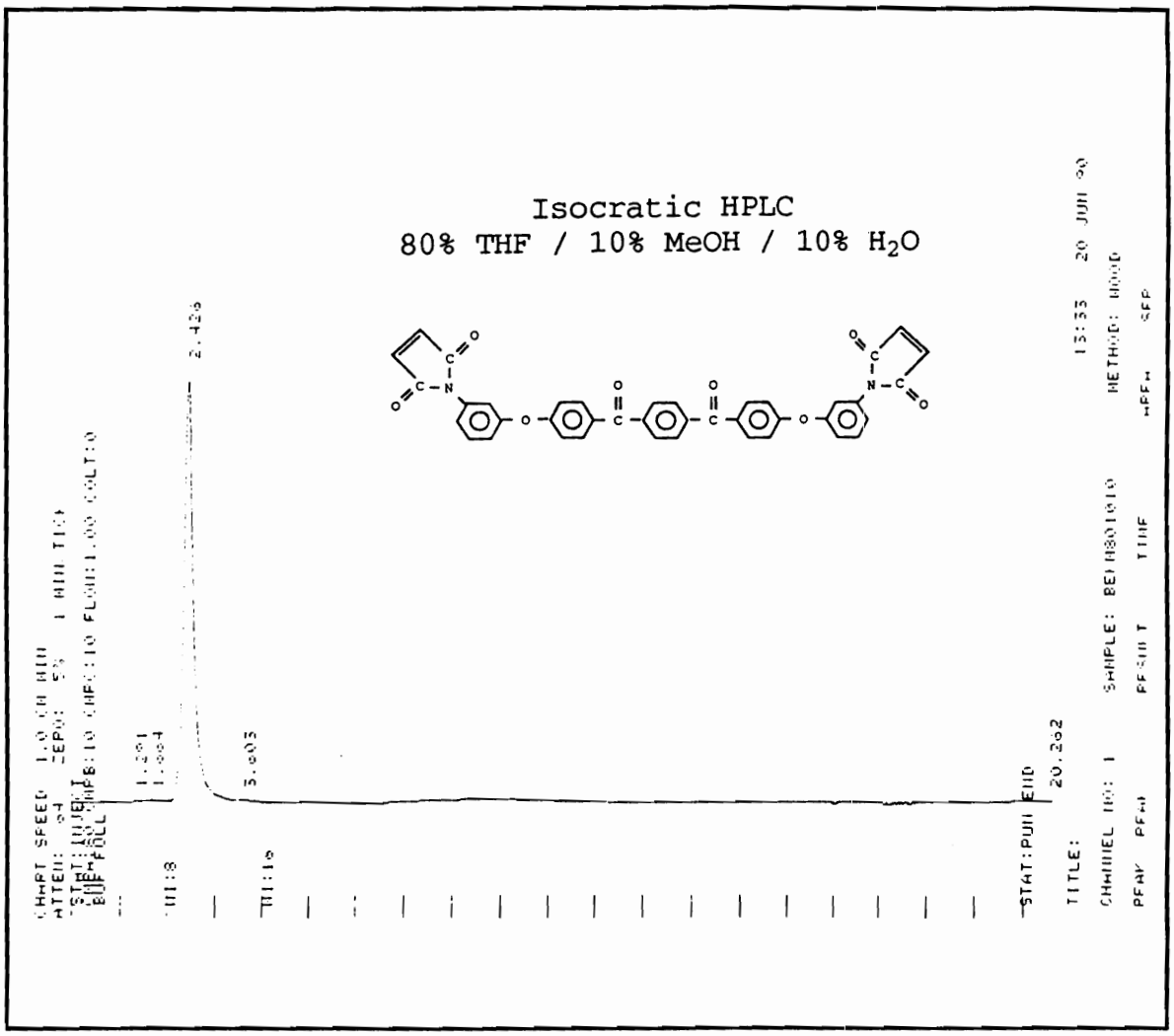

Figure 57

HPLC of Para-[bis(m-aminophenoxybenzoyl)]benzene

Titrating Reagent: HBr
Solvent: Chloroform

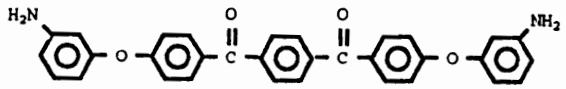

Calculated MW = 500.554 g/mole Titrated MW = 500.520 g/mole

Program Ver. US2.0
TITRATION T.= 3:42
ID-RNo: 4 - 2
NOTE :NH2 FSF SMPL :HBr
Pi: 240mv SS: 0.0226 g
A 474mv 3.843ml F 5=2000*SS/(N*A)

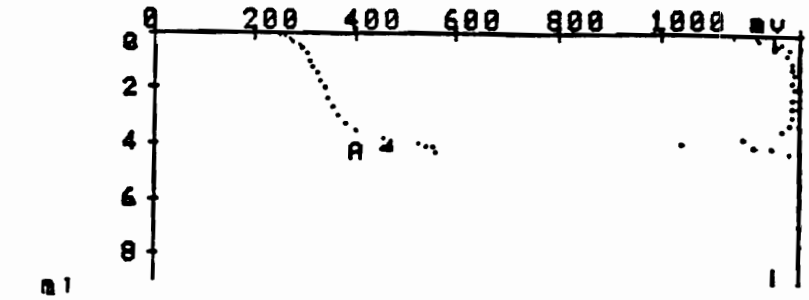

1990/12/06 20:43
T/File: 2 R/File: 2

C1 500.520 MW

Figure 58

Potentiometric Titration of

Para-[bis(m-aminophenoxybenzoyl)]benzene

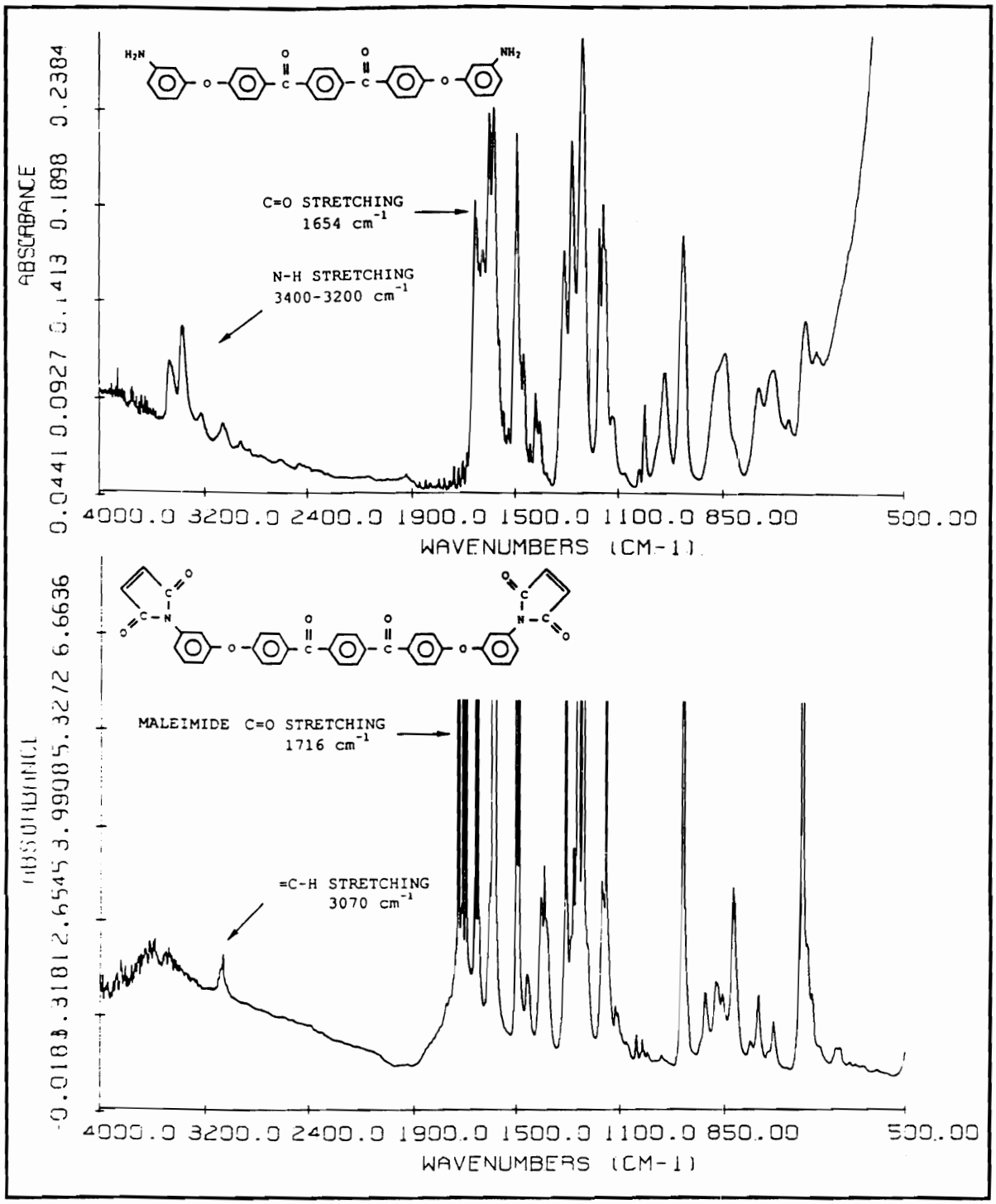

Figure 59

FTIR Spectra of Ether Ketone Monomers

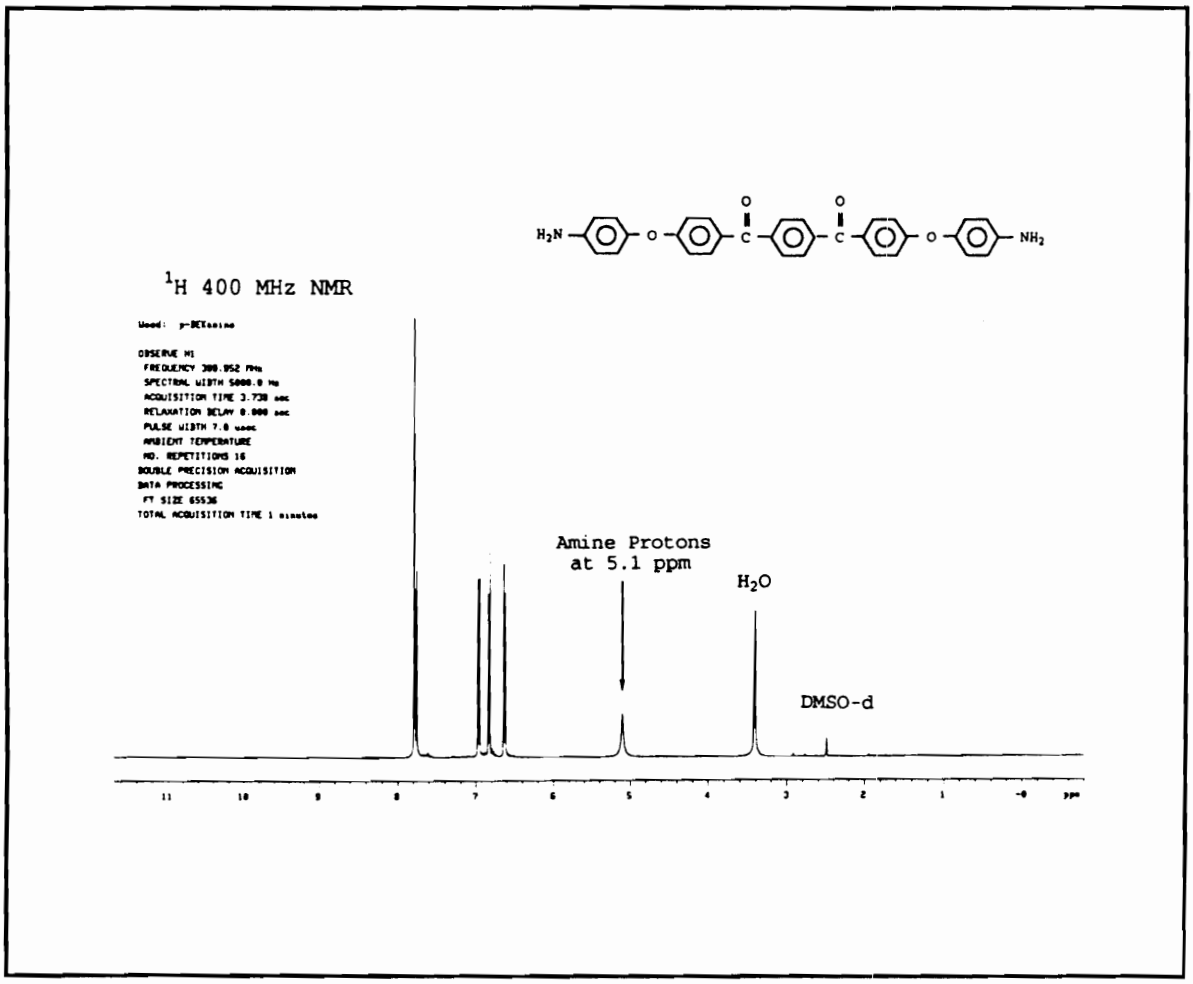

Figure 60

^{1}H-NMR of Para-[bis(p-aminophenoxybenzoyl)]benzene

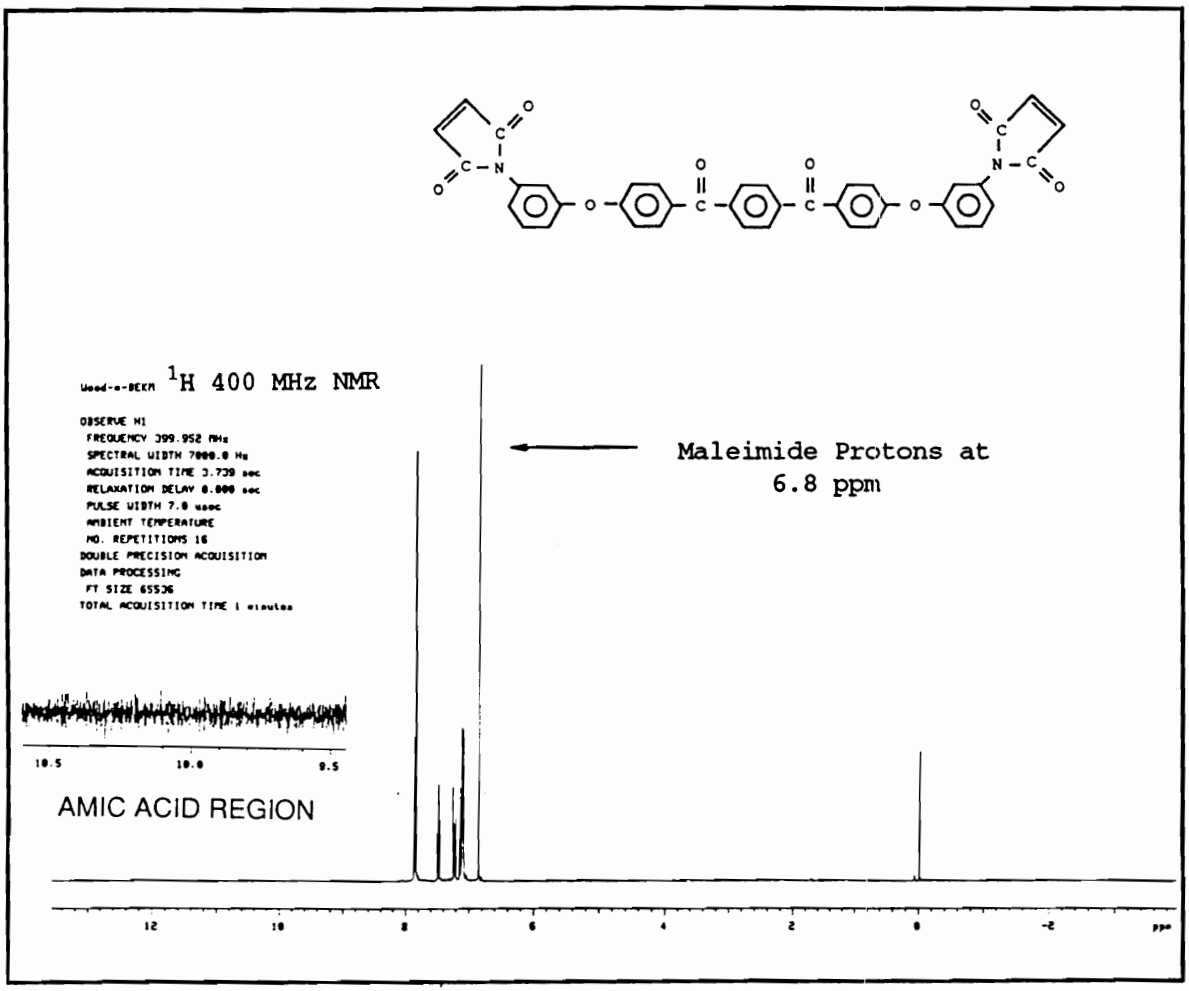

Figure 61

^{1}H-NMR of Para-[bis(m-maleimidophenoxybenzoyl)]benzene

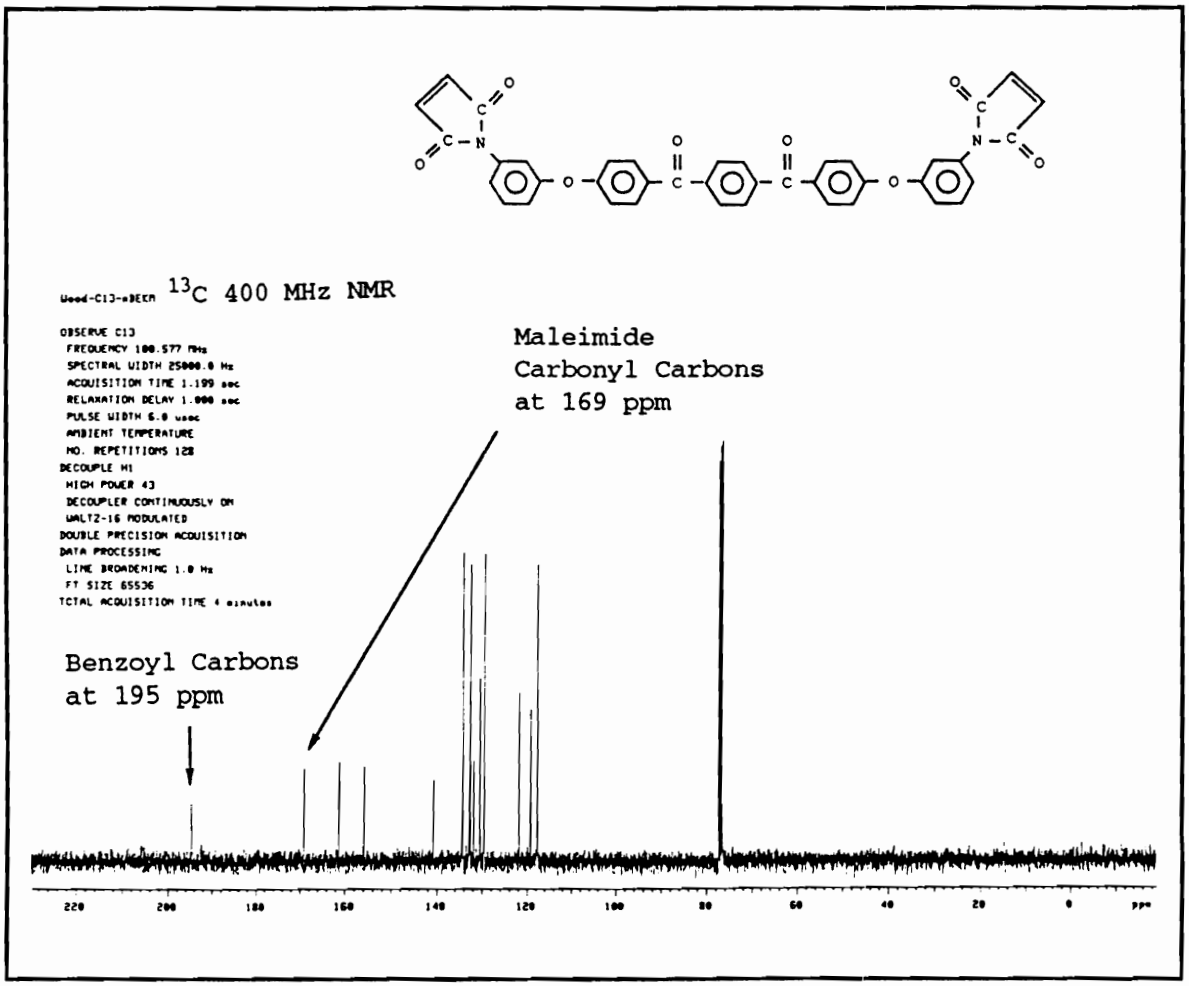

Figure 62

^{13}C-NMR of Para-[bis(m-maleimidophenoxybenzoyl)]benzene

presence of the maleimide and benzoyl carbons at 169 and 195 ppm, respectively.

However, in contrast to the phosphine oxide bismaleimides, the ether ketone meta- and para-bismaleimides melt around 200°C and immediately begin to crosslink as presented in Figure 63 for the dynamic DSC scan of ether ketone meta-bismaleimide. Both of the ether ketone meta- and para-bismaleimide networks have high glass transition temperatures, also around 400°C. The T_g as determined by TMA and DMTA are shown in Figures 64 and 65, respectively, for the ether ketone meta-bismaleimide network, post-cured at 300°C for 4 hours. Like the phosphine oxide bismaleimides the ether ketone bismaleimides exhibit a β-transition in the DMTA scan, which should again indicate improved toughness relative to the methylene dianiline based bismaleimides. Solid state carbon NMR was also utilized to confer the chemical structure of the ether ketone bismaleimide networks. Figure 66 indicates that the uncured maleimide carbonyl carbon shifts downfield from 169 to 175 ppm upon curing as was the case for the phosphine oxide bismaleimides.

The ether ketone bismaleimide networks demonstrate thermal stabilities similar to the phosphine oxide bismaleimides. Figure 67 indicates the thermo-oxidative stability of p-[bis(m-maleimidophenoxybenzoyl)]benzene network in air by dynamic and isothermal TGA, while Figure 68

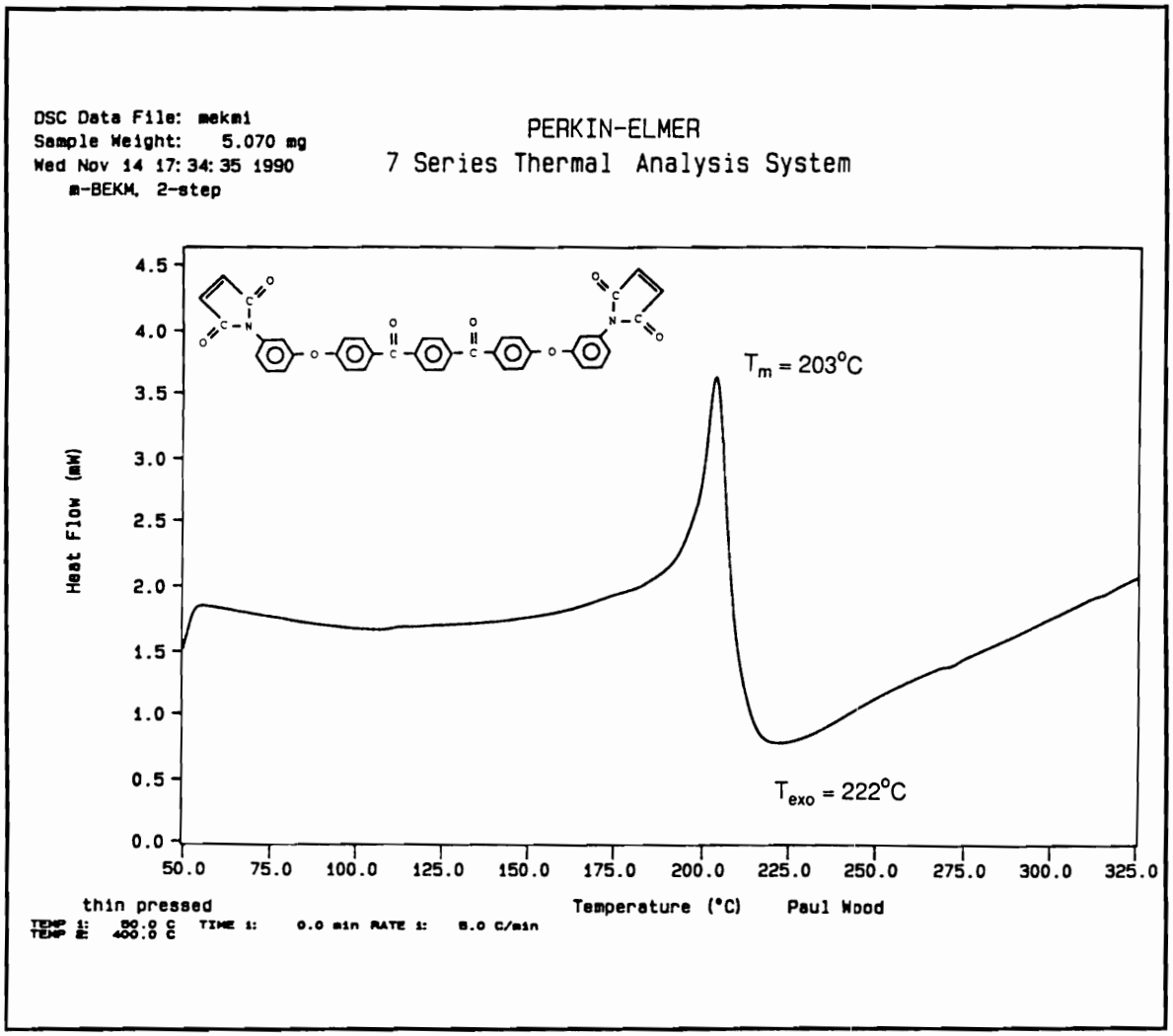

Figure 63

Dynamic DSC Scan of Para-[bis(m-maleimidophenoxybenzoyl)]benzene

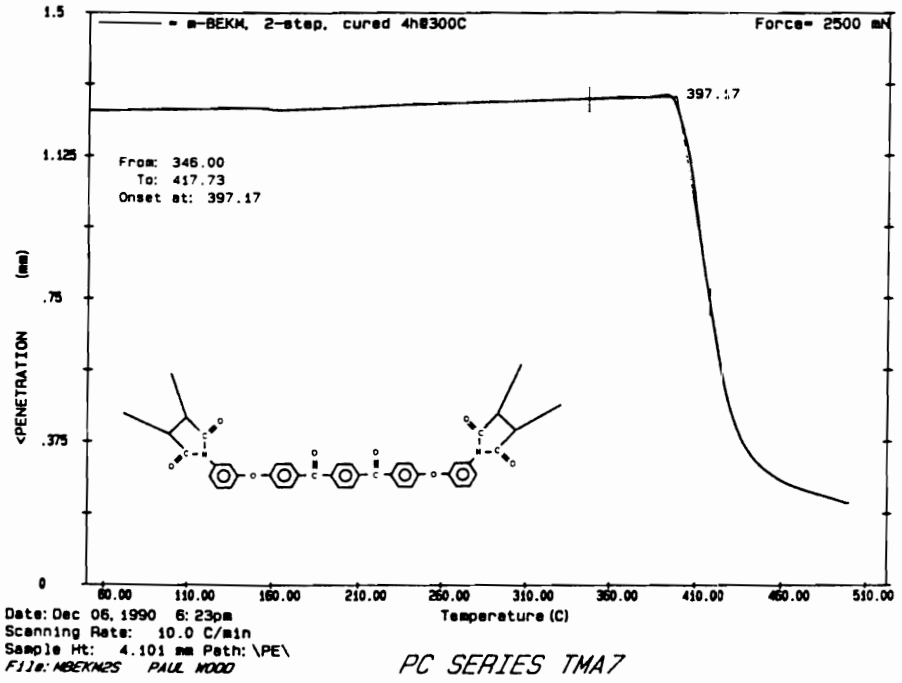

Figure 64

Dynamic TMA Scan of Para-[bis(m-maleimidophenoxybenzoyl)]benzene

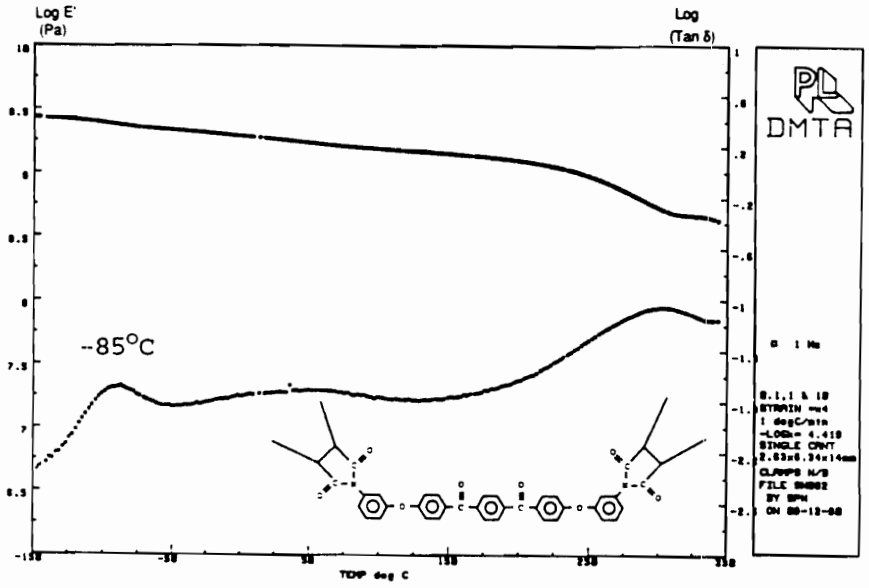

Figure 65

Dynamic Mechanical Behavior of

Para-[bis(m-maleimidophenoxybenzoyl)]benzene at 1 Hz

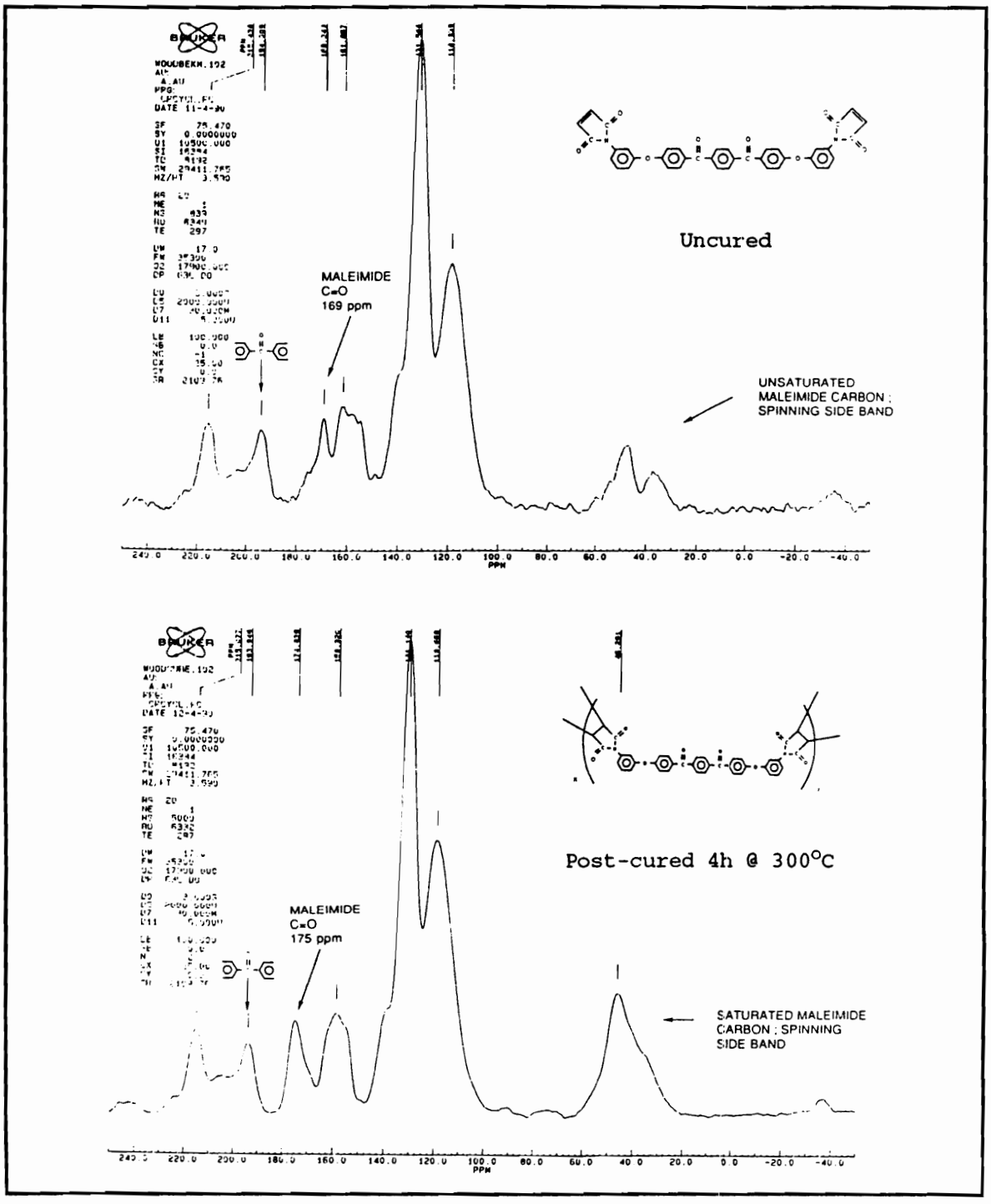

Figure 66

^{13}C-Solid State NMR of Uncured and Cured Para-[bis(m-maleimidophenoxybenzoyl)]benzene

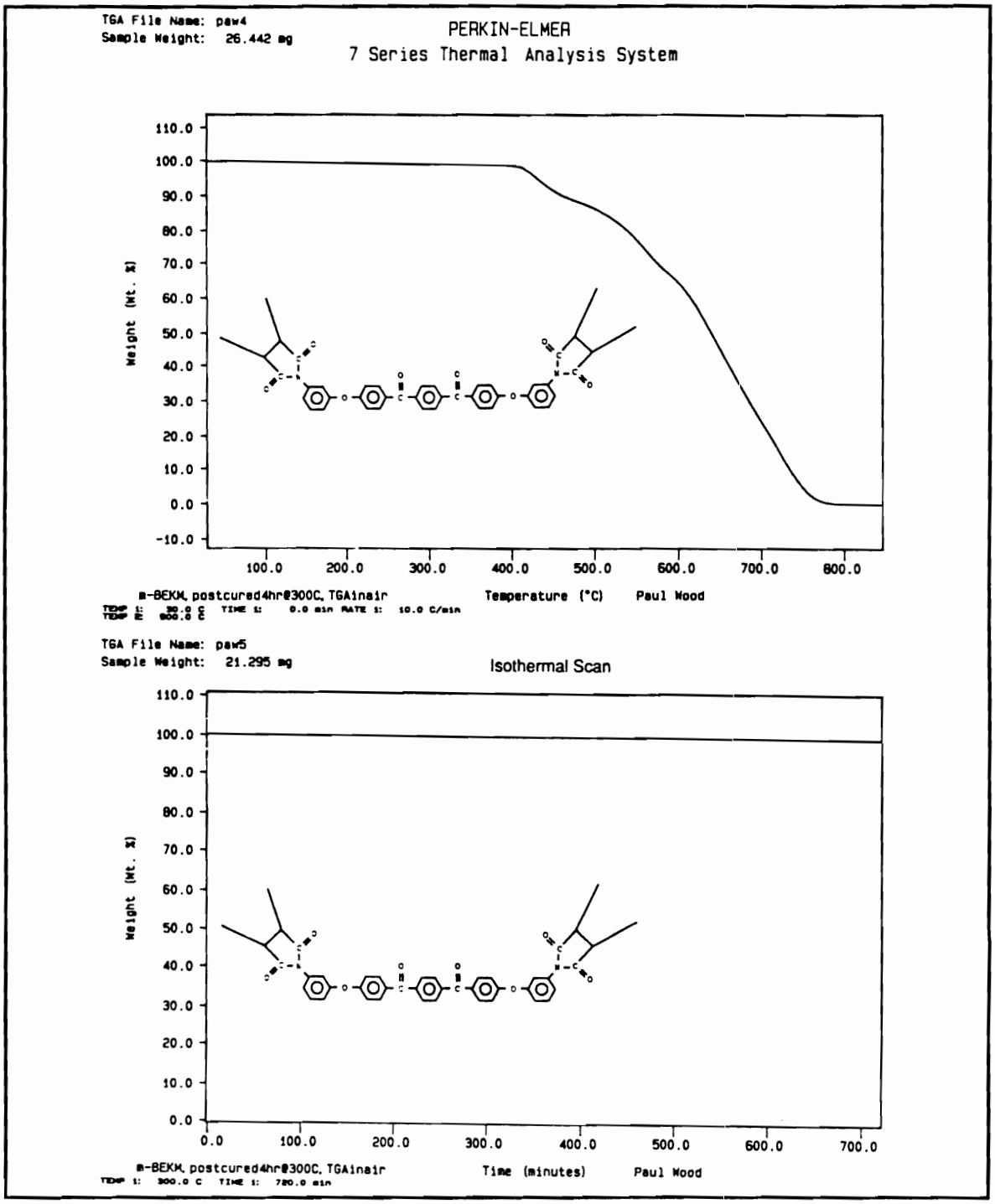

Figure 67

Dynamic and Isothermal TGA Scan of Para-[bis(m-maleimidophenoxybenzoyl)]benzene in Air

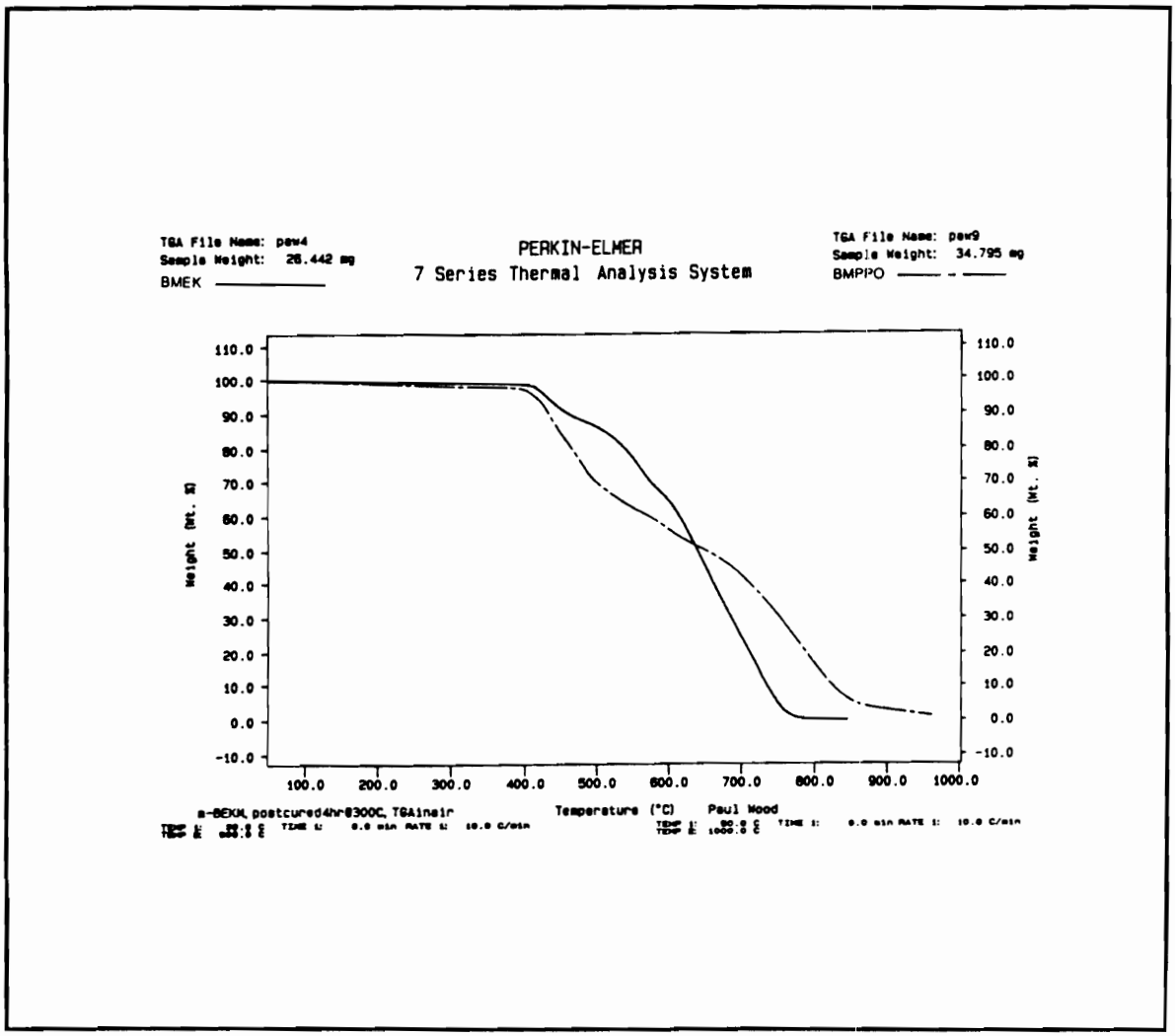

Figure 68

TGA Comparison of Para-[bis(m-maleimidophenoxybenzoyl)]benzene (BEKM) and bis(m-maleimidophenoxy)triphenyl phosphine oxide (BMPPO) in Air

compares the TGA of p-[bis(m-maleimidophenoxybenzoyl)]benzene to the bis(m-maleimidophenoxy)triphenyl phosphine oxide. The ether ketone bismaleimides are also stable in air up to 400°C and show no weight loss at 300°C for 12 hours. Poly(arylene ether ketones) are known to be flame resistant as a consequence of their molecular structure (309). The ether ketone bismaleimides also appear to have good flame resistance based on a similar char yield relative to the phosphine oxides as indicated in Figure 68.

The aminophenol, 2,2'-(4-hydroxyphenyl-4-aminophenyl)-propane was also used to prepared an ether ketone bismaleimide with the goal of having a lower melting point and better processability compared to the ether ketone meta- and para-bimaleimides, due to the flexible isopropylidene incorporation. The 2,2'-(4-hydroxyphenyl-4-aminophenyl)-propane based ether ketone monomer was synthesized in the same manner as the ether ketone meta- and para-bismaleimides. Clearly the amine and methyl protons; the maleimide carbonyl and isopropylidene carbons are seen in Figure 69 for the NMR spectra of the 2,2'-(4-hydroxyphenyl-4-aminophenyl)propane based ether ketone monomers. The dynamic DSC scan shown in Figure 70 confirms that indeed the isopropylidene linkages lowered the melting point without sacrificing the thermal stability, since the dynamic TGA scan shown in Figure 71 verifies stability up to 400°C in air.

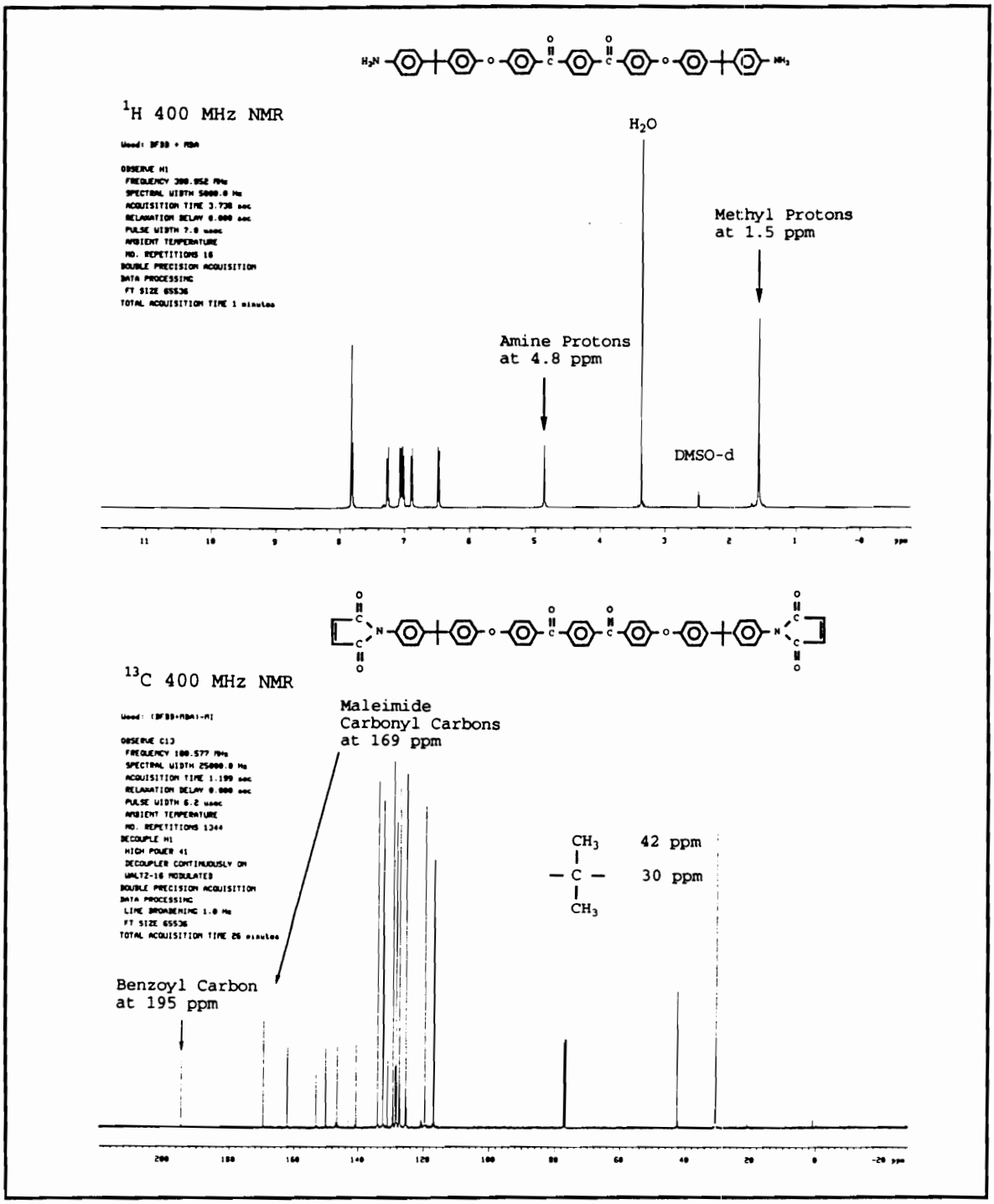

Figure 69

NMR Spectra of 2,2'-(4-Hydroxyphenyl-4-aminophenyl)propane Derived Ether Ketone Monomers

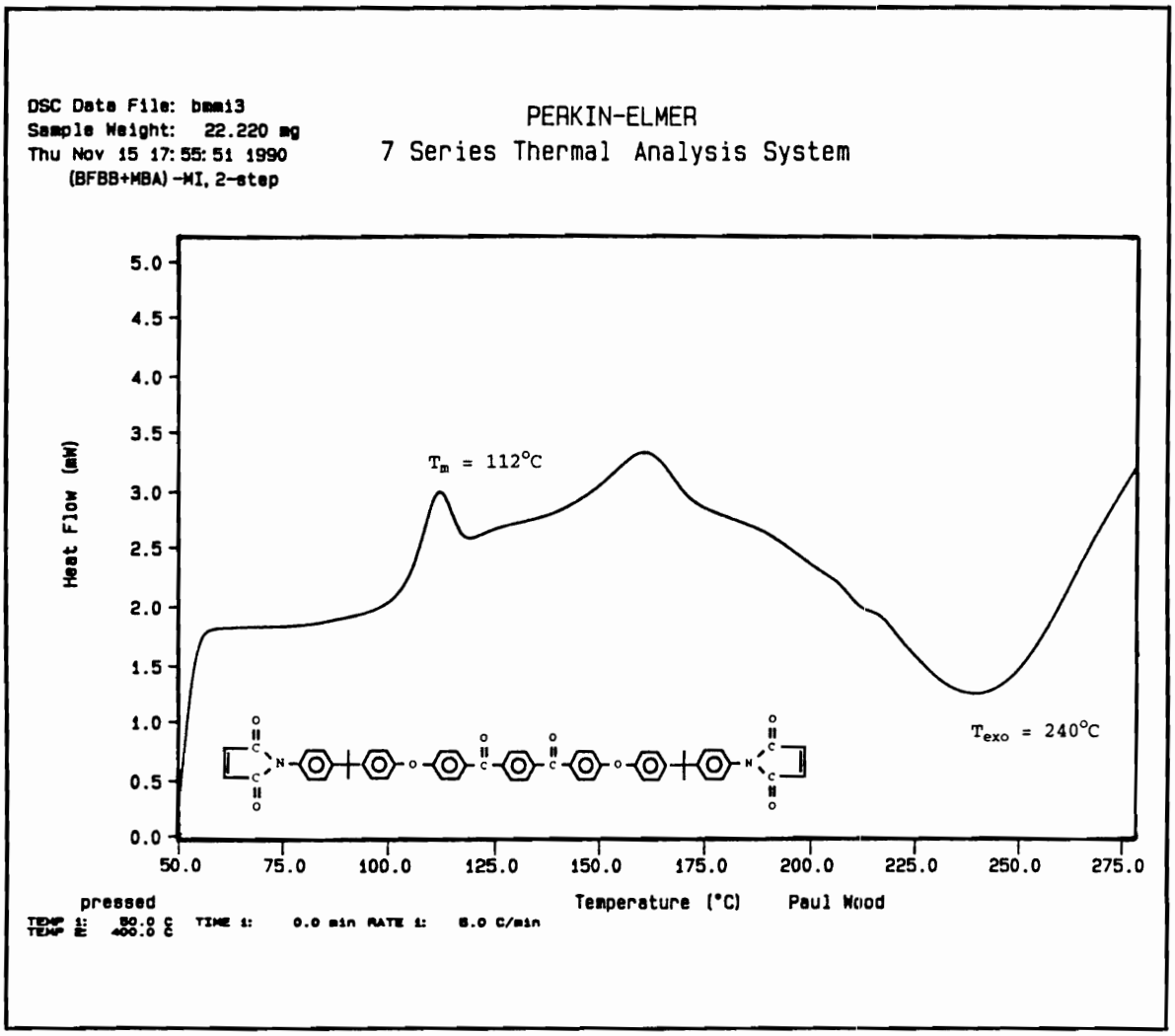

Figure 70

Dynamic DSC Scan of 2,2'-(4-Hydroxyphenyl-4-aminophenyl)propane Derived Ether Ketone Bismaleimide

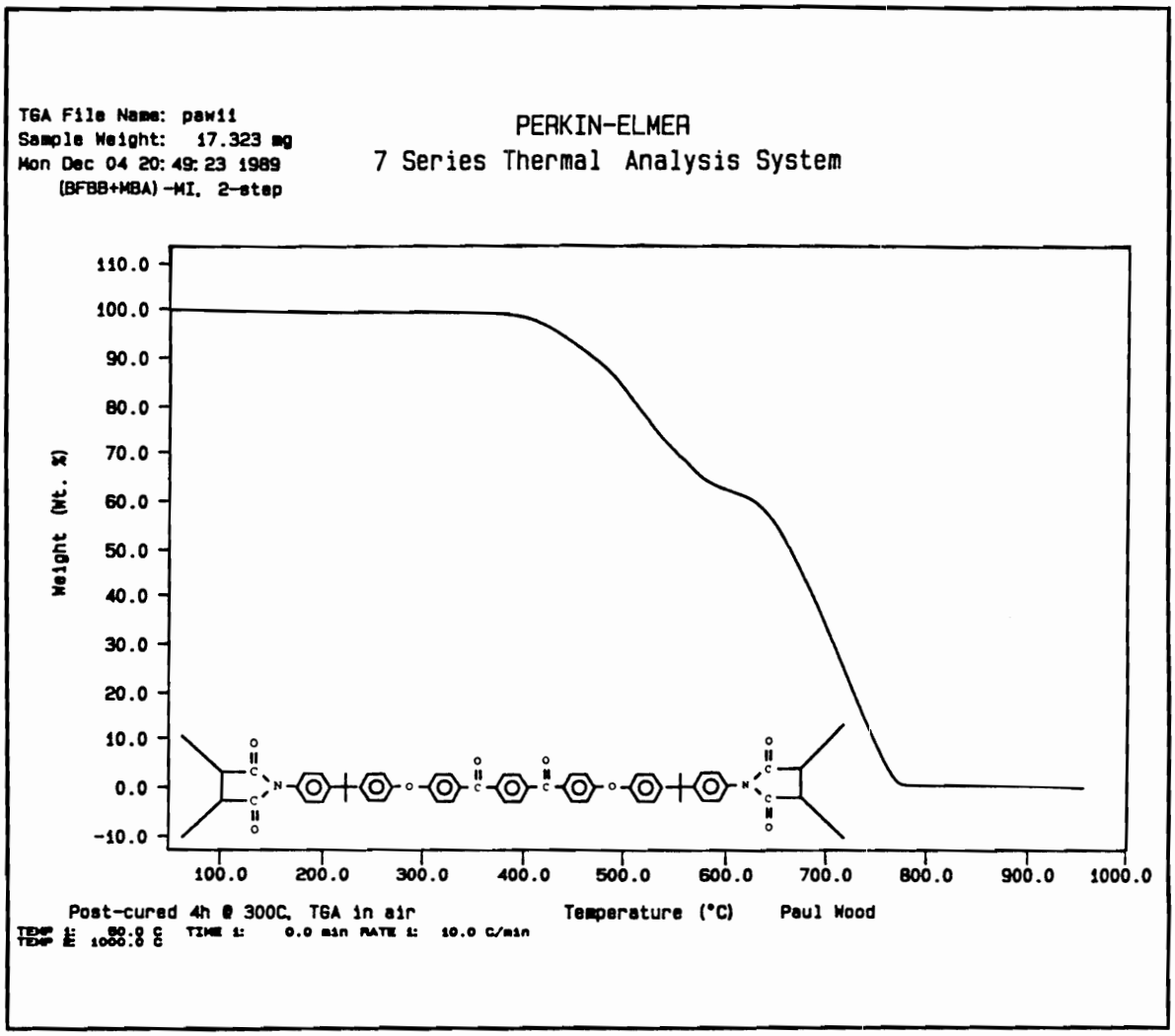

Figure 71

Dynamic TGA Scan of 2,2'-(4-Hydroxyphenyl-4-aminophenyl)propane Derived Ether Ketone Bismaleimide in Air

The 2,2'-(4-hydroxyphenyl-4-aminophenyl)propane bismaleimide has a melting point of 112°C and the network post-cured at 300°C for 4 hours has a T_g as shown in Figure 72 around 10°C lower than the ether ketone meta- and para-bismaleimides.

C. Cycloaliphatic Bismaleimides

Cycloaliphatic bismaleimides were made by the same imidization procedure used to prepare the phosphine oxide and ether ketone bismaleimides. The six cycloaliphatic diamines listed in Table 19 were used to synthesize the bismaleimide, as shown in Scheme 13 for 4,4'-methylenebis (cyclohexylmaleimide)-20. The FTIR and NMR characterization of the cycloaliphatic bismaleimides is outlined in Table 20.

These cycloaliphatic diamines were of interest because all of them were liquids at room temperature with the exception of 4,4'-methylenebis(aminobenzyl)cyclohexylamine which was a paste. The maleimides were of interest in the hope of preparing liquid bismaleimides, however all of the bismaleimides were solids, probably due to the rigid maleimide ring incorportion. All of the bismaleimides appeared to have very broad endotherms and then had poorly defined exotherms as represented in Figure 73 for the DSC of the bismaleimide 4,4'-methylenebis(cyclohexylmaleimide)-48. Melting points could not be detected using a melting point apparatus. The bismaleimide show no tendency to melt or flow

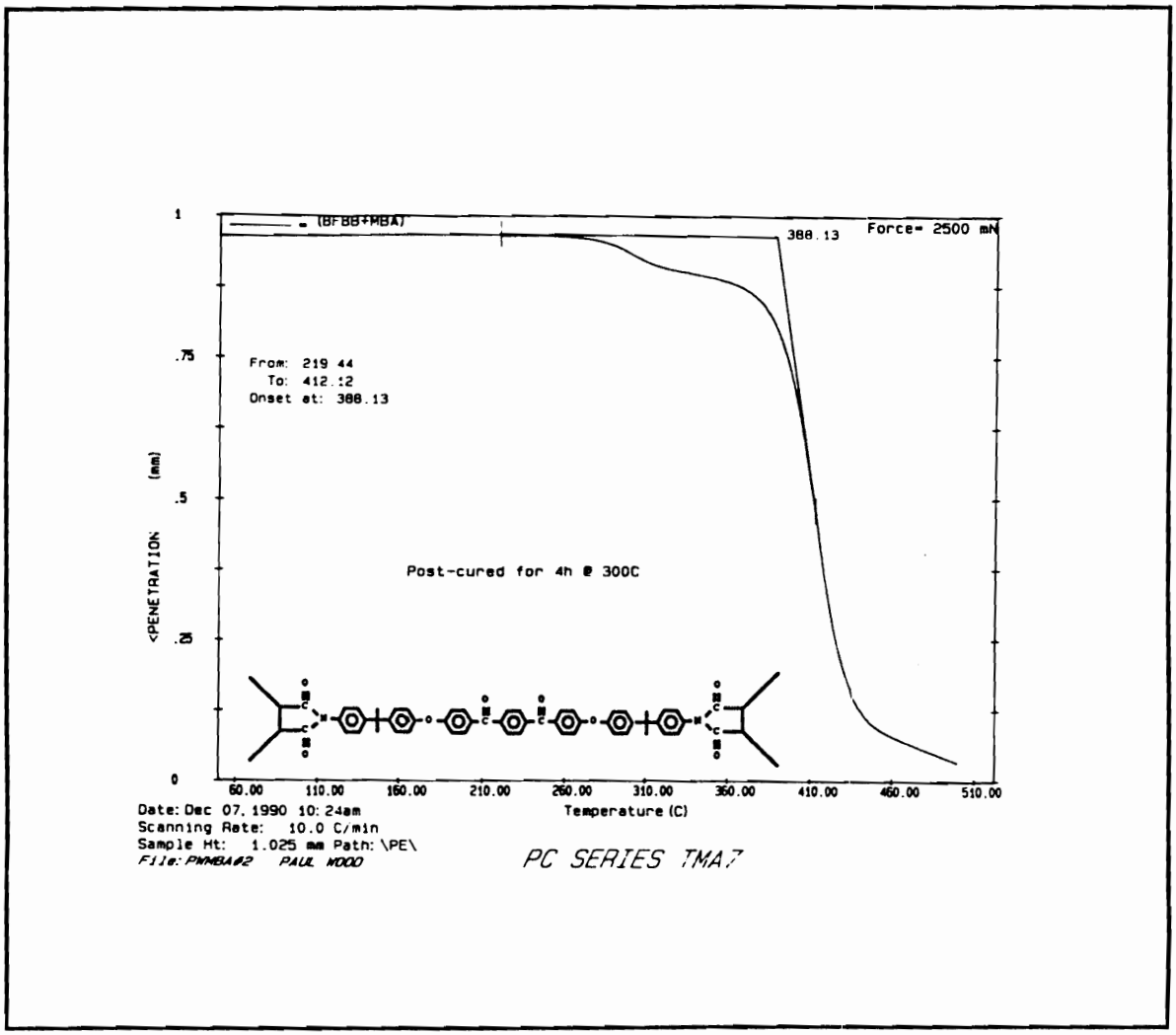

Figure 72

TMA Scan of 2,2'-(4-Hydroxyphenyl-4-aminophenyl)propane Derived Ether Ketone Bismaleimide

Table 19

Cycloaliphatic Diamines

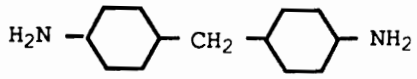

4,4'-Methylene-
bis(cyclohexylamine)-20

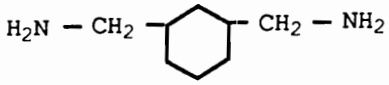

1,3-Bis(aminomethyl)-
cyclohexane

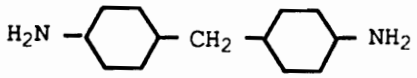

4,4'-Methylenebis-
(cyclohexylamine)-48

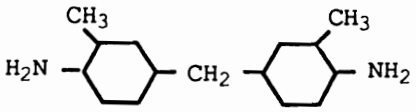

(3,3'-Dimethyl-4,4'-diamino-
dicyclohexylmethane

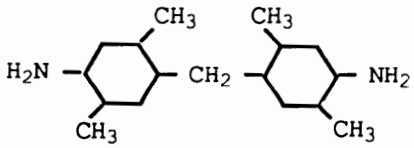

(2,2',5,5'-Tetramethylmethylene-
di(cyclohexylamine)

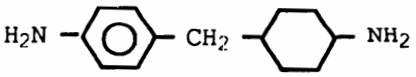

4,4'-methylene(aminobenzyl)-
cyclohexylamine

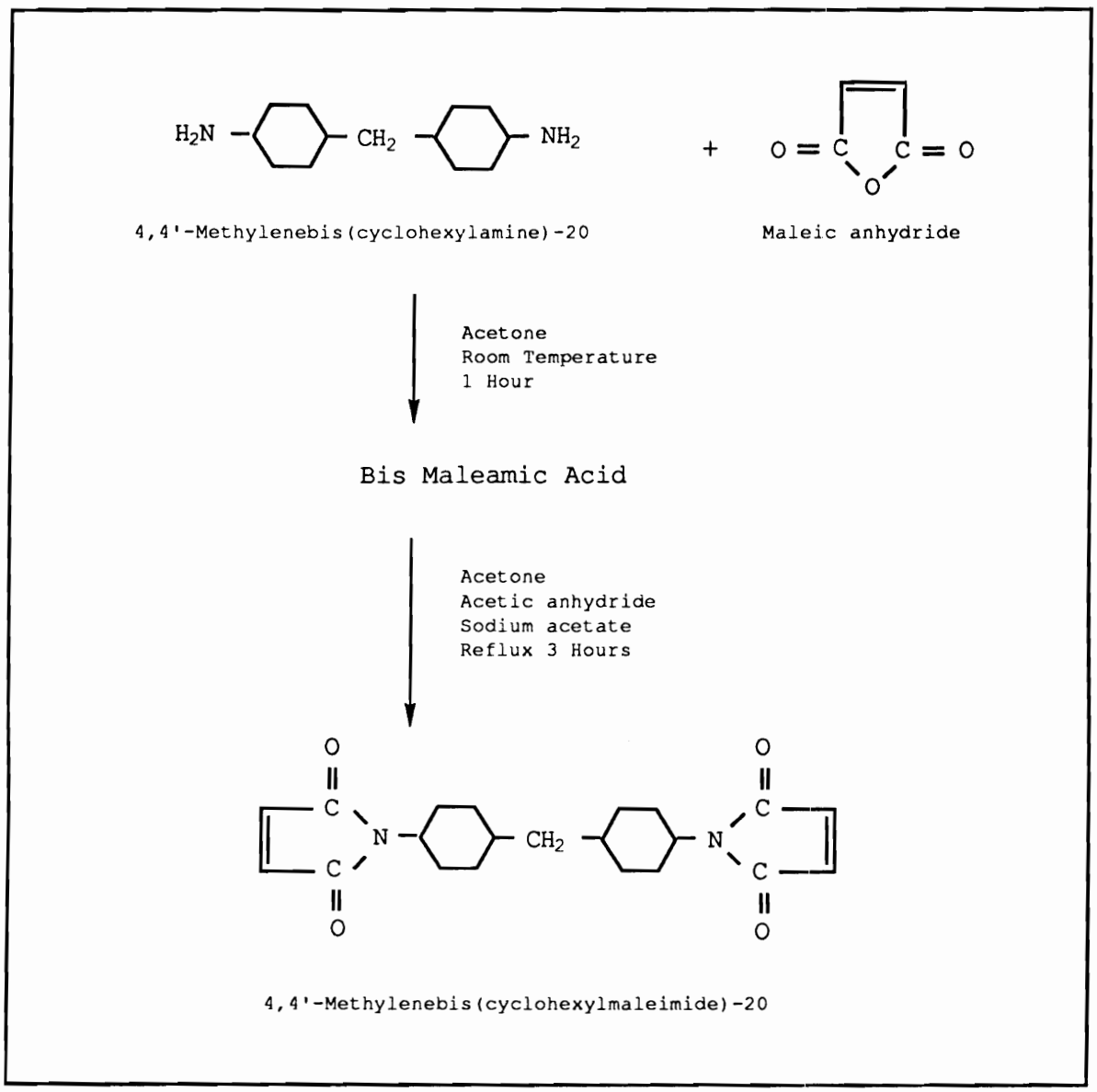

Scheme 13

Synthesis of Bismaleimides Derived from Cycloaliphatic Amines

Table 20

FTIR and NMR Characterization of Cycloaliphatic Bismaleimides

Bis Maleimide	FTIR	NMR	
	cm^{-1}	^{1}H (ppm)	^{13}C (ppm)
4,4'-Methylenebis-(cyclohexylmalemide)-20	3090 =C-H stretching 1703 maleimide carbonyl stretching	6.9 maleimide proton	169 maleimide carbonyl carbon
4,4'-Methylenebis-(cyclohexylmalemide)-48	3090 1703	6.9	171
2,2'-,5,5'-Tetra-methylmethylenedi-(cyclohexylmalemide)	3090 1710	6.9	171
1,3-bis(maleimido-methyl)cyclohexane	3090 1730	6.9	171
3,3'-dimethyl-4,4'-dimaleimidodicyclo-hexylmethane	3090 1710	6.9	165
4,4'-Methylene-maleimidobenzyl) cyclohexylmalemide	3090 1716	7.1	169

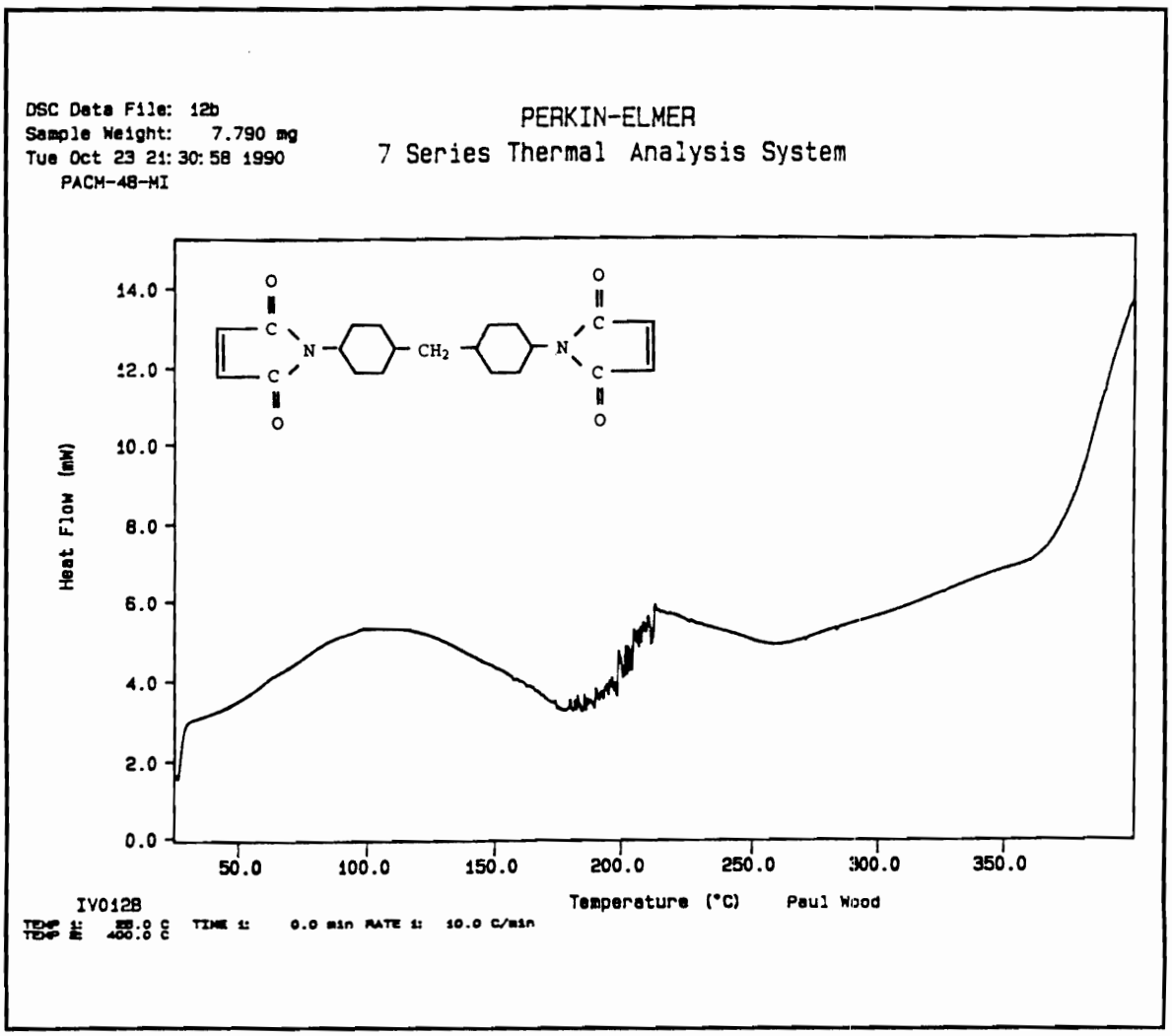

Figure 73

Dynamic DSC Scan of 4,4'-Methylenebis(cyclohexylmaleimide)-48

even up to a temperature of 250°C and are of less interest because of that.

D. Maleimide-terminated Poly(arylene ether ketones)

Maleimide-terminated poly(arylene ether ketones) were synthesized by a two step process via preparation of amine-terminated poly(arylene ether ketones) followed by imidization to the bismaleimide as described in Scheme 14 (50). Amine-terminated poly(arylene ether ketones) were prepared by end capping using meta-aminophenol, controlling the molecular weight according to the Carothers equation via addition of a monofunctional reagent. Very accurate molecule weights were prepared as verified in Figure 74 for the potentiometric titrations. The amine-terminated poly(arylene ether ketones) were imidized using maleic anhydride while refluxing in chlorobenzene. Table 21 shows the intrinsic viscosities of both the amine and maleimide-terminated poly(arylene ether ketones) increasing with increasing molecular weight, as expected. Figure 75 present the proton NMR for a maleimide-terminated with a calculated average molecular weight of 10,000 g/mole. The isopropylidene methyl protons clearly show up at 1.7 ppm, however at this molecular weight, the maleimide protons do not, at least for the number of acquisitions taken. But in Figure 76, for the carbon NMR and a 2,900 g/mole maleimide-terminated moiety, the maleimide

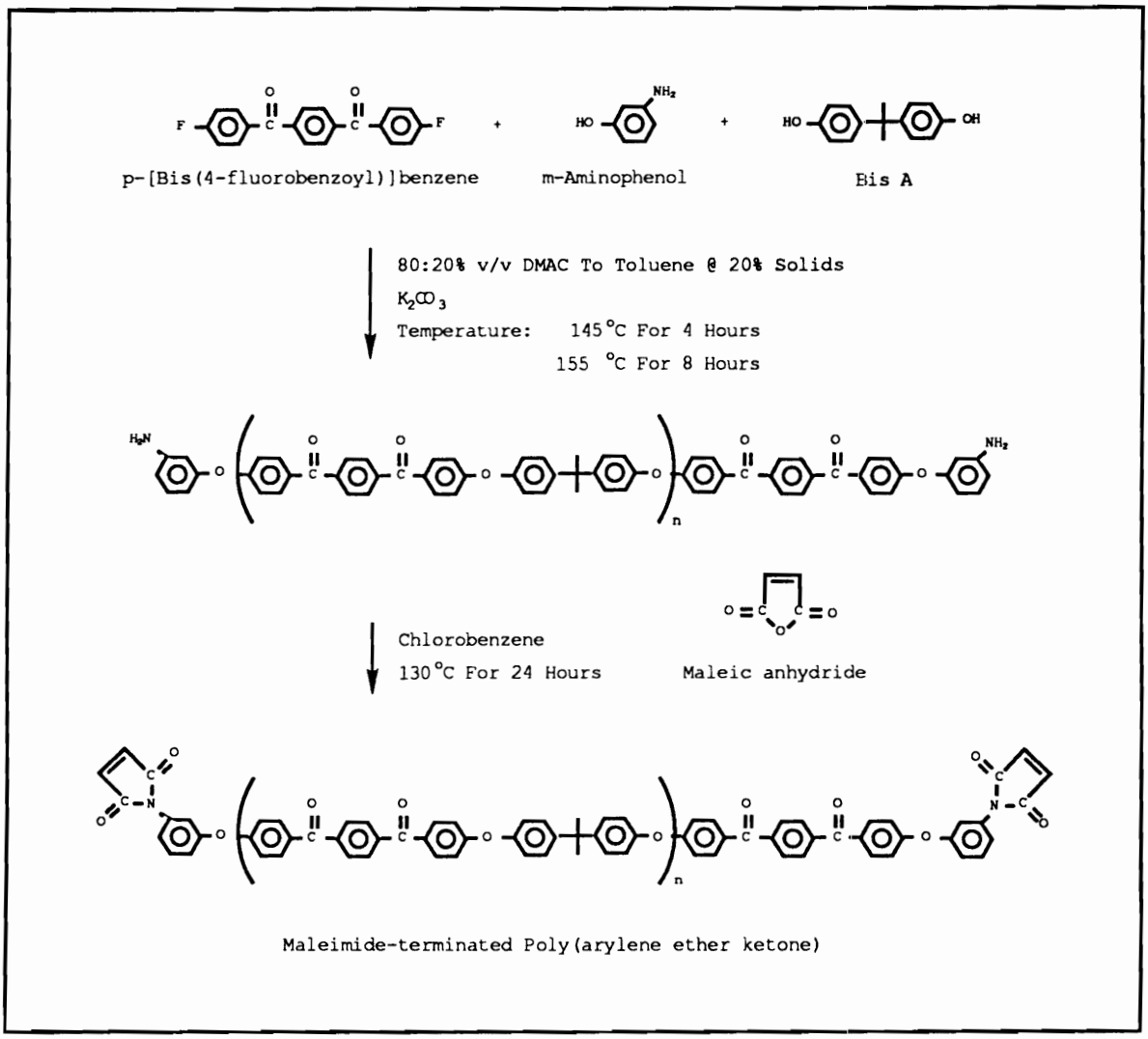

Scheme 14

Synthesis of Maleimide-terminated

Poly(arylene ether ketone) (50)

Titrating Reagent: HBr
Solvent: Chloroform

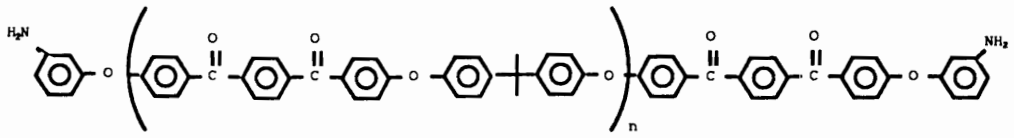

n	Calculated MW	Titrated MW
5	2900	3000
10	5500	5700
20	10500	11200

Figure 74

Molecular Weight Determination of Amine-terminated Poly(arylene ether ketones) via Potentiometric Titrations

Table 21

Poly(arylene ether ketones)

Intrinsic Viscosities and Glass Transition Temperatures

Amine-terminated Poly(arylene ether ketones)

Sample	$[\eta]^{25^{\circ}C}_{CHCl_3}$	T_g °C
2900	0.15	135
5500	0.27	150
10500	0.52	162

Maleimide-terminated Poly(arylene ether ketones)

Sample	$[\eta]^{25^{\circ}C}_{CHCl_3}$	T_g °C Cured
2900	0.26	179
5500	0.38	173
10500	0.66	167

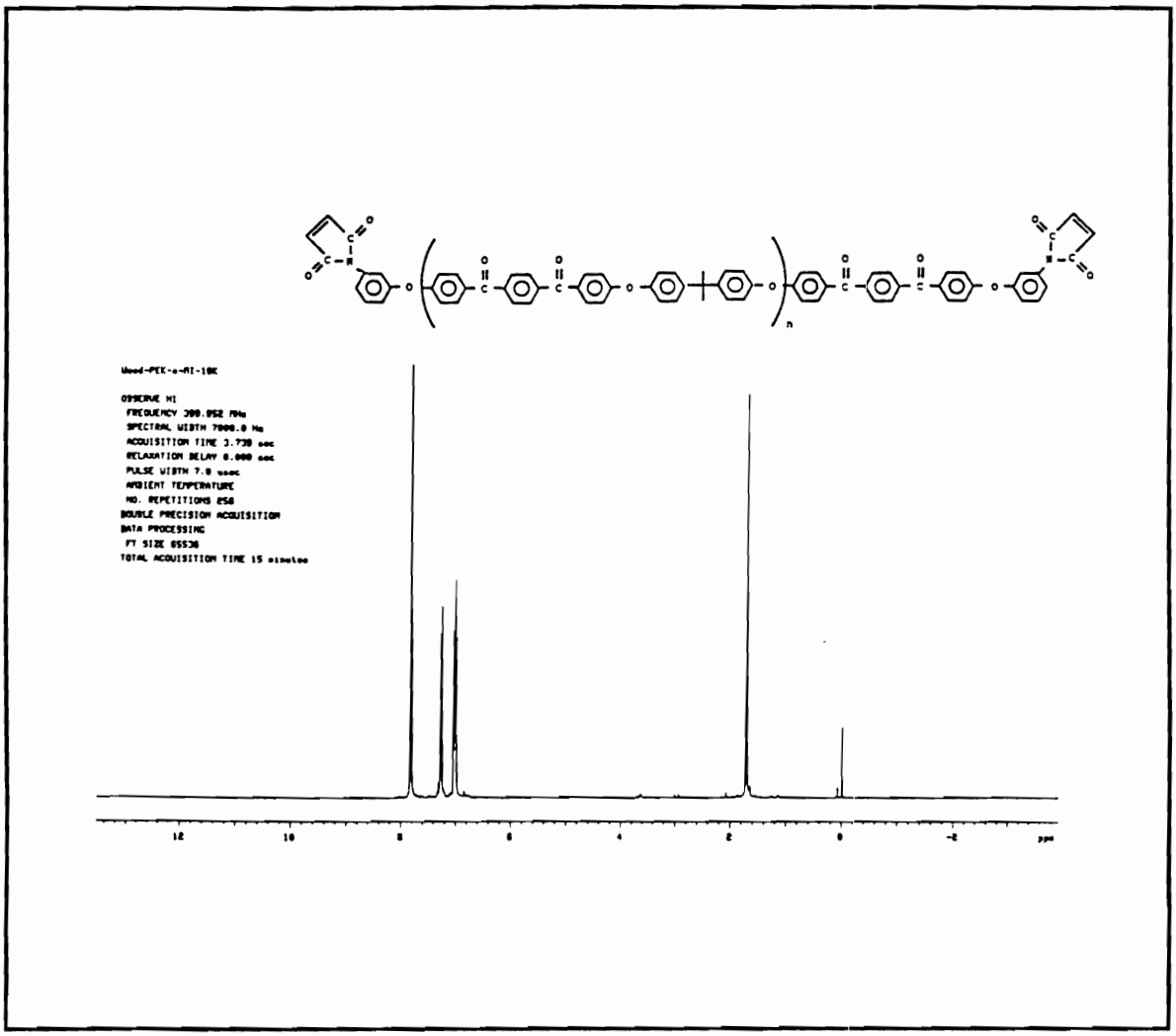

Figure 75

^{1}H-NMR of 10K Maleimide-terminated

Poly(arylene ether ketone)

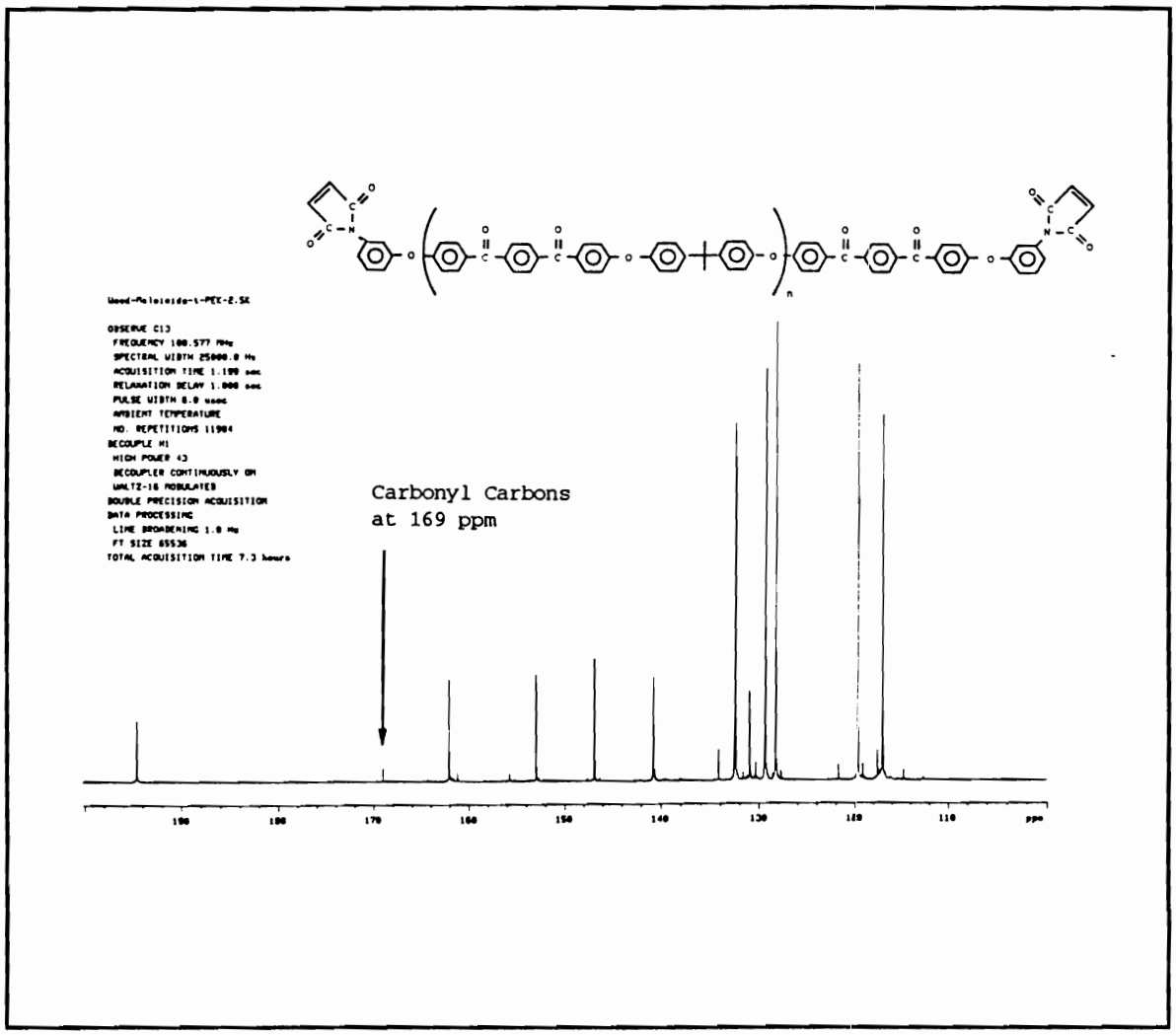

Figure 76

^{13}C-NMR of 2.9K Maleimide-terminated

Poly(arylene ether ketone)

carbonyl carbon at 169 ppm establishes that indeed the amine was imidized to the maleimide.

The glass transition temperatures for the amine and maleimide-terminated polymers are outlined in Table 21. As expected the amine-terminated polymers increase in T_g with increasing molecular. But interesting it has been demonstrated by Lyle that the ability to control the final T_g of the crosslinked maleimide-terminated poly(ether ketones) could be accomplished by varying the molecular weight of the starting poly(ether ketone)(50). As the oligomer molecular weight was lowered, the crosslink density increased leading to a corresponding increase in the T_g of the network as a result of decreased chain mobility. This is clearly shown in Table 21 for the cured maleimides. A representative DSC scan is shown in Figure 77 for the 2.9K fully cured system. While these system show thermal stability up to 450°C as shown in Figure 78, they are limited by their T_g for high temperature applications. However, the main interest with regards to the phosphine oxide and ether ketone bismaleimides would be to blend them with maleimide-terminated poly(arylene ether ketones), poly(arylene phosphine oxides) or poly(phosphine oxide imides) and others. In this manner it is predicted that both the glass transition temperature and fracture toughness could be controlled. Blending of the phosphine oxide bismaleimides with maleimide-terminated polyimides

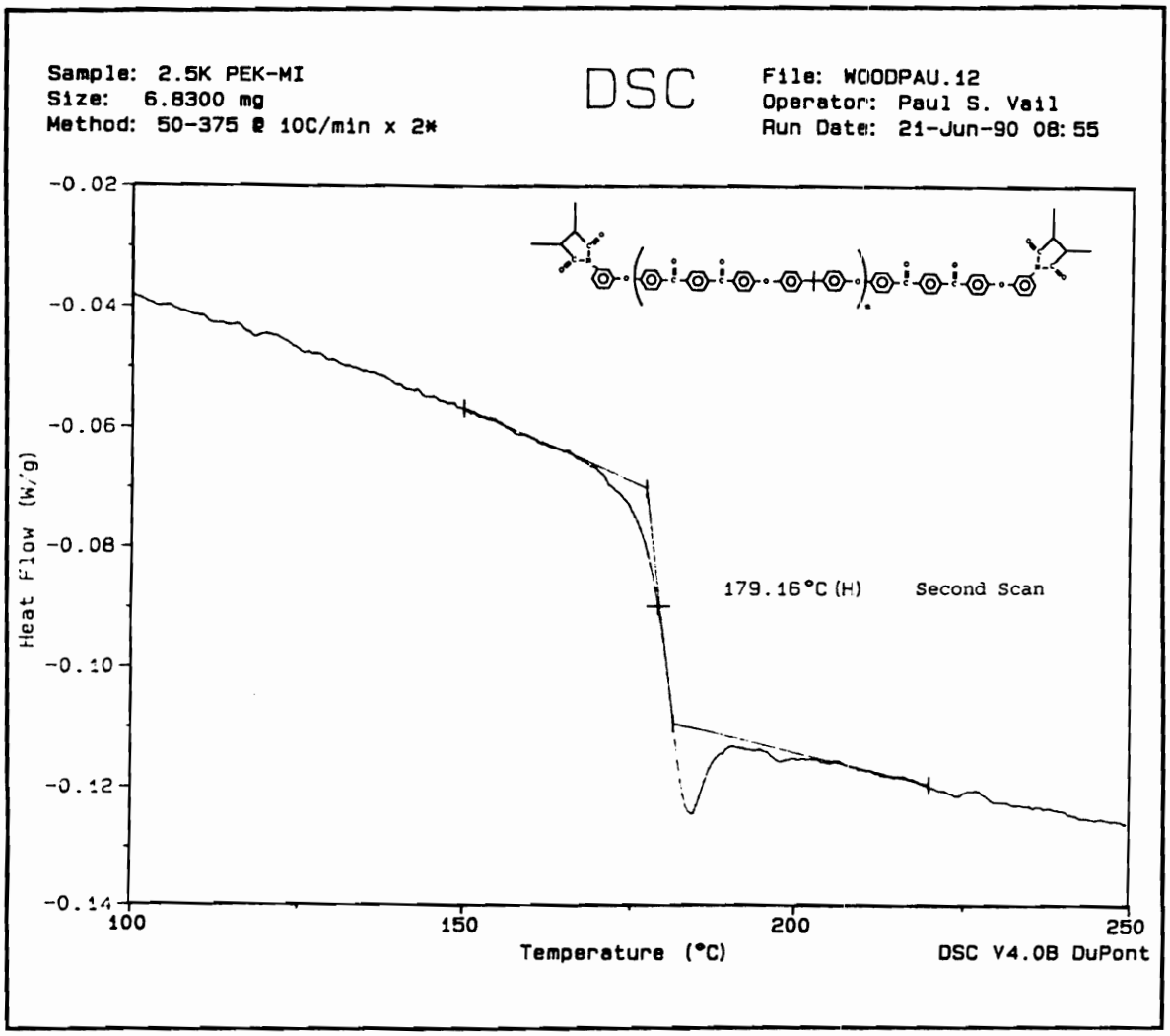

Figure 77

T_g of 2.9K Maleimide-terminated

Poly(arylene ether ketone)

via DSC

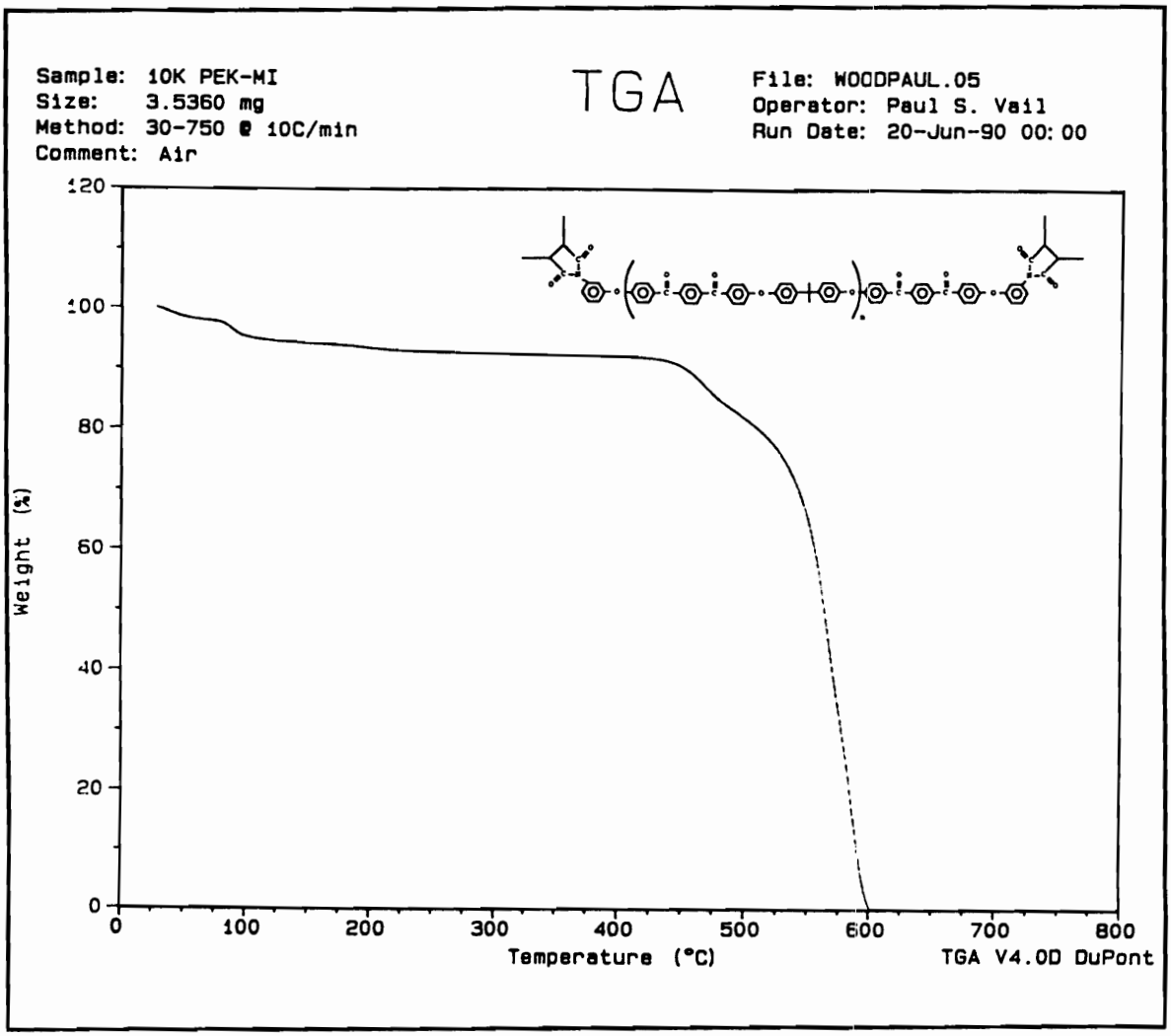

Figure 78

Dynamic TGA Scan of Maleimide-terminated

Poly(arylene ether ketone)

in Air

based on triphenyl phosphine oxide should have T_g's in the range of high temperature applications.

V. Conclusions

Ether phosphine oxide and ether ketone bismaleimides have been synthesized by a two-step procedure via preparation of aromatic diamine by a S_NAr reaction and subsequent cyclodehydration to the bismaleimide using maleic anhydride. Characterization verified the difunctionality of the diamines while bisamic acids were completely imidized to the bismaleimide. Characterization by HPLC, titration, FTIR and NMR has shown the materials to be obtainable in high yields and high purity.

Several structural variations of the phosphine oxides were prepared utilizing meta-aminophenol, para-aminophenol and 2,2'-(4-hydroxyphenyl-4-aminophenyl)propane in conjunction with the central triphenyl or diphenylmethyl phosphine oxide moieties. Thermal analysis by DSC has shown that all of the phosphine oxide bismaleimides to melt in the proximity of 100°C and cure at >180°C, demonstrating a usable processing window. The cured triphenyl phosphine oxide bismaleimide moieties prepared with the meta and para-aminophenols demonstrated glass transition temperatures around 400°C, while the incorporation of isopropylidene linking units from the 2,2'-(4-hydroxyphenyl-4-aminophenyl)propane based bismaleimide lowered the T_g as expected. Substitution of the pendent phenyl group in the meta-triphenyl phosphine oxide bismaleimide for a methyl

group lowered the T_g by approximately 35°C, still in the range of desired applications. All of the cured phosphine oxide bismaleimides exhibited excellant thermo-oxidative stability as indicated by TGA, showing thermal stability up to 400°C in air. These materials had unusually good fire resistance.

Three structural variations of the ether ketone bismaleimide were investigated utilizing the central p-(bis benzoyl)benzene unit along with meta, para and 2,2'-(4-hydroxyphenyl-4-aminophenyl)propane aminophenols. These materials also demonstrated exceptional thermooxidative stability in air up to 400°C and high glass transition temperatures around 400°C. However, the meta and para-bismaleimides prove to be high melting which resulted in a narrow processing window. A wider processing window was gained by inserting the flexible isoproylidene linkages along the network's main chains via 2,2'-(4-hydroxyphenyl-4-aminophenyl)propane derived ether ketone bismaleimide. This incorporation was achieved with little sacrifice to the glass transition temperature or to the thermo-oxidative stability of the network.

Cycloaliphatic liquid diamines were of interest because of the prospect of preparing liquid bismaleimides via the same successful imidization procedure used for the phosphine oxide and ether ketone bismaleimides. However, all of the

cycloaliphatic bismaleimides turned out to be high melting solids and probably less interesting because of that.

It was demonstrated that amine and maleimide-terminated poly(arylene ether ketones) could be prepared by procedures established in our laboratories that had precise control on molecular weight according to the Carothers equation. Maleimide end capping could also easily be amenable to other polymeric system like poly(arylene phosphine oxides) and polyimides. Bismaleimides developed in this investigation could then be blended with maleimide-terminated polymers to control the glass transition temperature and likely the fracture toughness of these networks.

This investigation has demonstrated the successful preparation of novel phosphine oxide and ether ketone bismaleimides with good processing windows, good thermal properties and excellent flame resistance. The stiffness behavior as defined by glass transition temperature would suggest that these materials could be used as structural adhesive or matrix resins. The networks also exhibited β-relaxation peaks via DMTA which indicates the materials may have improved fracture toughness relative to the commercial methylenedianiline based bismaleimides. Further mechanical properties need to be developed on these networks, but the first observations are that they are much tougher material than the methylenedianiline bismaleimides.

VI. References

1. B. C. Trivedi and B. M. Culbertson, "Maleic Anhydride," Plenum Press, New York (1982).

2. J. M. Barrales-Rienda, J. I. Campa and J. G. Ramos, "Free-Radical Copolymerizations of N-Phenyl Maleimide," J. Macromol. Sci. Chem. A11(2), 267 (1977).

3. J. R. Grawe and B. G. Bufkin, "Use of Maleimide Acceptors As a Means of Developing Crosslinking Emulsions," J. Coat. Tech. 53(676), 45 (1981).

4. R. C. P. Cubbon, "The Free Radical and Anionic Polymerization of Some N-Substituted Maleimides," Polymer 6, 419 (1965).

5. Y. Okamoto, T. Nakano, H. Kobayashi and K. Hatada, "Asymmetric Polymerization of N-Phenylmaleimide," Polym. Bull. 25, 5 (1991).

6. S. R. Turner, R. A. Arcus, C. G. Houle and W. R. Schleigh, "High-T_g Base-Soluble Copolymers as Novalac Replacements for Positive Photoresists," Polym. Eng. Sci. 26(16), 1096 (1986).

7. W. R. Brunsvold, L. P. Bushnell, M. F. Chow and C. F. Lyons (IBM), "Alkali-Soluble Ultraviolet Photoresist Containing Maleimide-Styrene Derivative Copolymer," Euro. Patent 272,498 (1988).

8. L. M. Minsk and H. L. Cohen (Eastman Kodak Co.), "Polymeric Hardeners for Gelatin," U. S. Patent 3,308,075 (1967).

9. M. P. Stevens and A. D. Jenkins, "Crosslinking of Polystyrene via Pendant Maleimide Groups," J. Polym. Sci.: Polym. Chem. Ed. 17, 3675 (1979).

10. R. E. Hefner, Jr. (Dow Chemical), "Cyanate Functional Maleimide Thermosetting Composition," U. S. Patent 4,683,276 (1987).

11. J. R. Wolfe, Jr. and I. C. Kogon, "Maleimide Cure Systems," Rubber Age 103(6), (1971).

12. K. Ho and R. Steevensz, "Diels-Alder Reaction Curing of Chlorobutyl Rubber by Bismaleimides," Rubber Chem. Technol. 62(1), 42 (1989).

13. H. D. Stenzenberger, "Recent Advances in Thermosetting Polyimides," Br. Polym. J. 20, 383 (1988).

14. M. Chaudhari, J. King and B. Lee, "A New Bismaleimide Matrix Resin For High Performance Advanced Composites," 32nd International SAMPE Symp. 32, 24 (1987).

15. H. D. Stenzenberger, "Bismaleimide Resins," in "Structural Adhesives: Developments in Resins and Primers," ed. by A. J. Kinloch, Elsevier Applied Science Publishers, New York, 77 (1986).

16. D. Landman, "Advances in the Chemistry and Applications of Bismaleimides," in "Developments in Reinforced Plastics, Vol. 5," ed. by G. Pritchard, Elsevier Applied Science Publishers, New York, Chp. 2, 39 (1986).

17. H. D. Stenzenberger, M. Herzoq, W. Römer and R. Scheiblich, "Compimides: A Family of High Performance Bismaleimide Resins," 30th National SAMPE Symp. 30, 1568 (1985).

18. H. D. Stenzenberger, et al., "Bismaleimide Resins: Past, Present, Future," 34th International SAMPE Symp. 34, 1877 (1989).

19. H. D. Stenzenberger, P. König, M. Herzog and W. Römer, "Toughened Bismaleimides: Concepts, Achievements, Directions," 19th International SAMPE Tech. Conf. 19, 372 (1987).

20. Chemical Abstract Search conducted on 11-3-90.

21. J. V. Crivello, "Polyimidothioethers," J. Polym. Sci., Polym. Chem. Ed. 14, 159 (1976).

22. P. Kovacic and R. W. Hein, "Cross-linking of Polymers with Dimaleimides," J. Am. Chem. Soc. 81, 1187 (1959).

23. H. Stenzenberger, K. U. Heinen and D. O. Hummel, "Thermal Degradation of Poly(Bismaleimides)," J. Polym. Sci., Polym. Chem. Ed. 14, 2911 (1976).

24. H. D. Stenzenberger, "The Preparation and Properties of High Performance Polyimide Composites," Appl. Polym. Symp. 22, 77 (1973).

25. J. L. Little (U.S. Rubber) , "Vulcanization of Polymer with N,N'-Bismaleimide and Compositions Thereof," U. S. Patent 2,989,504 (1961).

26. J. E. Moore and W. M. Ward, "Cross-Linking of Bovine Plasma Albumin and Wool Keratin," J. Am. Chem. Soc. 78, 2414, (1956).

27. P. Kovacic (Du Pont), "Elastomeric Reaction Products of Bismaleimides with Organic Diamines," U. S. Patent 2,818,405 (1957).

28. F. Grundschober and J. Sambeth (Societe Rhodiaceta), "Preparation of Crosslinked Polyimides from N,N'-Bismaleimide," U. S. Patent 3,533,996 (1970).

29. H. D. Cole and W. F. Gruber (Du Pont), "Preparation of m-Phenylene Dimaleimide," U. S. Patent 3,127,414 (1964).

30. N. E. Searle (Du Pont), "Synthesis of N-Aryl-Maleimides," U. S. Patent 2,444,536 (1948).

31. G. T. Kwiatkowski, L. M. Roberson, G. L. Brode and A. W. Bedwin, "Thermosetting Diphenyl Sulfone-Based Maleimides," J. Polym. Sci.: Polym. Chem. Ed. 13, 961 (1975).

32. L. A. Domeier and H. C. Gardner (Amoco), "Bismaleimides and Prepreg Resins Therefrom," U. S. Patent 4,691,025 (1987).

33. J. Harvey, R. P. Chartoff and J. M. Butler, "New Aromatic-Ether Bismaleimide Matrix Resins," 18th International SAMPE Tech. Conf. 18, 705 (1986).

34. L. A. Domeier (Amoco), "Aromatic Bismaleimides and Prepreg Resin Therefrom," U. S. Patent 4,654,407 (1987).

35. I. K. Varma, G. M. Fohlen, Ming-ta Hsu and J. A. Parker, "New Phosphorus-Containing Bisimide Resins," in "Contemporary Topics in Polymer Science," ed. by W. J. Bailey and T. Tsuruta, Plenum Press, New York, Vol. 4, 115 (1984).

36. I. K. Varma, G. M. Fohlen and J. A. Parker, "Phosphorus-Containing Imide Resins. I.," J. Macromol. Sci.-Chem., A, 19(2), 209 (1983).

37. D. Kumar, S. Extension, G. M. Fohlen, J. A. Parker (NASA), "Maleimido Substituted Aromatic Cyclotriphosphazenes," U. S. Patent 4,550,177 (1985).

38. D. Kumar, S. Extension, G. M. Fohlen and J. A. Parker (NASA), "Fire and Heat Resistant Laminating Resins Based on Maleimido Substituted Aromatic Cyclotriphosphazene Polymers," U. S. Patent 4,634,759 (1987).

39. K. Sugawara, A. Takahashi, M. Ono and T. Narahara (Hitachi, LTD.), Euro. Patent Appl. 269,021 (1988).

40. I. K. Varma and S. Sharma, "Thermal Behavior of Bismaleimides," Indian J. Technol. 25(3), 136 (1987).

41. H. D. Stenzenberger, W. Römer, M. Herzog and P. König, "Toughened Bismaleimides: Modification with Thermoplastics," 33rd International SAMPE Symp. 33, 1546 (1988).

42. M. Bergain, A. Combet and P. Grosjean (Rhone-Poulenc), "Heat-Stable Resins Derived From Bisimides of Unsaturated Dicarboxyl Acids," Brit. Patent Spec. 1,190,718 (1970).

43. J. J. King, M. Chaudhari and S. Zahir, "A New Bismaleimide System for High Performance Applications," 29th International SAMPE Symp. 29, 392 (1984).

44. T. Abraham, "New Bismaleimide Resin Systems: Decreased Moisture Absorption and Increased Impact Strength," J. Polym. Sci., C, Polym. Lett. 26, 521 (1988).

45. S. Zahir, M. A. Chaudhari and J. King, "Novel High Temperature Resins Based on Bis(4-Maleimidophenyl) Methane," Makromol. Chem., Makromol. Symp. 25, 141, (1989).

46. K. A. Barrett, B. Fu and A. Wang, "Injectable Bismaleimide Systems," 35th International SAMPE Symp. 35, 1007 (1990).

47. I. K. Varma, M. S. Choudhary, B. S. Rao, Sangita and D. S. Varma, "Thermal Behavior of Bismaleimide-Amine/Vinyl Ester Resin-Styrene Blends," J. Macromol. Sci.-Chem., A, 21(6&7), 793 (1984).

48. H. D. Stenzenberger and P. König, "Comonomers for Bismaleimides: o,o'-Diallylbisphenols," High Performance Polymers 1(2), 133 (1989).

49. H. D. Stenzenberger, "High-Temperature Composites From Bismaleimide Resins: A Binder Concept," J. Appl. Polym. Symp. 31, 91 (1977).

50. G. D. Lyle, J. S. Senger, D. H. Chen, S. Kilic, S. D. Wu, D. K. Mohanty and J. E. McGrath, "Synthesis, Curing and Physical Behavior of Maleimide-Terminated Poly(Ether Ketones)," Polymer 30, 978 (1989).

51. G. T. Kwiatkowski and G. L. Brode, "Polyarylimides," U. S. Patent 3,839,287 (1974).

52. S. P. Wilkinson, S. C. Liptak, P. A. Wood, J. E. McGrath and T. C. Ward, "Reactive Blends of Amorphous Functionalized Engineering Thermoplastics and Bismaleimide/Diallyl Bisphenol-A Resins For High Performance Composite Matrices," 36th International SAMPE Symp. 36, 482 (1991).

53. T. L. St. Clair, "Matrix Resin Development At NASA Langley Research Center," in "High Temperature Polymer Matrix Composites," ed. by T. T. Serafini, Noyes Data Corp., New Jersey, 35 (1987).

54. D. Kruh and R. J. Jablonske, "Maleimide-Terminated Amide-Imide Prepolymers: Synthesis and Basic Properties," J. Polym. Sci.: Polym. Chem. Ed. 17, 1945 (1979).

55. J. A. Mikroyannidis, "Crosslinkable Aromatic Polyketones with Maleimide Pendent Groups," J. Polym. Sci.: Part A: Polym. Chem. 28, 669 (1990).

56. A. J. Kinloch and R. J. Young, "Fracture Behavior of Polymers," Applied Science Publishers, London (1983).

57. C. K. Riew and J. K. Gillham, "Rubber-Modified Thermoset Resins," Am. Chem. Soc., Washington, DC, Advances in Chemistry Series No. 208 (1984).

58. C. B. Buckmall and I. K. Patridge, "Phase Separation in Epoxy Resins Containing Polyethersulphone," Polymer 24(5), 639 (1983).

59. J. Diamant and R. J. Moulton, "Development of Resins for Damage Tolerant Composites - A Systemic Approach," 29th National SAMPE Symp. 29, 422 (1984).

60. R. C. Laible and R. J. McGarry, "Toughening of High-Temperature Epoxy Resins," Polym. Plast. Technol. Eng. 27, (1976).

61. S. Takeda and H. Kakiuchi, "Toughening Bismaleimide Resins by Reactive Liquid Rubbers," J. Appl. Polym. Sci. 35, 1351 (1988).

62. M. T. Blair, P. A. Steiner and E. N. Willis, "The Toughening Effects of PBI in a BMI Matrix Resin," 33rd International SAMPE Symp. 33, 524 (1988).

63. S. A. Zahir and A. Renner (Ciba-Geigy), "Process for the Manufacture of Crosslinked Polymers Which Contain Imide Groups," U. S. Patent 4,100,140 (1978).

64. "Matrimid® 5292 System," Product Data Sheet: CR921C3M80, Ciba-Geigy Corp., Hawthorne, New York (1990).

65. J. J. King, M. Chaudhari and S. Zahir, "A New Bismaleimide System for High Performance Applications," 29th National SAMPE Symp. 29, 392 (1984).

66. S. Zahir, M. A. Chaudhari and J. King, "Novel High Temperature Resins Based on Bis(4-Maleimidophenyl) Methane," Makromol. Chem., Macromol. Symp. 25, 141 (1989).

67. H. D. Stenzenberger and P. König, "Bis[3-(2-Allylphenoxy) Phthalimides]: A New Class of Comonomers for Bismaleimides," High Performance Polymers 1(2), 133 (1989).

68. H. D. Stenzenberger and P. König, "Comonomers for Bismaleimides: o,o'-Diallylbisphenols," High Performance Polymers 1(3), 239 (1989).

69. K. A. Barrett, B. Fu and A. Wang, "Injectable Bismaleimide Systems," 35th International SAMPE Symp. 35, 1007 (1990).

70. H. D. Stenzenberger, P. König, W. Römer, S. Pierce and M. Canning, "Bismaleimide Matrix Resin for Graphite Fiber Composites," 29th National SAMPE Symp. 29, 1043 (1984).

71. R. C. P. Cubbon, "The Free Radical and Anionic Polymerization of Some N-Substituted Maleimides," Polymer 6, 149 (1965).

72. H. D. Stenzenberger, "Chemistry and Properties of Addition Polyimides," in "Polyimides," ed. by D. Wilson, H. D. Stenzenberger and P. M. Hergenrother, Blackie & Son Ltd., New York, Chp. 4, 79 (1990).

73. T. V. Sheremeteva, G. N. Larina, V. N. Tsvetkov and I. N. Shtennikova, "Influence of the Structure of Unsaturated Imides of Their Polymerizability and on the Polymer Properties," J. Polym. Sci.: Part C, 22, 185 (1968).

74. H. E. Green, S. Beach, R. J. Jones, H. Beach, M. K. O'Rell and M. Beach (TWA, Inc.), "Bis(Difluoromaleimide) Capped Propolymers and Polymers," U. S. Patent 4,173,700 (1979).

75. W. Flitsch and S. R. Schindler, "Alkenylation of Imides and Activated Amides," Synthesis 11, 685 (1975).

76. J. L. Lang, W. A. Pavelich and H. D. Clarey, "Homopolymerization of Maleic Anhydride. I. Preparation of the Polymer," J. Polym. Sci. A, 1, 1123 (1963).

77. R. M. Joshi, "Calorimetric Determination of Maleimide," Makromol. Chem. 62, 140 (1963).

78. T. Bartnik and B. Baranowske, "Homopolymerization of Maleimide in Methanol Solutions at High Pressure," Pol. J. Chem. 53(3), 741 (1979).

79. P. O. Tawney, R. H. Snyder, R. P. Conger, D. A. Leibbrand, C. H. Stiteler and A. R. Williams, "The Chemistry of Maleimide and Its Derivatives. II. Maleimide and N-Methylmaleimide," J. Org. Chem. 26, 15 (1961).

80. Y. Nakayama and G. Smets, "Radical and Anionic Homopolymerization of Maleimide and N-n-Butylmaleimide," J. Polymer Sci., Part A-1, 5, 1619 (1967).

81. L. E. Coleman and J. A. Conrady, "Nitrogen-Containing Monomers. I. Copolymerization Reactions of N-Alkyl Maleamic Acids and N-Alkyl Maleimides," J. Polym. Sci. 38, 241 (1959).

82. F. Grundschober and J. Sambeth (Rhone Poulenc), "Reticulated Polyimides and Method of Producing Same From N,N'-Bisimide," U. S. Patent 3,380,964 (1968).

83. D. O. Hummel, K. U. Heinen, H. Stenzenberger and H. Siesler, "Infrared Spectroscopic Determination of the Kinetic Data of the Polymerization of Aliphatic Bismaleimides," J. Appl. Polym. Sci. 18, 2015 (1974).

84. G. Odian, "Principles of Polymerization," 2nd ed., John Wiley & Son, New York (1981).

85. B. Rånby and J. F. Rabek, "ESR Spectroscopy in Polymer Research," Springer-Verlag, New York (1977).

86. G. Moad, E. Rizzardo and D. H. Solomon, "Other Initiating Systems," in "Comprehensive Polymer Science, Vol.3(10)," ed. by Sir G. Allen and J. C. Bevington, Pergamon Press, New York (1989).

87. I. M. Brown and T. C. Sandreczki, "Characterization of Bismaleimide Cure Reactions by Electron Spin Resonance Techniques," Poly. Mater. Sci. Eng. 59, 612 (1989).

88. T. V. Sheremeteve, B. N. Larina, M. G. Zhenevskaya and V. A. Gusinskaya, "Preparation of High Molecular Weight Compounds on the Basis of Cyclic Imides and Diimides of Dicarboxylic Acids," J. Polym. Sci., Part C, 16, 1631 (1967).

89. J. E. White, "Synthesis and Properties of High Molecular Weight Step Growth Polymers from Bismaleimides," Ind. Eng. Chem. Prod. Res. Dev. 25, 395 (1986).

90. D. H. Marrian, "322. The Reactions of Substituted Maleimides with Thiols," J. Chem. Soc., Part 2, 1515 (1949).

91. H. M. Relles and R. W. Schluenz, "Dichloromaleimide Chemistry. III. The Reaction of N-Aryldichloromaleimide with Phenols. The Preparation and Mass Spectral Rearrangements of N-Aryl-3-Aryloxy-4-Chloromaleimides and N-Aryl-3,4-Bis(Aryloxy)Maleimides," J. Org. Chem. 37(23), 3637 (1972).

92. T. Hagiwara, J. Mizota, H. Hamama and T. Narita, "Anionic Polymerization of N-Substituted Maleimide, 1: Polymerization of N-Phenylmaleimide," Makromol. Chem., Rapid Commun. 6, 169 (1985).

93. K. Kojima, N. Yoda and C. S. Marvel, "Base-Catalyzed Polymerization of Maleimide and Some Derivatives and Related Unsaturated Carbonamides," J. Polym. Sci.: Part A-1, 4, 1121 (1966).

94. T. Hagiwara, T. Someno, H. Hamana and T. Narita, "Anionic Polymerization of N-Substituted Maleimide. II. Polymerization of N-Ethylmaleimide," J. Polym. Sci.: Polym. Chem. Ed. 26, 1011 (1988).

95. T. Hagiwara, M. Takeda, H. Hamana and T. Narita, "Anionic Polymerization of N-Substituted Maleimide, 3: Polymerization of N-Phenylmaleimide by 'ate' Complexes," Makromol. Chem., Rapid Commun. 8, 167 (1987).

96. T. Hagiwara, T. Shimizu, T. Someno, T. Yamagishi, H. Hamana and T. Narita, "Anionic Polymerization of N-Substituted Maleimide. 4. "Living" Characteristics of Anionic Polymerization of N-Phenylmaleimide," Macromol. 21, 3324 (1988).

97. T. Hagiwara, T. Shimizu, T. Uda, H. Hamana and T. Narita, "Anionic Polymerization of N-Substituted Maleimide. V. A Study on the Kinetic Features of Anionic Polymerization of N-Phenylmaleimide," J. Polym. Sci.: Part A: Polym. Chem. 28, 185 (1990).

98. T. Hagiwara, H. Hamana and T. Narita, "Living Characteristics of Anionic Polymerization of N-Phenylmaleimide Initiated with Alkali Metal Tert-Butoxides," Polym. Prepr., Am. Chem. Soc., Div. Polym. Chem. 29(2), 100 (1988).

99. P. Hodge, E. Khoshdel and A. A. Naim, "Polymerization of Maleimides and Maleic Anhydride Initiated by Triphenylphosphine: A ^{31}P-NMR End-Group Study," Polym. Comm. 27, 322 (1986).

100. D. G. Smyth, A. Nagamatsu and J. S. Fruton, "Some Reactions of N-Ethylmaleimide," J. Am. Chem. Soc. 82, 4600 (1960).

101. D. Ishii, T. Enoki and S. Shibahara, "Effects of Catalyst on the Polymerization of N-Phenylmaleimide," Netsu Dokasei Jushi 9(2), 67 (1988).

102. P. A. Wood, "Radical and Nucleophilic Assisted Homo- and Network Polymerizations of Maleimides and Bismaleimides," Ph.D. Research Proposal, presented to Graduate Advisory Committee, Virginia Polytechnic

Institute and State University, Blacksburg, Virginia, July 26 (1989).

103. T. M. Pyriadi and H. J. Harwood, "Cyclopolymerization of N-Allylmaleimide," Polym. Prepr., Am. Chem. Soc., Div. Polym. Chem. 11(1), 60 (1970).

104. L-S. Tan, E. J. Soloski and F. E. Arnold, "Benzocyclobutene-Maleimide Terminated Aromatic Imide AB-Monomers: Synthesis, Characterization and Diels-Alder Polymerizations," Polym. Prepr., Am. Chem. Soc., Div. Polym. Chem. 27(2), 240 (1986).

105. P. M. Hergenrother, S. J. Havens and J. W. Connell, "Acetylene Terminated Aspartimides," Polym. Prepr. Am. Chem. Soc., Div. Polym. Chem. 27(2), 408 (1986).

106. A. Pickering, A. J. Thorne (Du Pont), "Initiators Systems for Polymerization of Polar Arylic or Maleimide Monomers," Euro. Pat. 278,668 A2 (1988).

107. W. R. Hertier (Du Pont), "Group-Transfer Polymerization and Initiators Therefor," Euro. Pat. 265,091 A1 (1988).

108. S. Y. Sogah (Du Pont), "Group-Transfer Polymerization and Initiators Therefor," Euro. Pat. 249,436 A1 (1987).

109. E. A. Kraiman (Union Carbide), "Maleimide Polymers," U. S. Patent 2,890,206 (1959).

110. E. A. Kraiman (Union Carbide), "Maleimide Polymers," U. S. Patent 2,890,207 (1959).

111. S. W. Chow and J. M. Whelan (Du Pont), "Maleimide Polymers," U. S. Patent 2,971,944 (1961).

112. J. A. Reeder (Du Pont), "Polyimides from Dimaleimide and Bisfuvlenes," U. S. Patent 3,334,071 (1967).

113. S. Street and D. A. Beckley (Hitco), "Bis-maleimide/-Divinyl Aryl Crosslinking Agent Resin System," U. S. Patent 4,351,932 (1982).

114. S. Street, "V-378A, A New Modified Bismaleimide Matrix Resin for High Modulus Graphite," 25th National SAMPE Symp. 25, 366 (1980).

115. S. Street, "V-378A, A New Modified Bismaleimide Matrix Resin for High Modulus Graphite," in "Polyimides," ed. by D. L. Mittal, Plenum Press, New York, 77 (1984).

116. M. P. Stevens, "Polymer Chemistry, An Introduction," Oxford University Press, New York (1990).

117. K. R. Carduner and M. S. Chattha, "Carbon-13 NMR Investigation of the Oligomerization of Bismaleimidodiphenyl Methane with Diallyl Bisphenol A," in "Cross-Linked Polymers Chemistry, Properties and Application," Am. Chem. Soc., Symp. Ser. 367, Washington DC, Chp. 26, 379 (1988).

118. K. R. Carduner and M. S. Chattha, "Carbon-13 NMR Investigation of the Oligomerization of Bismaleimidodiphenyl Methane With Diallyl Bisphenyl A," ACS Polym. Mat. Sci. & Eng. 56, 660 (1987).

119. A. Renner and A. Kramer, "Allylnadic Imides: A New Class of Heat-Resistant Thermosets," J. Polym. Sci. Part A: Polym. Chem. Ed. 27, 1301 (1989).

120. C. T. Vijayakumar, K. Lederer and A. Kramer, "Thermogravimetric Study of Nadic-, Methylnadic- and Allylnadic-Bisimide Monomers," J. Polym. Sci.: Part A: Polym. Chem. 29, 929 (1991).

121. R. A. Kirchhoff, C. E. Baker, J. A. Gilpin, S. F. Hahn and A. K. Schrock, "Benzocyclobutenes in Polymer Synthesis," 18th International SAMPE Tech. Conf. 18, 478 (1986).

122. D. A. Shimp, J. R. Christenson and S. J. Ising, "AroCy®Cyanate Ester Resins Chemistry, Properties and Applications," Technical Booklet: Rhone-Poulenc Inc., Performance Resins & Coatings Division, Louisville, 2nd ed. (1990).

123. J. A. Midroyannidis, "Thermostable Laminating Resins Based on Aromatic Diketone Bis- and Tetramaleimides," J. Polym. Sci.: Part A: Polym. Chem. 28, 679 (1990).

124. R. B. Prime, "Thermosets," in "Thermal Characterization of Polymeric Materials," ed. by E. A. Turi, Academic Press, Orlando, 435 (1981).

125. R. J. J. Williams, "Curing of Thermosets," in "Developments in Plastics Technology-2," ed. by A. Whelan and J. L. Craft, Elsevier Applied Science Pub., Belfast, Vol. 2, Chp. 8, 339 (1985).

126. J. B. Enns and J. K. Gillham, "Time-Temperature-Transformation (TTT) Cure Diagram: Modeling the Cure Behavior of Thermosets," J. Appl. Polym. Sci. 28, 2567 (1983).

127. M. Gordon, T. C. Ward and R. S. Whitney, "Chemical And Physical Aspects of the Three Stages in Forming Polymer Networks," in "Polymer Networks Structure and Mechanical Properties," ed. by A. J. Chompff and S. Newman, Plenum Press, New York, 1 (1971).

128. J. K. Gillham, "Cure and Properties of Thermosetting Polymers," in "Structural Adhesives: Developments in Resins and Primers," ed. by A. J. Kinloch, Elsevier Applied Science Publishers, New York, 1 (1986).

129. M. T. Aronhime and J. K. Gillham, "Time-Temperature-Transformation (TTT) Cure Diagram of Thermosetting Polymeric Systems," in "Epoxy Resins and Composites III," ed. by K. Dusek, Springer-Verlag, Berlin, Adv. Polym. Ser. 78, 84 (1986).

130. J. K. Gillham, "Curing," in "Encyclopedia of Polymer Science and Engineering," Editor in Chief, J. I. Kroschwitz, Wiley-Interscience, New York, Vol. 4, 519 (1984).

131. T. Kaiser, "Highly Crosslinked Polymers," Prog. Polym. Sci. 14, 373 (1989).

132. P. J. Flory, "Principles of Polymer Chemistry," Cornell University Press, Ithaca, New York, Chp. IX (1986).

133. S. H. Goodman, "Introduction," in "Handbook of Thermoset Plastics," ed. by S. H. Goodman, Noyes Publications, New Jersey, Chp. 1, 1 (1986).

134. F. C. Robertson, "Resin Transfer Moulding of Aerospace Resins - A Review," Br. Polym. J. 20, 417 (1988).

135. J. K. Gillham, "Formation and Properties of Thermosetting and High T_g Polymeric Materials," Polym. Eng. & Sci. 26(20), 1429 (1986).

136. J. E. Adabbo and R. J. J. Williams, "The Evolution of Thermosetting Polymers in a Conversion-Temperature-Phase Diagram," J. Appl. Polym. Sci. 27, 1327 (1982).

137. X. Wang and J. K. Gillham, "Cure/Property Diagrams of Thermosetting Systems," Polym. Mat. Sci. Eng. 65, 347 (1991).

138. G. Wisanrakkit and J. K. Gillham, "Effect of Physical Annealing on the Dynamic Mechanical Properties of a High-T_g Amine-Cured Epoxy System," J. Appl. Polym. Sci. 42, 2465 (1991).

139. C. DI Giulio, M. Gautier and B. Jasse, "Fourier Transform Infrared Spectroscopic Characterization of Aromatic Bismaleimide Resin Cure States," J. Appl. Polym. Sci. 29, 1771 (1984).

140. C. M. Tung, "The Effect of Cure States on the Mechanical Properties of Bismaleimides IV. Fourier Transform Infrared Spectroscopy," Polym. Prepr., Am. Chem. Soc., Div. Polym. Chem. 28(1), 7 (1987).

141. C. G. Fry and A. C. Lind, "Curing of Bismaleimide Polymers: A Solid-State ^{13}C-NMR Study," New Polymer Materials 2(3), 235 (1990).

142. R. Istratoiu, M. Farcasiu and C. Nicolau, "ESR Spectra of Some Gamma-Irradiated N-Substituted Maleamic Acids and Maleimides," Bulletin de la Societe Royale des Sciences de Liege 36(3-4), 245 (1968).

143. H. Zott and H. Heusinger, "Intermediates of Radiation-Induced Polymerisation of Maleimides Studied by ESR," Euro. Polym. J. 14, 89 (1978).

144. R. M. Silverstein, G. C. Bassler and T. C. Morrill, "Spectrometric Identification of Organic Compounds," John Wiley & Sons, New York (1981).

145. C. Yang and S. Wang, "Studies on the Imidization of N-Substituted Polyamic Acids," J. Polym. Sci., Polym. Chem. 27, 15 (1989).

146. M. K. Hargreaves, J. G. Pritchard and H. R. Dave, "Cyclic Carboxylic Monoimides," Chem. Rev. 70(4), 439 (1970).

147. E. Pretsch, T. Clerc, J. Seibl and W. Simon, "Spectral Data for Structure Determination of Organic Compounds," Springer-Verlag, Hemsbach (1983).

148. D. Kumar, "An Efficient *in situ* Preparation of Bismaleimides Derived From Aromatic Diamines," Chemistry and Industry 21, 189 (1981).

149. D. J. Williams, "Addition Polyimides Offer High-Performance Options," Modern Plastics, Feb., 74 (1991).

150. F. Colucci, "Building Air Superiority," Aerospace Composites & Materials 3(2), 17 (1991).

151. N. J. Johnston, "Polyimides in Aerospace Applications," presented at the ACS Div. of Polym. Chem. Symp. on "Polyimides & Other High-Performance Polymers," Reno, NV, July (1987).

152. L. M. Poveromo, "Polyimide Composites-Application Histories," in "High Temperature Polymer Matrix Composites," ed. by T. T. Serafini, Noyes Data Corp., New Jersey, 336 (1987).

153. S. W. Street, "V-378A, A Modified Bismaleimide For Advanced Composites," in "High Temperature Polymer Matrix Composites," ed. by T. T. Serafini, Noyes Data Corp., New Jersey, 356 (1987).

154. R. A. Stonier, "Stealth Aircraft & Technology From World War II To The Gulf," SAMPE J. 27(4), 9 (1991).

155. P. M. Hergenrother and N. J. Johnston, "Organic Polymeric Composites For Aerospace Applications," Polym. Mater. Sci. Eng. 59, 697 (1988).

156. P. M. Hergenrother, "High-Temperature Polymer Composites," presented at "Teaching Macromolecular Chemistry And Engineering in the Undergraduate Curriculum," Am. Chem. Soc. Continuing Education Short Course at Virginia Polytechnic Institute & SU, Aug. (1991).

157. B. D. Smith, "The Cautious Approach," Modern Plastics, Feb., 74 (1991).

158. R. C. Larock, "Amines," in "Comprehensive Organic Transformations A Guide to Functional Group Preparations," VHC Publisher, New York, 385 (1989).

159. P. N. Rylander, "Nitro Compounds," in "Catalytic Hydrogenation Over Platinum Metals," Academic Press, New York, Chp. 11, 169 (1967).

160. P. N. Rylander, "Hydrogenation of Nitro Compounds," in "Hydrogenation Methods," Academic Press, Suffolk, Chp. 8, 104 (1990).

161. T. Takekoshi, "Polyimides," in "New Polymer Materials," ed. by C. G. Overberger, Springer-Verlag, Berlin (Advances in Polymer Science 94), 1 (1990).

162. J. W. Verbicky, Jr., "Polyimides," in "Encyclopedia of Polymer Science and Engineering," Editor in Chief, J. I. Kroschwitz, Wiley-Interscience, New York, Vol. 12, 364 (1984).

163. J. E. Schoenberg and S. P. Anderson (National Starch and Chemical Co.), "Novel Polyimides and Polyamic Acid and Ester Intermediates Thereof," U. S. Patent 4,405,770 (1983).

164. J. T. Scanton, "The Magenta Series. I. The Preparation and Spectrophotometric Study of the Lower Basic Members," J. Am. Chem. Soc. 57, 887 (1935).

165. W. M. Moore, "Aniline and Its Derivatives," in "Kirk-Othmer Encyclopedia of Chemical Technology," Wiley-Interscience, New York, 3rd ed., Vol. 2, 338 (1978).

166. A. L. Williams, R. E. Kinney and R. F. Bridger, "Solvent-Assisted Ullmann Ether Synthesis. Reactions of Dihydric Phenols," J. Org. Chem. 32, 2501 (1967).

167. Th. J. de Boer and I. P. Dirkx, "Activating Effect Of The Nitro Group in Aromatic Substitutions," in "The Chemistry of The Nitro and Nitroso Groups," ed. by H. Feuer, Interscience Publishers, New York, Part 1, Chp. 8, 487 (1987).

168. T. Tadekoshi, "Synthesis of High Performance Aromatic Polymers via Nucleophilic Nitro Displacement Reaction," Polym. J. 19(1), 191 (1987).

169. J. F. Bunnett and R. E. Zahler, "Aromatic Nucleophilic Substitution Reactions," Chem. Rev. 49, 273 (1951).

170. R. N. Johnson, A. G. Farnham, R. A. Clendinning, W. F. Hale and C. N. Merriam, "Poly(Aryl Ethers) by Nucleophilic Aromatic Substitution. I. Synthesis and Properties," J. Polym. Sci., Part A-1, 5, 2375 (1967).

171. J. H. Kawakami, G. T. Kwiatkowski, G. L. Brode and A. W. Bedwin, "High Temperature Polymers. I. Sulfone Ether

Diamines as Intermediates for Tractable High Temperature Polymers," J. Polym. Sci., Polym. Chem. Ed. 12, 565 (1974).

172. G. L. Brode, J. H. Kawakami, G. T. Kwiatkowski and A. W. Bedwin, "High Temperature Polymers. II. High Temperature Polymers from 4,4'-[Sulfonylbis(p-phenyleneoxy)]-dianiline," J. Polym. Sci.: Polym. Chem. Ed. 12, 575 (1974).

173. G. T. Kwiatkowski, G. L. Brode and A. W. Bedwin, "Chloroaromatic Ether Amines," J. Polym. Sci.: Polym. Chem. Ed. 14, 2649 (1976).

174. P. M. Hergenrother, N. T. Wakelyn and S. J. Havens, "Polyimides Containing Carbonyl and Ether Connecting Groups," J. Polym. Chem.: Part A: Polym. Chem. 25, 1093 (1987).

175. J. L. Hedrick, "Synthesis, Properties And Modifications of Engineering Polymers," Ph.D. Dissertation, Virginia Polytechnic Institute and State University, Blacksburg, Virginia (1985).

176. M. K. Jurek and J. E. McGrath, "Synthesis And Characterization of Amine-Terminated Poly(Arylene Ether Sulphone) Oligomers," Polymer 30, 1552 (1989).

177. J. March, "Aromatic Nucleophilic Substitution," in "Advanced Organic Chemistry," McGraw-Hill, New York, 2nd ed., Chp. 13, 584 (1977).

178. J. Miller, "Aromatic Nucleophilic Substitution," Elsevier Publishing Co., Amsterdam (1968).

179. R. F. Brown, "Organic Chemistry," Wadsworth Publishing Co., Belmont, CA, 460 (1975).

180. L. M. Robeson, A. G. Farnham and J. E. McGrath, "Synthesis and Dynamic Mechanical Characteristics of Poly(Aryl Ethers)," in "Polymerization and Polycondensation Processes," ed. by N. A. J. Platzer, John Wiley & Sons, New York, (J. Applied Polym. Sci., Appl. Polym. Symp. No. 26), 373 (1975).

181. B. E. Jennngs, M. E. B. Jones and J. B. Rose, "Synthesis of Poly(Arylene Sulfones) and Poly(Arylene Ketones) by Reactions Involving Substitution at Aromatic Nuclei," J. Polym. Sci., Part C, 16, 715 (1967).

182. A. B. Newton and J. B. Rose, "Relative Reactivities of the Functional Groups Involved in Synthesis of Poly(Phenylene Ether Sulphones) from Halogenated Derivatives of Diphenyl Sulphone," Polymer 13, 465 (1972).

183. J. B. Rose, "Preparation and Properties of Poly(Arylene Ether Sulphones)," Polymer 15, 456 (1974).

184. J. Miller, "The S_N Mechanism in Aromatic Compounds. VI. Carbonyl and Nitrile Substituents," J. Am. Chem. Soc. 76(2), 448 (1954).

185. J. F. Bunnett, E. W. Garbisch, Jr. and K. M. Pruitt, "The 'Element Effect' as a Criterion of Mechanism in Activated Aromatic Nucleophilic Substitution Reactions," J. Am. Chem. Soc. 79(2), 385 (1957).

186. S. D. Ross, "Nucleophilic Displacement Reaction in Aromatic Systems. IV. Rates of Reaction of 1-Halo-2,4-dinitrobenzene with n-Butylamine in Chloroform and with n-Butylamine and t-Butylamine in Dimethylformamide," J. Am. Chem. Soc. 81(9), 2113 (1959).

187. J. D. Reinheimer, R. C. Taylor and P. E. Rohrbaugh, "Chemical Kinetics of the Reaction of 2,4-Dinitrohalobenzenes with Ammonia," J. Am. Chem. Soc. 83(4), 835 (1961).

188. S. Maiti and B. K. Mandal, "Aromatic Polyethers by Nucleophilic Displacement Polymerization," Prog. Polym. Sci. 12, 111 (1986).

189. R. Viswanathan, B. C. Johnson and J. E. McGrath, "Synthesis, Kinetic Observations and Characteristics of Polyarylene Ether Sulphones Prepared via a Potassium Carbonate DMAC Process," Polymer 25, 1827 (1984).

190. E. Radlmann, W. Schmidt and G. E. Nischk, "A New Synthesis for Poly(Ether-Ketone)," Makromol. Chem. 130, 45 (1969).

191. C. K. Ingold, "Structure and Mechanism in Organic Chemistry," Cornell University Press, Ithaca (1969).

192. A. J. Parker, "The Effects of Solvation on the Properties of Anions in Dipolar Aprotic Solvents," Q. Rev. (London) 16, 163 (1962).

193. A. J. Parker, "Protic-Dipolar Aprotic Solvent Effects on Rates of Bimolecular Reactions," Chem. Rev. 69(1), 1 (1969).

194. R. Anschutz, "Uber die Bildung von Anilsäuren aus Anhydriden Zweibasischer Säuren," Ber. 20, 3214 (1887).

195. A. Piutti and E. Giustiniani, "Sui Cerivali Maleinice di Alcune Ammine Grasse," Gazz. Chim. Ital 26, I, 431 (1896).

196. J. M. Weiss and R. P. Weiss (Research Corp.), "Amine Reaction Product," U. S. Patent 2,306,918 (1942).

197. L. E. Coleman, Jr., J. F. Bork and H. Dunn, Jr., "Reaction of Primary Aliphatic Amines with Maleic Anhydride," J. Org. Chem. 24, 135 (1959).

198. I. J. Rinkes, "The Action of Sodium Hypochlorite on Acid Amides," Rec. Trav. Chim. 48, 961 (1929).

199. N. B. Mehta, A. P. Phillips, F. Fu, Lui and R. E. Brooks, "Maleamic and Citraconamic Acids, Methyl Esters and Imides," J. Org. Chem. 25(6), 1012 (1960).

200. C. Yang and S. Wang, "Studies on the Imidization of N-Substituted Polymaleamic Acids," J. Polym. Sci.: Part A: Polym. Chem. 27, 15 (1989).

201. A. Piutti, "Maleic and Fumaric Derivatives of p-Aminophenols," Atti Accad. Lincei 18, II, 312 (1909).

202. W. H. Warren and R. A. Briggs, "Action of Thionyl Chloride on Some Anilic Acids," Ber. 64B, 26 (1931).

203. G. Vanags and A. Veinsbergs, "Condensations of Primary Amino Compounds with Phthalic Anhydride in AcOH," Ber. 75B, 1558 (1942).

204. L. H. Flett and W. H. Gardner, "Maleic Anhydride Derivatives," John Wiley & Sons, New York, 128 (1952).

205. G. B. Hoey and C. T. Lester, "The Reaction of Succinic and Glutaric Acid with Amines," J. Am. Chem. Soc. 73(9), 4473 (1951).

206. A. K. Bose, F. Greer and C. C. Price, "Procedure for Phthaloylation Under Mild Conditions," J. Org. Chem. 23, 1335 (1958).

207. J. M. Butler, R. P. Chartoff, J. A. Harvery (Univ. of Dayton), "Process for the Preparation of Aromatic Ether Bismaleimides," U. S. Patent 4,855,450 (1989).

208. M. Lancaster (BP), "Cyclodehydration of Diamine-Maleic Anhydride Adducts," Euro. Patent 342,823 A1 (1989).

209. M. Lancaster (BP), "Synthesis of Bisimides," Euro. Patent 367,599 A1 (1990).

210. Y. Kita, S. Nakagawa, H. Kanai and Akio Fukui (Nippon Shokubai Kagaku Kogyo Co.), "Preparation of Maleimides," Jap. Patent 1,242,568 A2 (1989).

211. R. J. Cotter, Carol D. Sauers and J. M. Whelan, "The Synthesis of N-Substituted Isomaleimides," J. Org. Chem. 26(1), 10 (1961).

212. F. V. Boyd and R. L. Monteil, "Synthesis and Reactions of Cyclic Isoimidium Salts," J. Chem. Soc., Perkin I, 11, 1338 (1978).

213. M. Narita, M. Akiyama and M. Okawara, "The Dehydration of N-Benzyloxy and N-Hydroxymaleamic Acid and the Isomerization of N-Benzyloxyisomaleimide, Bull. Chem. Soc. Jap. 44, 437 (1971).

214. K. C. Tsou, R. J. Barrnett and A. M. Seligman, "Preparation of Some N-(1-Naphthyl)maleimides as Sulfhydryl-group Reagents," J. Am. Chem. Soc. 77, 4613 (1955).

215. W. R. Roderick, "Dehydration of N-(p-Chlorophenyl)-phthalamic Acid by Acetic and Trifluoroacetic Anhydrides," J. Org. Chem. 29(3), 745 (1964).

216. A. E. Kretov, N. E. Kul'chitskaya and A. F. Mal'nev, "Isomerism of N-Arylmaleimides," Zh. Obshch. Khim. 31, 2588 (1961).

217. J. P. Critchley, G. J. Knight and W. W. Wright, in "Heat-Resistant Polymers," Plenum Press, New York (1983).

218. T. M. Bogert and R. R. Renshaw, "4-Amino-o-Phthalic Acid and Some of Its Derivatives," J. Am. Chem. Soc. 30, 1135 (1908).

219. R. W. Thomas, T. M. Aminabhavi and Patrick E. Cassidy, "Polyimidines - A New Class of Polymers," in "New Monomers and Polymers," ed. by B. M. Culbertson and C. U. Pittman, Jr., Plenum Press, New York, 1 (1984).

220. W. Sweeny (DuPont), "Poly-meta-Phenylene Isophthalamides," U. S. Patent 3,287,324 (1966).

221. W. M. Edwards and I. M. Robinson (DuPont), "Polyimides of Pyromellitic Acid," U. S. Patent 2,710,853 (1955).

222. P. M. Hergenrother, "High Temperature Polymers from Thermally Curable Oligomers," in "Reactive Oligomers," ed. by F. W. Harris and H. J. Spinelli, Am. Chem. Soc., Symp. Ser. 282, Chp. 1, 1 (1985).

223. P. M. Hergenrother and N. J. Johnston, "Status of High-Temperature Laminating Resins and Adhesives," in "Resins for Aerospace," ed. by C. A. May, Am. Chem. Soc., Symp. Ser. 132, 3 (1980).

224. P. E. Cassidy, "Polymers For Extreme Service Conditions," J. Chem. Education 58, 951 (1981).

225. J. Preston, "Heat-Resistant Polymers," in "Kirk-Othmer Encyclopedia of Chemical Technology," Wiley-Interscience, New York, 3rd ed., Vol. 12, 203 (1978).

226. P. E. Cassidy, "Thermally Stable Polymers, Syntheses and Properties," Marcel Dekker, Inc., New York (1980).

227. D. Wilson, "Polyimides as Resin Matrices For Advanced Composites," in "Polyimides," ed. by D. Wilson, H. D. Stenzenberger and P. M. Hergenrother, Chapman and Hall, New York, Chp. 7, 187 (1990).

228. G. Lubin and S. J. Dastin, "Aerospace Applications of Composites," in "Handbook of Composites," ed. by G. Lubin, Van Nostrand Reinhold Co., Chp. 28, 722 (1982).

229. G. H. Moelter, R. F. Tetrault and M. J. Hefferon, "Polybenzimidazole Fiber," Polym. News 9, 134 (1983).

230. A. Walch, H. Lukas A. Kimmer and W. Pusch, "Structure and Hyperfiltration Properties of Polyimide Membranes," J. Polym. Sci.: Lett. Ed. 12, 697 (1974).

231. P. M. Hergenrother and H. H. Levine, "Phenyl-Substituted Polyquinoxalines," J. Polym. Sci. A-1, 5, 1453 (1967).

232. P. M. Hergenrother, "Introduction To High Temperature Polymer Synthesis," in "American Chemical Society Intensive Polymer Synthesis Short Course Notes," ed. by J. E. McGrath, ACS, Blacksburg, VA (1991).

233. P. M. Hergenrother, "Heat-Resistant Polymers," in "Encyclopedia of Polymer Science and Engineering," Editor in Chief, J. I. Kroschwitz, Wiley-Interscience, New York, Vol. 7, 639 (1984).

234. A. H. Frazer, "High Temperature Resistant Polymers," John Wiley & Sons-Interscience, New York (1968).

235. J. E. Mulvaney, "Heat-Resistant Polymers," in "Encyclopedia of Polymer Science and Technology," ed. by N. M. Bikales, Wiley-Interscience, New York, Vol. 7, 478 (1967).

236. J. I. Jones, "The Synthesis of Thermally Stable Polymers: A Progress Report," J. Macromol. Sci.:-Revs. Macromol. Chem., C, 2(2), 303 (1968).

237. P. W. Atkins, "Physical Chemistry," W. H. Freeman and Company, San Francisco, 2nd ed., 111 (1978).

238. T. L. Cottrell, "The Strength of Chemical Bonds," Butterworths, London, 2nd ed. (1958).

239. G. Lyle, J. C. Hedrick, D. A. Lewis, J. S. Senger, D. H. Chen, S. D. Wu and J. E. McGrath, "Synthesis and Characterization of Maleimide Terminated Poly(Arylene Ether Ketone)s," in "Polyimides: Materials, Chemistry and Characterization," ed. by C. Feger, M. M. Khojaster and J. E. McGrath, Elsevier Science Publisher, Amsterdam, 213 (1989).

240. C. S. Marvel, "Thermally Stable Polymers with Aromatic Recurring Units," Soc. Plast. Eng. J. 20, 220 (1964).

241. C. Arnold, Jr., "Stability of High-Temperature Polymers," J. Polym. Sci.: Macromol. Revs. 14, 265 (1979).

242. C. J. Lee, "Polyimides, Polyquinolines and Polyquinoxalines: T_g-Structure Relationships," J. Macromol. Sci.:-Rev. Macromol. Chem. Phys., C, 29(4), 431 (1989).

243. C. J. Lee, "Assessments of T_g's for Semi-Rigid Polymers," in "Proceedings of the 34th International SAMPE Symp.," 34, 929 (1989).

244. B. C. Anderson and R. D. Lipscomb, "Carl Shipp Marvel: Speed at 90," Macromol. 17, 1641 (1984).

245. C. S. Marvel and G. E. Hartzell, "Preparation and Aromatization of Poly-1,3-Cyclohexadiene," J. Am. Chem. Soc. 81, 448 (1959); D. A. Frey, M. Hasegawa and C. S. Marvel, "Preparation and Aromatization of Poly-1,3-Cyclohexadiene. II," J. Polym. Sci. A, 1, 2057 (1963); C. S. Marvel, P. E. Cassidy and S. Ray, "Preparation and Aromatization of Poly-1,3-Cyclohexadiene and Subsequent Crosslinking. III," J. Polym. Sci. A, 3, 1553 (1965).

246. G. Rabilloud, B. Sillion and G. de Gaudemaris (Institut Francais du Petrole des Carurants et Lubrifiants), "Mixed Imide-Isoindoloquinazolinediones Heterocyclic Polymers," U. S. Patent 3,678,005 (1972).

247. A. Saiki, K. Mukai, S. Harada and Y. Miyadera, "Development of New Polyimide Type Resin, PIQ®, for LSI Multilevel Interconnections," Org. Coat. Plast. Chem. 43, 459 (1980).

248. W. J. Bailey, "Ladder and Spiro Polymers," in "Encyclopedia of Polymer Science and Engineering," Editor in Chief, J. I. Kroschwitz, Wiley-Interscience, New York, Index Vol., 158 (1984).

249. J. N. Hay, J. D. Boyle, P. G. James, J. R. Walton and D. Wilson, "Polymerization Mechanisms in PMR-15 Polyimide," in "Polyimides: Materials, Chemistry and Characterization," ed. by C. Feger, M. M. Khojaster and J. E. McGrath, Elsevier Science Publisher, Amsterdam, 305 (1989).

250. L. K. McCune, "HT-1 High-Temperature Resistant Polyamide Fibers and Paper," Text. Res. H. 32(9), 762 (1962); J. H. Ross, "High Temperature Research," Text. Res. J. 32(9), 768 (1962).

251. J. Economy, R. S. Storm, V. I. Matkovich, S. G. Cottis and B. E. Nowak, "Synthesis and Structure of the p-Hydroxybenzoic Acid Polymer," J. Polym. Sci.: Polym. Chem. Ed. 14, 2207 (1976).

252. G. Montaudo, P. Finocchiaro and S. Caccamese, "Synthesis and Properties of Anthracene-Containing Polybenzyls," J. Polym. Sci. A-1, 9, 3627 (1971).

253. P. W. Morgan, "Liquid-Crystalline Solutions of Polyhydrazindes and Poly(Amide-Hydrazides) in Sulfuric Acids," J. Polym. Sci.: Polym. Symp. No. 65, 1 (1978).

254. J. G. Speight, P. Kovacic and F. W. Koch, "Synthesis and Properties of Polyphenyls and Polyphenylenes," J. Macromol. Sci.: Rev. Macromol. Chem., C, 5(2), 295 (1971).

255. W. H. Bonner (DuPont), "Aromatic Polyketone and Preparation Thereof," U. S. Patent 3,065,205 (1962).

256. H. L. Finkbeiner, A. S. Hay and D. M. White, "Polymerization by Oxidative Coupling," in "Polymerization Process," ed. by C. E. Schildknecht, Wiley-Interscience, Chp.15, 537 (1977); J. T. Edmonds and H. W. Hill, "Production of Polymers from Aromatic Compounds," U. S. Patent 3,354,129 (1967).

257. "Polyimides: Materials, Chemistry, and Characterization," ed. by C. Feger, M. M. Khojaster and J. E. McGrath, Elsevier Science Publisher, Amsterdam (1989); "Polyimides," ed. by D. Wilson, H. S. Stenzenberger and P. M. Hergenrother, Blackie, New York (1990).

258. T. Shono, M. Hachihama and K. Shinra, "Aromatic Poly(Phenyleneoxazoles)," J. Polym. Sci., Polym. Lett., B, 5, 1001 (1967).

259. G. F. D'Alelio, D. M. Feigl, T. Ostdick, M. Saha and A. Chang, "Arylsufimide Polymers. VII. The Polythiazones," J. Macromol. Sci. Chem., A, 6(1), 1 (1972).

260. G. P. de Gaudemaris and B. J. Sillion, "New Polymers Obtained by Polyheterocyclization: Polyquinozalines," J. Polym. Sci., Polym. Lett., B, 2, 203 (1964).

261. K. C. Brinker, D. D. Kameron and I. M. Robinson (DuPont), "Polybenzoxazoles," U. S. Patent 2,904,537 (1959).

262. H. Vogel and C. S. Marvel, "Polybenzimidazoles, New Thermally Stable Polymers," J. Polym. Sci. 50, 511 (1961).

263. C. J. Abshire and C. S. Marvel, "Some Oxadiazole and Triazole Polymers," Makromol. Chem. 44-46, 388 (1961).

264. C. G. Overberger and S. Fujimoto, "Polycycloaddition of Terephthalonitrile Oxide," J. Polym. Sci., B, 3, 735 (1965).

265. W. Bracke, "Aromatization of Polydiethynylbenzene," J. Polym. Sci. A-1, 10(4), 975 (1972).

266. D. F. Loncrini, W. L. Walton and R. B. Hughes, "Aromatic Polyesteramideimides," J. Polym. Sci. A-1, 4, 440 (1966).

267. G. M. Bower and L. W. Frost, "Aromatic Polyimides," J. Polym. Sci. A-1, 1, 3135 (1963); "Polyimides," ed. by D. Wilson, H. S. Stenzenberger and P. M. Hergenrother, Blackie, New York (1990).

268. B. C. Johnson, "High Performance Polyimide Copolymers: Synthesis and Characteristics," Ph.D. Dissertation, Virginia Polytechnic Institute and State University, Blacksburg, Virginia (1984).

269. C. A. Arnold, J. D. Summers, Y. P. Chen, T. H. Yoon, B. E. McGrath, D. Chen and J. E. McGrath, "Soluble Polyimide Homopolymers and Poly(Siloxane Imide) Segmented Copolymers with Improved Dielectric Behavior," in " Polyimides: Materials, Chemistry and Characterization," ed. by C. Feger, M. M. Khojasteh and J. E. McGrath, Elsevier Sci. Publishers, Amsterdam, 69 (1989).

270. B. Culbertson and R. Murphy, "Poly(Phenylene-1,3,4-Oxadiazole Benzoxazoles)," J. Polym. Sci., Polym. Lett. B, 4, 249 (1966).

271. L. L. Bircumshaw, F. M. Tayler and D. H. Whiffen, "Paracyanogen: Its Formation and Properties. Part 1.," J. Chem. Soc., 931 (1954); H. M. Woodburn and J. R. Fisher, "Reaction of Cyanogen with Organic Compounds. X. Aliphatic and Aromatic Diamines," J. Org. Chem. 22(8), 895 (1957).

272. M. L. Kaplan, P. H. Schmidt, C. H. Chen and W. M. Walsh, Jr., "Carbon Films with Relatively High Conductivity," Appl. Phys. Lett. 36, 867 (1980).

273. V. L. Bell, "Polyimidazopyrrolones," in "Encyclopedia of Polymer Science and Technology," ed. by N. M. Bikales, Wiley-Interscience, New York, Vol. 11, 240 (1967).

274. N. G. Fisher and R. H. Wiley (DuPont), "Polymers," U. S. Patent 2,389,662 (1945).

275. W. J. Bailey and B. D. Feinberg, "The Synthesis of Ladder Polymers Containing Macrocyclic Esters," Polym. Prepr., Am. Chem. Soc. Div., Polym. Chem. 8(1), 165 (1967).

276. V. Percec and B. C. Auman, "Polyaromatics with Terminal or Pendant Styrene Groups," in "Reactive Oligomers," ed. by F. W. Harris and H. J. Spinelli, Am. Chem. Soc., Washington, DC, ACS Symp. Ser. 282, Chp. 8, 91 (1985).

277. F. W. Harris and K. Sridhar, "Ethynyl End-Capped Polyimide Oligomers Containing Oxyethylene Linkages," in "Reactive Oligomers," ed. by F. W. Harris and H. J. Spinelli, Am. Chem. Soc., Washington, DC, ACS Symp. Ser. 282, Chp. 7, 81 (1985).

278. L. C. Hsu and W. Philips, "Cyclopolymerization and Polymers with Chain-Ring Structures," ed. by G. B. Butler and J. E. Kresta, Am. Chem. Soc., Washington, DC, ACS Symp. Ser. 195, 285 (1982).

279. R. J. Kray, "The NCNS Resins For Potential Applications in Advanced Composites," 20th National SAMPE Symp. and Exhib. 20, 227 (1975).

280. S. C. Lin, "N-Cyanourea-Terminated Resins," in "Reactive Oligomers," ed. by F. W. Harris and H. J. Spinelli, Am. Chem. Soc., Washington, DC, ACS Symp. Ser. 282, Chp. 9, 105 (1985).

281. F. W. Harris, et al., "Synthesis and Characterization of Reactive End-Capped Polyimide Oligomers," J. Macromol. Sci.-Chem., A, 21(8 & 9), 1117 (1984).

282. B. Sillion, "Polymerization of Reactive Telechelic Oligomers. Formation of Thermostable Networks," in "Recent Advances in Mechanistic and Synthetic Aspects of Polymerization," ed. by M. Fontanille and A. Guyot, D. Reidel Publishing Co., Dordrecht, Holland, 237 (1987).

283. L. S. Tan and F. E. Arnold, "New High-Temperature Thermoset Systems Based on Bis-Benzocyclobutene," Polym.

Prepr., Am. Chem. Soc., Div. Polym. Chem. 26(2), 176 (1985).

284. J. P. Droske and J. K. Stille, "Biphenyl End-Capped Polyquinoline Prepolymers: Synthesis, Processing and Curing Reactions," Macromol. 17(1), 1 (1984).

285. R. C. MacKenzie, "Nomenclature for Thermal Analysis IV," Pure Appl. Chem. 57, 1737 (1985).

286. J. H. Flynn, "Thermal Analysis," in "Polymers: Polymer Characterization and Analysis," ed. by J. I. Kroschwitz, Wiley-Interscience, New York, 837 (1990).

287. W. W. Wendlandt and P. K. Gallagher, "Instrumentation," in "Thermal Characterization of Polymeric Materials," ed. by E. A. Turi, Academic Press, Orlando, Chp. 1, 1 (1981).

288. E. A. Turi, Y. P. Khanna and T. J. Taylor, "Thermal Analysis," in "A Guide to Materials Characterization and Chemical Analysis," ed. by J. P. Sibilia, VHC, New York, Chp. 9, 205 (1988).

289. C. S. Marvel, "Trends in High-Temperature Stable Polymer Synthesis," J. Macromol. Sci.:-Revs. Macromol. Chem., C, 13(2), 219 (1975).

290. J. R. MacCallum, "Thermogravimetric Analysis," in "Comprehensive Polymer Science," ed. by C. Booth and D. Price, Pergamon Press, Oxford, Vol. 1, Chp. 37, 903 (1989).

291. H. Vogel and C. S. Marvel, "Polybenzimidazoles II.," J. Polym. Sci. A, 1, 1531 (1963).

292. R. C. Gann, R. A. Dipert and M. J. Drews, "Flammability," in "Encyclopedia of Polymer Science and Engineering," Editor in Chief, J. I. Kroschwitz, Wiley-Interscience, New York, Vol. 7, 639 (1984).

293. C. F. Cullis and M. M. Hirschler, "The Combustion of Organic Polymers," Clarendon Press, Oxford (1981).

294. D. W. Van Krevelen, "Some Basic Aspects of Flame Resistance of Polymeric Materials," Polymer 16(8), 615 (1975).

295. J. E. McGrath, "Chain Reaction Polymerization," J. Chem. Education 58, 844 (1981).

296. A. Factor, "The Chemistry of Polymer Burning and Flame Retardance," J. Chem. Educ. 51, 453 (1974).

297. E. M. Pearce, Y. P. Khanna and D. Raucher, "Thermal Analysis in Polymer Flammability," in "Thermal Characterization of Polymeric Materials," ed. by E. A. Turi, Academic Press, Orlando, Chp. 8, 793 (1981).

298. A. Factor, "Char Formation in Aromatic Engineering Polymers," in "Fire and Polymers, Hazards Identification and Prevention," ed. by G. L. Nelson, Am. Chem. Soc., Washington, DC, Chp. 19, 274 (1990).

299. Y. P. Khanna and E. M. Pearce, "Flammability of Polymers," in "Applied Polymer Science," ed. by R. W. Tess and G. W. Poehlein, ACS Symp. Ser. 285, Am. Chem. Soc., Washington, DC, Chp. 14, 305 (1985).

300. A. Granzow, "Flame Retardation by Phosphorus Compounds," Acct. Chem. Res. 11(5), 177 (1978).

301. J. W. Hastie and C. L. McBee, "Mechanistic Studies of Triphenylphosphine Oxide-Poly(Ethyleneterephthalate) and Related Flame Retardant Systems," National Bureau of Standards Final Report, NBSIR 75-741, Aug.(1975), COM-75-11136/9GA.

302. I. K. Varma, G. M. Fohlen, M. Hsu and J. A. Parker, "New Phosphorus-Containing Bisimide Resins," in "Contemporary Topics in Polymer Science," ed. by W. J. Bailey and T. Tsuruta, Plenum Press, New York, Vol. 4, 115 (1984).

303. E. D. Weil, "Flame Retardants, Phosphorus Compounds," in "Kirk-Othmer Encyclopedia of Chemical Technology," Wiley-Interscience, New York, 3rd ed., Vol. 10, 396 (1978).

304. P. A. Wood, G. D. Lyle, A. Gungor, C. D. Smith and J. E. McGrath, "Synthesis of New Bismaleimides Derived From Bis(3-Amino Phenoxy) Triphenylphosphine Oxide and Bis(4-Fluoro Benzoyl) Benzene," 36th International SAMPE Symposium 36(2), 1355 (1991).

305. C. D. Smith, "Synthesis and Characterization of Phosphorus Containing Poly(Arylene Ether) Systems," Ph.D. Dissertation, Virginia Polytechnic Institute and State University, Blacksburg, Virginia (1991).

306. M. J. Jurek, "Synthesis and Characterization of Poly(Arylene Ethers) and Functionalized Oligomers," Ph.D. Dissertation, Virginia Polytechnic Institute and State University, Blacksburg, Virginia (1987).

307. G. D. Lyle, Ph.D. Dissertation, Virginia Polytechnic Institute and State University, Blacksburg, Virginia (1992).

308. A. Gungor, C. D. Smith, J. Wescott, S. Srinivasan and J. E. McGrath, "Synthesis of Fully Imidized Phosphorous-Containing Soluble Polyimides," Polym. Prepr., Am. Chem. Soc. Div., Polym. Chem. 32(1), 172 (1991).

309. R. May, "Polyetheretherketones," in "Encyclopedia of Polymer Science and Engineering," Editor in Chief, J. I. Kroschwitz, Wiley-Intersicence, New York, Vol. 12, 313 (1984).

310. Harvey J. Grubbs, "High Performance Monomer Synthesis and Polymer Pyrolysis," Ph.D. Dissertation, Virginia Polytechnic Institute and State University, Blacksburg, Virginia (1992).

Vita

Paul A. Wood, III was born on September 27, 1954, in Roanoke, Virginia. Paul received his high school diploma from Roanoke's Patrick Henry High School in 1973. He then entered Emory & Henry College and completed a B.A. in Biology in 1977. Paul finished a B.S. in Chemistry from Roanoke College in 1983 while employed as the Chemist for the City of Salem, Virginia Water Department from 1977-1984. He then completed his M.S. in Chemistry under Professor James E. McGrath in 1988 at Virginia Tech with interest in anionic polymerization of block copolymers. Paul received his Ph.D. in Chemistry in 1991 and joined Dow Chemical USA to do "great things".